5-2012

Characterization of the Function of the *Azospirillum brasilense* Che1 Chemotaxis Pathway in the Regulation of Chemotaxis, Cell Length and Clumping

Amber Nicole Bible
abible@utk.edu

To the Graduate Council:

I am submitting herewith a dissertation written by Amber Nicole Bible entitled "Characterization of the Function of the *Azospirillum brasilense* Che1 Chemotaxis Pathway in the Regulation of Chemotaxis, Cell Length and Clumping." I have examined the final electronic copy of this dissertation for form and content and recommend that it be accepted in partial fulfillment of the requirements for the degree of Doctor of Philosophy, with a major in Biochemistry and Cellular and Molecular Biology.

Gladys Alexandre, Major Professor

We have read this dissertation and recommend its acceptance:

Beth Mullin, Barry Bruce, Alison Buchan, Elena Shpak

Accepted for the Council:
Dixie L. Thompson

Vice Provost and Dean of the Graduate School

(Original signatures are on file with official student records.)

Characterization of the Function of the *Azospirillum brasilense* Che1 Chemotaxis Pathway in the Regulation of Chemotaxis, Cell Length and Clumping

A dissertation presented for the Doctor of Philosophy Degree

The University of Tennessee, Knoxville

Amber Nicole Bible

May 2012

Abstract

Azospirillum brasilense is a gram-negative alphaproteobacterium that lives in the soil where it colonizes the root surfaces of cereals and grasses. The genome of *A. brasilense* has recently been sequenced and shown to possess four different chemotaxis-like operons. This dissertation project focused on characterizing the Che1 chemotaxis-like signal transduction pathway, which was initially implicated in regulation of the chemotaxis behavior. Deletions of individual genes within the Che1 pathway did not exhibit a null chemotaxis phenotype, leading us to investigate the role of this pathway in the lifestyle of *A. brasilense* and the mechanism(s) by which it functions. We have used a combination of microbiology and molecular genetics methods, including construction and characterization of several mutant strains lacking *che1* genes, as well as molecular biology and microscopy. The data obtained suggest that Che1 is involved in regulating multiple cellular behaviors such as cell length and swimming speed, as well as having indirect effects on cell-to-cell clumping behavior, cell surface properties, and a minor role in regulating the motility bias. The data obtained also shed light on the function of the N-terminal HlyIII-like domain of CheA1 in *A. brasilense* which is also found in other bacterial species, as a single domain protein. Using *A. brasilense*, *Escherichia coli* and *Bacillus subtilis*, evidence is provided that HlyIII-like domains function to modulate membrane properties with effects on fatty acid composition that appear to also impair protein localization and function, including the control of cell length at division and chemotaxis.

Table of Contents

List of Tables

List of Figures

List of Symbols and Abbreviations

Ap:	Ampicillin
Asp:	Aspartic Acid
Che:	“chemotaxis”, “chemotaxis-like”, or “chemosensory”
DIC:	Differential Interference Contrast
EDTA:	Ethylenediaminetetraacetate
EPS:	Exopolysaccharide
FITC:	Fluorescein Isothiocyanate
GFP:	Green Fluorescent Protein
Gm:	Gentamycin
GPCR:	G-Protein Coupled Receptor
His:	Histidine
HK:	Histidine kinase
HlyIII:	Hemolysin III (domain)
IPTG:	Isopropyl-β-D-1-thiogalactopyranoside
Km:	Kanamycin
MCPs:	Methyl-accepting chemotaxis proteins
ORF:	Open reading frame
PAQR:	Progestin and AdipoQ Receptor (family)
Rec:	Receiver (domain)
RR:	Response regulator
SDS-PAGE:	Sodium dodecyl sulfate-polyacrylamide gel electrophoresis
Tc:	Tetracycline

TRITC:	Texas Red Isothiocyanate
YFP:	Yellow Fluorescent Protein

Introduction

Azospirillum brasilense

Sensing and adaptation to various environmental cues is an important survival strategy of soil-dwelling bacteria. Bacteria can take advantage of motility behavior and chemotaxis in order to overcome situations such as low nutrient availability or to sense differences in the relative viscosity of their environment (15). The gram-negative alphaproteobacterium, *Azospirillum brasilense*, resides in the soil where it colonizes the root surfaces of certain cereals and grasses. These bacteria possess a variety of important traits which are important to its survival. First of all, *A. brasilense* is a microaerophilic organism, which means that it grows optimally under low oxygen conditions, 0.4% dissolved oxygen, in this case (67). This trait is especially important to the process of nitrogen fixation, in that it is only under microaerophilic conditions that *A. brasilense* can fix nitrogen, because the nitrogenase enzyme, NifH, is highly sensitive to and its activity is inhibited by oxygen (22, 41). The ability of *A. brasilense* to grow under low oxygen conditions and fix nitrogen is beneficial for a soil-dwelling lifestyle, where oxygen and nitrogen can be limiting.

Flagella and motility in A. brasilense

A. brasilense possesses a dual flagellar system consisting of a single polar flagellum, which is expressed under all growth conditions and is used for swimming, as well as lateral flagella which are utilized for swarming on solid surfaces (52) (Figure 1). The polar flagellum has been shown to play a key role in the adsorption of *A. brasilense* to wheat roots (16), and it is believed that the glycosylation of this flagellum plays a role in this attachment, perhaps via

lectins (39). Under more viscous conditions, genes encoding the lateral flagella are expressed and are used for swarming motility (24). Swarming motility has been poorly characterized in *A. brasilense*, but in the studies thus far, it was shown that *A. brasilense* can sense differences in growth surface properties (high versus low agar concentrations), most likely viscosity, in order to induce either swimming via the polar flagellum (low viscosity or liquid media), or swarming (higher viscosity) with the use of lateral flagella (24). Generally speaking, the means by which cells detect conditions suitable for production of lateral flagella are not clearly understood. One hypothesis is that cells have a "mechanosensor" that recognizes the surface conditions where swarming behavior is required; however, identification of this mechanosensor and the mechanism by which it measures the surface conditions is unclear (27, 37). However, such a role for the polar flagellum has been hypothesized with reduction in flagellar rotation acting as a cue for lateral flagellar expression (21, 35, 36). In some bacteria, it has been shown that the ability to move across surfaces using lateral flagella is important to the process of surface colonization (37, 38), suggesting that the capability of exhibiting swarming behavior in *A. brasilense* may enhance plant root colonization.

Cellular differentiation in A. brasilense

A. brasilense can also differentiate into other cell types under specific growth conditions. When growth conditions become limiting, such as under conditions of low nitrogen and high aeration (higher levels of aeration are due to vigorous shaking), azospirilla lose motility and their elongated shape to become round, finally forming large aggregates of non-motile cells known as "flocs". If these deleterious conditions persist, the flocculated cells will eventually form

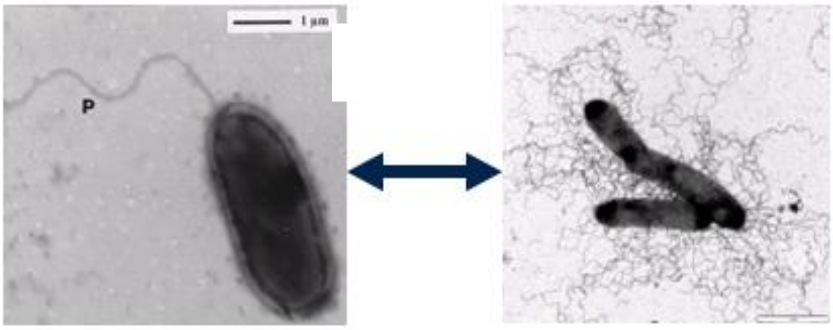

Figure 1. Polar and lateral flagella in *Azospirillum brasilense*. Electron micrographs showing polar flagella used for swimming (left) and lateral flagella used for swarming (right).

dessication-resistant cysts (46). Many cellular factors are known to play a role in floc formation (or "flocculation"), including exopolysaccharide (EPS) production and the presence of surface-exposed outer membrane proteins, such as lectins (13, 14, 17, 40, 46). Flocculation, and other key factors which affect this behavior, will be described in more detail in Chapter 2.

Chemotaxis and the A. brasilense *genome*

The genome of *A. brasilense*, strain Sp245, was recently sequenced (59). It consists of 1 chromosome, 3 "chromids", and 3 plasmids with a total genome size of 7.53 Mb. The term "chromid" has recently been coined to refer to regions of bacterial DNA previously known as "second chromosomes" or "megaplasmids", many of which encode key housekeeping genes (20). Analysis of the *A. brasilense* Sp245 genome has led to the identification of four chemotaxis-like pathways and 48 chemoreceptors known as methyl-accepting chemotaxis proteins (MCPs, chemoreceptors). The predicted functions of these chemotaxis-like pathways are based primarily on sequence homology to the closely related bacterium *Rhodospirillum centenum*. The predicted function for the Che1 pathway, based on sequence homology to the Che1 pathway of *R. centenum*, as well as by functional complementation of generally non-chemotactic mutants, was in the regulation of motility bias and chemotactic behavior (23); however, in Chapter 1, evidence are presented which shows that in addition to chemotaxis and motility behavior, other cellular functions are regulated by Che1 signaling. The Che2 pathway has a predicted function in flagellar biosynthesis, based on sequence homology to *R. centenum*, the only organism for which the homologous pathway has been experimentally characterized (9); whereas, the function for the Che3 pathway is predicted to be in cyst cell production, based on sequence homology to *R. centenum* (10). The Che4 pathway does not yet have a predicted or

experimentally determined role, but is currently under investigation in the Alexandre lab. A figure summarizing the four chemotaxis-like operons of *A. brasilense* is shown in Figure 2.

Taxis behaviors in *Azospirillum brasilense*

A. brasilense resides in the soil where it can colonize the roots of many cereals and grasses. Both soil and aquatic environments contain a highly diverse population of bacterial organisms which have developed various strategies in order to compete and survive in nutrient-limiting environments. Under these conditions, characteristics which lend a competitive advantage to the organisms are a must for survival. One such characteristic is taxis behavior. Taxis behaviors are generally described as the directed movement of a motile organism in response to a gradient of a particular environmental cue. For example, chemotaxis is a motile response to chemical gradients, phototaxis is the directed movement in gradients of light, aerotaxis, the movement in gradients of oxygen, and energy taxis is the directed movement of cells in gradient of cues that elicit changes in intracellular energy status (usually, metabolic cues) (53).

Taxis behaviors in *A. brasilense* have only been characterized in terms of polar-flagellum dependent motility (i.e. swimming behavior) thus far, despite this organism possessing a dual flagellar system. In fact, very little is known thus far about the role of chemotaxis in swarming behavior using lateral flagella, not just in *A. brasilense* but among other bacterial species as well. A recent review describes the role of chemotaxis in swarming behavior as being both "mysterious" and "controversial" in that although running and tumbling behaviors are not

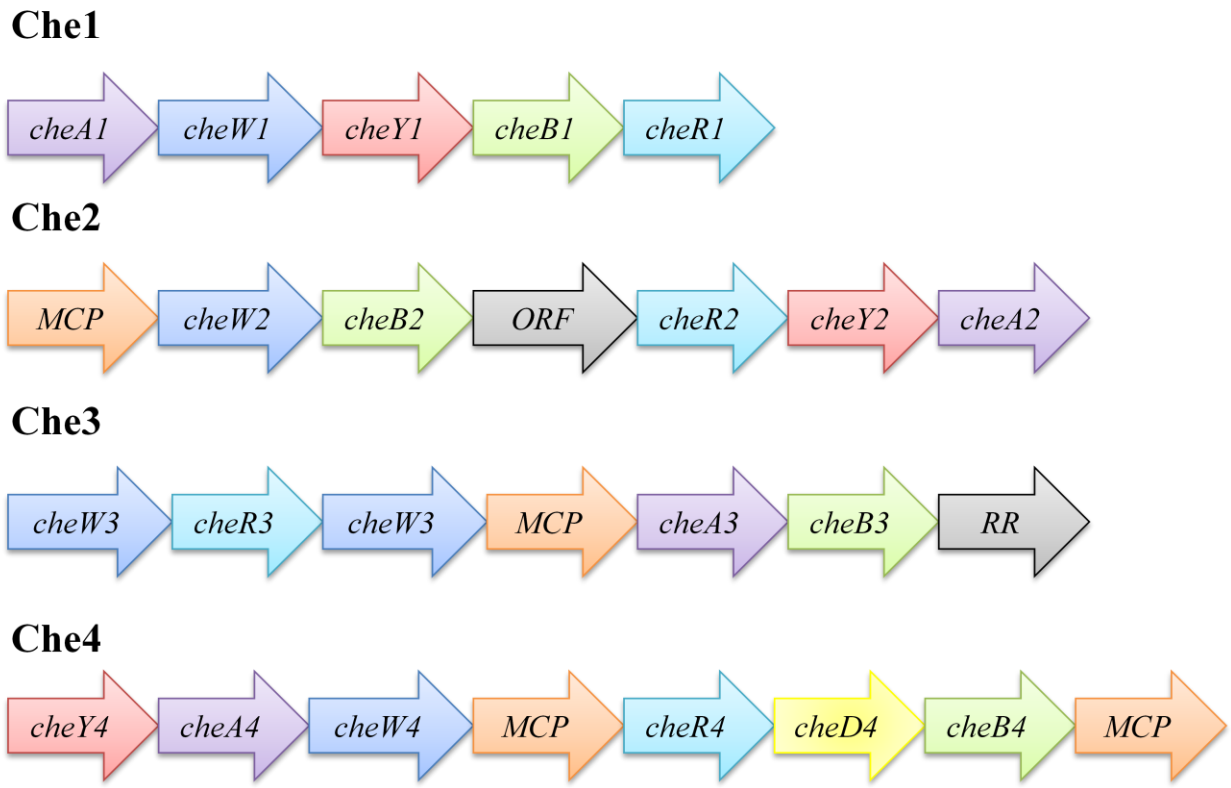

Figure 2. Chemotaxis operons of *Azospirillum brasilense*. Diagrams of the four chemotaxis operons of *A. brasilense* based on Wisniewski-Dye *et al.*, 2011 are shown above. Each gene is colored to facilitate identification within each operon. For example, *cheA* is purple, *cheW* is blue, etc. **Key**: CheA, histidine kinase. CheW, coupling protein. CheY, response regulator. CheB, methylesterase. CheR, methyltransferase. MCP, methyl-accepting chemotaxis proteins. RR, response regulator. ORF, open reading frame.

typically observed in swarming bacterial cells, mutations affecting chemotaxis can often affect these swarming capabilities (27). Although chemotaxis and chemotaxis-like pathways have not been shown to regulate the motility bias of lateral flagella, there are organisms such as *R. centenum* which possess a chemotaxis-like pathway (designated as Che2) which regulates flagella biosynthesis and mutations within this pathway were shown to affect swarming motility (9). Homology of the Che2 pathway of *A. brasilense* to the Che2 pathway of *R. centenum* would suggest that the *A. brasilense* Che2 pathway may also play a key role in regulating swarming motility; however, this has yet to be experimentally determined. Here, I will describe three different, yet related types of polar flagellum-dependent taxis behaviors in *A. brasilense*: chemotaxis, aerotaxis, and energy taxis.

Measuring bacterial taxis responses

One of the most common assays used for the study of chemotaxis in *E. coli* and *B. subtilis* is the capillary assay, first described by Julius Adler in 1973 (1). In this assay, a capillary filled with a chemical (either attractant or repellent) is placed into a suspension of cells and after a sufficient period of time, the capillary is then analyzed for the number of cells inside. The strength of the attractant is measured by the number of cells inside the capillary. Specifically, higher numbers of cells indicate stronger attractants. A significant problem with this assay is in measuring responses to repellents, for which other assays described later were developed (56). Another common assay is the swim-plate assay (or "swarm plate assay" or "soft agar plate assay") in which a petri dish containing minimal media prepared with a low percentage of agar (around 0.3%), compatible with bacterial swimming motility through the agar is supplemented with a chemical-of-interest. Motile bacteria are inoculated into the center of the

petri dish and as cells grow and nutrients are depleted at the point of inoculation and of initial growth, a gradient is established where chemotaxis (and thus swimming behavior) is required in order to move up the gradient of nutrients hence created. The swimming ring diameters (i.e. how far the cells have swum away from the inoculation point) are used as proxy for the taxis responses providing that growth is constant, i.e. larger ring diameters indicate a stronger attractant response. An example of cells analyzed using this assay is shown in Figure 3. Problems with this assay include confusing chemotaxis defects with growth or motility defects, or other behavioral issues, such as aggregation. Other common assays include the mini-plug agar assay and the temporal gradient assay, both of which work by a similar mechanism to the other chemotaxis assays described here. The mini-plug agar assay was first developed as a means of studying repellent responses, since other common assays like the capillary assay are not a good technique for quantitating "negative chemotaxis" (56). In this assay, a chemical that is to be tested is concentrated into a solid agar "plug" that is then placed in semi-solid media uniformly inoculated with bacteria. The chemical then diffuses away from the plug into the surrounding medium, creating a spatial concentration gradient of that chemical. In the case of an attractant, there will be an increase in cell density near the agar plug, but in the case of a repellent, a zone of clearing will be observed close to the plug. Although this assay can be useful in measuring chemotactic responses, a recent paper pointed out that this assay is also prone to false positives and recommended using non-chemotactic mutants as controls (32). The temporal gradient assay was developed as a means of finding an improved and more quantitative method for measuring attractant/repellent responses to a specific stimulus (33, 48, 55). In the temporal gradient assay, a chemical to be tested is added to a "pool" of cells and the frequency at which

cells tumble, as in the case of *E. coli*, is calculated. Repellents will increase the tumble frequency, whereas attractants will suppress the tumble frequency. Generally speaking, experts in the field of chemotaxis would agree that no one assay is sufficient to definitively determine chemotactic responses to specific cues. In fact, combinations of these assays are commonly used in order to arrive at conclusive and reliable results.

Chemotaxis behavior and plant association in Azospirillum

Early studies of chemotactic behavior in *A. brasilense* were performed with the plant-bacterium association in mind. Because *A. brasilense* was known to colonize the root surfaces of plants, it was anticipated, and later shown, that these bacteria would be chemotactic towards chemicals commonly found in plant root exudates, such as amino acids, organic acids, and sugars (6, 42). Interestingly, in these early studies of chemotactic behavior in *A. brasilense* using the capillary assay, it was found that *A. brasilense* was chemotactic towards water and phosphate buffer. Upon further study, it was determined that *A. brasilense* was actually attracted to the oxygen available in the water and phosphate buffer, indicating aerotactic behavior (5, 6, 42). In fact, the aerotactic response of *A. brasilense* was so strong, the capillary assay could not be used to assess chemotactic behavior due to an inability to differentiate between chemotaxis and aerotaxis responses. Therefore, the initial studies of chemotaxis behavior were performed using the swim plate assays (6) and later supplemented with the mini-plug agar and temporal gradient assays (2, 65, 66). Analysis of chemicals as attractants were carried out using three methods: semi-solid swarm plates, the miniplug assay, and the temporal gradient assay. Results from all three methods were analyzed in order to classify each chemical as being strong, moderate, or weak attractants. The best chemo-attractants were found to be organic acids (such as malate,

succinate, and pyruvate) and fructose, while sugars such as galactose, ribose, and arabinose as well as amino acids such as aspartate, glutamate, and asparagine were moderate chemoeffectors (2). However, most amino acids had little or no effect on chemotaxis behavior (2). It was observed that there was a correlation between the efficiency of chemicals as growth substrates with their efficiency as attractants, and substrates which were poor for growth were also poor for inducing chemotaxis responses. For a more comprehensive list of attractants and details about the respective chemotactic responses, see Alexandre *et al*., 2000 (2). Interestingly, within the family of azospirilla sp., different strains are attracted to different chemicals and a correlation between the type of plants (and root exudates) that the isolates were obtained from and the chemotactic response suggested a type of chemotactic "specificity" dependent upon the environment that the isolates dwelled in (44). For example, it was found that azospirilla strains isolated from C4 plants such as maize, were strongly attracted to organic acids like malate alone, which is commonly produced by these plant roots. On the other hand, azospirilla isolated from wheat roots were attracted to both sugars and organic acids. Taken together, it was suggested that this specificity towards particular root exudates is likely an adaptive response of these bacteria based upon the environment from which they were isolated (44).

Aerotaxis, the strongest behavioral response in Azospirillum

As mentioned earlier, it was discovered while performing capillary assays to measure chemotaxis that *A. brasilense* is highly aerotactic (5). Aerotaxis behavior is described as the directed movement of a bacterial cell to a favorable oxygen gradient. The definition of a "favorable" oxygen gradient depends on the bacteria itself. For instance, *Bacillus subtilis* is an obligate aerobe and prefers a 200 µM oxygen concentration (58), while *Escherichia coli* is a

facultative anaerobe and prefers a 50 µM oxygen concentration (53). *Azospirillum brasilense* is a microaerophilic organism and prefers an oxygen concentration of approximately 4 µM, under which conditions energy production and nitrogen fixation are optimal (67). The initial aerotaxis assays that were performed in *A. brasilense* used the capillary assay, as described by J. Adler (1). Since then, aerotaxis assays have been performed by collecting cells in a small capillary tube and observing the formation of an aerotactic band near the air-liquid interface (meniscus), at the desired oxygen concentration, using microscopy (67). An example of this type of assay is shown in Figure 3. In this assay, it takes approximately 0.5 to 3 minutes to form a distinct aerotactic band that is 400-900 µm from the meniscus (67).

Energy taxis is a dominant locomotor behavior in Azospirillum

A discussion of taxis behaviors in *A. brasilense* would not be complete without describing energy taxis, which is considered as the "dominant behavior in *Azospirillum brasilense*" (2). Energy taxis relies heavily on both chemotactic and aerotactic behaviors. Energy taxis could be summarized as taxis behavior that results in the movement of cells to the most energetically favorable environments, i.e., to local positions in gradients where energy generation is maximum. A key question to the study of chemotaxis is ***how*** this energy is sensed. Some ways that intracellular energy may be sensed is in the form of proton motive force, changes in pH or membrane potential, or in the rate of electron transport (4, 53, 67). Energy taxis in *A. brasilense* takes place in the form of aerotaxis, as well as chemotaxis to various electron donors and acceptors (2). The dominance of energy taxis in *A. brasilense* was clearly

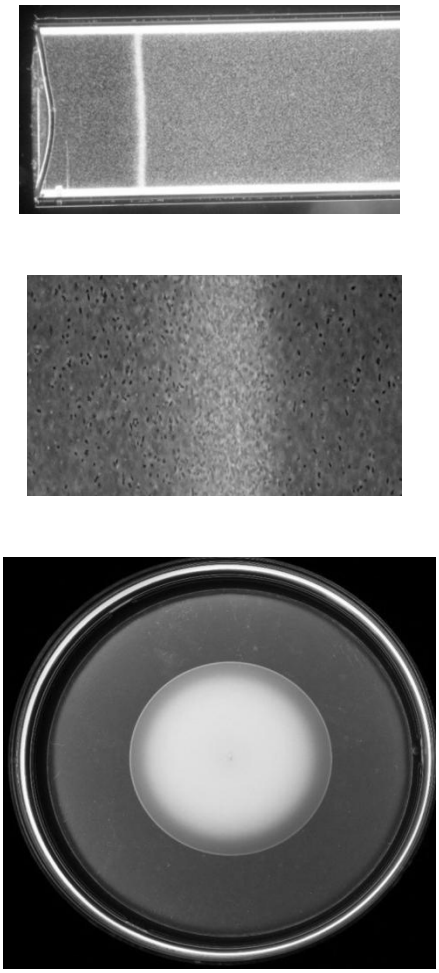

Figure 3. Taxis behaviors in *Azospirillum brasilense*. (Top) Aerotactic band of cells in a capillary tube (dark-field microscopy at 40X magnification). (Middle) Aerotactic band of cells in a capillary tube (phase-contrast microscopy at 400X magnification). (Bottom) Semi-solid agar plate showing chemotactic behavior.

shown in the use of metabolic inhibitors that resulted in a repellent response, such as myxothiazol which affects the cytochrome bc_1 complex while chemicals which bypassed cytochrome bc_1, such as TMPD (N,N,N',N'-tetramethyl-*p*-phenylenediamine) resulted in an attractant response (2). A mutant lacking the *cbb3* cytochrome (FAJ851) was affected in both aerotaxis and chemotaxis, further supporting these results (2). Although the mechanistic details behind how intracellular energy levels are detected remains largely unclear, research has pointed to two chemoreceptors thus far in *A. brasilense* which have been shown to play a role in measuring intracellular energy levels, Tlp1 and AerC (18, 60). The Tlp1 chemoreceptor was shown to measure parameters associated with the electron transport system, although the details surrounding how Tlp1 measures such parameters are not yet clear (18). AerC, on the other hand, is similar to Aer from *E. coli*, with the differences being that AerC from *A. brasilense* possesses two PAS domains while Aer from *E. coli* contains only one PAS domain (60). The PAS domains of both Aer and AerC have been shown to bind flavin adenine dinucleotide (FAD) as a means of measuring internal cellular energy, and are then able to pass this signal along to the chemotaxis signal transduction pathway (which will be described below) (3, 11, 45, 60).

In summary, these taxis behaviors (chemotaxis, aerotaxis, and energy taxis) in *A. brasilense* provide this bacterium with an amazing capability of finding plant roots to colonize at the most optimal oxygen concentration for nitrogen fixation (providing the plants with a source of nitrogen), as well as finding the best possible location within the rhizosphere for survival, which together provides *A. brasilense* with a powerful competitive edge against other bacteria in its environment.

Molecular Mechanisms of Chemotaxis

The Escherichia coli *prototypical chemotaxis signal transduction system*

As explained previously, bacterial chemotaxis can take place in the form of swimming towards attractants, such as nutrients, or away from repellents, such as toxins. Bacterial chemotaxis has been best characterized in the gram-negative bacteria *Escherichia coli*. In the absence of chemical gradients, cells exhibit a "random walk" type of motility (8). A "random walk" motility consists of alternating "runs" (smooth swimming without changes in direction) and "twiddles" or "tumbles" in *E. coli*, or "reversals" in *A. brasilense* (66). Without stimulation, cells will swim in a "run" pattern and randomly "twiddle", "tumble", or "reverse". However, upon stimulation by an attractant, the chemotaxis machinery will suppress changes in swimming direction; but, in the presence of a repellent, signaling via the chemotaxis proteins will result in an increase in tumbling, or any other behavior which results in a change of swimming direction (8).

At the molecular level, chemotaxis takes place using a conserved set of dedicated chemotaxis proteins which comprise a two-component signal transduction pathway (for a review, see 57). In *E. coli*, signals are received by chemoreceptors known as methyl-accepting chemotaxis proteins (MCPs). Upon signal perception by these MCPs, conformational changes take place that are sensed by the histidine kinase, CheA, via interactions with the adaptor protein CheW. CheA is then autophosphorylated at a conserved histidine residue and can then phosphorylate the response regulator, CheY, at a conserved aspartate site, Asp57 (47). The phosphorylated CheY can then bind the flagellar motor, FliM, in order to change the direction of

rotation from counter-clockwise to clockwise. Because *E. coli* is peritrichously flagellated (meaning that it possesses multiple flagella that are located around the cell), counter-clockwise rotation of the flagella results in the formation of a flagellar bundle that allows the cell to swim forward. However, when the rotation of the flagella is changed to clockwise, the flagellar bundle comes apart resulting in a tumble (flagella behavior is also described in 8). Repellents in *E. coli* result in activation of the chemotaxis signal transduction pathway and result in cell tumbling and ultimately a change in swimming direction, whereas attractants suppress activation of the chemotaxis signal transduction pathway, resulting in a smoother swimming pattern. CheA can also phosphorylate the methylesterase, CheB. CheB, along with the methyltransferase CheR, functions to add and remove methyl groups from the MCPs in order to "reset" them to receive new signals (for a review, see 57). In recent years, the use of antibodies, fluorescent protein labels, and cryo-electron microscopy has facilitated localization studies for chemotaxis proteins in many bacterial organisms. Such studies have shown that MCPs, which associate in arrays of trimers of dimers, are commonly (but not exclusively) found at the cell pole in several organisms (7, 12, 64). Because CheW binds to both CheA and MCPs, CheW and CheA are also typically found at the cell pole. CheY binds to both CheA at the cell pole, as well as its target (the flagellar motor in *E. coli*, for example, which is also located at the cell pole).

Diversity in chemotaxis signal transduction systems

Analysis of completely sequenced bacterial genomes has indicated that many bacterial organisms, particularly those from soil and aquatic environments, possess more than one chemotaxis-like signal transduction pathway (51, 68). For example, *Myxococcus xanthus*

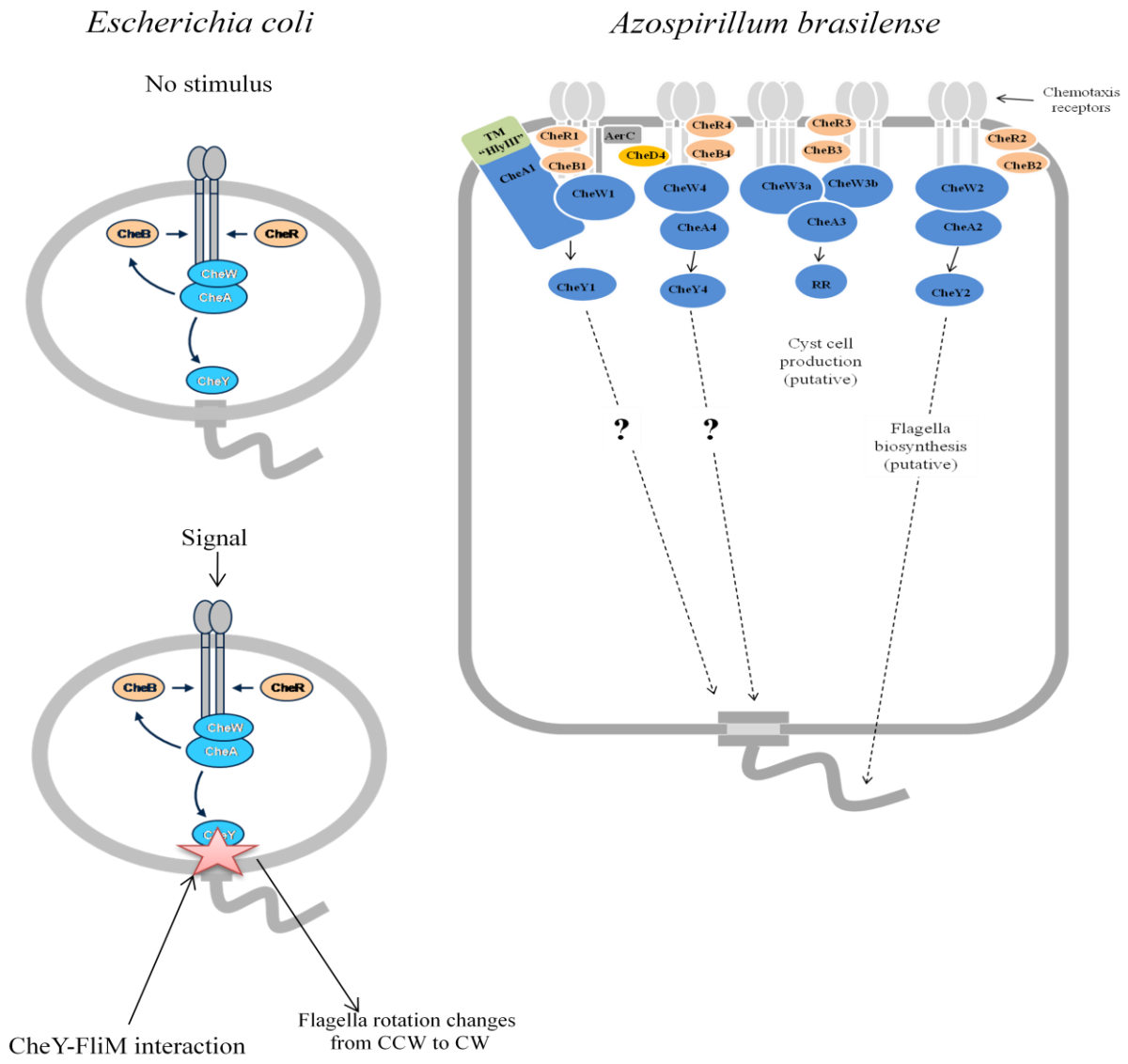

Figure 4. Chemotaxis signal transduction pathway(s) in *Escherichia coli* and *Azospirillum brasilense*. In the *E. coli* model (top), the image on the left represents a cell that has no stimulus. The image on the right shows what takes place upon signal perception. The red star represents a protein-protein interaction between CheY and the flagellar motor, FliM, in order to induce a switch in flagellar rotation from counter-clockwise to clockwise. In the *A. brasilense* model (bottom), based on homology with *R. centenum* and experiments where the Che1 pathway complemented for chemotaxis behavior in non-chemotactic mutants, it is expected that CheY1 will interact with the flagellar motor, as well. Also shown are the predicted outputs of Che2 and Che3, as well as a possible function for Che4. Arrows are not shown for phosphorylation of CheB by CheA, or methylation/demethylation of chemoreceptors by CheB, CheR, or CheD.

possesses eight chemotaxis-like pathways and *Rhodospirillum centenum* has three chemotaxis-like pathways (26, 69) and many of these chemotaxis-like pathways deviate from the *E. coli* paradigm in that they regulate behaviors other than swimming motility (30). Some examples include the Wsp signal transduction pathway in *Pseudomonas aeruginosa* which regulates biofilm formation (25), the Dif pathway in *Myxococcus xanthus* which regulates exopolysaccharide (EPS) production (62), and the Che2 pathway of *Rhodospirillum centenum* which regulates flagellar expression (9). Although the functions of many of these pathways have been characterized, the mechanism(s) by which they take place remain poorly understood.

Although the general consensus is that chemosensory pathways are "wired" in order to avoid any means of cross-talk among these pathways (31), some recent studies have suggested a mechanism for cross-talk between chemotaxis-like pathways. One such example includes the Dif and Frz systems of *Myxococcus xanthus* which sense phosphatidylethanolamine and signals perceived by the Dif pathway can modulate proteins within the Frz pathway (61). The mechanism of cross-talk here happens when signals perceived by DifA affect methylation of the FrzCD receptors which can then activate the Frz pathway. Because much of the current research in bacterial chemotaxis focuses on organisms such as *Escherichia coli* or *Bacillus subtilis*, each of which possess only a single chemotaxis pathway, it is not surprising that this type of cross-talk has not yet been characterized in other organisms. However, given the prevalence of organisms with multiple chemotaxis-like pathways and numerous methyl-accepting chemotaxis proteins, the identification of such mechanisms of cross-talk among chemotaxis-like pathways in the future are likely.

A. brasilense chemotaxis signal transduction and regulation of multiple cellular behaviors

The subject of my dissertation research is the Che1 chemotaxis-like pathway of *A. brasilense*. Previous work in the study of chemotaxis in *A. brasilense* has shown that energy taxis is a dominant behavior for this organism, and other taxis behaviors of *A. brasilense* are likely influenced by energy taxis (2). Earlier studies that looked into the motility of *A. brasilense* and the role of chemoreceptor methylation in these motility behaviors suggested that chemotaxis in *A. brasilense* takes place using a methylation-independent system of chemotaxis (66). In methylation-independent chemotaxis, sugars are transported across the membrane by the phosphoenolpyruvate (PEP) carbohydrate phosphotransferase system (PTS) and the phosphorylation state of key enzymes (Enzyme I and HPr) of this pathway can affect the phosphorylation status of CheA, which can then signal through the chemotaxis signal transduction pathway (3). In further studies of chemotaxis in *A. brasilense*, chemical mutagenesis was utilized in order to generate the generally non-chemotactic mutants IZ15 and IZ21 and complementation of these mutants resulted in the identification of the Che1 set of genes from *A. brasilense*, indicating that the Che1 pathway regulates chemotaxis and motility behavior in this organism (23).

Role of methylation via CheB and CheR in the A. brasilense *Che1 pathway*

The Che1 operon of *A. brasilense* possesses both a CheB and a CheR homolog (Figure 2). The presence of CheB and CheR in this operon was surprising given that prior research had suggested that chemotaxis in *A. brasilense* takes place primarily via a methylation-independent mechanism (66); however, the presence of a CheB and a CheR would seem to contradict this

conclusion. In order to determine whether CheB and CheR function in a methylation-dependent chemotaxis mechanism, first mutants were generated lacking CheB, CheR, CheB-CheR (a double mutant), or Che1 (the entire operon) in order to analyze swimming behavior in response to various cues. Next, a methanol release assay (a common assay for measuring the activity of CheB and CheR adaptation proteins on chemoreceptors by measuring the release of methanol as a result of CheB activity) was utilized to measure the activity of CheB and CheR. Intriguingly, it was found that the motility bias in mutants lacking either CheB or CheR was highly variable dependent on the substrate present (50), whereas in the model organism *E. coli*, the swimming behavior in mutants that lack CheB is always "tumbly" (63) and in mutants that lack *cheR* is always "smooth" (49). It was also found that addition of some chemoeffectors resulted in methanol release, while the removal of others also resulted in methanol release (50). The results from this assay were unlike those of any other organism studied thus far. In the model organism, *E. coli*, methanol release is observed upon removal of an attractant (28) and in *B. subtilis*, both addition and removal of attractant results in methanol release (29, 54). However, *Rhodobacter sphaeroides*, an organism shown to exhibit methylation-independent (or metabolism-dependent) chemotaxis (43), as was suggested for *A. brasilense*, was shown to release methanol only upon addition of attractant (34). The methanol release profile for *A. brasilense* was different from organisms that exhibit primarily methylation-dependent chemotaxis and organisms that exhibit methylation-independent chemotaxis, suggesting that (i) *A. brasilense* utilizes both methylation-dependent and methylation-independent chemotaxis, and (ii) based on mutant phenotypes, there may be other receptor methylation/demethylation systems and/or other Che pathways at work in *A. brasilense* (50).

The results described above suggest that the mechanisms governing chemotaxis in *A. brasilense* are complex and do not follow the paradigm of model organisms such as *E. coli* or *B. subtilis*. Adding to the complexity of this behavior, it was also observed that a mutant where the entire Che1 operon was deleted did not result in a null chemotaxis phenotype, as expected (50). Taken together, these results suggested the possibility that another Che pathway in *A. brasilense* primarily regulates chemotaxis behavior, where Che1 could modulate chemotaxis behavior indirectly by affecting the methylation status of receptors. These modified receptors could then signal through another Che pathway which is responsible for regulating chemotaxis behavior. In an attempt to address these questions, mutants were generated lacking *cheA* and *cheY* from the Che1 operon to determine the role of these two proteins in the chemotactic behavior of *A. brasilense*. Based on previous studies suggesting that Che1 primarily regulated chemotaxis behavior (23), it was expected that mutations affecting *cheA* or *cheY* would result in a null chemotaxis phenotype; however, this was not so (Chapter 1). These results were the beginning of what would be (and what will continue to be) an interesting story with the central questions in mind: (i) If this operon does not directly regulate motility behavior, what does it regulate? and (ii) Is there another operon in this organism that is primarily responsible for the regulation of motility behavior? This is the point at which my dissertation project was initiated with the goal of identifying a role for this chemotaxis operon in *A. brasilense* and then to identify the molecular mechanism(s) by which this operon is able to regulate certain cellular behaviors.

Introduction

References

1. **Adler, J.** 1973. A method for measuring chemotaxis and use of the method to determine optimum conditions for chemotaxis by *Escherichia coli*. J. Gen. Microbiol. **74**: 77-91.

2. **Alexandre, G., Greer, S. E., Zhulin, I. B.** 2000. Energy taxis is the dominant behavior in *Azospirillum brasilense*. J. Bacteriol. **182**: 6042-6048.

3. **Alexandre, G., Zhulin, I. B.** 2001. More than one way to sense chemicals. J. Bacteriol. **183**: 4681-4686.

4. **Alexandre, G., Greer-Phillips, S., Zhulin, I. B.** 2004. Ecological role of energy taxis in microorganisms. FEMS Micro. Rev. **28**: 113-126.

5. **Barak, R., Nur, I., Okon, Y., Henis, Y.** 1982. Aerotactic response of *Azospirillum brasilense*. J. Bacteriol. **152**: 643-649.

6. **Barak, R., Nur, I., Okon, Y.** 1983. Detection of chemotaxis in *Azospirillum brasilense*. J. Appl. Bacteriol. **53**: 399-403.

7. **Bardy, S. L., Maddock, J. R.** 2005. Polar localization of a soluble methyl-accepting protein of *Pseudomonas aeruginosa*. J. Bacteriol. **187**: 7840-7844.

8. **Berg, H. C., Brown, D. A.** 1972. Chemotaxis in *Escherichia coli* analyzed by three-dimensional tracking. Nature. **239**: 500-504.

9. **Berleman, J. E., Bauer, C. E.** 2005. A *che*-like signal transduction cascade involved in controlling flagella biosynthesis in *Rhodospirillum centenum*. Mol. Micro. **55**: 1390-1402.

10. **Berleman, J. E., Bauer, C. E.** 2005. Involvement of a *che*-like signal transduction cascade in regulating cyst cell development in *Rhodospirillum centenum*. Mol. Micro. **56**: 1457-1466.

11. **Bibikov, S. I., Barnes, L. A., Gitin, Y., Parkinson, J. S.** 2000. Domain organization and flavin adenine dinucleotide-binding determinants in the aerotaxis signal transducer Aer of *Escherichia coli*. Proc. Natl. Acad. Sci. USA. **97**: 5830–5835.

12. **Briegel, A., Ortega, D. R., Tocheva, E. I., Wuichet, K., Li, Z., Chen, S., Müller, A., Iancu, C. V., Murphy, G. E., Dobro, M. J., Zhulin, I. B., Jensen, G. J.** 2009. Universal architecture of bacterial chemoreceptor arrays. Proc. Natl. Acad. Sci. USA. **106**: 17181-17186.

13. **Burdman, S., Jurkevitch, E., Schwartsburd, B., Hampel, M., Okon, Y.** 1998. Aggregation in *Azospirillum brasilense*: effects of chemical and physical factors and involvement of extracellular components. Microbiology. **144**: 1989-1999.

14. **Burdman, S., Jurkevitch, E., Soria-Diaz, M. E., Serrano, A. M., and Okon, Y.** 2000. Extracellular polysaccharide composition of *Azospirillum brasilense* and its relation to cell aggregation. FEMS Microbiol. Lett. **189**: 259-264.

15. **Clayton, R. K.** 1958. On the interplay of environmental factors affecting taxis and motility in *Rhodospirillum rubrum*. Arch. Microbiol. **29**: 189-212.

16. **Croes, C. L., Moens, S., Bastelaere, E. V., Vanderleyden, J., Michiels, K. W.** 1993. The polar flagellum mediates *Azospirillum brasilense* adsorption to wheat roots. J. Gen. Microbiol. **139**: 2261-2269.

17. **Del Gallo, M., Negi, M., Neyra, C. A.** 1989. Calcofluor- and lectin-binding exocellular polysaccharides of *Azospirillum brasilense* and *Azospirillum lipoferum*. J. Bacteriol. **171**: 3504-3510.

18. **Greer-Phillips, S. E., Stephens, B. B., Alexandre, G.** 2004. An energy taxis transducer promotes root colonization by *Azospirillum brasilense*. **186**: 6595-6604.

19. **Grishanin, R. N., Chalmina, I. I., Zhulin, I. B.** 1991. Behaviour of *Azospirillum brasilense* in a spatial gradient of oxygen and in a 'redox' gradient of an artificial electron acceptor. J. Gen. Microbiol. **137**: 2781-2785.

20. **Harrison, P. W., Lower, R. P., Kim, N. K., Young, J. P.** 2010. Introducing the bacterial 'chromid': not a chromosome, not a plasmid. Trends Microbiol. **18**: 141–148.

21. **Harshey, R. M., Matsuyama, T.** 1994. Dimorphic transition in *Escherichia coli* and *Salmonella typhimurium*: surface-induced differentiation into hyperflagellate swarmer cells. Proc. Natl. Acad. Sci. USA. **92**: 8631-8635.

22. **Hartmann, A., Zimmer, W.** 1994. Physiology of *Azospirillum*, p. 15-39. In Y. Okon (ed.), *Azospirillum*/plant associations. CRC Press, Boca Raton, Fla.

23. **Hauwaerts, D., Alexandre, G., Das, S. K., Vanderleyden, J., Zhulin, I. B.** 2002. A major chemotaxis gene cluster in *Azospirillum brasilense* and relationships between chemotaxis operons in α-proteobacteria. FEMS Microbiol. Letters. **208**: 61-67.

24. **Hall, P. G., Krieg, N. R.** 1983. Swarming of *Azospirillum brasilense* on solid media. Can. J. Microbiol. **29**: 1592-1594.

25. **Hickman, J. W., Tifrea, D. F., Harwood, C. S.** 2005. A chemosensory system that regulates biofilm formation through modulation of cyclic diguanylate levels. Proc. Natl. Acad. Sci. USA. **102**: 14422-14427.

26. **Jiang, Z. Y., Gest, H., Bauer, C. E.** 1997. Chemosensory and photosensory perception in purple photosynthetic bacteria utilize common signal transduction components. J. Bacteriol. **179**: 5720-5727.

27. **Kearns, D. B.** 2010. A field guide to bacterial swarming motility. Nature Rev. Microbiol. **8**: 634-644.

28. **Kehry, M. R., Doak, T. G., Dahlquist, F. W.** 1984. Stimulus-induced changes in methylesterase activity during chemotaxis in *Escherichia coli*. J. Biol. Chem. **259**: 11828-11835.

29. **Kirby, J. R., Kristich, J. S., Feinberg, S. L., Ordal, G. W.** 1997. Methanol production during chemotaxis to amino acids in *Bacillus subtilis*. Mol. Microbiol. **24**: 869-878.

30. **Kirby, J. R.** 2009. Chemotaxis-like regulatory systems: unique roles in diverse bacteria. Annu. Rev. Microbiol. **63**: 45-59.

31. **Laub, M. T., Goulian, M.** 2007. Specificity in two-component signal transduction pathways. Annu. Rev. Genet. **41**: 121-145.

32. **Li, J., Go, A. C., Ward, M. J., Otteman, K. M.** 2010. The chemical-in-plug bacterial chemotaxis assay is prone to false positive responses. BMC Res. Notes. **3**: 77.

33. **Macnab, R., Koshland, D. E., Jr.** 1972. The gradient-sensing mechanism in bacterial chemotaxis. Proc. Natl. Acad. Sci. USA. **69**: 2509-2512.

34. **Martin, A. C., Wadhams, G. H., Shah, D. S., Porter, S. L., Mantotta, J. C., Craig, T. J., Verdult, P. H., Jones, H., Armitage, J. P.** 2001. CheR- and CheB-dependent chemosensory adaptation system of *Rhodobacter sphaeroides*. J. Bacteriol. **183**: 7135-7144.

35. **McCarter, L. L., Silverman, M.** 1990. Surface-induced swarmer cell differentiation of *Vibrio parahaemolyticus*. Mol. Microbiol. **4**: 1057-1062.

36. **McCarter, L. L.** 2004. Dual flagellar systems enable motility under different circumstances. J. Mol. Microbiol. Biotechnol. **7**: 18-29.

37. **Merino, S., Shaw, J. G., Tomás, J. M.** 2006. Bacterial lateral flagella: an inducible flagella system. FEMS Microbiol. Letters. **263**: 127-135.

38. **Mobley, H. L., Belas, R.** 1995. Swarming and pathogenicity of *Proteus mirabilis* in the urinary tract. Trends Microbiol. **3**: 280-284.

39. **Moens, S., Michiels, K., Vanderleyden, J.** 1995. Glycosylation of the flagellin of the polar flagellum of *Azospirillum brasilense*, a gram-negative nitrogen-fixing bacterium. Microbiology. **141**: 2651-2657.

40. **Mora, P., F. Rosconi, L. Franco Franguas, and Susana-Sowinski.** 2008. *Azospirillum brasilense* Sp7 produces an outer-membrane lectin that specifically binds to surface-exposed extracellular polysaccharide produced by the bacterium. Arch. Microbiol. **189**: 519-524.

41. **Okon, Y., Houchins, J. P., Albrecht, S. L., Burris, R. H.** 1977. The growth of *Spirillum lipoferum* at constant partial pressures of oxygen and the properties of nitrogenase in cell free extracts. J. Gen. Microbiol. **98**: 87-93.

42. **Okon, Y., Cakmakci, L., Nur, I., Chet, I.** 1980. Aerotaxis and chemotaxis of *Azospirillum brasilense*: a note. Microb. Ecol. **6**: 277-280.

43. **Poole, P. S., Smith, M. J., Armitage, J. P.** 1993. Chemotactic signalling in *Rhodobacter sphaeroides* requires metabolism of attractants. J. Bacteriol. **175**: 291-294.

44. **Reinhold, B., Hurek, T., Fendrik, I.** 1985. Strain-specific chemotaxis of *Azospirillum* spp. J. Bacteriol. **162**: 190-195.

45. **Repik A., Rebbapragada, A., Johnson, M. S., Haznedar, J. O., Zhulin, I. B., Taylor, B. L.** 2000. PAS domain residues involved in signal transduction by the Aer redox sensor of *Escherichia coli*. Mol. Microbiol. **36**: 806–816.

46. **Sadasivan, L., Neyra, C. A.** 1985. Flocculation in *Azospirillum brasilense* and *Azospirillum lipoferum*: exopolysaccharides and cyst formation. J. Bacteriol. **163**: 716-723.

47. **Sanders, D. A., Gillece-Castro, B. L., Stock, A. M., Burlingame, A. L., Koshland, D. E., Jr.** 1989. Identification of the site of phosphorylation of the chemotaxis response regulator, CheY. J. Biol. Chem. **264**: 21770-21778.

48. **Spudich, J. L., Koshland, D. E., Jr.** 1975. Quantitation of the sensory response in bacterial chemotaxis. Proc. Natl. Acad. Sci. USA. **72**: 710-713.

49. **Springer, W. R., Koshland, D. E., Jr.** 1977. Identification of a protein methyltransferase as the *cheR* gene product in the bacterial sensing system. Proc. Natl. Acad. Sci. USA. **99**: 123-127.

50. **Stephens, B. B., Loar, S. N., Alexandre, G.** 2006. Role of CheB and CheR in the complex chemotactic and aerotactic pathway of *Azospirillum brasilense*. J. Bacteriol. **188**: 4759-4768.

51. **Szurmant, H., and G. H. Ordal.** 2004. Diversity in chemotaxis mechanisms among the bacteria and archaea. Microbiol. Mol. Biol. Rev. **68**: 301-319.

52. **Tarrand, J. J., Krieg, N. R.** 1978. A taxonomic study of the *Spirillum lipoferum* group, with descriptions of a new genus, *Azospirillum* gen. nov. and two species, *Azospirillum lipoferum* (Beijerinck) comb. nov. and *Azospirillum brasilense* sp. nov. Can. J. Microbiol. **24**: 967-980.

53. **Taylor, B. L., Zhulin, I. B., Johnson, M. S.** 1999. Aerotaxis and other energy-sensing behavior in bacteria. Annu. Rev. Microbiol. **53**: 103-128.

54. **Thoelke, M. S., Kirby, J. R., Ordal, G. W.** 1989. Novel methyl transfer during chemotaxis in *Bacillus subtilis*. Biochemistry. **28**: 5585-5589.

55. **Tsang, N., Macnab, R., Koshland, D. E., Jr.** 1973. Common mechanism for repellents and attractants in bacterial chemotaxis. Science. **181**: 60-63.

56. **Tso, W., Adler, J.** 1974. Negative chemotaxis in *Escherichia coli*. J. Bacteriol. **118**: 560-576.

57. **Wadhams, G.H., Armitage J. P.** 2004. Making sense of it all: bacterial chemotaxis. Nat. Rev. Mol. Cell Biol. **5**: 1024-1037.

58. **Wong, L. S., Johnson, M. S., Zhulin, I. B., Taylor, B. L.** 1995. Role of methylation in aerotaxis in *Bacillus subtilis*. J. Bacteriol. **177**: 3985-3991.

59. **Wisniewski-Dye, F., Borziak, K., Khalsa-Moyers, G., Alexandre, G., Sukharnikov, L.O., Wuichet, K., Hurst, G.B., McDonald, W.H., Robertson, J.S., Barbe, V., Calteau, A., Rouy, Z., Mangenot, S., Prigent-Combaret, C., Normand, P., Boyer, M., Siguier, P., Dessaux, Y., Elmerich, C., Condemine, G., Krishnen, G., Kennedy, I., Paterson, A.H., Gonzalez, V., Mavingui, P., Zhulin, I.B.** 2011. *Azospirillum* genomes reveal transition of bacteria from aquatic to terrestrial environments. PLoS Genetics **7**: e1002430.

60. **Xie, Z., Ulrich, L. E., Zhulin, I. B., Alexandre, G.** 2010. PAS domain containing chemoreceptor couples dynamic changes in metabolism with chemotaxis. Proc. Natl. Acad. Sci. **107**: 2235-2240.

61. **Xu, Q., Black, W. P., Cadieux, C. L., Yang, Z.** 2008. Independence and interdependence of Dif and Frz chemosensory pathways in *Myxococcus xanthus* chemotaxis. Mol. Microbiol. **69**: 714-723.

62. **Yang, Z., Ma, X., Tong, L., Kaplan, H. B., Shimkets, L. J., Shi, W.** 2000. *Myxococcus xanthus dif* genes are required for biogenesis of cell surface fibrils essential for social gliding motility. J. Bacteriol. **182**: 5793–5798.

63. **Yonekawa, H., Hayashi, H., Parkinson, J. S.** 1983. Requirement of the *cheB* function for sensory adaptation in *Escherichia coli*. J. Bacteriol. **156**: 1228-1235.

64. **Zhang, P., Khursigara, C. M., Hartnell, L., Subramaniam, S.** 2007. Direct visualization of *Escherichia coli* chemotaxis receptor arrays using cryo-electron microscopy. Proc. Natl. Acad. Sci. USA. **104**: 3777-3781.

65. **Zhulin, I. B., Tretyakova, S. E., Ignatov, V. V.** 1988. Chemotaxis of *Azospirillum brasilense* towards compounds typical of plant root exudates. Folia Microbiol. **33**: 277-280.

66. **Zhulin, I. B., Armitage, J. P.** 1993. Motility, chemokinesis, and methylation-independent chemotaxis in *Azospirillum brasilense*. J. Bacteriol. **175**: 952-958.

67. **Zhulin, I. B., Bespalov, V. A., Johnson, M. S., Taylor, B. L.** 1996. Oxygen taxis and proton motive force in *Azospirillum brasilense*. J. Bacteriol. **178**: 5199-5204.

68. **Zhulin, I. B.** 2001. The superfamily of chemotaxis transducers: from physiology to genomics and back. Adv. Microbiol. Physiol. **45**: 157-198.

69. **Zusman, D. R., Scott, A. E., Yang, Z., Kirby, J. R.** 2007. Chemosensory pathways, motility and development in *Myxococcus xanthus*. Nature Rev. Microbiol. **5**: 862-872.

Chapter 1

Function of a chemotaxis-like signal transduction pathway in modulating motility, cell clumping, and cell length in the alphaproteobacterium *Azospirillum brasilense*

Disclosure

Chapter 1 is reproduced in part with permission from Amber N. Bible; Bonnie B. Stephens; Davi R. Ortega; Zhihong Xie; Gladys Alexandre. "Function of a chemotaxis-like signal transduction pathway in modulating motility, cell clumping, and cell length in the alphaproteobacterium *Azospirillum brasilense*". *Journal of Bacteriology*, 2008. 190 (19): 6365-6375.

In this article, Dr. Gladys Alexandre is the principal investigator from whom guidance and experimental advice was obtained. Bonnie B. Stephens and Dr. Gladys Alexandre generated the Δ*cheA1* (AB101), Δ(*cheB1cheR1*) (BS104), and Δ*cheY1* (AB102) mutants and performed the aerotaxis assays, reversal frequency and cell length measurements (while fluorescent staining of cells for cell length measurements and measurements of complemented strains were my own work), as well as flocculation assays. Davi R. Ortega performed the nutrient uptake calculations based on cell length. Dr. Zhihong Xie generated the Δ*che1* (AB103) mutant and in collaboration with Dr. Gladys Alexandre generated the complementation constructs for the Δ*cheA1* (AB101), Δ(*cheB1cheR1*) (BS104), and Δ*cheY1* (AB102) mutants. All other work was my own.

Abstract

A chemotaxis signal transduction pathway (thereafter named Che1) has been previously identified in the alpha-proteobacterium *Azospirillum brasilens*e. Previous experiments have demonstrated that although mutants lacking CheB and/or CheR homologs from this pathway are defective in chemotaxis, a mutant in which the entire chemotaxis pathway has been mutated displayed a chemotaxis phenotype mostly similar to that of the parent strain, suggesting that the primary function of this Che1 pathway is not the control of motility behavior. Here, we report that mutants carrying defined mutations in the *cheA1* (AB101) and the *cheY1* (AB102) genes and a newly constructed mutant lacking the entire operon (Δ(*cheA1-cheR1)::Cm,* AB103) were defective, but not null, for chemotaxis and aerotaxis and had a minor defect in swimming pattern. We found that mutations in genes of the Che1 pathway affected the cell length of actively growing cells, but not their growth rate. Mutants lacking functional *cheB1* and *cheR1* genes (BS104) were significantly longer than the wild type, whereas cells of mutants impaired in the *cheA1* or *cheY1* genes, as well as a mutant lacking a functional Che1 pathway were significantly shorter than the wild type. Both the modest chemotaxis defects and the observed differences in cell length could be complemented by expressing the wild type genes from a plasmid. In addition, under conditions of high aeration, cells of mutants lacking functional *cheA1*, *cheY1* genes or the Che1 operon formed clumps due to cell-to-cell aggregation, whereas the mutant lacking functional CheB1 and CheR1 (BS104) clumped poorly, if at all. Further analysis suggested that the nature of the EPS produced, rather than the amount, may be involved in this behavior. Interestingly, mutants that displayed clumping behavior (lacking *cheA1*, *cheY1* genes or the Che1 operon) also flocculated earlier and quantitatively more than the wild type cells,

whereas the mutant lacking both CheB1 and CheR1 was delayed in flocculation. We propose that the Che1 chemotaxis-like pathway modulates the cell length as well as clumping behavior, suggesting a link between these two processes. Our data are consistent with a model in which the function of the Che1 pathway in regulating these cellular functions directly affects flocculation, a cellular differentiation process initiated under conditions of nutritional imbalance.

Section A: Introduction

To survive and compete under fluctuating environmental conditions, bacteria must rapidly adjust their behavior to maintain an optimum metabolism. Signal transduction systems enable cells to detect and adapt to these changes by executing appropriate cellular responses, such as regulation of gene expression or modulation of the swimming pattern. Two-component signal transduction systems are found in phylogenetically diverse organisms, but they are most prevalent in Bacteria where they modulate many cellular adaptive responses including development, virulence and chemotaxis (38, 41). The best characterized of such systems is the one regulating the run/tumble swimming bias (chemotaxis) in *Escherichia coli* (for a review, see 42). This signal transduction system consists of a set of conserved proteins which includes CheA, CheW, CheY, CheB, and CheR and a set of chemoreceptors (known as methyl-accepting proteins or MCPs) that perceive environmental cues. Signals sensed by MCPs modulate the activity of the histidine kinase CheA associated to chemoreceptors via CheW. Phosphotransfer from CheA to CheY results in P~CheY that can trigger a switch in the direction of flagellar rotation (tumble). The activity of CheB and CheR modulates the methylation status of MCPs which affects their sensitivity. CheB, a methylesterase activated through phosphorylation by CheA, removes methyl groups added to MCPs by the constitutive methyltransferase CheR. The

analysis of completely sequenced bacterial genomes has revealed that some bacterial species have multiple homologous chemotaxis-like signal transduction pathways (41, 47). Interestingly, Che-like pathways have been recently implicated in controlling cellular functions other than motility, including flagella biosynthesis, cyst formation, biofilm formation and the initiation of developmental programs (8, 9, 10, 22, 27). In cases where a response regulator (CheY homolog) is present, the mechanism by which the Che-like pathways regulate functions other than the swimming pattern remains unknown. It is also unclear whether cellular responses modulated by parallel chemosensory systems, which function simultaneously in a single organism may be coordinated.

The alpha-proteobacteria *Azospirillum brasilense* are soil diazotrophs (bacteria which fix nitrogen) that colonize the roots of cereals and grasses. *A. brasilense* cells are motile, and similarly to *E. coli*, respond to temporal gradients of stimuli by modulating their swimming pattern toward a higher or lower probability of change in swimming direction in response to repellents and attractants, respectively (1). We previously identified a chemotaxis-like signal transduction pathway in this bacterium that is comprised of CheAWYBR homologs (21). An orthologous pathway was shown to exclusively control the motility behavior in a closely related species (21). The on-going sequencing project of the first *A. brasilense* genome (http://genome.ornl.gov/microbial/abra) indicates that there are three other chemotaxis-like gene clusters in addition to the one identified previously (21) which we now name Che1 (Figure 5). We demonstrated that the CheB1 and CheR1 proteins from this pathway function as a chemoreceptor-specific methylesterase and methyltransferase, respectively; however, experimental evidence strongly suggested that the primary function of this Che1 pathway is not

the control of motility behavior (39). The main line of evidence for this hypothesis is the observation that although mutants lacking CheB and/or CheR functions are impaired in chemoreceptor-specific modifications and are defective in chemotaxis, a mutant in which the entire chemotaxis operon was mutated displays a chemotaxis phenotype mostly similar to that of the parent strain (39). Thus, we hypothesized that this signal transduction system in *A. brasilense* may control a cellular function(s) other than motility and we tested this by characterizing the physiology and growth of a set of defined chemotaxis mutants. Here we confirm that this Che pathway contributes to the cell motility pattern and we also provide evidence that this is not its only and primary function. Our results suggest a function for this chemotaxis pathway in modulating the propensity of cells for clumping under conditions of high aeration as well as cell length. Mathematical modeling of the rates of nutrient uptake predicts that shorter cells may have a reduced diffusive nutrient uptake, suggesting that changes in cell length affect cell physiology in order to optimize metabolism. Our data are consistent with a model in which the function of the Che1 pathway in regulating these cellular functions directly affects flocculation, a cellular differentiation process initiated under conditions of nutritional imbalance.

Section B. Materials and Methods

Bacterial strains and growth conditions

A wild type *A. brasilense* Sp7 (ATCC 29145) strain was used throughout this study. The Che1 pathway and genes therein (*cheA1*, *cheY1* etc.) were previously known as the Che pathway (21, 39). The mutant lacking functional CheB1 and CheR1 (Δ(*cheB1-cheR1)::km*; BS104) (39), the Che1 pathway insertion mutant (BS110) (39) as well as the IZ15 and IZ21 mutants (21) were

described previously. A map detailing the genetic organization of the *che1* region and the location of the mutation is shown in Figure 5. *A. brasilense* cells were grown in minimal medium (MMAB), supplemented with a carbon source of choice as described previously (21). To visualize Congo Red binding by individual colonies, cells to be tested were grown in liquid minimal medium with malate as a carbon source, and placed as 5 µl drops on solid TY plates (per liter, 10 g bacto-tryptone and 5 g yeast extract, 15 g Noble agar) containing Congo Red (40 µg ml^{-1}). The plates were incubated at 28°C for 1 to 4 days before being photographed. Cell aggregation and flocculation was performed as follows. Overnight cultures in liquid TY medium were normalized to an $O.D._{600\ nm}$ of 1.0 and 100 µl was inoculated into 5 ml of liquid minimal medium containing 8 mM fructose and 0.5 mM $NaNO_3$ and incubated at 28°C with shaking. Flocculation was quantified after 24 and 48 hours incubation as described (13). At least three independent cultures were used for each strain. The doubling time of individual strains was determined in at least two independent experiments in minimal medium supplemented with a carbon source of choice during early exponential phase by serial dilution in sterile PBS, and plating on minimal medium plates.

Behavioral assays

To compare chemotaxis responses to different carbon sources, minimal medium plates containing 0.3% agar and lacking a carbon source were supplemented with 10 mM malate, 10 mM succinate, or 10 mM fructose. These plates were then inoculated with wild-type *A. brasilense* strain Sp7 or the mutant derivatives Δ*(cheA1)::gusA-km (AB101),* Δ*(cheY1)::km* (AB102), Δ(*cheA1-cheR1)::Cm (AB103),* Δ*(cheB1-cheR1)::km* (BS104), IZ15, and IZ21 as

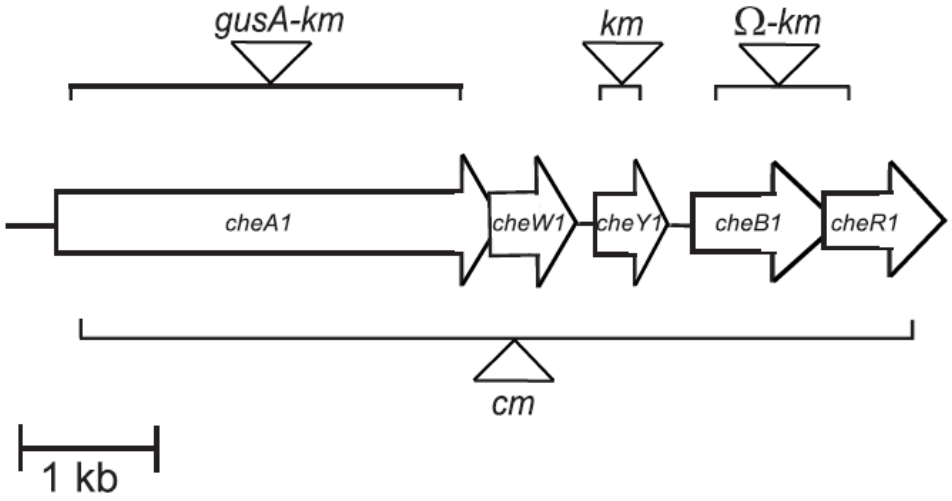

Figure. 5. Genetic organization of the *Azospirillum brasilense che1* operon and location of mutations. The diagram of the *che1* operon is derived from that published previously (21). The bars represent the regions deleted to construct each mutant strain. The triangles represent the insertion of a non-polar *gusA-km* cassette within Δ*cheA1* (AB101), of a non-polar km cassette within Δ*cheY1* (AB102 strain), of a polar omegon-km cassette within Δ(*cheB1-cheR1*) (BS104 strain)(39), and of a non-polar Cm cassette within Δ(*cheA1-cheR1*)(AB103), as described in detail in the Material and Methods. Abbreviations: km, kanamycin resistance; cm; chloramphenicol resistance.

described previously (39). Measurements of chemotactic ring diameter were performed after 48 hours. Aerotaxis assays using the capillary method were performed as described previously (39). In order to determine the reversal frequency (probability of change in the swimming direction) of cells under steady-state conditions, free-swimming cells were first grown in MMAB supplemented with malate or fructose (final concentrations of 10 mM) to early exponential phase, observed with a dark-field microscope, and videotaped. Malate and fructose are the strongest chemoattractants for *A. brasilense* (1) and wild-type cells of *A. brasilense* grown with malate have a different swimming motility pattern under steady-state conditions than when grown with fructose (39). Reversal frequency under steady-state was measured by determining the number of reversals of a single cell during a 4-s time frame, corresponding to the average time a single cell can be tracked, as described previously (39). The reversal frequencies of at least 90 cells (from three independent cultures) were measured in each experiment.

Construction and characterization of mutants

To construct a mutant lacking a functional *cheA1* gene, pGA115 containing a Δ(*cheA1)::gusA-km* deletion-insertion was introduced into *A. brasilense* by triparental mating (38). Double homologous recombinants carrying a deletion-insertion in *cheA1* were selected. Southern hybridization and PCR were used to verify the correct insertion and the loss of the recombinant plasmid and one such mutant strain was named AB101 (Figure 5). The mutant lacking a functional *cheY1* gene Δ*(cheY1)::km* was constructed by deletion of an internal 320-bp fragment in-frame and inserting a nonpolar kanamycin cassette from pCM184 (29). A 531-bp fragment directly upstream of *cheY1* and containing the start codon was amplified from the pFAJ451 cosmid (21) using the primers pair: cheY1UF (5'GCCACCACCAAGAAGTCCAAG)

and cheY1UR (5’CATGGTGAACGGGCCTCAGGC). This fragment was cloned in the pCR2.1TOPO vector (Invitrogen). A 554-bp fragment directly downstream of *cheY1* and encompassing the last 43-bp at the 3’-end of the gene was amplified from pFAJ451 using the primers pair: cheY1DF (5’CGACATCATCCAGACCAAGTTC) and cheY1DR (5’CTTGACCTTCGACACCAGCTC) and cloned into pGEM-T (Promega). Individual fragments were verified by sequencing and subsequently isolated by digestion with NcoI and NotI (upstream fragment) and ApaI and SacI (downstream fragment) before being cloned into corresponding sites in the pCM184 vector. In the resulting construct, the kanamycin cassette from pCM184 is inserted in-frame between the two cloned fragments, yielding a Δ*(cheY1)::km* construct. The entire Δ*(che1Y)::km* construct was amplified using the primers cheY1UF and cheY1DR and blunt-cloned into the pSUP202 suicide vector (digested with EcoRI followed by end-repair for blunt) which was used for allelic exchange (39). Correct allelic replacement was verified by PCR and one such mutant strain was named AB102 (Figure 5).

We also constructed a second mutant deleted for most of the genes encoded within Che1. A 614-bp region immediately upstream of the *che1* gene cluster and including 222 bp of the first gene in the operon (*cheA1*) was PCR amplified with the primer pair CheA1TMupFwd (5'-CCCAAGCTTCAGCGCGATGAACTGGTTG) including a 5' HindIII site (engineered restriction sites are underlined) and CheA1TMupRev (5'-CTTGAGCAGGGACATGTTGTAGGCGGC). A 831 bp region beginning 12 bp from the end of the last gene in the operon, *cheR1*, and extending downstream of the operon was PCR amplified with the primer pair CheR1dwnFwd (5'-AACATGTCCCTGCTCAAGCAGCGTTCC) and CheR1dwnRev (5'-CGG GGTACCTTAGACGGCCGCCCGGAG) including a 5' KpnI site

(engineered restriction sites are underlined). DNA fragments with the *cheA1* to *cheR1* deletion were generated by a two-step, overlap PCR procedure (36) by using DNA polymerase (Epicentre Biotechnologies, Inc.). The fragments with appropriate deletions were excised with the restriction enzymes HindIII and KpnI and inserted into the vector pUC19 at the appropriate restriction sites to generate the new construct pUCAR. A cassette encoding resistance to chloramphenicol (Cm) was excised as a SmaI fragment from the p34SCm vector (15) and cloned into the pUCAR to create plasmids pUCARCm. A 2,363 bp region encompassing the Δ(*cheA1-cheR1)::Cm* construct was then amplified by PCR using the primer pair CheA1TMupFwd and CheR1dwnRev (5' XbaI site replaced KpnI site). The PCR fragments were excised with the restriction enzymes HindIII and XbaI and inserted into the suicide vector pKGmobGII (24) at the appropriate restriction sites to generate the deletion construct pKGmobGARCm. The deletion construct was transferred into *A. brasilense* wild type strain Sp7 by biparental conjugation for allelic exchange (39). PCR was used to verify the correct replacement in Δ(*cheA1-cheR1)::Cm* mutants obtained and one such mutant strain was named AB103 (Figure 5). All intermediate constructs were verified by sequencing prior to being transferred into *A. brasilense*.

Chemotaxis mutant complementation

Functional complementation of the AB101 strain carrying the Δ*(cheA1)::gusA-km* mutation was performed by using a wild-type gene expressed from a broad host range plasmid. First, PCR amplification of *cheA1* and 545-bp of DNA sequence upstream of the chemotaxis operon was performed by using the previously described pGA111 vector (39), a pBluescript (Stratagene) derivative, as a template. The *cheA1* region was isolated by EcoRV-XhoI digestion and cloned into a SmaI-XhoI linearized medium-copy vector pBBR-MCS3 (28) to generate

pBBR-*cheA1*. This *cheA1* DNA region was also cloned into the low-copy plasmid pRK415 (25) by purifying an XbaI-KpnI fragment from pBBR-*cheA1*, yielding pRK415-*cheA1*. Both constructs were then introduced into the *A. brasilense cheA1* mutant using triparental mating with pRK2013 as a helper (20), as described previously (21). As a control, the empty pRK415 and pBBR-MCS3 vectors were introduced into the *A. brasilense* wild type strain (Sp7) and the AB101 strain carrying the Δ*(cheA1)::gusA-km* mutation. Complementation of the BS104 and AB102 strains was performed essentially as described previously, with the exception that a ribosome binding site (5'-AGGAGGA-3') was engineered at the 5'-end of each sequence to facilitate expression from the plasmid promoters (16). In order to complement the BS104 strain carrying a mutation deleting a region encompassing the *cheB1-cheR1* genes, the *cheB1-cheR1* genes were amplified by PCR from genomic DNA using the CheB1R1 forward primer (5'-CCCAAGCTTTA**AGGAGA**GGCCCGTATGTCCGATGGTTTCGGCAGAC-3) and CheB1R1 reverse primer (5'- GCTCTAGATTAGACGGCCGCCCGGAGC - 3') (the restriction sites are underlined and the ribosome-binding site is in bold type). The PCR product was cloned into the pCR2.1TOPO (Invitrogen) vector and verified by sequencing. The *cheB1-cheR1* region was then digested with the restriction enzymes HindIII and XbaI, prior to cloning into pRK415, yielding pRK415-*cheB1R1* (24). The wild-type *cheY1* gene was cloned in a similar manner using the CheY1 forward primer (5'-CCCAAGCTTTA**AGGAGA**GGCCCGTATGAAAGTTTGTCTGGTC - 3') and the CheY1 reverse primer (5'- CGGATTTCTCACAGCAGCCCGACCTCGAAC - 3') into the pCR2.1TOPO vector and the construct was verified by sequencing. Next, *cheY1* was isolated by digestion with HindIII and XbaI and cloned into pRK415, yielding pRK415-*cheY1* (25). The

pRK415-*cheB1R1* and pRK415-*cheY1* constructs were then introduced into the *A. brasilense* BS104 and AB102 strains respectively, using triparental mating, as described previously. As a control, an empty pRK415 (and pBBR1 MCS3 vector for *cheA1* complementation) was introduced into *A. brasilense* wild type (Sp7), AB101, BS104, and AB102 strains using triparental mating. The BS104 strain carrying the pRK415-*cheB1R1* vector did not require IPTG for complementation (perhaps due to "leaky" expression), whereas the AB102 strain carrying the pRK415-*cheY1* vector was complemented using 1 mM IPTG. We also complemented the previously described IZ15 and IZ21 mutants (21) using the pRK415 and pBBR-MCS3 vector derivatives containing *cheA1*, *cheB1-cheR1*, or *cheY1* genes described above. The transconjugants from each mating were inoculated *en masse* as a straight line in semi-solid (0.3 % w/v agar) MMAB medium (lacking nitrogen) and incubated at 28°C for 48 hours before being photographed. Complemented strains (but not controls) are expected to move away from the inoculation sites under these conditions. All constructs were verified by sequencing prior to being transferred into *A. brasilense* strains.

Measurements of cell size parameters

Transmission electron micrographs were taken on cells grown to mid-exponential phase ($O.D._{600\ nm} < 0.5$) in the medium indicated, washed twice in sterile phosphate-buffered saline (PBS), spotted on formvar coated nickel grids, and negatively stained with 2% uranyl acetate or 0.75% uranyl formate. The TEM images were taken at random within a particular grid. Several grids were collected for each experiment. For cell length measurements, all cells within the field of view were measured from one cell pole to the other at the longest axis provided that both poles of the cells were clearly visible. Only cells for which both poles were not clearly seen

either because of cell-to-cell overlap or because they were not entirely within the image, were not measured. Both the images of the cells and the measurements of cell length were taken blindly to avoid bias in the collection of data, i.e. the particular mutant studied at a given time was identified only by grid number until all data (both images and measurements) were collected. Cell size data were collected from at least three independent experiments for the wild type and each mutant under all growth conditions.

We also measured cell length using fluorescence microscopy of actively growing cells stained with the live fluorescent dye FM4-64 (Invitrogen Molecular Probes) in order to ensure that the differences detected did not result from the fixation protocol used for preparing samples for TEM. Briefly, aliquots of the cultures were stained with 1 μM FM4-64 for 5 minutes at room temperature (Invitrogen Molecular Probes). Stained cells were immobilized on slides using molten 1% agarose in PBS. Pictures were taken using a Nikon ECLIPSE 80i fluorescence microscope equipped with a Nikon CoolSnap HQ2 cooled CCD camera and cell lengths were measured using the NIKON NIS-Elements BR program for a minimum of 50 cells per sample taken from at least 4 different fields of view.

Exopolysaccharides isolation and quantitation

Extraction and quantitation of exopolysaccharides was performed as described by Enos-Berlage and McCarter (18) with the following modifications. Cells were grown overnight at room temperature with shaking in 250 ml of minimal media supplemented with 5 mM malate and 5 mM fructose. Cells were harvested via centrifugation at 8000 rpm for 10 minutes in a Sorvall GSA rotor. Cells were resuspended in phosphate-buffered saline (20 mM sodium

phosphate [pH 7.3], 100 mM NaCl) and then vortexed at high speed for 1 minute. Cells were then incubated at 30^{o}C on a gyratory shaker for 1.5 hours. The vortexing and incubation steps were repeated once. Cells were then pelleted at 8000 rpm for 15 minutes in a PTI F18S-12 x 50 rotor. An aliquot of the cell pellet was set aside for protein quantitation according to Bradford (11). The supernatant was collected and treated with Proteinase K to a final concentration of 200 µg/ml and incubated on a gyratory shaker overnight at 37^{o}C. The samples were then extracted using phenol:chloroform and precipitated with 95% ethanol. The pellets were washed once with 70% ethanol before being resuspended in water. Quantitation of EPS production was then determined using a 5% phenol: sulfuric acid solution according to the method described by Dubois *et al*. (17).

Mathematical analysis of nutrient uptake by diffusion

We have used the Berg and Purcell model (7) modified by Wagner *et al.* (43) for comparing the diffusion rates of nutrient uptake in each of the mutants relative to the wild type strain. We calculated the rate of nutrient uptake for each mutant using a model for cells with prolate spheroid shapes (43), assuming constant concentration of the nutrient and the same diffusion constant for each cell type. In addition, we estimated the number of receptors to be around 50,000 per cell (7) assuming the same density of receptors on the surface for cells used on the reference (2) and assuming the diameter of each receptor to be 1 nm. Changing the values of these assumptions for all strains did not affect the results.

Statistical analysis. First, one-way ANOVA tests (alpha level of 0.05) were performed to compare cell length between all strains and all growth conditions. Significant differences were found in cell length (cells grown on malate, P = 3.38e-41; cells grown on malate and fructose, P

= 2.85e-51) among the strains in the ANOVA tests. Similar differences were also found for septating cells (cells grown in malate, P = 2.45e-8; cells grown in malate and fructose, P = 2.61e-22). Next, the mean cell length values of wild type and mutants or between the mutant populations of actively growing cells were compared in pair wise two-sample t-tests assuming equal variances (alpha level of 0.05) (Microsoft Excel (Microsoft, Inc.)). The differences between the means analyzed were considered statistically significant if the P-value was < 0.05.

Section C: Results

CheA1 and CheY1 play a minor role in chemotaxis

The chemotaxis pathway in *A. brasilense* has been identified in a cosmid library of *A. brasilense* Sp7 by functional complementation of generally non-chemotactic mutants generated by chemical mutagenesis (hereby referred to as Che1) (21). Although the exact gene(s) mutated in these mutants (IZ15 and IZ21) (21) have not been previously characterized, each mutant is locked into a specific motility pattern (highly reversing for IZ15 and smooth swimming for IZ21), consistent with a defect in chemotaxis signal transduction. However, we previously found that a strain carrying a *che1* insertion mutation (strain BS110; generated by a Campbell mutation) disrupting the entire operon had a random swimming pattern similar to that of the wild type strain and a minor (if any) defect in chemotaxis in soft agar plates (39). This atypical result suggested that the primary function of the Che1 pathway may not be control of the motility pattern (chemotaxis) (39). To extend these observations and clarify the function of the *che1* operon in chemotaxis and aerotaxis, we have characterized the motility and tactic behaviors of strains carrying mutations in *cheA1* (strain AB101) and *cheY1* (strain AB102) as well as a strain

carrying a newly constructed deletion-insertion mutation that disrupts the entire *che1* operon (strain AB103) (Figure 5). We have found that strains carrying mutations in *cheA1*, *cheY1* and *che1* have a defect in chemotaxis in soft agar plates but they are not fully defective (Figure 6A and 6B). The chemotactic defect of strains AB101, AB102 as well as that of BS104 (carrying a Δ*(cheB1-cheR1)::km* mutation) (39) could be complemented by expressing the corresponding genes from a plasmid (Figure 7), indicating that the chemotactic defects are not due to polar effects (i. e. effects on genes downstream).

Interestingly, all mutant strains were capable of forming typical "chemotactic" rings on all substrates tested. This contrasts with the phenotypes of the original nonchemotactic mutants (IZ15 and IZ21) that were complemented by this operon (21) (Figure 8A). All strains were capable of forming an aerotactic band in the spatial gradient assay (Figure 9). Although equivalent cell concentrations were placed in the capillaries, strain AB101 formed an aerotactic band significantly faster relative to the wild type strain (less than 1 minute versus about 2 minutes for the wild type strain), resulting in the formation of an aerotactic band with a greater density of motile cells. As shown previously, the time required for the formation of the aerotactic band by *A. brasilense* cells in the capillary assay is reproducible and consistent (about 2 minutes) because it depends on the ability of cells to efficiently sense the oxygen gradient and navigate toward its optimum concentration (1, 4, 48). Strain AB102 also formed an aerotactic band but the band formed slightly slower (about 5 minutes) and farther away from the meniscus relative to the wild type or AB101 (Figure 9). Strain AB103 was the most affected in aerotaxis: the band formed farther away from the meniscus and it also formed significantly slower (if at all) (about

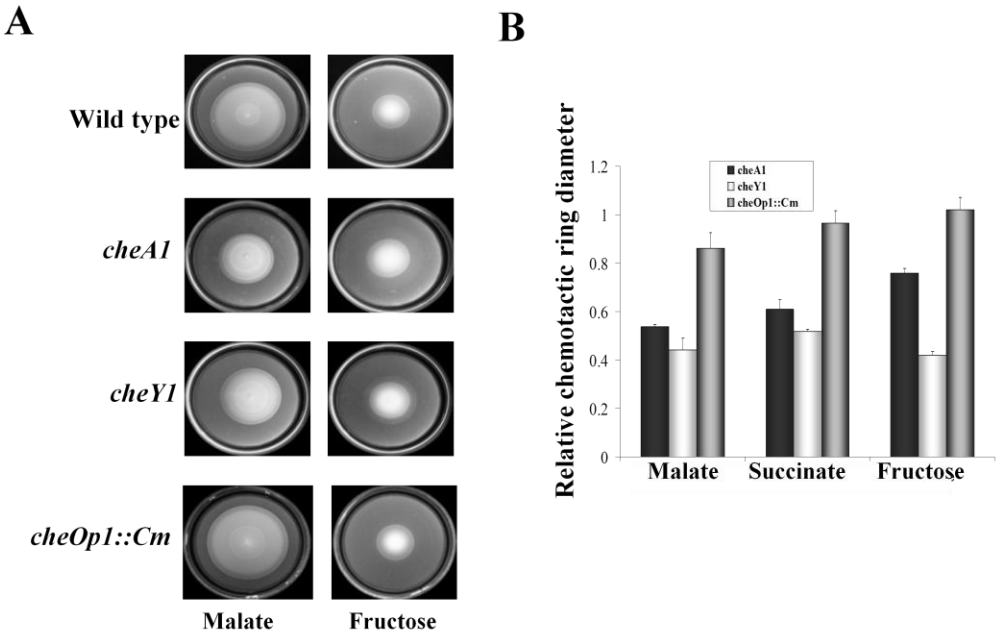

Figure 6. *che1* mutant strains are impaired, but not null in chemotaxis. (A) Chemotaxis of the wild type *A. brasilense* strain Sp7 and strains carrying mutations in the *che1* operon in the soft agar plate assay, with malate (Left) or fructose (Right) as the sole carbon source. Representative plates are shown for each strain and conditions. (B) The average chemotactic ring diameters are expressed relative to that of the wild type strain (defined as 1). Error bars represent standard deviation from the mean, calculated from at least three repetitions. The chemotactic-ring diameters of the mutants were found to be significantly different from the wild type with all chemoeffectors tested except for AB103 on succinate and fructose.

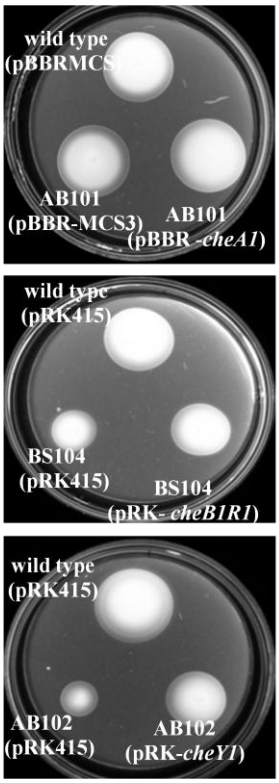

Figure 7. The chemotaxis defect of the strains carrying deletions for *cheA1*, *cheY1*, and *cheB1-cheR1* can be complemented by expressing *cheA1*, *cheY1*, and *cheB1-cheR1* from a plasmid. Representative results (out of 3 repetitions) from the soft agar plate assays are shown. Complementation was performed as described in **Section B: Materials and Methods**.

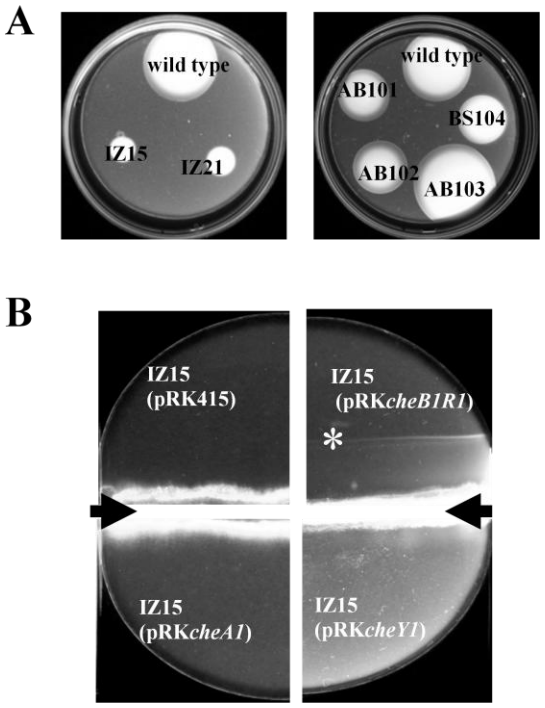

Figure 8. Complementation of the generally non-chemotactic mutants IZ15 and IZ21. (A) Chemotaxis in the soft agar plate assay of the wild-type A. brasilense, the non-chemotactic mutants IZ15 and IZ21 and the *che1* mutant strains, after 24 hours incubation at 28°C. (B) Representative results of chemotaxis in the semi-soft agar plate assay are shown for IZ15 complemented with the pRK415 vector (control), pRK-cheA1, pRK-cheB1R1, or pRK-cheY1. The arrows indicate the inoculation line within the soft agar in each plate. The asterisk points to the chemotaxis ring (indicative of functional complementation). No complementation was observed with the other genes for IZ15 and no complementation was observed for IZ21 when the same plasmids as well as pBBRMCS3 and pBBRcheA1 were tested in this assay.

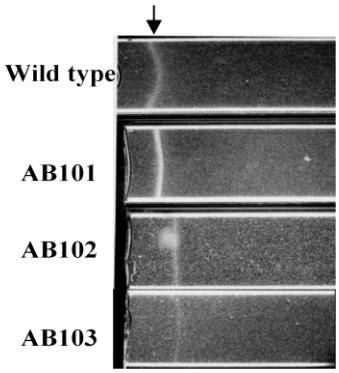

Figure 9. *che1* mutant strains have different aerotaxis defects. Aerotaxis of the wild type *A. brasilense* and the *che1* mutant strains in the capillary tube assay. The arrow indicates the position of the center of the aerotactic band. Cell suspensions of similar density were used in the assay. The picture was taken after 10 minutes incubation at room temperature.

15 to 20 minutes), resulting in a low density of motile cells within the "band". It is noteworthy to mention that cells from all strains were actively motile within the band as well as outside of it.

If the primary function of the *che1* operon is chemotaxis, then mutants lacking any component of the excitation pathway (such as CheA and CheY homologs) should have a locked smooth swimming motility pattern, similar to equivalent mutants in *E. coli* (40, 42). To test this hypothesis, we determined the steady-state (constant concentration of an attractant) swimming pattern of free-swimming cells by using motion tracking analysis (Figure 10). Consistent with our previous observations of the motility pattern in the wild-type *A. brasilense* and the BS104 strains (39), we found that the steady-state motility pattern of strains carrying mutations in *cheA1*, *cheY1* and *che1* was dependent upon the substrate present: the probability of changes in the swimming direction (reversal frequency) was higher when cells were grown on fructose than when cells were grown on malate. However, strains carrying mutations in *cheA1* (strain AB101) and *cheY1* (strain AB102) tended to swim with a "smoother" motility pattern (changed swimming direction less frequently) relative to the wild type cells (statistically significant; $P<0.05$) under all conditions. Noticeably, in both the semi-soft agar plate assay and in analysis of the motility pattern under steady-state conditions, AB101 and AB102 had more pronounced defects than AB103 which carries a mutation encompassing the *che1* cluster. The AB103 strain had a similar motility pattern than AB101 and AB102 in the presence of malate, but it did not have a distinct motility pattern in the presence of fructose. Taken together, these data strongly suggest that the function of the Che1 pathway in chemotaxis may be indirect.

The lack of a null chemotactic phenotype in any of the Che1 pathway mutants prompted us to re-examine the original mutants IZ15 and IZ21 from the complementation of which the

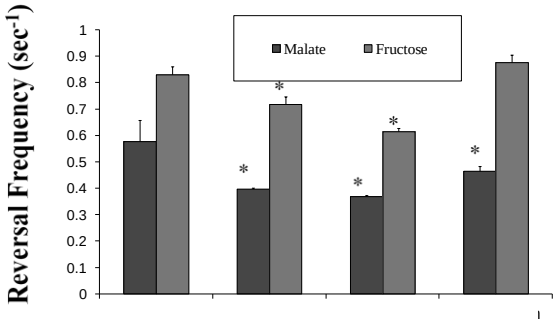

Figure 10. *che1* mutant strains are affected in their steady-state swimming pattern. The steady state swimming pattern is represented by the reversal frequency (Probability of changes in the swimming direction) of free-swimming cells grown in minimal MMAB medium containing either 10 mM malate (dark bars) or 10 mM fructose (light bars) as the sole carbon source. Reversal frequencies are expressed as the number of events per second (sec^{-1}). Error bars represent standard deviation from the mean calculated from at least 90 cells. Statistically significant differences ($P < 0.05$) with the wild type are indicated by a star.

Che1 operon was originally isolated (21). These mutant derivative strains have a locked highly reversal (IZ15) and smooth swimming (IZ21) motility phenotype on all substrates tested (21). Consistent with previous observations, these mutants also failed to spread much beyond the inoculation point and they did not form any chemotactic ring on semi-soft agar plates, even under conditions where the wild type parental strain, the AB101, AB102, AB103 and BS104 strains formed sharp chemotactic rings (Figure 8A). While a cosmid carrying the entire operon, except for the very end of the *cheR1* gene could complement both IZ15 and IZ21 (21), we have found that the IZ15 mutant could be complemented by expressing *cheB1-cheR1* from a plasmid while IZ21 was not complemented by expressing either *cheA1*, *cheY1* or *cheB1-cheR1* (Figure 8B). These data suggest that the IZ15 mutant strain may carry a mutation in either *cheB1* or in another gene that may be suppressed through the expression of *cheB1-cheR1*. Sequencing *cheB1* and *cheR1* from the IZ15 and IZ21 genomes did not reveal any mutation, supporting the latter hypothesis that the complementation of the IZ15 defect by a plasmid expressing *cheB1-cheR1* is a multicopy suppression. On the other hand, the genetic defect responsible for the IZ21 (21) phenotype (complemented by expressing the full Che1 cluster from a cosmid) remains to be determined. These results are consistent with the hypothesis that Che1 may have an indirect role in chemotaxis, perhaps via CheB1.

Che1 mutants have different cell lengths under specific growth conditions

As mentioned previously, strains carrying mutations in genes of the Che1 pathway had modest defects in chemotaxis, prompting us to hypothesize that this operon controls other cellular functions. Thus, we systematically analyzed the wild type and the *che1* mutant strains by transmission electron microscopy (TEM). Interestingly, we found that most cells in an actively

growing culture of the BS104 strain appeared to be longer than similar cultures of the wild type strain, suggesting that mutations in *che1* affected cell morphology under these growth conditions (low O.D., standard shaking conditions). We compared the cell lengths of wild-type and mutant cells grown with different substrates by using TEM and by staining cells taken directly from cultures with the vital fluorescent membrane dye FM4-64 (Figure 11A). Similar results were obtained in all experiments for the BS110 strain (carrying a mutation disrupting Che1 function by Campbell insertion; 39) and the AB103 strain (carrying a Δ(*cheA1-cheR1)::cm* mutation) indicating that the constructs used to make each mutant strain were not responsible for the phenotypes observed. We found that in populations of actively growing cells, strains lacking functional *cheA1*, *cheY1*, and *che1* tended to be shorter than the wild-type cells, whereas cells lacking functional *cheB1-cheR1* tended to be longer (Figure 11A). Furthermore, cells lacking functional *cheY1* and *che1* were significantly shorter than cells of the other mutant strains, including AB101 (P <0.05 in pair wise t-tests). The biased cell length distribution of the mutant strains could be complemented to wild-type length values *in trans* by a cosmid carrying the wild-type *che1* cluster (21) (data not shown) or specific *che1* genes expressed from plasmids (Table 1). There was a similar bias toward shorter or longer cell lengths for a subpopulation of cells undergoing septation (Figure 11B). Cells that tended to be longer divided at a longer cell length relative to the wild type, and shorter cells divided at a shorter cell length. Given that the doubling times of strains carrying mutations in *che1* were similar to that of the wild type, we concluded that the Che1 pathway must modulate cell length independently of cell division. This observation is consistent with the fact that the timing of chromosome replication and cytokinesis are independent from each other, as well as being independent of cell length at division in bacteria

(19). This finding also suggests that the Che1 pathway modulates cell length independently of the events leading to cell size increase and growth during cell cycle progression. The changes in cell length as detected here were relatively small, but statistically significant and experimentally reproducible. The differences were especially significant when comparing the BS104 strain mutated in *cheB1-cheR1* with that of the wild type or any of the other mutants. Our experimental approach for measuring cell size parameters was carefully designed to guard against unintentional bias of locating and measuring unusually long and short cells (see Materials and Methods). Interestingly, differences in cell length between the wild type and the mutant strains as described above were best observed in actively growing cultures maintained in early exponential phase of growth ($O.D._{600nm} < 0.5$) and were less pronounced at other growth stages. These subtle differences in the cell lengths of individual and septating cells were also best observed at lower cell density in cultures in the early exponential phase of growth, suggesting that this effect of the *che1* mutations prevailed in the early stages of the cell cycle.

Changes in cell length do not affect the growth rate

Changes in the average cell length of the mutants in the presence of different substrates are correlated with the growth rate, consistent with the fact that cells growing faster tend to be larger (19) (Table 2). However, differences in cell length between the strains could not be attributed to differences in growth rate because the doubling times of the mutant strains were not different from that of the wild type (Table 2). Further comparison of the growth rates and the cell length in actively growing populations of cells revealed that at faster growth rates, the average cell length increased for wild-type cells and some (but not all) mutant cells (Table 2 and Figure 11). When comparing the length of cells grown on malate versus that of cells grown on malate

and fructose, the differences in the average cell length between the two growth conditions were found to be statistically significant (t-test, alpha level 0.05) for the wild type strain (P = 0.0043) and BS104 (P = 9.02e-8), but not the AB101, AB102, AB103 or BS110 strains. This result indicates that although the average length of wild-type cells can change under different nutrient conditions, the cell lengths of strains carrying mutations in *cheA1*, *cheY1*, and *che1* remained constant regardless of the growth conditions. This implies that strains carrying mutations in *cheA1*, *cheY1* and *che1* cannot sense and/or transduce the signal(s) that lead to an increased cell length at faster growth rates, as opposed to the wild type or a strain carrying a mutation disrupting both *cheB1* and *cheR1*.

Altogether, these data indicate that the Che1 pathway may contribute to the ability to regulate changes in cell length under conditions of optimal growth (low O.D., low aeration).

The changes in cell length are predicted to affect nutrient uptake in shorter but not longer cells

In order to assess whether the subtle changes in cell length could impact the physiology of the cells, we used a previously developed mathematical model (7, 43) to compare the rates of diffusive nutrient uptake of the mutant strains (Figure 12). The model predicted that the changes in cell length would not significantly affect nutrient uptake in the BS104 strain but it would result in a significant decrease in the nutrient uptake abilities of the shorter cells (strains AB101, AB10 and AB103). These predictions also imply that the Che1 pathway could function to reduce cell length in order to decrease nutrient uptake.

Table 1. Complementation of *che1* mutant strains for cell length.

Strain	Mean Cell Length (μm) ± SD *
Sp7(pRK415)	2.61 ± 0.0055
AB101(pRK415)	2.35 ± 0.0038
AB101(pRK-*cheA1*)	2.71 ± 0.0061
BS104(pRK415)	2.84 ± 0.0085
BS104(pRK-*cheB1R1*)	2.50 ± 0.0106
AB102(pRK415)	2.46 ± 0.0045
AB102(pRK-*cheY1*)	2.56 ± 0.0047

* The mean values are given ± standard deviation to the mean (SD). Mean cell length was determined on cells grown in MMAB with malate (5mM) and fructose (5 mM).

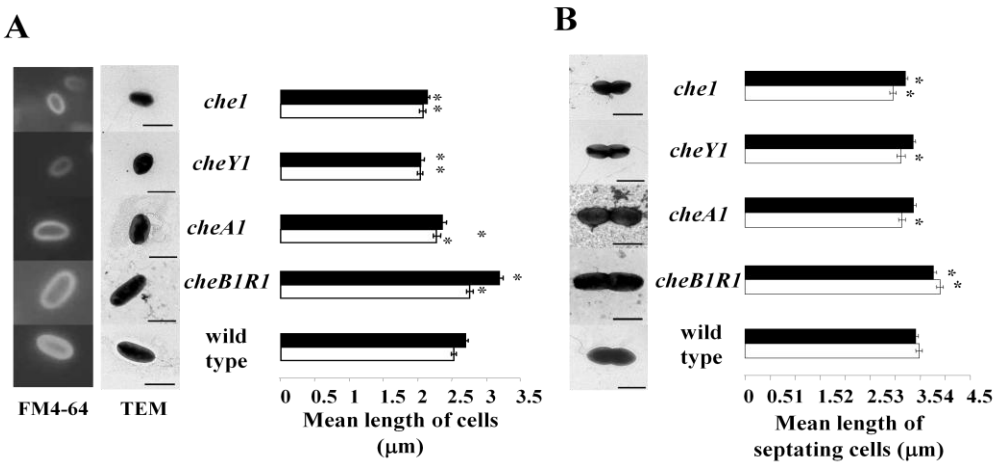

Figure 11. *che1* mutant strains have different cell length. (A) Mean cell length from actively growing populations of the wild type *A. brasilense* and the strains carrying mutations in genes of the *che1* operon**.** Cells were grown in minimal medium supplemented with 10 mM malate (white columns) or 5 mM malate and 5 mM fructose (black columns) as the carbon sources. Cell length values were measured on transmission electron micrographs or on images obtained by fluorescence microscopy after staining the cells with the membrane fluorescent dye FM4-64 along the length of individual cells, as specified in *Materials and Methods*. (B) Mean cell lengths of septating cells from actively growing cultures of the wild-type *A. brasilense* and of strains carrying mutations in genes of the *che1* operon. Cells were grown in minimal medium supplemented with 10 mM malate (white bars) or 5 mM malate and 5 mM fructose (black bars) as the carbon sources. The cell length values for individual cells were obtained from transmission electron micrographs or fluorescent images as described in (A). Cells were identified as undergoing septation during division by the presence of a clear constriction located at midcell. In both (A) and (B), the asterisks indicate statistically significant differences in mean cell length values from that of the wild type strain as determined by a t-test (at the $P < 0.05$ level). Representative images of cells stained with the fluorescent membrane dye FM4-64 or transmission electron micrographs are shown on the left side of each graph as typical examples of non-proliferating (A) or septating (B) cells grown on malate and fructose (5 mM each). In both panels, the bars represent the standard deviation to the mean. The scale bar on the TEM pictures represents 2 μm.

Che1 mutants have a different ability to clump under certain growth conditions

In addition to the effect of mutations in *che1* genes on cell length, we have also observed that the AB101, AB102, AB103, BS110 strains, but not the wild type or BS104 strains, were capable of cell-to-cell aggregation and clumping under conditions of growth at high aeration (Figure 13A). Clumps were not observed under conditions of growth at low aeration for any of the strains tested (Figure 13A), indicating that this behavior was induced under conditions of high aeration and that it was not constitutive. Under these conditions of growth at high aeration, the AB101, AB102, AB103, BS110 strains still exhibited different cell lengths and they also formed clumps due to cell-to-cell contacts initiated at the non-flagellated poles. The cell clumps were very dynamic in that some cells were capable of leaving the clumps. We have analyzed clumped cells by light microscopy, transmission electron microscopy, scanning electron microscopy as well as fluorescence microscopy using various fluorescent lectins (data not shown), but we were unable to detect any specific extracellular bacterial structure(s), such as pili, polysaccharide fibrils or holdfasts that could be invoked to mediate such interactions between cells. Clumping and cell-to-cell interactions have been described previously and have been studied in detail in *A. brasilense* because it is one of the first observable steps in flocculation, a cellular differentiation event that occurs when cells are grown under conditions of nutrient stress at high aeration (12). In order to determine if the clumping observed was related to flocculation, we compared the wild type strain and the chemotaxis mutant strains for the ability to flocculate and found that strains carrying mutations in *cheA1, cheY1* and *che1* not only flocculated sooner, but also quantitatively more than the wild type strain (Figure 13B and 13C). We also observed that these mutant strains formed clumps earlier and in greater numbers than the wild type under

Table 2. Effect of mutations in genes of the *che1* operon of *A. brasilense* on the doubling times of cells grown with different substrates.

	Doubling time (minutes)	
	Malate	Malate+Fructose
Sp7	138	117
BS104	136	109
AB101	145	107
AB102	138	118
AB103	145	108

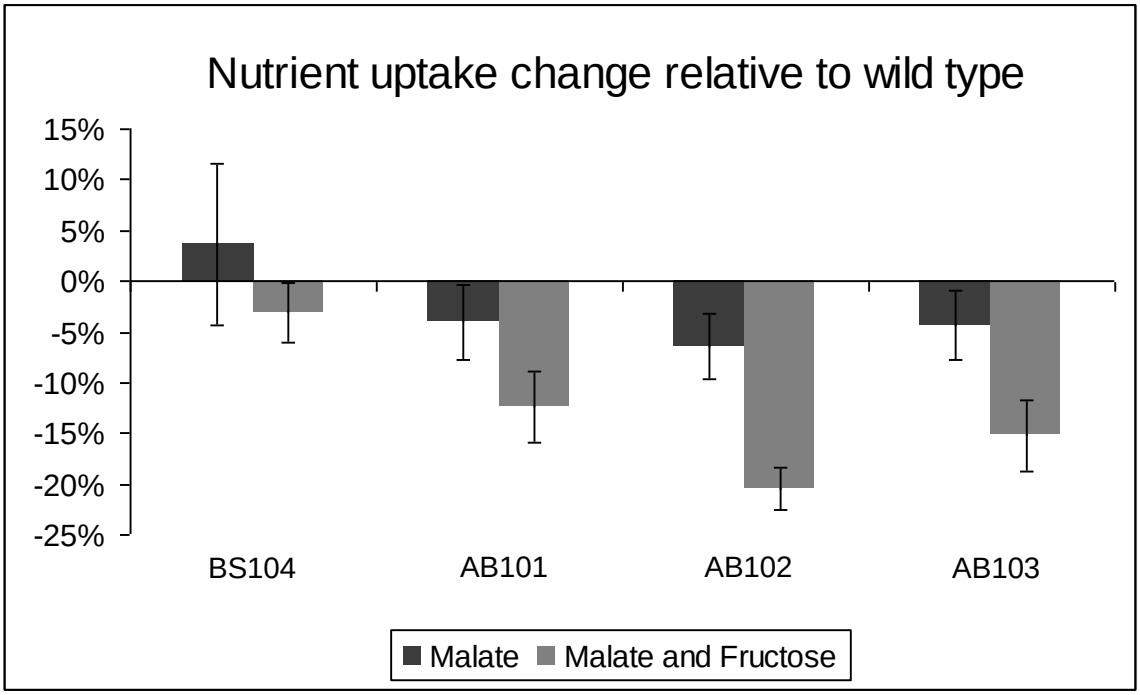

Figure 12. Modelling of the effect of changes in cell length on the rates of diffusive nutrient uptake. The changes in the rate on nutrient uptakes are expressed as percent change relative to the wild type strain. The rates of nutrient uptake for each mutant strain were calculated as described in the Material and Methods for cells grown in minimal MMAB medium with malate (10 mM) or malate (5 mM) and fructose (5 mM) as carbon sources. The bars represent standard deviation to the means. Stars indicate statistically significant changes.

these conditions (about 6 hours post inoculation into the flocculation medium versus about 9 hours for the wild type). Conversely, BS104 flocculated very poorly even after prolonged incubation, suggesting that this strain is significantly delayed rather than impaired in flocculation (Figure 13B and 13C). Taken together, these data indicate that the Che1 pathway modulates the propensity of cells for clumping under conditions of high aeration and that this behavior directly affects the timing of flocculation.

Che1 mutants are affected in the production of exopolysaccharides

The ability of *A. brasilense* cells to aggregate, to form large clumps and to flocculate in liquid cultures under conditions of unbalanced growth was previously correlated with changes in the concentration and composition of exopolysaccharides (EPS) (13, 35). The production of Congo Red–binding EPS has been correlated with the ability of cells to flocculate under certain conditions (22). Therefore, we compared strains carrying mutations in *che1* genes to the wild type strain for the ability of colonies to bind the Congo Red dye (Figure 14A). We noticed dramatic differences in the appearance of colonies (both color and morphology) formed by the *che1* mutant strains in comparison with the wild type (Figure 14A). Four-day old colonies of the wild type and of the BS104 strain bound Congo Red moderately and mostly at the center of the colony whereas AB101 and AB102 bound more Congo Red homogeneously throughout the colony (Figure 14A). In contrast, four-day old colonies of AB103 (and BS110; not shown) did not bind Congo Red under these conditions. When comparing one-week old colonies grown on medium containing Congo Red, we observed that all colonies, including that of AB103, bound the Congo Red dye included in the plates. These observations suggest that the mutants are affected in the amount and/or timing of production of at least some Congo Red-binding EPS.

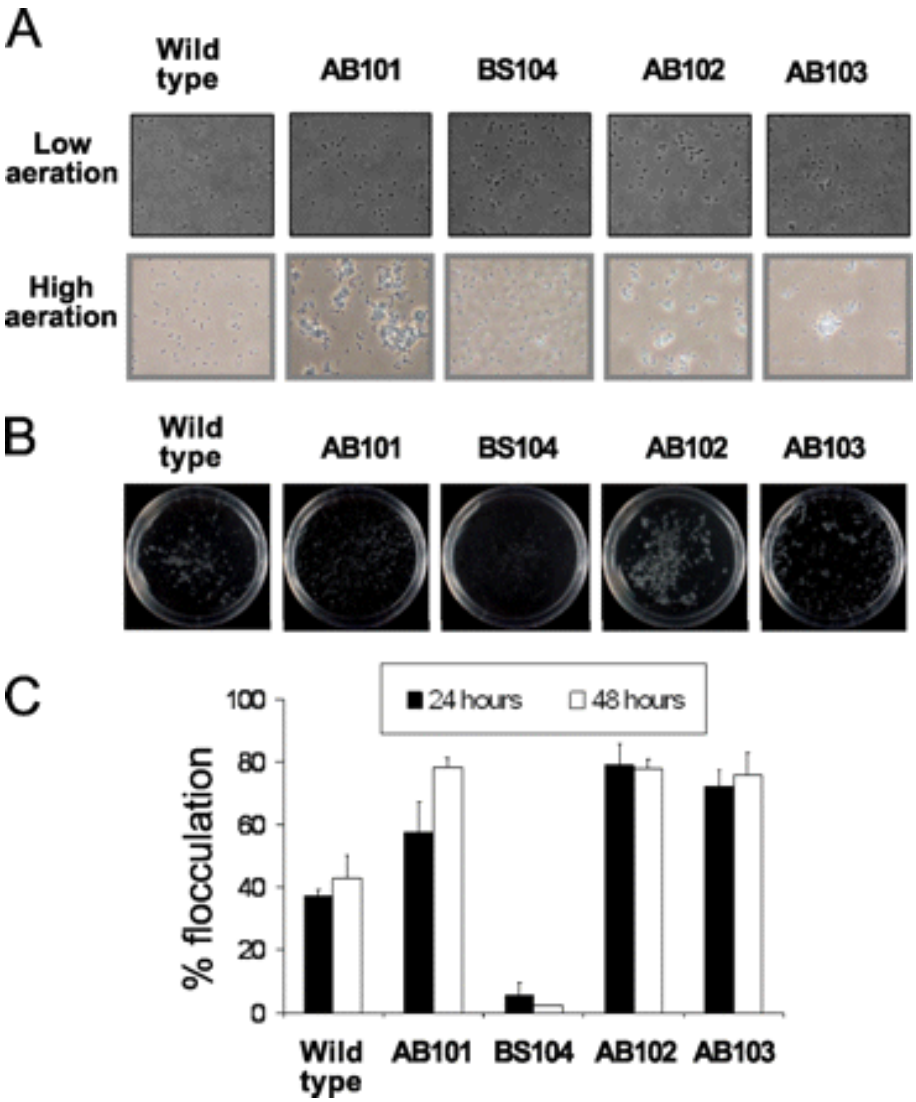

Figure 13. The *che1* mutants are affected in the ability to clump and to flocculate under specific growth conditions. (A) Actively growing cells of *A. brasilense* do not clump under conditions of low aeration (top) whereas cells of AB101, AB102 and AB103, but not that of the wild type or BS104, clump under these conditions (bottom). Pictures were from actively growing cultures in MMAB with 5 mM malate and 5 mM fructose as the carbon sources, observed by phase contrast. Magnification, X 400. (B) Visible aggregates of flocculated cells. Petri dishes (60 x 15 mm) containing flocculated liquid cultures are shown. (C) Quantitative analysis of flocculation. The data represent the fraction of flocculated cells relative to the total number of cells in the culture, after gentle homogenization, expressed as a percentage as detailed in *Material and Methods*. The bars represent the standard deviation to the mean.

Consistent with the hypothesis that the *che1* mutant strains are impaired in the production of EPS, we found that the surfaces of one-week old colonies were different (Figure 14A). The surface of colonies of AB101, and to a lesser extent that of AB102, were wrinkled and appeared "dried" in aspect. In contrast, colonies of AB103 were smooth and appeared "wet" under the same conditions while colonies of the wild type and of the BS104 strains were similar and appeared intermediate between those of strains carrying mutations disrupting *che1* or *cheA1* (Figure 14A). Comparing the total amount of EPS produced by each strain revealed that AB102, AB103 and BS104 produced significantly less total EPS under these conditions while AB101 produced EPS in amounts equivalent to that extracted from the wild type strain (Figure 14B). However, the amount of EPS produced by the different strains did not correlate with a particular Congo Red-binding phenotype on plates or the ability of any of the mutants to clump or to flocculate. We have also directly tested the hypothesis that EPS could be responsible for the clumping behavior by attempting to induce clumping by adding EPS isolated from clumped and flocculated cells in suspensions of free-swimming cells. However, none of the isolated EPS fractions could induce the clumping behavior. This result does not rule out the possibility that the EPS may modulate clumping, since it is possible that the structure of the EPS could be involved in this behavior; however, the EPS structure may have been compromised by the extraction procedure. Collectively, these data suggest that it is most likely the nature, composition and/or structure of the EPS, rather than the total amount of EPS produced alone, that contribute to the different cell surface properties and associated clumping abilities of the *che1* mutants.

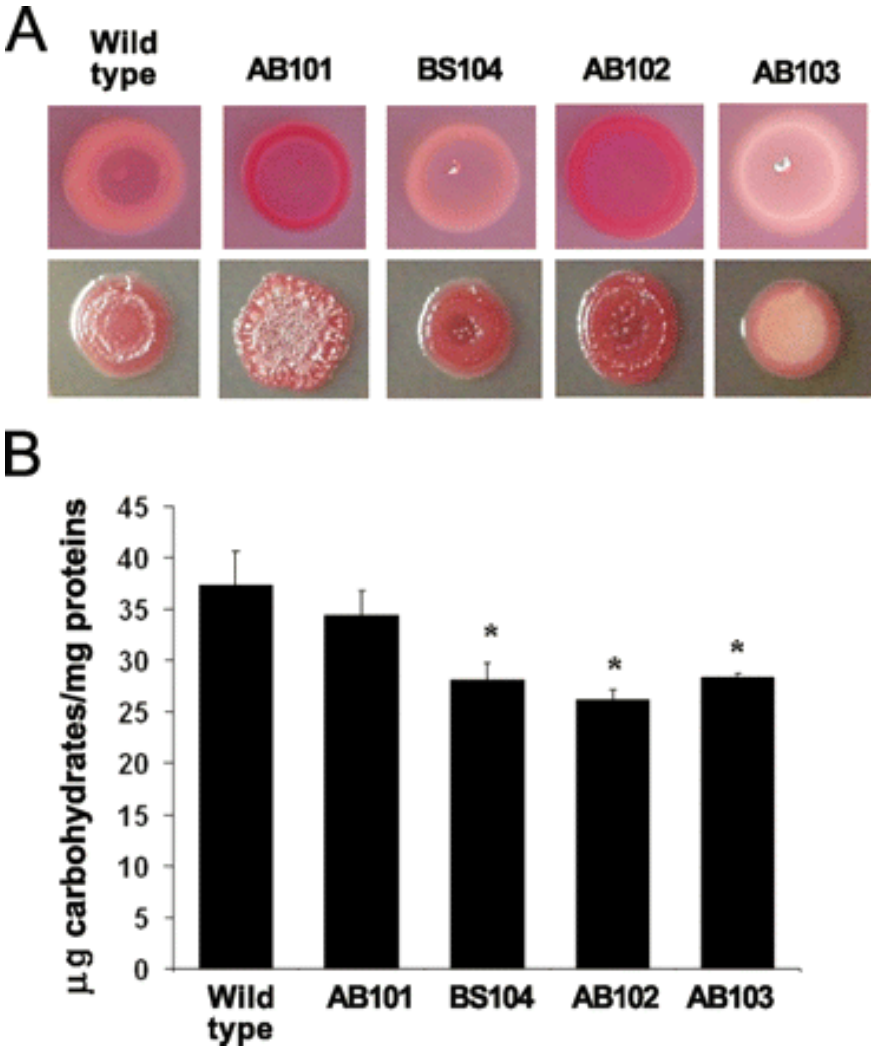

Figure 14. The *che1* mutants are affected in the production of EPS. (A) Colony morphologies of the wild-type and the *che1* mutants observed on solid agar plates containing Congo Red on minimal medium (top) or TY medium (bottom), after 4 days of incubation. Although the exact patterns of Congo Red binding varied with the growth conditions, patterns produced by the mutants were always different from those produced by the wild-type. The colony morphology was also different under different conditions and between the wild type and some of the mutant strains (AB101 and AB102 in particular). (B) Quantitation of the EPS produced by the wild type *A. brasilense* strain and the *che1* mutants. The extraction and quantification of EPS was performed as described in *Materials and Methods*. The bars represent the standard deviation to the mean for each sample. Asterisks indicate statistically significant differences as compared to that of the wild type strain (at the $P<0.05$ level).

Section D: Discussion

The *che1* cluster was initially identified by functional complementation of two generally non-chemotactic mutants (IZ15 and IZ21) that each had a distinct swimming pattern (21). Here, we confirmed that the Che1 pathway contributes to chemotaxis and we also show that this control is likely to be indirect. We further demonstrate that the Che1 pathway of *A. brasilense* functions to modulate the propensity of cells for clumping, likely in response to changes in oxygen concentrations and that this pathway can also bias the cell length, suggesting a link between these two cellular processes.

Evidence for a complex role of Che1 in chemotaxis

Our data indicate an indirect role for the Che1 pathway in chemotaxis, perhaps mediated by the adaptation proteins CheB1 and/or CheR1. The following lines of evidence support this hypothesis: (i) a mutant lacking the entire *che1* cluster is capable of chemotaxis and it is affected only subtly in its swimming pattern; (ii) strains with mutations in *cheB1* and/or *cheR1* have the strongest chemotaxis and aerotaxis phenotypes (39); (iii) strains carrying mutations in *cheB1* and/or *cheR*1, but not strains with mutations in *cheA1* or *cheY1*, have a distinct motility pattern (39; Figure 9); (iv) the motility pattern of the different *che1* mutant strains is more pronounced on malate than it is on fructose, consistent with our previous findings that CheB1-dependent demethylation of chemoreceptors is required in response to malate but not to fructose (39); (v) the IZ15 mutant (21) can be complemented by expressing CheB1 and CheR1 from a plasmid. Interestingly, the $CheB_{II}$ adaptation protein from the *che2* operon of *R. leguminosarum* bv. *viciae* was also suggested to indirectly modulate chemotaxis mediated by the *che1* operon which is

essential for all chemotactic behaviors in this species (30). The role of the Che1 pathway of *A. brasilense* in aerotaxis is puzzling since each *che1* mutant is differently affected, consistent with an indirect role of the Che1 pathway in mediating this behavior. Previously, we have shown that a strain carrying a mutation in both *cheB1* and *cheR1* (BS104) was impaired in aerotaxis while strains carrying a mutation only in *cheB1* or *cheR1* were null for aerotaxis (39). Our finding that the AB103 strain had an impaired aerotactic phenotype mostly similar to that of BS104 (39) lends further support to this hypothesis.

Several mechanisms can be invoked to explain how CheB1 and/or CheR1 proteins, but not other Che1 pathway components, could mediate chemotaxis. One possibility is that CheB1 and CheR1 together with other adaptation proteins, including some directly involved in controlling chemotaxis, contribute to the overall methylation status of chemotaxis transducers, and thus fine-tune the sensitivity of the chemotactic response. In this scenario, in the absence of components of the Che1 pathway, there is a change in the sensitivity of the chemotactic response and an impaired, rather than a null chemotactic phenotype, is expected. Our observation that strains carrying mutations in *cheB1* and *cheR1* have the most severe defect in chemotaxis (39) and that several *che1* mutant strains, but not AB103 or BS110 (both lacking a functional Che1 pathway), are generally affected, but not null for chemotaxis would fit such a model. An alternative possibility is that the methylation status of chemoreceptors and/or the activity of CheB1 and CheR1 affect the activity of other protein(s) that directly regulates chemotaxis. Candidates for such functions are CheC and CheD homologs, which have been studied in most detail in *B. subtilis* (33). CheC was shown to have a dual role as a phosphatase for P~CheY as well as in adaptation by interacting with CheB and affecting its activity on chemoreceptors in a

methylation-independent process (33). CheC has also been proposed to bind directly to the switch of the flagellar motor and to affect the motility pattern (37). It is interesting to note that methylation-independent adaptation was previously shown to be important in chemotaxis in *A. brasilense* (39) and that the genome of *A. brasilense* encodes two CheC homologs (http://genome.ornl.gov/microbial/abra), whose function remains to be determined. CheD modifies chemoreceptors by deamidation and can modulate their sensitivity and/or signal transduction abilities (34). There are two homologs of CheD encoded within the *A. brasilense* genome (http://genome.ornl.gov/microbial/abra). A third possibility, that does not exclude the previous two hypotheses, is that the Che1 pathway contributes directly to chemotaxis but competes with other chemotaxis pathway(s) for the flagellar motor targets and thus provides a redundant function. In this latter alternative, other pathway(s) or protein(s) are expected to compensate for the lack of activity of Che1 on the flagellar motors. There are three other chemotaxis-like operons in addition to Che1, as well as an additional genetically unlinked CheY homolog within the *A. brasilense* genome (http://genome.ornl.gov/microbial/abra). Any of the possibilities described above, alone or in combination, could possibly account for our data. Insights into the function of other chemotaxis clusters and adaptation proteins should refine these hypotheses.

Che1 modulates changes in cell morphology

The effect of *che1* mutations on the clumping behavior depended on the growth conditions whereas the effects on cell length were observed under all conditions at low O.D. The changes in cell length were predicted to significantly reduce nutrient uptake in shorter cells (strains carrying mutation in *cheA1*, *cheY1* and *che1*) compared to longer cells (strain carrying

mutation in both *cheB1* and *cheR1*), suggesting that the Che1 pathway may function to modulate cell length as an adaptive response to optimize nutrient uptake. The effects on clumping were observed under conditions of growth at high (but not low) aeration, suggesting a role for oxygen (or a related parameter such as intracellular energy) in this process. *Azospirillum* spp. are microaerophilic in that they generate maximum intracellular energy at low oxygen concentrations and they actively seek environments with low oxygen tensions by aerotaxis (48). Interestingly, when motile cells of *A. brasilense* accumulate within an aerotactic band, cells in front of the aerotactic band experience higher oxygen concentrations and these cells tend to form clumps that are dynamic with some cells joining the clumps as they leave the optimal conditions of the aerotaxis band (4, 48). These clumps are similar to those formed by strains carrying mutations in *cheA1*, *cheY1* and *che1* under conditions of high aeration. Given that cell clumping is only observed under conditions of growth at high aeration (growth with vigorous shaking, front of an aerotaxis band and growth under flocculation conditions), this behavior may represent an adaptive response to high oxygen concentrations which is known to decrease the energy levels in *A. brasilense* (48). One possibility is that in clumped cells, the cell surfaces involved in cell-to-cell clumping are no longer (or less) available for exchanges with the surrounding medium, regardless of cell size or shape, thus providing a possible advantage to limiting oxygen diffusion under these conditions. It also suggests that the changes in the cell length observed under conditions where *A. brasilense* generates maximum energy (48) (low aeration, low O.D.) may be an alternative response to clumping and that both behaviors would represent adaptive responses in order to optimize metabolism. However, we can not rule out the possibility that the changes in cell length are secondary i.e. that changes in cell length are morphological manifestations of

other primary effects not detected here. Irrespective of that, the observation that the Che1 pathway affects (even if only indirectly) the cell length in *A. brasilense*, as well as clumping, is intriguing as it suggests that these two functions are linked.

Based on the *E. coli* paradigm for chemotaxis, the CheA1 and CheY1 homologs are expected to comprise the excitation pathway with CheY1 as the signaling output (31, 41, 42). If CheY1 is the signaling output of the pathway described in this study, then strains carrying mutations in *cheA1*, *cheY1* and *che1* are expected to have similar phenotypes and should no longer be capable of transducing signals and causing an adequate cellular response. Indeed, we found that these strains (AB101, AB102, AB103, BS110) are biased toward shorter cell lengths and toward a higher propensity to clump under conditions of high aeration, suggesting that CheY1 provides the signaling output for this pathway. In *E. coli* chemotaxis, CheB and CheR comprise an adaptation system that allows the cells to return to a pre-stimulus motility pattern (12, 38). By analogy, we propose that cells of the BS104 strain that lacks functional CheB1 and CheR1 receive the positive signal for cell elongation, or negative signal for clumping, but do not adapt, yielding a population of cells significantly biased toward longer cells or free-swimming, non-clumping cells, respectively. The different clumping behaviors of strains with mutations in the *che1* cluster would also explain their different flocculation phenotypes since clumping is a prerequisite to flocculation (13). Taken together, our data strongly support the notion that the main output activity of the *che1* operon in *A. brasilense* results in a positive signal for cell elongation and a negative signal for clumping (under high aeration conditions). The sugar composition of EPS produced by *A. brasilense* was shown to change depending on the stage of growth and the growth conditions (3). Furthermore, it was recently shown that *A. brasilense*

constitutively produces an outer membrane lectin that interacts with an unidentified oligosaccharide structure found in arabinose-rich EPS, which is specifically produced in aggregating *A. brasilense* cells, suggesting that this lectin may be required for flocculation (3, 14, 32). Here we show that strains with mutations in *che1* are affected in their ability to produce Congo Red-binding EPS, suggesting that the Che1 pathway affects the production of some EPS. Thus, although the exact mechanism responsible for the clumping behavior is still unknown, we hypothesize that it involves changes in cell surface properties such as changes in the structure and/or composition of EPS. Interestingly, the effect of the Che1 pathway of *A. brasilense* in modulating the cell surface properties (cell length and possibly clumping via EPS production) is reminiscent of the effect of the *che2* chemotaxis-like signal transduction pathway which regulates flagella biogenesis in *Rhodospirillum centenum* (8) and the Dif pathway which modulates fibril polysaccharide biogenesis in *Myxococcus xanthus* (5, 46). Similarly to Che1 of *A. brasilense*, the exact mechanism(s) by which these chemotaxis-like signal transduction pathways affect non-chemotactic cellular properties remains to be determined. While we have yet to identify the molecular targets of the Che1 pathway, our results suggest that this pathway may affect molecular machinery responsible for concomitantly regulating cell elongation (positive regulation), and clumping behavior, likely via production of specific EPS (negative regulation).

Potential implications for the role of Che1 in modulating changes in cell surface properties

Why would *A. brasilense* use a Che-like signal transduction pathway to coordinate such dynamic changes in cell surface properties? Several features of information processing by Che-like pathways make them particularly well-suited for the regulation of dynamic cellular

behaviors. First, multiple cues sensed by independent putative chemoreceptors may be integrated into a single cellular response by interaction with a particular chemotaxis-like pathway. Thus, chemotaxis-like responses are initiated when a set of conditions, rather than a single trigger, are met. Second, the activity of CheB and CheR homologs on chemoreceptors modulates chemosensory sensitivity so that a response to concentration changes is initiated under a broad range of background conditions. Although we have not identified a particular chemoreceptor for the Che1 pathway, we have shown that CheB1 and CheR1 are functional and essential for at least some behavioral responses (39), indicating that these proteins function to modulate sensory input. Furthermore, we have described phenotypes of strains carrying mutations in *che1* genes that are dependent on growth conditions, suggesting that environmental input is required to modulate the observed responses. Comparative genomics indicate that many bacterial genomes encode multiple chemotaxis-like pathways including some that were shown to regulate cellular behaviors *a priori* not directly related to flagellar motility (45). In addition, as shown here and elsewhere (30, 21), orthologous chemotaxis-like operons may modulate different cellular functions in closely related bacterial species. This observation thus suggests that these signal transduction systems evolve rapidly as they are likely to provide significant advantages to the organisms that must constantly seek optimum conditions for growth in ever-changing environments. The function of Che1 in modulating dynamic changes in cell morphology expands the range of cellular functions modulated by such versatile signal transduction pathways.

ACKNOWLEDGMENTS

We thank Annie Lin for the initial characterization of the Congo Red phenotypes of some of the mutants and help with the some of the chemotaxis assays. The authors thank M. Lidström for the gift of the pCM184 plasmid and Matt Russell, Beth Mullin, Igor Zhulin and anonymous reviewers for insightful comments on the manuscript. This work was supported by a NSF CAREER award (MCB-0622277) and generous start-up funds from the University of Tennessee, Knoxville to G.A.

Chapter 1

Function of a chemotaxis-like signal transduction pathway in modulating motility, cell clumping, and cell length in the alphaproteobacterium *Azospirillum brasilense*

References

1. **Alexandre, G., S.E. Greer, and I. B. Zhulin.** 2000. Energy taxis is the dominant behaviour in *Azospirillum brasilense*. J. Bacteriol **182**: 6042-6048.

2. **Ames, P., C. A. Studdert, R. H. Reiser, and J. S. Parkinson. 2002.** Collaborative signalling by mixed chemoreceptor teams in *Escherichia coli.* Proc. Natl. Acad. Sci**.** USA **99**:7060-7065.

3. **Bahat-Samet, E., S. Castro-Sowinski, and Y. Okon.** 2004. Arabinose content of extracellular polysaccharide plays a role in cell aggregation of *Azospirillum brasilense*. FEMS Microbiol. Lett. **237**:195-203.

4. **Barak, I., I. Nur, Y. Okon, and Y. Henis.** 1982. Aerotactic response of *Azospirillum brasilense*. J. Bacteriol. **152**:643–649.

5. **Bellenger, K. , X. Ma. W. Shi, and Z. Yang.** 2002. A CheW homologue is required for *Myxococcus xanthus* fruiting body development, social gliding motility and fibril biogenesis. J. Bacteriol. **184**:5654-5660.

6. **Berg, H. C., and D. A. Brown.** 1972. Chemotaxis in *Escherichia coli* analyzed by three-dimensional tracking. Nature **239**:500-504.

7. **Berg, H. C., and E. M. Purcell.** 1977. Physics of chemoreception. Biophys. J. **20**:193-219.

8. **Berleman, J. E., and C. E. Bauer.** 2005a. A che-like signal transduction cascade involved in controlling flagella biosynthesis in *Rhodospirillum centenum*. Mol. Microbiol. **55**:1390-1402.

9. **Berleman, J. E., and C. E. Bauer.** 2005b. Involvement of a Che-like signal transduction cascade in regulating cyst cell development in *Rhodospirillum centenum*. Mol. Microbiol. **56**:1457-1466.

10. **Blackhart, B. D. and D. R. Zusman.1985.** "Frizzy" genes of *Myxococcus xanthus* are involved in control of frequency of reversal of gliding motility. Proc. Natl. Acad. Sci. USA **82**:8767-8770.

11. **Bradford, M. M.** 1976. A rapid and sensitive method for the quantitation of microgram quantities of protein utilizing the principle of protein dye binding. Anal. Biochem. **72**:248-254.

12. **Borkovitch, K. A., Alex, L. A., and M. I. Simon.** 1992. Attenuation of sensory receptor signaling by covalent modification. Proc. Natl. Acad. Sci.USA **89**:6756-6760.

13. **Burdman, S., E. Jurkevitch, M. E. Soria-Diaz., A. M. Serrano, and Y. Okon.** 1998. Aggregation of *Azospirillum brasilense*: effects of chemical and physical factors and involvement of extracellular components. Microbiology **144**:1989-1999.

14. **Burdman, S., E. Jurkevitch, M. E. Soria-Diaz., A. M. Serrano, and Y. Okon.** 2000. Extracellular polysaccharide composition of *Azospirillum brasilense* and its relation to cell aggregation. FEMS Microbiol. Lett. **189**:259-264.

15. **Dennis, J., G. Zylstra.**1998. Improved antibiotic-resistance cassettes through restriction site elimination using Pfu DNA polymerase PCR. Biotechniques **25**:72-776.

16. **Dombrecht B., J. Vanderleyden, and J. Michiels.** 2001. Stable RK2-derived cloning vectors for the analysis of gene expression and gene function in gram-negative bacteria. Mol. Plant-Microbe Interact. **14**:426-430.

17. **Dubois M., K. A. Gilles, J. K. Hamilton, P. A. Rebers, and Fred Smith.** 1956. Colorimetric method for determination of sugars and related substances. Anal. Chem. **28**:350-356.

18. **Enos-Berlage J. L., and L. L. McCarter.** 2000. Relation of capsular polysaccharide production and colonial cell organization to colony morphology in *Vibrio parahaemolyticus*. J. Bacteriol. **182**: 5513-5520.

19. **Errington, J., R. A. Daniel, and D. J. Scheffers.** 2003. Cytokinesis in bacteria. Microbiol. Mol. Biol. Rev. **67**:52-65.

20. **Figurski, D. H., and D. R. Helinski.** 1979. Replication of an origin-containing derivative of plasmid RK2 dependent on a plasmid function provided *in trans*. Proc. Natl. Acad. Sci. USA **76**:1648–1652.

21. **Hauwaerts, D., G. Alexandre, S. K. Das, J. Vanderleyden, and I. B. Zhulin**. 2002. A major chemotaxis gene cluster in *Azospirillum brasilense* and relationships between chemotaxis operons in alpha-proteobacteria. FEMS Microbiol. Lett. **208**: 61-67.

22. **Hickman, J.W., T. F. Tifrea, and C. S. Harwood.** 2005. A chemosensory system that regulates biofilm formation through modulation of cyclic diguanylate levels. Proc. Natl. Acad. Sci. USA **102**:14422-14427.

23. **Jiang, Z. J., H. Gest, and C. E. Bauer.** 1997. Chemosensory and photosensory perception in purple photosynthetic bacteria utilize common signal transduction components. J. Bacteriol. **179**: 5720–5727.

24. **Katzen, F., A. Becker, M. V. Ielmini, C. G. Oddo, and L. Ielpi.** 1999. New mobilizable vectors suitable for gene replacement in gram-negative bacteria and their use in mapping of the 3' end of the *Xanthomonas campestris* pv. *campestris* gum operon. Appl. Environ. Microbiol. **65**:278–282.

25. **Keen N.T., S. Tamaki, D. Kobayashi, and D. Trollinger.** 1988. Improved broad-host-range plasmids for DNA cloning in gram-negative bacteria. Gene **70**:191-197.

26. **Katupitya, S., J. Millet, M. Vesk, L. Viccars, A. Zeman, Z. Lidong, C. Elmerich, and I. R. Kennedy.** 1995. A mutant of Azospirillum brasilense Sp7 impaired in flocculation with a modified colonization pattern and superior nitrogen fixation in association with wheat. Appl. Environ. Microbiol. **61**:1987-1995.

27. **Kirby, J. R. and D. R. Zusman.** 2003. Chemosensory regulation of developmental gene expression in *Myxococcus xanthus*. Proc. Natl. Acad. Sci. USA **100**:2008- 2013.

28. **Kovach M. E., P. H. Elzer, D. S. Hill, G. T. Robertson, M. A. Farris, R. M. Roop 2nd, and K. M. Peterson.** 1995. Four new derivatives of the broad-host-range cloning vector pBBR1MCS, carrying different antibiotic-resistance cassettes. Biotechniques **166**:175-176.

29. **Marx, C. J., and M. E. Lidström**. 2002. Broad-host-range *cre-lox* system for antibiotic marker recycling in gram-negative bacteria. Biotechniques **33**:1062-1067.

30. **Miller, L. D., C. K. Yost, M. F. Hynes and G. Alexandre.** 2007. The major chemotaxis gene cluster of *Rhizobium leguminosarum* bv. *viciae* is essential for competitive nodulation. Mol. Microbiol. **63**:348-362.

31. **Montrone, M., M. Eisenbach, D. Oesterhelt, and W. Marwan.** 1998. Regulation of switching frequency and bias of the flagellar motor by CheY and fumarate. J. Bacteriol. **180**:3375-3380.

32. **Mora, P., F. Rosconi, L. Franco Franguas, and Susana-Sowinski.** 2008. *Azospirillum brasilense* Sp7 produces an outer-membrane lectin that specifically binds to surface-exposed extracellular polysaccharide produced by the bacterium. Arch. Microbiol. **189**:519-524.

33. **Rosario M. M., J. R. Kirby, D. A. Bochar, and G. W. Ordal.** 1995. Chemotactic methylation and behavior in *Bacillus subtilis*: role of two unique proteins, CheC and CheD. Biochemistry **21**: 3823-3831.

34. **Rosario M. M., and G. W. Ordal.** 1996. CheC and CheD interact to regulate methylation of *Bacillus subtilis* methyl-accepting chemotaxis proteins. Mol. Microbiol. **21**:511-518.

35. **Sadasivan L. and C. A. Neyra.** 1985. Flocculation in *Azospirillum brasilense* and *Azospirillum lipoferum*: exopolysaccharides and cyst formation. J. Bacteriol. **163**:716-723.

36. **Sambrook J. and D. W. Russell.** 2001. Molecular cloning: a laboratory manual, 3rd ed. Cold Spring Harbor Laboratory Press, Cold Spring Harbor, N.Y.

37. **Saulmon M. M., E. Karatan, and G. W. Ordal.** 2004. Effect of loss of CheC and other adaptational proteins on chemotactic behaviour in *Bacillus subtilis*. Microbiology **150**:581-589.

38. **Segall, J. E., S. M. Block, and H. C. Berg.** 1986. Temporal comparisons in bacterial chemotaxis. Proc. Natl. Acad. Sci. USA **83**:8987-8991.

39. **Stephens, B. B. Loar, S. N., and G. Alexandre**. 2006. Role of CheB and CheR in the complex chemotactic and aerotactic pathway of *Azospirillum brasilense*. J. Bacteriol. **188**: 4759-4768.

40. **Swanson, R. V., L. A. Alex, and M. I. Simon.** 1994. Histidine and aspartate phosphorylation: two-component systems and the limits of homology. Trends Biochem**.** **19**: 485-490.

41. **Szurmant, H., and G. H. Ordal.** 2004. Diversity in chemotaxis mechanisms among the bacteria and archaea. Microbiol. Mol. Biol. Rev. **68**:301-319.

42. **Wadhams, G. H., and J. P. Armitage.** 2004. Making sense of it all: bacterial chemotaxis. Nat. Rev. Mol. Cell Biol. **5**:1024-1037.

43. **Wagner, J. K., S. Setayeshgar, L. A. Sharon, J. P. Reilly, and Y. V. Brun.** 2006. A nutrient uptake role for bacterial cell envelope extensions. Proc. Natl. Acad. Sci. USA **103**:11772-11777.

44. **West, A. H., and A. M. Stock.** 2001. Histidine kinases and response regulator proteins in two-component signaling systems. Trends Biochem. Sci. **26**:369-376.

45. **Wuichet, K., R. P. Alexander, and I. B. Zhulin.** 2007. Comparative genomic and protein sequence analyses of a complex system controlling bacterial chemotaxis. Methods Enzymol. **422:**3-31.

46. **Yang, Z., Geng, D., Xu, H,m H. B. Kaplan, and W. Shi.** 1998. A new set of chemotaxis homologues is essential for *Myxococcus xanthus* social motility. Mol. Microbiol. **30**:1123-1130.

47. **Zhulin, I. B.** 2001. The superfamily of chemotaxis transducers: from physiology to genomics and back. Adv. Microbiol. Physiol. **45**:157-198.

48. **Zhulin, I. B., V. A. Bespalov, M. S. Johnson, and B. L. Taylor.** 1996. Oxygen taxis and proton motive force in *Azospirillum brasilense*. J. Bacteriol. **178**:5199–5204.

Chapter 2

The *Azospirillum brasilense* Che1 chemotaxis pathway controls the swimming velocity which affects transient cell-to-cell clumping

Disclosure

Chapter 2 is reproduced in part with permission from Amber N. Bible; Matthew H. Russell; Gladys Alexandre. "The *Azospirillum brasilense* Che1 chemotaxis pathway controls the swimming velocity which affects transient cell-to-cell clumping". *Journal of Bacteriology*, just accepted, 2012.

In this article, Dr. Gladys Alexandre is the principal investigator from whom guidance and experimental advice was obtained. Matthew H. Russell performed the temporal assay and the measurements of clumping, reversal frequency, and speed associated with this assay. All other experiments were my own work.

Abstract

The Che1 chemotaxis-like pathway of *Azospirillum brasilense* contributes to chemotaxis and aerotaxis, and it has also been found to contribute to regulating changes in cell surface adhesive properties that affect the propensity of cells to clump and to flocculate. The exact contribution of Che1 to the control of chemotaxis and flocculation in *A. brasilense* remains poorly understood. Here, we show that Che1 affects reversible cell-to-cell clumping, a cellular behavior in which motile cells transiently interact by adhering to one another at their non-flagellated pole before swimming apart. Clumping precedes and is required for flocculation and both processes appear independently regulated. The phenotypes of an Δ*aerC* receptor mutant and of mutant strains lacking *cheA1*, *cheY1*, *cheB1*, *cheR1* (alone or in combination) or deleted for *che1* show that Che1 directly mediates changes in the flagellar swimming velocity and that this behavior directly modulates the transient nature of clumping. Our results also suggest that additional receptor(s) and signaling pathway(s) are implicated in mediating other Che1-independent changes in clumping identified in the present study. Transient clumping precedes the transition to stable clump formation, which involves the production of specific extracellular polysaccharide (EPS); however, production of these clumping-specific EPS is not directly controlled by Che1 activity. Che1-dependent clumping may antagonize motility and prevent chemotaxis, thereby maintaining cells in a metabolically favorable niche.

Section A. Introduction

The ability of bacteria to sense and adapt to changes within their environment is an essential survival strategy. At the molecular level, signal transduction pathways couple sensing of environmental changes with adaptive responses which includes modulation of gene expression, enzyme activities or protein-protein interactions (34).

Chemotaxis in *Escherichia coli* is considered the best studied signal transduction pathway. The *E. coli* chemotaxis signal transduction pathway functions to control the probability of changes in the flagellar motility pattern in response to physicochemical cues detected by dedicated chemotaxis receptors. These receptors form ternary signaling complexes with cytoplasmic chemotaxis proteins that include a histidine kinase, CheA, and an adaptor protein, CheW. Following repellent signal reception, CheA becomes autophosphorylated at a conserved histidine residue and phosphorylates its cognate response regulator, CheY. Phosphorylated CheY controls the probability of changes in the direction of flagellar rotation. The signaling activity of chemoreceptors is modulated by antagonistic activities of the methyltransferase CheR and the methylesterase CheB, thus allowing sensory adaptation. CheR constitutively adds methyl groups to specific glutamate residues in the C-terminal signaling region of receptors, while CheB esterase activity depends on phosphorylated CheA. CheA is thus the central regulator of the chemotaxis response as it links the forward excitation pathway that triggers the CheY-dependent signaling output with the feedback adaptive loop dependent on CheB activity (28, 34). This prototypical chemotaxis signal transduction pathway is conserved in closely and distantly related bacterial species (36). Emerging evidence from the analysis of completely sequenced genomes

indicates that most bacterial species possess more than one chemotaxis signal transduction pathway (30, 41). Additional chemotaxis-like signal transduction pathways (also named chemosensory signal transduction pathways) have been shown to be implicated in the regulation of non-motility behaviors (15).

Azospirillum brasilense is an alphaproteobacterium and diazotrophic motile microorganism found in soil and rhizosphere habitats. *A. brasilense* have an oxidative metabolism that is optimum under microaerophilic conditions, with maximum energy generated at about 0.4% dissolved oxygen (40). Motile cells actively seek low oxygen concentrations for optimum metabolism by aerotaxis as well as by monitoring changes in the metabolic status via energy taxis (1, 3). Energy taxis is mediated by dedicated energy sensing receptors that allow *A. brasilense* to locate environments that are optimum for growth (1, 9, 40). Monitoring fluctuations in intracellular energy levels is the preeminent mode of sensing in *A. brasilense* (1), suggesting that in this organism, adaptive cellular behaviors such as aerotaxis, are tightly coupled with metabolism.

The *A. brasilense* Che1 chemotaxis signal transduction pathway comprises homologs of CheA, CheW, CheY, CheB and CheR that mediate energy taxis responses. Despite similarity to prototypical chemotaxis pathways, the *A. brasilense* Che1 pathway has been shown to be functionally divergent in that it appears to regulate taxis behaviors, as well as other cellular functions, including cell-to-cell clumping and flocculation (4). Experimental evidence indicates that *che1* pathway mutants display changes in cell surface adhesive properties, likely in the structure and/or composition of EPS, that ultimately modulate the ability of cells to clump and to flocculate (4, 7, 11, 27, 29). Furthermore, the contribution of Che1 to the control of motility-

dependent taxis responses seems to be more complex than those in other bacterial species, perhaps involving additional chemotaxis signal transduction pathways and/or auxiliary chemotaxis proteins (4, 29, 35). The Che1 pathway was also shown to indirectly affect changes in the swimming direction of cells, and thus the motility bias (4, 29). Prior biochemical and genetic evidence have suggested that CheB1 and CheR1 from the Che1 pathway participate in signaling cross-talk with other chemotaxis pathway(s) by altering the methylation status of chemoreceptors (29). In support of this possibility, the genome of *A. brasilense* encodes for three chemotaxis-like signal transduction pathways, in addition to Che1, as well as several ancillary chemotaxis proteins (35). The functions of these chemotaxis-like pathways and proteins have not been determined.

In *A. brasilense*, flocculation results from the differentiation of motile, rod-shaped cells into aggregates of non-motile, spherical cells that are encased in a dense fibrillar polysaccharide material (flocs) visible to the naked eye (25). Flocculated cells are not dormant, but are highly resistant to various environmental insults (25). To date, the only known regulator affecting this differentiation process is an orphan transcriptional regulator, named FlcA, for which no cognate sensor kinase has been identified (13, 22, 23). Che1 signaling output might mediate changes in EPS production by directly affecting transcription of putative EPS biosynthetic genes. However, evidence for this hypothesis or in support of a genetic link between Che1 effects on taxis responses and on cell surface adhesive properties is lacking. In addition, the link between Che1 function and flocculation (and FlcA) remains uninvestigated.

In this study, we clarify the role of Che1 in flocculation. By characterizing a set of *che1* mutant strains and an energy taxis receptor mutant, we provide evidence that Che1 modulates

reversible cell-to-cell interactions between motile cells, that we call "clumping". We also show that Che1 does not directly regulate changes in EPS production. Interestingly, we found that the mechanism by which Che1 affects clumping behavior is by modulating the swimming velocity of cells. The role for Che1 in modulating transient cell-to-cell clumping via direct regulation of the swimming velocity provides insight into how this chemotaxis pathway may function to coordinate taxis behaviors with reversible cell-to-cell interactions in clumping.

Section B. Materials and Methods

Bacterial Strains and Growth Conditions

Table 3 describes the strains and plasmids used in this study. Cells were grown at 28ºC with shaking in rich TY (1 liter contains 10 grams Tryptone and 5 grams Yeast extract) media or MMAB (minimal media) (11). In order to induce clumping behavior and flocculation, 100 µl of an overnight culture of cells grown in TY media (OD_{600nm} = 1) was used to inoculate 5 ml of flocculation media (MMAB containing 0.5 mM Sodium Nitrate as sole nitrogen source and 8 mM Fructose as sole carbon source) and then grown with shaking at 28ºC. For the time course of clumping and flocculation, cells were inoculated into flocculation media and grown with high aeration and vigorous shaking (225 rpm). Aliquots of cultures were observed microscopically at the time of inoculation, 3 hours post-inoculation (hpi), 6 hpi, 9 hpi, 14 hpi, and 24-30 hpi (time at which wild type cells are flocculated). The times (along with standard deviations) indicated in Table 2 were determined from multiple independent experiments (n = 5). Cells were visualized using a Nikon Eclipse E200 phase-contrast microscope at a final magnification of 400X and

Table 3. Strains and plasmids used in this study

Strain or plasmid	Genotype, relevant characteristics	Reference or Source
Plasmids		
pBBR1MCS3	Cloning vector (Tc)	16
pRK415	Cloning vector (Tc)	14
pBBR-*cheA1*	pBBR1MCS3 containing *cheA1*	4
pBBR-$cheA1_{H252Q}$	pBBR1MCS3 containing $cheA1_{H252Q}$	this work
pBBR-*cheB1*	pBBR1MCS3 containing *cheB1*	this work
pBBR-$cheB1_{D78N}$	pBBR1MCS3 containing $cheB1_{D78N}$	this work
pRK-*cheY1*	pRK415 containing *cheY1*	4
pRK-$cheY1_{D52N}$	pRK415 containing $cheY1_{D52N}$	this work
Strains		
Escherichia coli		
TOP10	General cloning strain	Invitrogen
S17-1	*thi endA recA hsdR* with RP4-2Tc::Mu-Km::Tn7 integrated in chromosome	26
Azospirillum brasilense		
Sp7	Parental strain, "wild type"	ATCC29145
AB101	Δ(*cheA1*)::*gusA-Km* (Km)	4
GA3	Δ(*cheB1*)::*gusA-Km* (Km)	29
BS109	Δ(*cheR1*)::*Gm* (Gm)	29
BS104	Δ(*cheB1cheR1*)::*Km* (Km)	29
AB102	Δ(*cheY1*)::*Km* (Km)	4
AB103	Δ(*cheA1-cheR1*)::*Cm* (Cm), also named Δ*che1*	4
AB301	Δ*aerC*::*Km* (Km)	37
AB302	Δ(*cheA1-cheR1*) Δ(*aerC*)::*Km* (Cm, Km), also named Δ*che1* Δ*aerC*	this work
Sp72002	*flcA*::Tn5 (Km)	22
AB104	Δ(*cheA1-cheR1*), *flcA*::Tn5 (Cm, Km)	this work
Wild type (pRK415)	Wild type strain (Sp7) containing pRK415 (Tc)	4
Wild type (pBBR)	Wild type strain (Sp7) containing pBBR1MCS3 (Tc)	4
AB101 (pBBR)	AB101 containing pBBR1MCS3 (Tc)	4
AB101 (pBBR-*cheA1*)	AB101 containing pBBR-*cheA1* (Tc)	4
AB101 (pBBR-$cheA1_{H252Q}$)	AB101 containing pBBR-$cheA1_{H252Q}$ (Tc)	this work
GA3 (pBBR)	GA3 containing pBBR	this work
GA3 (pBBR-*cheB1*)	GA3 containing pBBR-*cheB1*	this work
GA3 (pBBR-$cheB1_{D78N}$)	GA3 containing pBBR-$cheB1_{D78N}$	this work
AB102 (pRK415)	AB102 containing pRK415	4
AB102 (pRK-*cheY1*)	AB102 containing pRK-*cheY1*	4
AB102 (pRK-$cheY1_{D52N}$)	AB102 containing pRK-$cheY1_{D52N}$	this work

Antibiotic resistance abbreviations: Tc (tetracycline), Km (kanamycin), Gm (gentamycin), Cm (chloramphenicol)

photographs were taken of at least three different fields-of-view per sample per time point during this time course using a Nikon Coolpix P5000 camera. Digital videos were captured using a Sony Hyper HAD high resolution black and white camera at 400X (final) magnification and cover slips were added to enhance clarity. Timing of clumping and flocculation, as well as the accompanying behavioral and morphological changes observed were highly reproducible.

***Construction of* (Δ*che1-flcA*::Tn5) (AB104) mutant and of a Δ*aerC*Δ*che1* (AB302) mutant**

The Δ*che1-flcA* double mutant strain was generated using the previously described pKGmobGARCm construct, previously used to generate Δ*che1* (4). A biparental mating with the *flcA*::Tn5 (Sp72002) mutant strain as a recipient was performed as previously described (29) to construct the double mutant. Candidate Δ*che1-flcA* (AB104) mutants were verified using PCR. The same technique was used to introduce a *che1* mutation in the previously constructed Δ*aerC* (AB301) mutant background (37) and generate the Δ*aerC*Δ*che1* strain AB302.

Complementation and site-specific mutations of Che1 genes

Generation of constructs for complementation of Δ*cheA1* (AB101) was performed previously (4). The site-specific mutant, $cheA1_{H252Q}$, was generated previously (unpublished data) using the QuikChangeII Site-directed Mutagenesis Kit (Stratagene). The following primers were used to generate $cheA1_{H252Q}$: forward primer, 5'-CATCTTCCGTCTGGTGCAGACCATCAAGGG CACC-3' and reverse primer, 5'-GGTGCCCTTGATGGTCTGCACCAGACGGAAGATG-3' [underlined letter refers to the specific base which was mutated to change CAC (codon for histidine) to CAG (codon for glutamine)]. The $cheA1_{H252Q}$ was then cloned into pProEx-HTA

(yielding pIZ105). In order to generate pBBR-*cheA1*$_{H252Q}$ expressed from its own promoter in the pBBR-MCS3 vector , the promoter region of the *che1* operon, found upstream of *cheA1*, was first amplify from pBBR-*cheA1* (4) using cheA1promXho-F (5'-CCGCTCGAGCAGCGCGATGAACTGGTT-3' with the XhoI restriction site underlined) and cheA1HQup-R (5'-AAGCTTACGGACCAGTTCCAC-3' with the HindIII restriction site underlined). Next, primers cheA1HQdown-F (5'-AAGCTTCTGGAGCAGAATCCC-3' with the HindIII restriction site underlined) and cheA1fullXba-R (5'-GCTCTAGATCATGCGGCACCTTTCTGC-3' with the XbaI restriction site underlined) were used to amplify *cheA1*$_{H252Q}$ from pIZ105. Each PCR fragment was icloned into the pCR2.1 TOPO vector and sequenced prior to cloning into pBBR-MCS3 (16). These fragments were inserted into the pBBR-MCS3 vector using the following digestions: cheA1HQup (XhoI and HindIII), cheA1 HQ down (HindIII and XbaI), pBBR-MCS3 (XhoI and XbaI). The final product fuses the upstream region of cheA1 containing the putative promoter with *cheA1*$_{H252Q}$ in pBBR-MCS3. The final construct was introduced into wild type *A. brasilense* Sp7 and Δ*cheA1* (AB101) strain using biparental mating as described previously (29).

Constructs for complementation of Δ*cheY1* (AB102) were also generated previously (4). The site-specific mutant, *cheY1*$_{D52N}$, was generated by amplifying *cheY1*$_{D52N}$ from pIZ103 (2), using the primers used to amplify *cheY1* for complementation (4), and sub-cloning into the pCR2.1 TOPO vector. Upon verification by sequencing, *cheY1*$_{D52N}$ was isolated from this vector using restriction digestion with HindIII and EcoRI, and ligated into pRK415 digested with the same enzymes (14). The newly constructed pRK-*cheY1*$_{D52N}$ was introduced into the wild type Sp7 strain and the Δ*cheY1* mutant strain by biparental mating as described previously (29).

Complementation of the Δ*cheB1* mutant was performed by amplifying the *cheB1* gene from genomic DNA using the primers cheB1R1forward (5'-CCCAAGCTTTA**AGGAGA**GGCCCGTATGTCCGATGGTTTCGGCAGAC-3' with the HindIII site underlined and the ribosome binding site in bold) (4) and cheB1reverse (5'-GGGCTCGAGTCATGCTGCCCTCGATGCGAAC -3' with the XbaI site underlined). The amplified *cheB1* gene was sub-cloned into pCR2.1 TOPO and verified by sequencing. The *cheB1* gene was isolated by digestion with HindIII and XhoI, and ligated into pBBR-MCS3 digetsed with the same enzymes (16). The newly constructed pBBR-*cheB1* was introduced into the wild type Sp7 strain and Δ*cheB1* (GA3) strain by biparental mating.

The site-specific mutant, $cheB1_{D78N}$, was generated using the QuikChangeII Site-directed Mutagenesis Kit (Stratagene) accodirng to the manufacturer's instructions using mutagenic primers CheBDN-F (5'-GACGTCATCGTTCTCAACATCGAGATGCCGGTG-3') and CheBDN-R (5'-CACCGGCATCTCGATGTTGAGAACGATGACGTC-3') (underlined letter refers to the specific base which was mutated to change GAC (codon for aspartic acid) to AAC (codon for asparagine)) using *cheB1* subcloned into pCR 2.1 TOPO as a template using cheB1R1forward and cheB1reverse (see above). The fragment generated ($cheB1_{D78N}$) was cloned into pCR2.1 TOPO and the presence of the correct mutation was verified by sequencing of the entire open reading frame in both directions. In order to generate pBBR-$cheB1_{D78N}$, HindIII and XhoI were used to isolate $cheB1_{D78N}$ before cloning it into pBBR-MCS3 (16) digested with the same enzymes. pBBR-$cheB1_{D78N}$, was introduced into wild type *A. brasilense* Sp7and Δ*cheB1* (GA3) using biparental mating as described previously (29).

Gas perfusion chamber assay for clumping and image analysis

A 10 µl drop of cells grown under high aeration in MMAB supplemented with 0.1% (w/v) NH_4Cl and 0.5% (w/v) sodium pyruvate to late log phase ($O.D._{600}$ ~ 0.7), first washed before being re-suspended in MMAB supplied with 10 mM pyruvate, was placed in a gas perfusion chamber in which the humidified gas flowing above the drop can be controlled (17). First, compressed air (21% oxygen) is allowed to flow over the cell suspension until cells are equilibrated (usually 5 minutes) before recording of the cells' behavior begins. After one minute, a valve is switched to provide pure nitrogen to the atmosphere of the cell suspension (air removal). The cells remain motile under these conditions. After a period of 6 minutes, the nitrogen gas flowing into the chamber is switched back to air (air addition) and recording is stopped after 3 minutes (10 minutes recorded total). Each experiment was performed at least 3 times on independent samples and the behavior of the cells was highly reproducible.

The fraction of clumps in the cell suspension was determined as the number of clumps (rather than cells within clumps) relative to free-swimming cells. These ratios were measured using digital movies and the Cell Counter plug-in from ImageJ (http://rsbweb.nih.gov/ij/). Briefly, the number of clumps were identified as transient cell-to-cell contacts between motile cells in suspension, and counted manually for a given video frame or image. A minimum of 2 video frames were analyzed for each time point and each video frame comprised at least 100 cells in the field of view. Clumping in videos was verified by analyzing the motion of cells in the field of view just prior to and after the frame because the motion analysis software could not always accurately distinguish between clumps and free-swimming cells. The number of free-swimming cells was also counted for a single field-of-view in the same video frame in order to

determine the ratio of clumping cells to free-swimming cells. These measurements were repeated for at least two different fields-of-view per sample and per time point for each of the samples analyzed. The data shown are the average of these calculations. In the temporal assay in the gas perfusion chamber, the fractions of clumps were measured at given time points during the assay before and after air removal or addition. The determined ratios were then plotted over time using Microsoft Excel (Microsoft). The average swimming velocity of cells was determined on the same video files and frames described above, using computerized motion analysis (CellTrak 1.3, Santa Rosa, CA).

Extracellular complementation of clumping with extracted EPS

Extracellular polysaccharides (EPS) were extracted from 2-liter cultures of *A. brasilense* that were grown until clumping was observed. Samples of extracted EPS were used to treat 2 ml of wild type cells suspension grown under flocculation permissive conditions (but prior to clump formation), gently pelleted by centrifugation (2,500 x g for 2 minutes) and washed twice with 0.8% (w/v) sterile KCl in order to "remove" any EPS already present on the surface. We used this strategy because preliminary control experiments had shown that EPS present on the cell surface may mask the ability of exogenously added EPS to induce clumping. The cells were then re-suspended in 100 µl of flocculation medium (described above, under ***Bacterial strains and growth conditions***) with 100 µl of extracted EPS (at a final concentration of 15 µg/ml), followed by 1-2 hours incubation at room temperature with shaking. A control was incubated with water alone. Treated cells were then visualized using light microscopy. Photographs and digital videos were of cells treated with extracted EPS (or water, as a control). The fraction of

clumps was determined using both photographs and digital videos and manually counting the number of clumps (counting clumps rather than cells within clumps) relative to the total number of free-swimming cells in each field-of-view, with at least 3 distinct fields of view being analyzed per treatment and with counting a total of at least 100 cells per sample. The fold-increase in the clumping fraction was calculated relative to the control treated with water, which was taken as a reference and given the value of 1.00.

To test the effect of proteinase K treatment on the propensity of extracted EPS to mediate clumping, wild type *A. brasilense* cells were grown under flocculation conditions and collected at the onset of clumping. The cells were then concentrated by centrifugation at 2,500 x g for 2 minutes to a final volume of 100 μl. The control samples remained untreated. Test samples were treated using the following: 1) 100 μl of untreated wild type EPS and 2) 100 μl of Proteinase K-treated EPS. The EPS fraction was analyzed on a SDS-PAGE gel to verify the absence of protein after treatment with proteinase K. Cells were incubated for approximately 3-4 hours at room temperature with shaking before visualization using light microscopy. The motility or viability of cells did not appear affected by these treatments.

Western Blotting

In order to verify expression of CheA1 and CheY1 in the complementation constructs, we grew overnight cultures for each strain, then collected and lysed the cells. For samples from CheA1 complementation constructs, 250 ml of actively growing cultures were collected and cells were lysed using sonication in a lysis buffer containing 50 mM KH_2PO_4, 2 mM $MgCl_2$, and 1 mM PMSF (phenylmethanesulfonylfluoride, a serine protease inhibitor). The lysate was then

centrifuged for 5 minutes at 20,000 x g at 4°C and the supernatant was removed for analysis by SDS-PAGE. Protein concentrations were measured for each sample using the Bradford Assay (5) and each sample was adjusted to the same protein concentration. Next, a fresh solution of n-dodecyl-β-D-maltoside was added to each sample to a final concentration of 0.5% (w/v). Each sample was then boiled and analyzed using a 6% SDS-PAGE gel and an α-CheA1 antibody (against CheA1 from *A. brasilense*) at a 1:4,000 dilution with the HRP-tagged α-rabbit secondary antibody at a 1:10,000 dilution. For samples from CheY1 complementation constructs, 20 milliliters of an actively growing culture of cells were collected and lysed using sonication in phosphate-buffered saline (PBS). Each lysate was then centrifuged for 5 minutes at 20,000 x g at 4°C and the supernatant was removed for analysis by SDS-PAGE. Protein concentrations were measured for each sample using the Bradford Assay (5) and each sample was adjusted to the same protein concentration. Each sample was then boiled and analyzed using a 12% SDS-PAGE gel and an α-CheY1 antibody (against CheY1 from *A. brasilense*) at a 1:2,000 dilution and an HRP-tagged α-guinea pig secondary antibody at a 1:10,000 dilution. Analysis of CheB1 expression from the complementation constructs was not assessed due to the unavailability of an antibody against CheB1.

Section C. Results

Che1 affects clumping but not flocculation

We have shown previously that mutants carrying deletions in *cheA1*, *cheB1*, *cheY1* and *che1* flocculate more than wild type cells (4). We also found that a double mutant lacking both *cheB1* and *cheR1* flocculated very little, if at all (4). These data suggested that the Che1 pathway

directly regulates flocculation. To gain further insight into how the Che1 pathway regulates the amount of flocculation, we observed the behaviors of each strain during this process. Cells were inoculated into flocculation medium (low nitrogen and high aeration, see Materials and Methods) and the behaviors of the cells were analyzed at different times post inoculation (Fig. 15). We found that the strains carrying mutations within *che1* not only differed in the amount of flocculation, but also in the timing at which they form flocs. In comparison to the wild type strain, the Δ*cheA1* mutant flocculated after 17 hours of growth in the flocculation medium, as opposed to 24-30 hours in the wild type (Fig. 15). The Δ*cheB1* mutant flocculated the earliest, at 11 hours post-inoculation into the at observed for the Δ*cheA1* and the Δ*cheB1* mutant strain, in that it flocculated 14 hours post-inoculation. Deletion of the *che1* operon resulted in a strain (Δ*che1*) that flocculated slightly earlier than the wild type, at 19 hours. Consistent with previous data (4), the Δ*cheB1cheR1* mutant did not flocculate (4). Finally, the Δ*cheR1* mutant resembled the wild type, flocculating after 24-30 hours. Therefore, the *che1* mutant strains that flocculate more than the wild type, initiate flocculation earlier relative to the wild type strain.

Interestingly, when cells were grown under these conditions of flocculation, we observed that there was not only a difference in the amount and timing of flocculation between the strains, but there was also a difference in the amount and timing of clumping behavior. Free-swimming, wild type cells formed small, transient and highly dynamic "clumps" of two to five cells after approximately nine hours of incubation into the flocculation medium. These clumps consisted of cells that attached briefly (about 1 sec) at the cell poles before swimming apart (Supplemental movie S1). *A. brasilense* is motile by a single polar flagellum and cells in clumps appeared to adhere to one another at their non-flagellated pole: when clumping, the cells were seen rotating

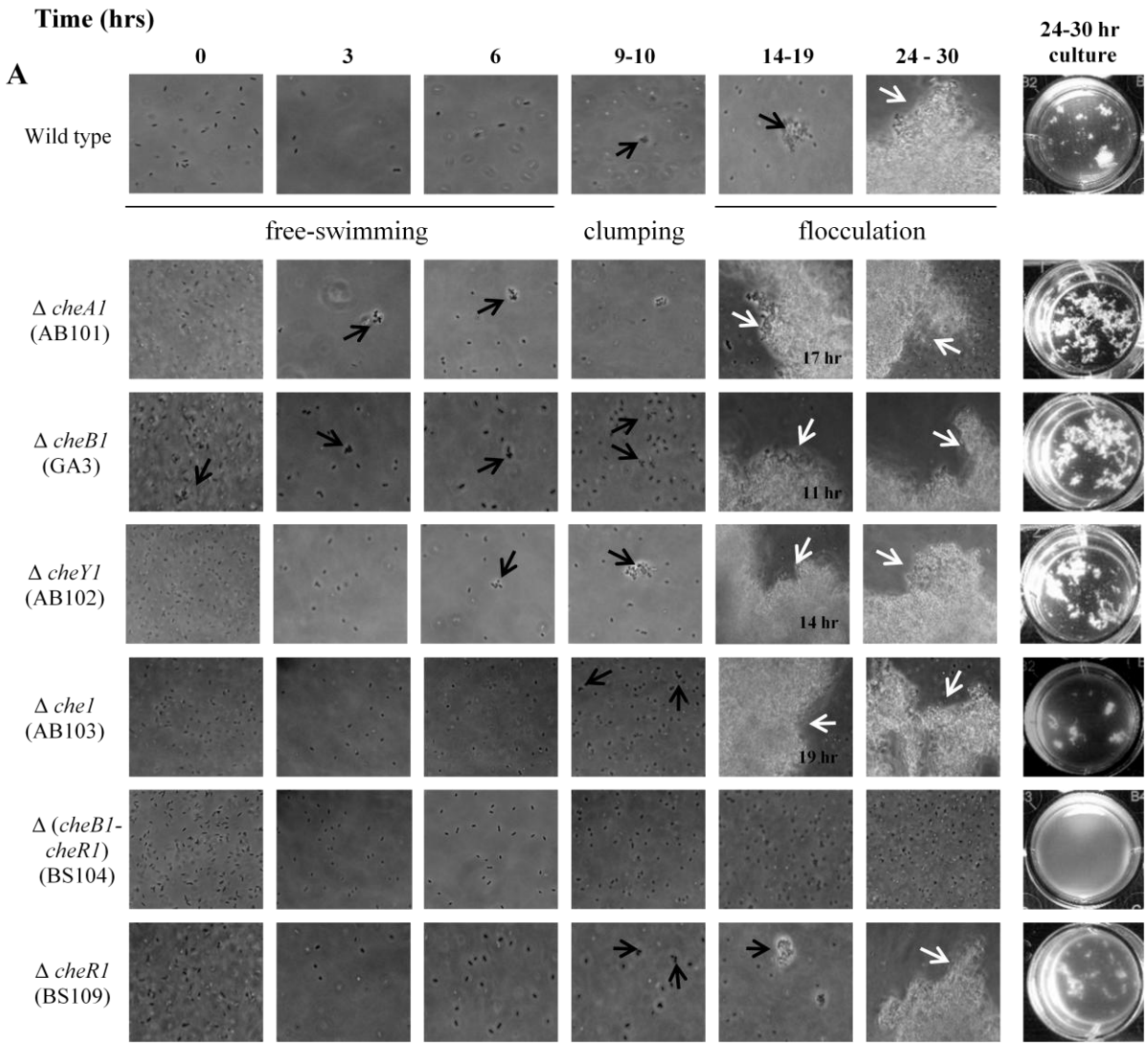

Figure 15. Time course of clumping and flocculation behaviors in wild type and *che1* mutant strains of *Azospirillum brasilense*. Cells grown under flocculation permissive conditions were analyzed by light microscopy and photographed at the indicated times. Black arrows indicate cells within clumps and white arrows indicate flocs. Times labeled in the 14-19 hour time frame indicate the time at which the strain formed visible flocs. (Right) Photographs of cultures at 24 - 30 hours post-inoculation are shown to illustrate flocculation (as seen as large aggregates) of the culture, if applicable.

around the contact point between cells and the cell-to-cell contact did not hinder polar flagellum rotation (Movie 1). Approximately two to three hours later, the number of clumps in the culture increased. The nature of these clumps were different, too, in that clumps consisted of more motile cells (about 8-10cells per clump), and these clumps appeared more stable (most cells did not leave the clumps when observed over a period of 10 minutes) in that some of the cells remained within the clumps without swimming away, while others were adherent only transiently (Fig. 15) (Movie 1). Starting around 15 hours post-inoculation, most cells appeared irreversibly attached to one another in larger clumps, and at about 18-19 hours post inoculation, larger aggregates comprised of non-motile, round-shaped cells ("mini-floc") were observed. Cells within "mini-flocs" appeared more refractile, suggesting that these cells contained intracellular polyhydroxybutyrate (PHB) granules (Fig. 15), an assumption confirmed by Nile red staining (Data not shown). Over the next several hours, the mini-flocs continued to grow larger by aggregation until the culture consisted primarily of large flocs (24-30 hours post-inoculation) (Fig. 15).

In comparison to the wild type, we observed that the Δ*cheA1* mutant began to form small, stable clumps after approximately three hours, much earlier than the wild type strain (Table 4). The *ΔcheB1* mutant showed clumping behavior resembling that of Δ*cheA1*. The Δ*cheY1* mutant formed clumps six hours post-inoculation, which was earlier than the wild type, but later than the Δ*cheA1* mutant. Clumps formed by the Δ*cheY1* mutant also appeared more transient initially than those produced by the Δ*cheA1* and Δ*cheB1* mutants. Clumping behavior was not observed in the Δ*cheB1cheR1* mutant, while the Δ*cheR1* mutant resembled the wild type. Differences in

Table 4. Time course of clumping and flocculation in wild type and mutant derivatives of *A. brasilense*.

Strain	Initiation of transient clumping [a] (in hours[b])	Transition to stable clumping [c] (in hours[b])	Time to flocculation (in hours[b])
Sp7	9 ± 1	11 ± 1	24 ± 3
Δ*cheA1* (AB101)	2 ± 1	3 ± 2	17 ± 1
Δ*cheB1* (GA3)	2 ± 1	3 ± 2	11 ± 1
Δ*cheY1* (AB102)	6 ± 2	9 ± 1	14 ± 1
Δ*che1* (AB103)	9 ± 1	11 ± 1	19 ± 2
Δ*cheR1* (BS109)	9 ± 1	11 ± 1	24 ± 3
Δ(*cheB1cheR1*)(BS104)	no clumping	no clumping	no flocculation
flcA::Tn5 (Sp72002)	9 ± 1	11 ± 1	no flocculation
Δ*che1 flcA::Tn5* (AB104)	9 ± 1	13 ± 1	no flocculation
Δ*aerC* (AB301)	2 ± 1	3 ± 2	14 ± 1
Δ*aerC*Δ*che1* (AB302)	9 ± 1	11 ± 1	19 ± 2

Values represent the time (along with the standard deviation) in hours post-inoculation into flocculation media (n = 5).

[a] Time at which transient cell-to-cell clumping is first detected. The fraction of transient clumps increases over time.

[b] Time shown represents the hours post-inoculation into flocculation medium.

[c] Time at which stable cell-to-cell clumping is first detected. The fraction of stable clumps increases over time.

the timing of clumping behavior suggested that effects of Che1 on floccculation instead reflect an effect of Che1 on clumping.

Formation of clumps and flocs earlier than the wild type could explain why some Che1 mutants were shown previously to flocculate more than the wild type (4). However, the Δ*che1* mutant does not form clumps earlier than wild type and flocculates only slightly earlier, making it difficult to explain why this mutant would flocculate more than the wild type. In order to gain insight into the mechanism by which the Δ*che1* mutant flocculates more than the wild type, we analyzed the amount of clumps (expressed as the fraction of clumps within the cell suspension) formed at different times post inoculation into the flocculation medium (Table 5). First, we compared the fraction of clumps in strains grown under flocculation-conducive conditions for 9-10 hours, the timing at which wild type cells and Δ*che1* mutant cells begin to form clumps. We found that strains which produced clumps earlier than the wild type also had a larger proportion of clumps, suggesting that clumps accumulate over time under these conditions. On the other hand, the wild type and Δ*che1* mutant formed comparable amount of clumps at this time point (9-10 hours). However, at a later time point (17-18 hours post inoculation), the Δ*che1* mutant strain had approximately twice as many clumps as the wild type cells (Table 5), an observation that support the hypothesis that greater clumping correlates with greater flocculation. Taken together, these data indicate that the *che1* mutant strains that flocculate more than the wild type strain do so because they are able to form clumps at greater rates relative to the wild type strain.

The data thus show that (i) clumping precedes flocculation, (ii) the extent of clumping correlates with the extent of flocculation, (iii) mutations affecting Che1 function correlate with increased clumping, and (iv) a mutation that prevents clumping also prevents flocculation. These

Table 5. Fraction of clumping cells in wild type (Sp7) *A. brasilense* and its *che1* mutant derivatives during growth under flocculation permissive conditions

Strain	9 – 10 hours[a]	17 – 18 hours[a]
Wild type (Sp7)	0.029[b]±0.006[c]	0.078±0.014
Δ*cheA1* (AB101)	0.069±0.004	Nd
Δ*cheB1* (GA3)	0.053±0.018	Nd
Δ(*cheB1-cheR1*) (BS104)	no clumping	no clumping
Δ*cheY1* (AB102)	0.040±0.007	Nd
Δ*che1* (AB103)	0.028±0.013	0.157±0.042

[a] Time represents the hours post-inoculation into flocculation medium.
[b] Fraction of clumping cells relative to free-swimming cells at the indicated times calculated from three representative fields-of-view and at least two independent experiments; Nd: not determined.
[c] Standard deviation.

results suggest that Che1 affects flocculation indirectly, perhaps by modulating the ability of cells to clump. To test this hypothesis, the behavior of a *flcA* mutant strain which is null for flocculation (22) was analyzed in this assay (Table 4). The *flcA* mutant behaved like the wild type strain for clumping; but, in contrast to the wild type, it did not flocculate. A mutant strain carrying both *flcA* and *che1* mutations (Δ*flcA-che1*) behaved similar to the Δ*che1* mutant cells for the timing to clumping, but like the *flcA* mutant, it did not flocculate (Table 4). FlcA is thus required for flocculation, but not clumping, and Che1 affects clumping independently of FlcA.

Stable but not reversible (transient) clumping involves changes in the extracellular EPS matrix

The time course analysis of clumping and flocculation revealed that clumping was initially a dynamic and reversible process. Over time, clumps became more stable with motile cells losing the ability to leave clumps in order to return to a free-swimming behavior. Formation of these stable clumps could be a result of changes in EPS or in the production of specific "adhesins". A role for EPS in mediating clumping and flocculation in *A. brasilense* has been previously suggested (4, 27), prompting us to test this hypothesis. The EPS were extracted at about 10 hours post inoculation into the flocculation medium which corresponds to the time where wild type cells have transitioned to formation of more stable clumps (Table 4). Under these conditions, cultures of the wild type, the Δ*cheA1* and the *flcA::*Tn5 mutant strains displayed a significant proportion of stable clumps (Table 4). In contrast, cultures of the Δ*che1* and Δ*cheY1* mutant strains were mostly comprised of cells displaying a transient clumping behavior (Table 4). As expected, clumping was not observed in cultures of the Δ*cheB1cheR1*

mutant. Extracted EPS samples were then added exogenously at similar concentrations to a suspension of wild type cells grown under flocculation permissive conditions. EPS extracted from the wild type, Δ*cheA1* and *flcA*::Tn5 strains were able to induce stable clumping behavior *per se* (and not flocculation) in wild type cells under these conditions, i.e., motile cells adhering to each other by their non-flagellated poles were observed in the EPS-treated samples but not in the control (Fig. 16A). Conversely, treatment of cells with EPS extracted from the Δ*cheB1cheR1* strain, which does not exhibit any clumping behavior, was not able to induce clumping, and in fact appeared to promote free-swimming (Fig. 16A and 16B). Noticeably, the exogenous addition of EPS extracted from the Δ*cheY1* and the Δ*che1* mutants failed to induce significant clumping under similar conditions (Fig. 16B). Exogenous application of EPS extracted from some, but not all, strains carrying mutations affecting Che1 function is thus sufficient to trigger the formation of stable clumps. EPS samples which were the most potent for inducing stable clumping behavior were extracted from strains that produced the most stable clumps at the time of EPS extraction: the wild type strain, the Δ*cheA1* and the *flcA*::Tn5 mutant strains. Strains that clumped only transiently at the time of EPS extraction (Δ*cheY1* and Δ*che1*) produced EPS that did not trigger stable clumping. Therefore, it is likely that EPS production contributes to stabilizing clumping. However, mutations within different *che1* genes appear to yield strains producing EPS of variable potency for inducing stable clumping, indicating some variation in the nature of the EPS produced by these strains. This observation supports the hypothesis of an indirect role for Che1 in modulating "clumping-specific" EPS production. To rule out any other indirect effects of the extracted EPS, the contribution of proteins potentially present within the

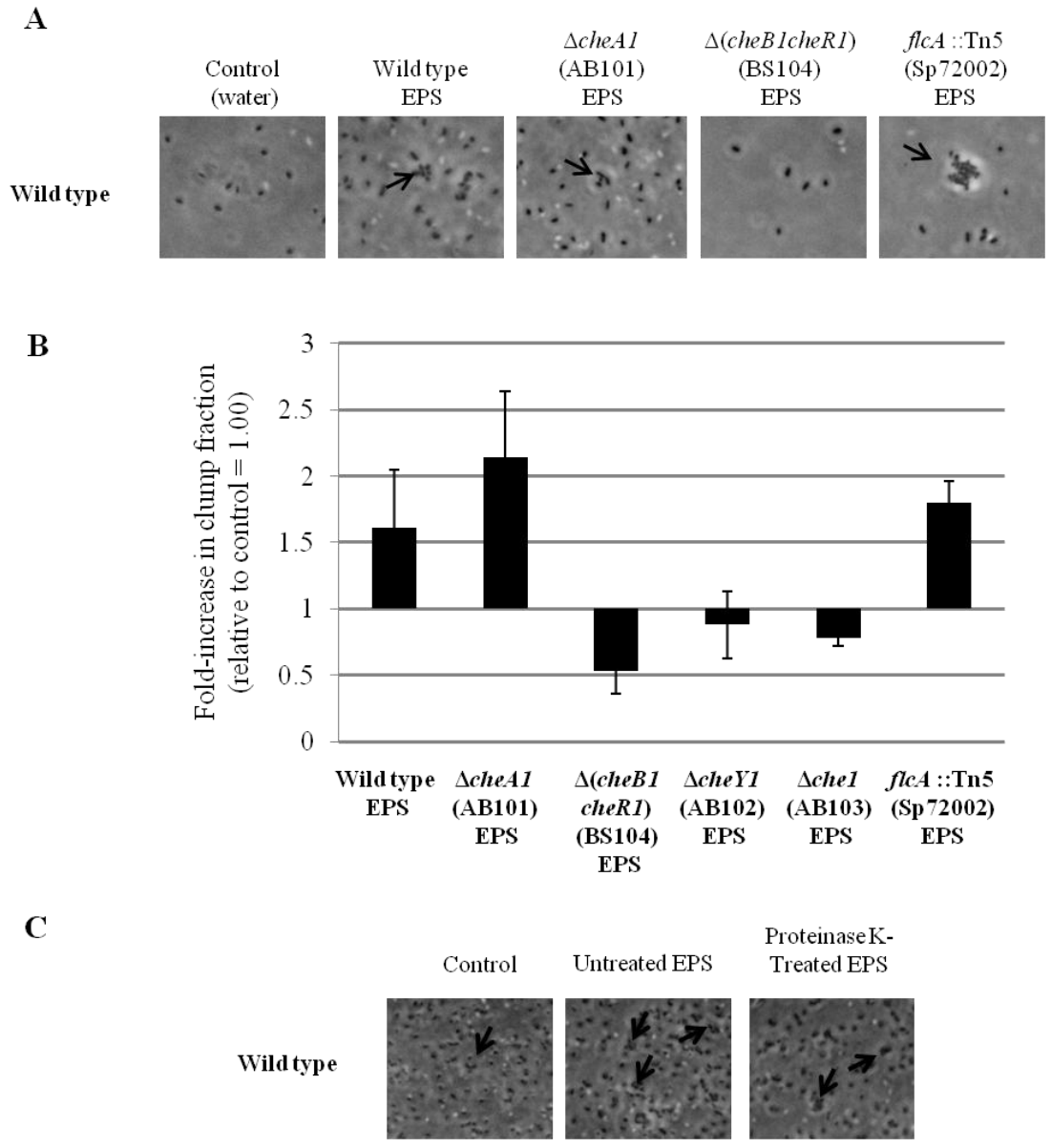

Figure 16. Effects of extracted exopolysaccharides (EPS) on clumping in *Azospirillum brasilense*. (A) Representative light microscopy photographs of wild type cells treated with EPS extracted from the strains indicated at the top. Arrows indicate clumping cells. (B) Fold increase in clumping upon treatment of wild type cells with EPS extracted from different strains. The fold-increase in the clumping fraction upon treatment with the extracted EPS as compared to the control treatment (water), taken as a value of 1. (C) Effect of proteinase K on the ability of extracted EPS to induce clumping. A suspension of wild type *A. brasilense* cells were prepared as in (A) and then treated as indicated. Arrows indicate clumping cells.

extracted EPS was tested by examining the effect of proteinase K treatment of EPS on induction of clumping in this assay. Treatment of EPS with proteinase K did not affect the propensity of the EPS to induce clumping, suggesting that EPS but not any other protein within the extracted EPS, modulates increased clumping (Fig. 16C). These results thus confirm that EPS produced by cells capable of forming stable clumps are potent inducers of clumping. Since different *che1* mutant strains produce EPS with different abilities to promote stable clumping, it follows that clumping-specific EPS production is most likely not directly regulated by Che1. Together with the observation that Che1 affects the timing to clumping in the flocculation assay, these results suggest that Che1 may function to modulate the transient nature of clumping which precedes the formation of stable clumps.

Clumping is modulated by temporal changes in aeration

Changes in aeration conditions are likely to modulate clumping because clumping is observed when cultures of *A. brasilense* are grown under conditions of high aeration (4). Therefore, we modified a gas perfusion chamber assay, typically used for aerotaxis (1), to directly measure temporal changes in clumping in order to further characterize the transient and reversible clumping behavior. In this assay, the gas atmosphere flowing above a suspension of cells can be controlled allowing one to analyze the behavioral responses of cells challenged with changes in the aeration conditions. In order to use the gas perfusion chamber assay to analyze clumping, we also grew all strains under high aeration conditions and to higher cell densities (late exponential phase) (see Material and methods). Under these growth conditions, all strains clumped in a pattern similar to that detected in the flocculation assay, i.e., the Δ*cheA1*, Δ*cheY1*, Δ*che1*, Δ*cheB1*, as well as the Δ*cheR1* mutant strains had more clumps relative to the wild type

while the Δ*cheB1cheR1* mutant did not clump (Fig. 15). When a suspension of wild type cells was analyzed in this assay, cells responded to a switching in the aeration (air removal) with a decrease in the overall amount of clumping (reduction by half relative to pre-stimulus levels; Fig. 17) followed by an adaptation period where the fraction of clumps detected in the suspension returned to pre-stimulus levels. We observed that the fraction of clumps decreased transiently upon air removal because clumped cells briefly returned to free-swimming behavior, before adapting to the ambient aeration conditions and returning to clumps (Fig. 17). Similarly, when air was returned to the atmosphere of the cell (air addition), cells displayed a similar response characterized by a similar decrease in clumping by half concomitant with the clumped cells becoming free-swimming for a short period before the clumps re-formed to return to pre-stimulus levels (Fig. 17).

The Δ*cheR1* mutant resembled wild type cells the most (Fig. 17). The Δ*cheR1* mutant differed from the wild type in that after the initial decrease in the clumping fraction (upon both air removal and air addition), cells were slower to return to pre-stimulus clumping levels. Where wild type cells would begin to re-form clumps after 30-40 seconds, the Δ*cheR1* mutant would take approximately 60 seconds to resume clumping behavior. The Δ*cheB1cheR1* mutant did not show any clumping behavior, regardless of the removal or addition of air (Fig. 17).

The clumping behavior of the Δ*cheA1* mutant differed in two key ways from that of the wild type strain which responded to both air addition and air removal with an initial decrease in clumping behavior (prior to adaptation where clumps are re-formed), in this assay. First, Δ*cheA1* responded to both air removal and air addition, but it did not adapt to the imposed aeration conditions since clumping did not return to pre-stimulus levels upon air removal or air addition

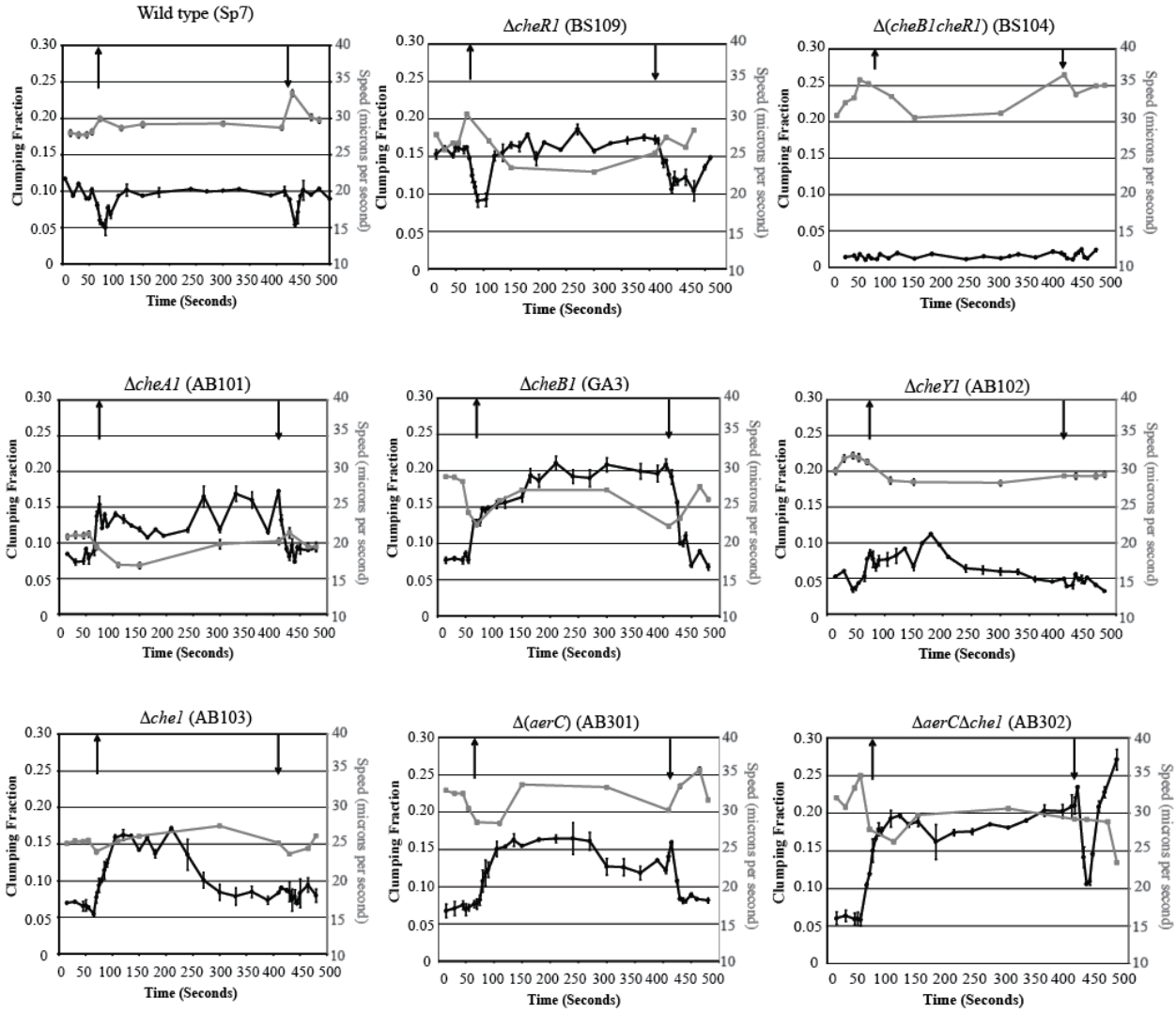

Figure 17. Clumping behavior of *A. brasilense* and the *che1* mutant strains in the gas perfusion chamber assay. The gas atmosphere of a suspension of cells placed in a gas perfusion chamber is changed from air to nitrogen gas (air removal) and back to air (air addition). Changes in the fraction of clumps (black line and axis) and the average speed of free-swimming cells (gray line and axis) within the cell suspension were determined at regular time intervals (x-axis, in seconds), upon air removal (up arrow) and after air addition (down arrow) for the strains indicated. Time is in seconds with the entire experiment representing about 10 minutes. The fraction of clumps and the swimming speed within the cell suspensions were determined from digital movies analyzed as described in Material and Methods.

(Fig. 17). Secondly, rather than experiencing a decrease in the number of clumps upon air removal, clumping levels in suspension of this mutant nearly doubled under these conditions. Upon air addition to the Δ*cheA1* cell suspension, the number of clumps decreased by half. Similar to Δ*cheA1*, the Δ*cheB1* mutant also responded to both air removal and air addition, but no adaptation to the changes in aeration conditions was observed. The number of clumps in the suspension of the Δ*cheB1* also doubled upon air removal and decreased upon air addition by the same amount, as in Δ*cheA1*.

In response to air addition, clumping also nearly doubled in suspension of the Δ*cheY1* which contrasted with the wild type response to similar changes in aeration conditions. In fact, the observed increase in clumping seen in the Δ*cheY1* upon air removal is similar to that observed in the Δ*cheA1* and Δ*cheB1* mutants; however, clumping in the Δ*cheY1* mutant slowly adapted to the new aeration conditions and decreased back to pre-stimulus levels (Fig. 17). No further change in clumping was detected when air was returned to the atmosphere of Δ*cheY1* (air addition). The Δ*che1* mutant increased clumping by more than 2-fold, which is slightly higher than that observed in the other mutants; however, like Δ*cheY1*, clumping in response to air removal slowly adapted and it returned to pre-stimulus levels (Fig. 17). Similar to Δ*cheY1*, the Δ*che1* mutant did not respond to air addition and no change in clumping was detected.

Collectively, we show that changes in transient clumping take place as a result of changes in aeration conditions. These results also indicate that Che1 functions to reduce clumping when cells experience a decrease in aeration (air removal), but its contribution to clumping under conditions of increased aeration (air addition) is not straightforward.

Clumping is not correlated with changes in reversal frequency

Changes in the clumping pattern of wild type cells detected in the gas perfusion chamber assay were reminiscent of changes in the swimming pattern of cells in a temporal assay for chemotaxis or aerotaxis, suggesting a functional link between clumping and motility. First, we analyzed the swimming motility bias of cells that have experienced changes in clumping upon changes in aeration conditions in the gas perfusion chamber assay described above. Under these conditions, the wild type strain was found to display a nearly 3-fold decrease in the swimming reversal frequency (number of reversals in the swimming direction per second and per cell) upon air removal or addition to the atmosphere of the cells (Fig. 18). While most of the che1 mutant strains responded to changes in aeration conditions by modulating the swimming motility bias under these conditions, no correlation between changes in clumping and changes in the reversal frequency of cells upon air removal or air addition could be established when analyzed in this assay (Fig. 18). The most striking illustration of this fact is that no change in the swimming bias of the Δ*cheR1* mutant strain could be detected upon air removal or addition, yet its clumping behavior most resembled that of the wild type strain, albeit with longer transient free-swimming responses (Fig. 17) (Fig. 18).

Clumping and swimming velocity correlate

While there was no detectable correlation between clumping behavior and changes in the motility bias, changes in swimming velocity appeared to correlate with changes in clumping detected upon air removal. For example, wild type cells showed a significant increase in swimming velocity by approximately 3 μm/sec upon air removal, which correlated with a transient decrease in the fraction of clumping cells by about

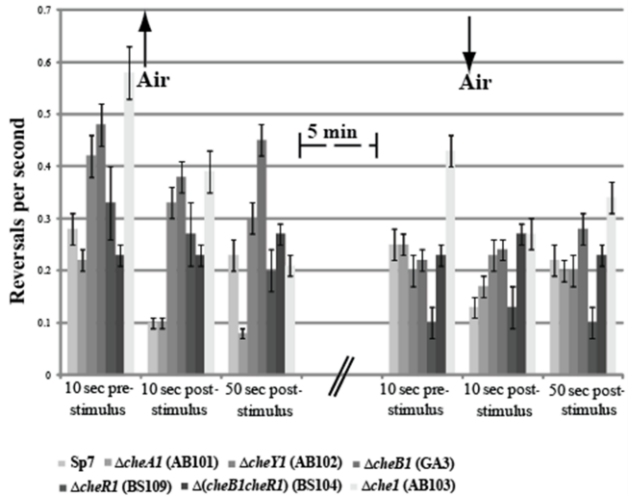

Figure 18. Motility bias of free-swimming *A. brasilense* wild type and *che1* mutant derivative cells. The swimming bias is represented as the number of reversals in the swimming direction per second, as determined using computerized motion analysis. Suspensions of cells displaying transient clumping were analyzed in the gas perfusion chamber assay. The arrows pointing upward and downward represent air removal and air addition to the atmosphere of the cells, respectively. The time elapsed between two events of air removal and air addition represents over 6 minutes, during which cells remain motile. Error bars represent standard deviations from the means, calculated from at least 90 cells from a minimum of 2 independent experiments.

half (Fig. 17). When the swimming velocity of wild type cells decreased to pre-stimulus levels upon adaptation, the clumping fraction increased to pre-stimulus levels, as well. Similar to the wild type strain, the Δ*cheR1* mutant cells also swam faster by about 5 μm/sec in response to air removal, with concomitant decrease in clumping by half. The Δ*cheB1cheR1* strain, on the other hand, did not respond to air removal by modulating clumping but it did respond by transiently swimming faster (a ~ 5 μm/sec increase in swimming velocity). Noticeably, the average swimming velocity of the Δ*cheB1cheR1* mutant strain was also the highest of all strains analyzed (ranging from 30-37 μm/sec), differing from wild type by about 4 μm/sec and from the Δ*cheA1* (the slowest of the Che1 mutants) mutant by nearly 14 μm/sec (Fig. 17). Given that clumping decreases with increased swimming velocities in the wild type, the higher average swimming velocity of the Δ*cheB1cheR1* mutant may explain the lack of clumping observed in this strain (Fig. 17). In contrast, the swimming velocity of the mutants lacking *cheA1*, *cheB1*, *cheY1*, or *che1* decreased by an average of 3 to 7 μm/sec upon air removal and it was concomitant with a doubling in the amount of clumping in cell suspensions of these mutants (Fig. 17). These results thus suggest that the inability of these *che1* strains to increase swimming velocity upon air removal correlates with the increase in clumping observed under these conditions (Fig. 17). These data further imply that changes in transient clumping upon air removal may be modulated by direct effects of Che1 on the swimming velocity.

Although changes in swimming velocity correlated with changes in clumping upon air removal in the *che1* mutant strains, we were unable to detect such a correlation upon air addition (Fig. 17). Changes in swimming velocity detected for the wild type and the various *che1* mutant strains upon air removal were also detected and followed a similar pattern upon air removal (Fig.

17). While the wild type cells as well as Δ*cheR1* and Δ*cheB1cheR1* mutant cells swam transiently faster by about 5 μm/sec upon air addition, the Δ*cheA1*, Δ*cheB1*, Δ*cheY1*, and Δ*che1* mutant cells swam with a reduced velocity (by 4 μm/sec on average) under these conditions. Similar to the behavior observed upon air removal, the transient increased in the swimming velocity correlated with a decrease in clumping by half for the wild type and the Δ*cheR1* mutant, while clumping was not detected for the Δ*cheB1cheR1* mutant for which the average swimming velocity remained the greatest (Fig. 17). In contrast and despite swimming transiently slower, clumping decreased by half in suspension of the Δ*cheA1* and the Δ*cheB1* mutant strains upon air addition, while there was no change in clumping (no response) in suspension of the Δ*cheY1*, and of the Δ*che1* (Fig. 17). These observations suggest that the effect of the decreased swimming velocity on clumping may be significant only when cells experience a decrease in aeration conditions (air removal). This suggests that transient clumping is modulated by direct effects of Che1 on the swimming behavior, as well as by other Che1-independent effects that are likely prevalent under conditions of increased aeration in the atmosphere of the cells.

Control of the swimming velocity is a signaling output of Che1

In order to gain further insight into how signaling via Che1 regulates the swimming velocity and clumping, the behavior of mutant strains expressing wild type *che1* genes or genes carrying mutations of conserved phosphorylation residues expressed from low copy plasmids was characterized under flocculation conditions (Table 6) and in the gas perfusion chamber assay (Fig. 19) (Fig. 20). Expression of CheA1, $CheA_{H252Q}$, CheY1 and $CheY1_{D52N}$ from the plasmids used for complementation was detected with antibodies to the *A. brasilense* wild type proteins and found

Table 6. Timing of clumping behavior in wild type A. brasilense and its che1 mutant strain derivatives complemented with wild type or mutant alleles of *cheA1*, *cheB1*, or *cheY1* (in hours)

Strain	Clumping*
Wild type (pRK415)	9
Wild type (pBBR)	9
Δ*cheA1* (pBBR)	3
Δ*cheA1* (pBBR-*cheA1*)	9
Δ*cheA1* (pBBR-$cheA1_{H252Q}$)	3
Δ*cheB1* (pBBR)	3
Δ*cheB1* (pBBR-*cheB1*)	9
Δ*cheB1* (pBBR-$cheB1_{D78N}$)	6
Δ*cheY1* (pRK415)	6
Δ*cheY1* (pRK415-*cheY1*)	9
Δ*cheY1* (pRK415-$cheY1_{D52N}$)	6

*Method used to assess the timing of clumping and flocculation is identical to that used for Figure 2. Noted times refer to the time at which clumping is observed (in hours) for each sample.

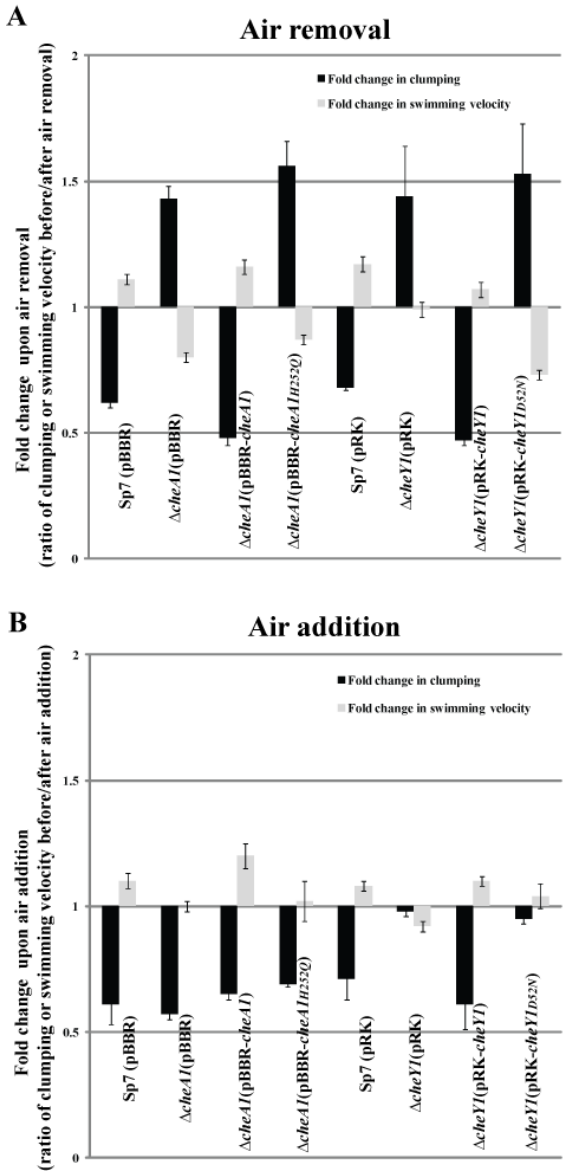

Figure 19. **Effects of CheA1 and CheY1 on the relative fold change in swimming speed and clumping upon air removal or air addition to the atmosphere of the cells.** The wild type strain (Sp7) and its *cheA1* and *cheY1* mutant were analyzed in the gas perfusion chamber assay. The strains carried either an empty vector (controls pRK or pBBR) or a vector in which a wild type *cheA1* or *cheY1* allele or mutant alleles (*cheA1*$_{H252Q}$ and c*heY1*$_{D52N}$) are expressed from low copy plasmids. The fold change in the swimming speed and clumping were determined on at least 3 video images by computerized image analysis with video frames with at least 100 cells in the field of view. Clumping represents the fraction of cells within clumps (clumping fraction) relative to the total number of cells in the video frame analyzed. The fold change in swimming speed and in clumping upon air removal or addition is calculated relative to the swimming speed or clumping prior to the switch in the atmosphere of the cells (air removal or addition).

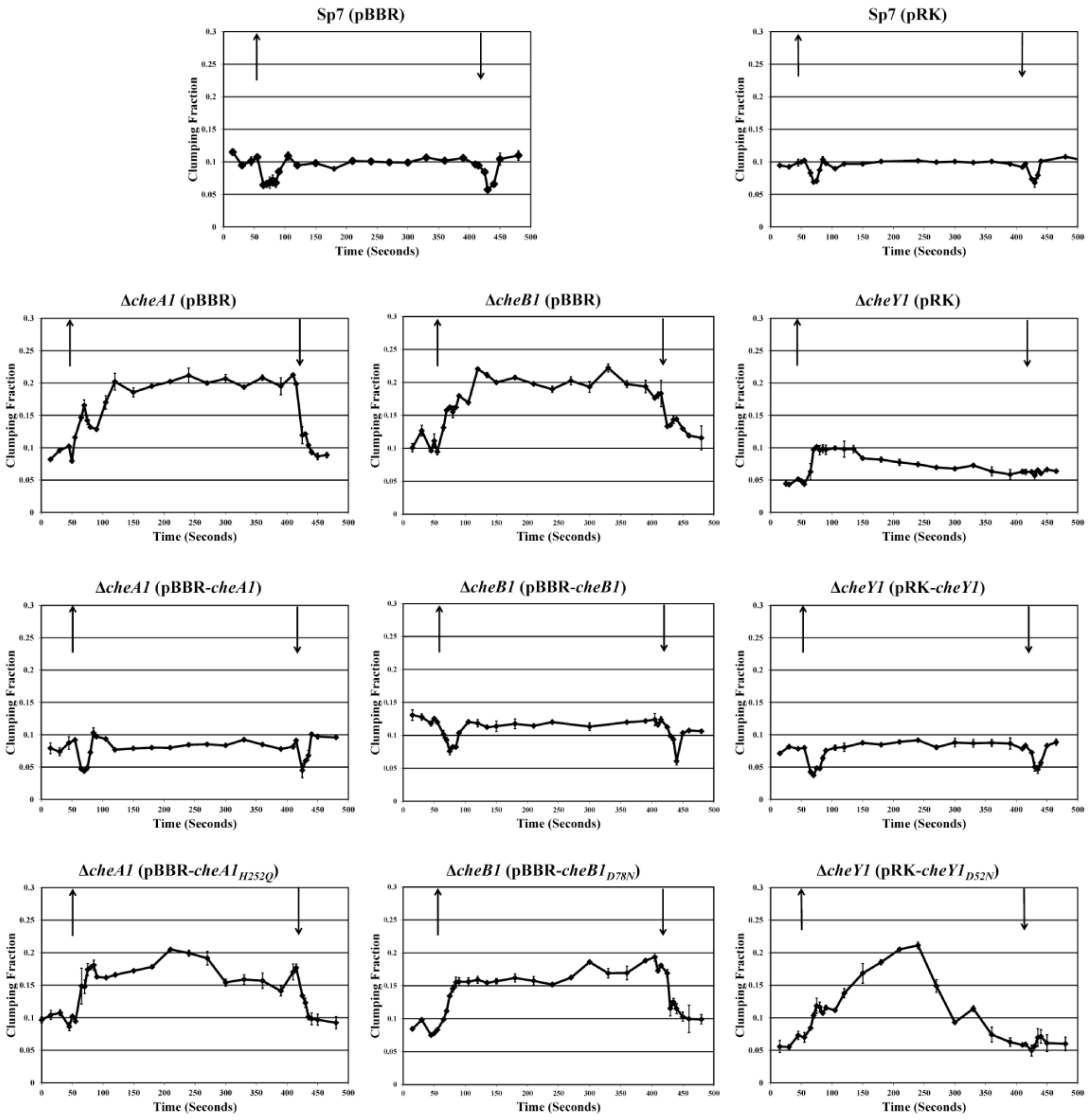

Figure 20. Complementation of *che1* mutant phenotypes with parental (wild type) and variant alleles of CheA1, CheB1, and CheY1 in the gas perfusion chamber assay. The fraction of clumps to free-swimming cells over the time course of the assay is shown. The total experiment time is 10 minutes. The up and down arrows indicate events of air removal and air addition to the atmosphere of the cells, respectively.

to be comparable to the level of the wild-type proteins (Fig. 21). Similar controls of protein expression could not be performed with CheB1 since we do not have any antibody to CheB1 and none of the antibodies against CheB of other bacterial species that we have tried cross-reacted with the CheB1 protein from *A. brasilense*. While functional complementation of Δ*cheA1* (AB101) with the wild type *cheA1* expressed from a plasmid restored wild-type clumping behavior in both the flocculation and the gas perfusion chamber assays, complementation with a plasmid expressing a mutated *cheA1* gene in which the codon for the conserved phosphorylatable histidine residue is replaced with glutamine ($CheA1_{H252Q}$) failed to restore the wild type phenotype: the pattern of changes in clumping within the suspension upon air removal or addition paralleled that of the mutant strain (Fig. 19) (Fig. 20). An intact CheA1 is thus required for its function in clumping. Similar functional complementation of Δ*cheY1* (AB102) with the wild type CheY1, but not with a $CheY1_{D52N}$ variant, restored the wild-type clumping phenotype, indicating that functional CheY1 is also essential for its function in clumping (Fig. 19) (Fig. 20). An intact phosphorylatable aspartate site (D78) in the receiver domain of CheB1 was found to be required to restore the wild type clumping behavior of a Δ*cheB1* mutant strain (Fig. 20). Functional CheA1 and CheY1, but not $CheA1_{H252Q}$ or $CheY1_{D52N}$ also restored the ability of strains to transiently increase swimming velocity upon air removal and air addition in the gas perfusion chamber assay, correlating with a transient reduction in the fraction of clumped cells (Fig. 19). Che1 thus modulates the cell's swimming velocity by a direct effect on CheY1 phosphorylation, likely via a phosphorelay between CheA1 and CheY1. The analysis of the Δ*cheA1*, Δ*cheY1* and Δ*che1* mutant phenotypes together with the effects of expressing non-

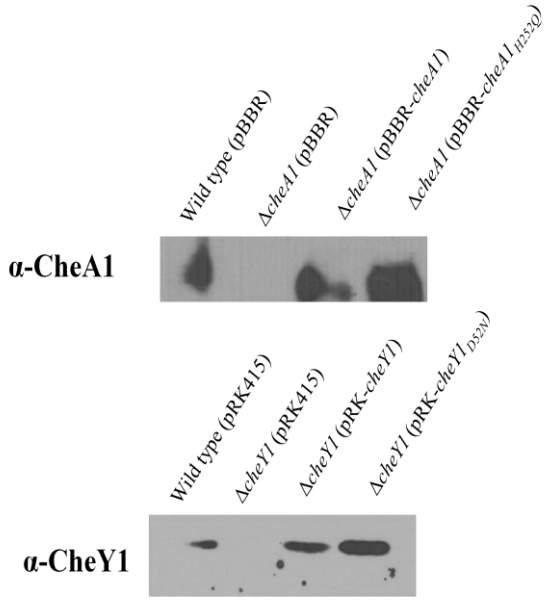

Figure 21. Expression of CheA1 and CheY1 from complementation constructs. Western blots were performed on whole cell extracts to analyze the expression levels of CheA1 and CheY1 using antibodies that were affinity-purified and that are specific to each of these proteins. Top panel, western blot of CheA1 and its variant, $CheA1_{H252Q}$, expressed from a low copy plasmid. Bottom panel, western blot of CheY1 and its variant, $CheY1_{D52N}$.

functional CheA1$_{H252Q}$ or CheY1$_{D52N}$ on the swimming velocity of cells also indicate that Che1 signaling output causes an increase in the swimming velocity of cells.

A taxis receptor modulates Che1-dependent effects on clumping

Mutations affecting the *A. brasilense* energy taxis receptor *aerC* were previously shown to possess small clumps under most growth conditions (37), suggesting that this receptor functions to modulate clumping. Consistent with this hypothesis, an Δ*aerC* mutant strain clumped after 1-3 hours post-inoculation (Table 4) and quantitatively more than the wild type strain, resulting in greater flocculation, as well (data not shown). A double mutant lacking both *aerC* and *che1* (Δ*aerC*Δ*che1*, strain AB302) behaved as the Δ*che1* mutant strain (Table 4) for clumping and flocculation. This is consistent with previous observations (37) and suggests that AerC functions upstream of Che1 to modulate clumping.

Next, the behavior of the Δ*aerC* (AB301) and the Δ*aerC*Δ*che1* (AB302) mutant strains were analyzed in the gas perfusion chamber assay (Fig. 17). The swimming velocity of both the Δ*aerC* and the Δ*aerC*Δ*che1* mutant strains decreased by at least 5 μm/sec immediately upon air removal. Upon air addition, the swimming velocity increased by approximately 5 μm/sec in the Δ*aerC* strain, but decreased by 5 μm/sec in the Δ*aerC*Δ*che1* strain. These results are consistent with the role of Che1 in modulating changes in swimming velocity as well as with the role of AerC in mediating Che1-dependent changes in the swimming velocity, likely by sensing conditions of decreased aeration.

Compared to the wild type strain, the Δ*aerC* mutant strain doubled in clumping, but with a significant delay (of about 15 seconds compared to the wild type) relative to the time of air removal. The delayed clumping response seen in the Δ*aerC* mutant strain upon air removal was

no longer observed in the Δ*aerC*Δ*che1* strain: clumping increased immediately upon air removal (Fig. 17). Similar to Δ*cheA1* and Δ*cheB1* mutants, clumping in each of these strains remained at levels higher than pre-stimulus conditions after it initially increased upon air removal. Clumping returned to lower levels only after air addition in the Δ*aerC* mutant strain (Fig. 3). Under conditions of increased aeration, the Δ*aerC*Δ*che1* mutant strain responded by decreasing the fraction of clumps by more than 2-fold (Fig. 17). In contrast to the response of the Δ*aerC* mutant, the decrease in clumping upon air addition was transient in the Δ*aerC*Δ*che1* strain (Fig. 17). The ability of the Δ*aerC*Δ*che1* mutant to respond to air addition by transiently decreasing clumping also lends support to the hypothesis that Che1 effects on the swimming speed does not directly contribute to clumping under conditions of increased aeration. The transient decreased clumping response of the Δ*aerC*Δ*che1* mutant upon air addition is similar to the response of the wild type strain, i.e. appears to correspond to adaptation; however, steady state clumping in suspension of the wild type strain remained at lower levels. In contrast, the steady-state levels of clumping remained at significantly higher levels relative to pre-stimulus in suspension of the Δ*aerC*Δ*che1* mutant, suggesting indirect effects of AerC on the steady-state levels of clumping. Taken together, these results argue that in addition to modulating Che1-dependent effects on transient clumping via an effect on the swimming speed, AerC may also mediate indirect effects that modulate the ability of cells to maintain constant steady-state levels of clumping, after changes in aeration conditions.

Section D. Discussion

The Che1 chemotaxis-like pathway of *A. brasilense* has been implicated in the control of chemo- and aerotaxis as well as cell surface adhesive properties, clumping and flocculation. Here, we show that clumping and flocculation are distinct processes and that Che1 contributes to the control of the initial reversible and transient cell-to-cell clumping behavior. While transient clumping correlates with changes in motility of cells, transition to stable clumps depends on the production of EPS that are produced independently of Che1. Our results demonstrate that the signaling output of Che1 is the modulation of the flagellar swimming velocity, illuminating its role in chemo- and aerotaxis.

The signaling output of Che1 is the control of the swimming velocity

Che1 appears to directly regulate the propensity of cells to increase swimming velocity with changes in aeration conditions. A functional Che1 pathway, including a phosphorylatable CheY1 response regulator is required for this response, identifying modulation (increase) of the swimming velocity as a signaling output of the Che1 pathway. This finding implies that changes in swimming velocity contribute to aerotaxis in *A. brasilense* with receptors signaling to Che1 upon changes in aeration conditions in order to modulate this response. AerC is an energy taxis receptor (37) that is shown here and elsewhere (37) to function in a Che1-dependent manner to modulate the swimming velocity and aerotaxis. Changes in swimming velocity have not been directly implicated in the tactic behaviors of *A. brasilense*. However, the results obtained here imply that changes in the swimming speed of cells represent a mechanism by which motile *A. brasilense* cells actively navigate in gradients. This assumption is supported by the observation

that wild type *A. brasilense* cells responded to temporal changes in aeration conditions by increasing the swimming speed, as well as decreasing the reversal frequency by nearly 3-fold (an attractant response). Further, the Δ*cheB1cheR1* mutant strain, in which CheA1 and CheY1 are supposed to be active (5), has a constantly greater swimming velocity than the wild type cells (Fig. 17). In addition to identifying the signaling output of the Che1 pathway, these results also shed light on how the Che1 pathway could contribute to chemotaxis and aerotaxis, while not having any apparent effect on the reversal frequency of the cells (4). Che1 signaling output could regulate swimming velocity either via direct effect(s) of phosphorylated CheY1 on the flagellar motor or switch complex to ultimately increase flagellar swimming velocity, or through indirect effects involving additional protein(s) capable of affecting flagellar motor rotation or torque. Direct effects of CheY proteins on flagellar rotation have been recently demonstrated in *R. sphaeroides*, a species that employs multiple CheY homologs which are able to bind to the flagellar motor and switch complex that act as a "brake" to stop flagellar rotation (21). The genome of *A. brasilense* encodes six CheY homologs that have not been characterized yet (35). The role of CheY1 in increasing the swimming velocity and the contribution of Che1 to chemo- and aerotaxis in *A. brasilense*, albeit minor (4, 11), collectively suggest the possibility of a similar function. However, other mechanisms are possible. For example CheY1 could counteract the effect of potential flagellar velocity braking protein(s) and thus act indirectly to increase the speed at which cells swim. The observation that mutations affecting *cheA1*, *cheY1* or deletion of *che1* cause the cells to respond to changes in aeration conditions by swimming slower relative to the wild type (Fig. 17) gives credence to this hypothesis. Several proteins from diverse bacteria have been recently shown to control the flagellar motor with typical effects observed on the

cell's swimming velocity. The proteins involved and the mechanisms by which they interact with flagellar motor components appear diverse, even within a single bacterial species, making their direct identification from sequences alone challenging (for a recent review, see 6).

Che1-dependent changes in the swimming speed modulate transient clumping

When wild type cells were analyzed in a temporal assay for clumping, a transient decrease in the fraction of clumps was observed upon air removal and air addition from the atmosphere of the cells. Concomitant with this transient change in cell-to-cell interactions, swimming was biased toward less frequent changes in the swimming direction (reversals per second) and the swimming speed increased, immediately in response to changes in aeration conditions. Changes in clumping paralleled changes in the swimming pattern (bias and velocity) of the cells. Results obtained here establish that changes in the swimming velocity mediated by Che1 are sufficient to promote a reduction in transient clumping upon downshifts in aeration conditions. Changes in the swimming speed could affect clumping, perhaps by increasing the likelihood of loosely adherent cells within clumps to detach and swim away and/or by decreasing the probability of initial cell-to-cell contacts, thus reducing the possibility of transient clump formation. A decrease in flagellar swimming bias and/or flagellar swimming velocity was previously shown to promote surface attachment and biofilm formation in many bacterial species (8, 18, 19, 32). Similarly, changes in the swimming motility of *A. brasilense* cells appear to contribute to the propensity of cells to interact within clumps. A major role for Che1-dependent changes in motility in modulating cell-to-cell interactions in transient clumps is consistent with the dynamic and short-lived nature of these associations and with the propensity of transient clumps to dissociate rapidly in response to changes in aeration conditions. While Che1 appears

to control the flagellar swimming velocity under all conditions, a significant effect of the swimming speed on transient clumping was detected only upon air removal, under the conditions of the gas perfusion chamber assay. This suggests that while the swimming velocity may significantly affect transient clumping under some conditions, other behavior(s) may modulate the dynamics of transient reversible clumping under other conditions, such as an increase in aeration. Given the changes in the motility pattern of the wild type cells detected upon air removal and air addition, it is likely that the swimming reversal frequency or perhaps other transient changes in the motility behavior that were not detected here could contribute to modulate clumping upon increases in aeration conditions. Given that clumping was correlated with increased biofilm formation in *A. brasilense* (27), these results also raise the intriguing possibility that changes in the swimming pattern of cells are directly implicated in the initiation of transient cell-to-cell and cell-to-surface interactions that precede most steps in colonization.

Cross-talk may be involved in modulating clumping

In addition to direct effects on the swimming velocity, Che1 also appears to have indirect effects on clumping behavior. For instance, some Che1 mutants show increased steady-state levels of clumping that do not return to pre-stimulus levels in the gas perfusion chamber assay, which did not appear to directly correlate with a generally lower swimming velocity of the cells. Indirect effects also include the observation that *che1* mutations affect the timing to clumping in the flocculation assay, consistent with effects of Che1 on the sensitivity of the clumping response under the conditions of this assay. Adaptation proteins in chemotaxis signal transduction function to maintain response sensitivity over a broad range of background conditions, and allow the behavior to return to pre-stimulus bias after a rapid response to environmental stimuli (15,

34). Loss of function in adaptation proteins is thus expected to affect the sensitivity and/or activity of chemotaxis receptors that are regulated by these proteins. The following lines of evidence support the hypothesis that indirect effects of Che1 on clumping are mediated through the activity of adaptation proteins and chemotaxis receptors. First, mutations affecting CheB1 directly or indirectly (e.g. mutations affecting CheA1 function), yielded the most dramatic clumping phenotypes. Second, increased clumping triggered in response to air removal from the atmosphere of the cells remained at high levels in strains with Δc*heA1* or Δ*cheB1* mutations or expressing nonfunctional CheA1 or CheB1 variant proteins. Persistent clumping at high levels was also detected in a mutant strain lacking a functional AerC receptor. This clumping response pattern suggested that a stimulus and an initial response must be implemented for this change in the steady-state clumping behavior to be detected, implicating defects in a response feedback loop. In contrast, higher clumping levels decayed slowly to reach lower levels in strains carrying Δc*heY1* (or non-functional $CheY1_{D52N}$ variant) and Δ*che1* mutations. Last, a strain carrying a Δ(*cheB1cheR1)* mutation does not clump under any growth conditions. Collectively, these results implicate both a receptor (AerC) and Che1 adaptation proteins, in particular CheB1, in mediating the indirect effects of Che1 on the sensitivity of cells that allows them to maintain clumping at constant steady-state levels. How could indirect effects of Che1 be mediated by adaptation proteins and/or receptors? One possibility is that other pathways in addition to Che1 contribute to modulating the swimming behavior and thus transient clumping. Results obtained here and in previous studies (5, 29) support this hypothesis. CheB1 and CheR1 of the Che1 pathway were previously implicated in a signaling cross-talk between Che1 and other unknown pathway(s) in regulation of aero- and chemotaxis responses in *A. brasilense*, with the most notable effects

being the relative sensitivity of receptors and associated pathway(s) to changes in environmental conditions (29). Genetic, biochemical and/or modeling data in a few other bacterial species support the hypothesis that cross-talk between different chemotaxis or Che-like operons may be mediated by the activity of CheB proteins (10, 20, 24, 31, 33). The methylation status of the FrzCD receptor also depends on signaling by two Che-like pathways in *Myxococcus xanthus* (38), lending further support to this possibility. In such a scenario, if receptors are modified by adaptation proteins from independent signaling pathways, then sensory input to one pathway could modulate the activity of the adaptation protein of this pathway, which in turn will affect the sensitivity and thus the response output of other pathway(s).

Clumping and its relationship with flocculation

While they are both formed as a result of cell-to-cell interactions, clumping cells are morphologically and behaviorally distinct from flocculated cells in that flocculated cells are non-motile, round and encased in large aggregates of polysaccharides (25). Consistent with this observation, FlcA, a key transcriptional regulator for flocculation (22), has no effect on clumping in *A. brasilense*. Mutant strains that lack FlcA could produce stable clumps but they fail to lose motility or to differentiate into round flocculated cells. Clumping thus precedes and appears required for flocculation. Our data are consistent with Che1 modulating transient cell-to-cell clumping in response to changes in aeration conditions. *A. brasilense* flocculates only under conditions of high aeration, as well as when the source of combined nitrogen for growth is limiting (7, 25). This observation further supports the hypothesis that clumping and flocculation are distinct processes. The effect that Che1 has on the ability of cells to flocculate is thus indirect

and is most likely the result of Che1-dependent effects on clumping. However, the identity of the kinase(s) or of the phosphorelay(s) that regulate(s) the activity of FlcA remains unknown.

Che1 modulates transient clumping behavior, which depends on changes in motility and precedes the formation of stable clumps and flocculation. Over time, stable clumps accumulate and data obtained in this study suggest that specific EPS are produced by cells in order to stabilize clumping. While our data clearly establish that the signaling output of Che1, and thus its main function, is not the regulation of clumping-specific EPS production, mutations within *che1* result in mutant strains differentially affected in their ability to transition from transient to stable clumping. These differences in timing for the transition to stable clumps suggest that Che1 may indirectly modulate clumping-specific EPS production. One possibility is if production of clumping-specific EPS depends on the activity of another chemotaxis-like pathway. Che-like pathways regulating EPS production have been identified in other bacterial species (12, 39). The genome of *A. brasilense* encodes for four Che-like pathways, with one of them predicted to have an alternative cellular function, distinct from motility (35). This or perhaps another pathway could ultimately function in modulating clumping-specific EPS production. Together with evidence obtained previously (4, 29) and discussed above, cross-talk involving CheB1 and CheR1 is plausible to explain the role of Che1 in modulating indirectly the signaling output of other signaling pathway(s), including perhaps some regulatory pathway controlling clumping-specific EPS production. In support of this hypothesis, clumping-specific EPS were produced in strains where the activity of CheB1 was affected (strains carrying *cheA1* and *cheB1* deletions) while the role of CheY1 in modulating the production of EPS yielding stable clumps was opposite.

What advantage could clumping afford *A. brasilense* cells with? Our results indicate that transient clumping is inversely correlated with free-swimming behavior such as aerotaxis. Motile cells within clumps are unlikely to be able to explore their surroundings using taxis-dependent behaviors. In turn, this suggests that clumping functions to transiently prevent motility-dependent responses. Clumping is initially a transient behavior, progressing over time toward increasingly more stable clumps of motile cells. Therefore, while motility changes may mediate transient clumping behaviors, additional physiological changes are implemented to allow for the transition to more stable clumps, with the production of EPS being such a prominent change. The finding that Che1, quite likely together with other pathway(s), regulates clumping in *A. brasilense* is consistent with the observation that clumping is a behavior extremely sensitive to ambient conditions in which clumping cells are able to rapidly transition between cell-to-cell interactions and free-swimming motility. Given the dynamic changes in clumping and the fact that it precedes the production of stable clumps, we hypothesize that clumping could afford the cells with the ability to maintain a relatively static position in a gradient without having to commit to a permanently attached lifestyle by remaining motile and able to respond to changes in ambient conditions.

Acknowledgements

The authors thank Dr. Z. Xie, for constructing strain AB104 and anonymous reviewers for their insightful comments and suggestions as well as members of the Alexandre laboratory for comments on the manuscript. This work was supported by NSF (MCB-0919819) to G.A.

Chapter 2

The *Azospirillum brasilense* Che1 chemotaxis pathway controls the swimming velocity which affects transient cell-to-cell clumping

References

1. **Alexandre, G., Greer, S. E., Zhulin, I. B.** 2000. Energy taxis is the dominant behavior in *Azospirillum brasilense*. J. Bacteriol. **182**: 6042-6048.

2. **Alexandre, G., Zhulin, I.B.** 2003. Different evolutionary constraints on chemotaxis proteins CheW and CheY revealed by heterologous expression studies and protein sequence analysis. J. Bacteriol. **185**: 544-552.

3. **Alexandre, G.** 2010. Coupling metabolism and chemotaxis-dependent behaviours by energy taxis receptors. Microbiology **156**: 2283-2293.

4. **Bible, A.N., Stephens, B.B., Ortega, D.R., Xie, Z., Alexandre, G.** 2008. Function of a chemotaxis-like signal transduction pathway in modulating motility, cell clumping, and cell length in the Alphaproteobacterium, *Azospirillum brasilense*. J. Bacteriol. **190**: 6365-6375.

5. **Bradford, M. M.** 1976. A rapid and sensitive method for the quantitation of microgram quantities of protein utilizing the principle of protein-dye binding. Anal. Biochem. **72**: 248-254.

6. **Brown, M. T., Delalez, N. J., Armitage J. P.** 2010. Protein dynamics and mechanisms controlling the rotational behaviour of the bacterial flagellar motor. Curr. Opin. Microbiol. **14**:734-740.

7. **Edwards, A.N., Siuti, P., Bible, A.N., Alexandre, G., Retterer, S.T., Doktycz, M.J., Morrell-Falvey, J.L.** 2011. Characterization of cell surface and extracellular matrix remodeling of *Azospirillum brasilense* chemotaxis-like1 signal transduction pathway mutants by atomic force microscopy. FEMS Microbiol. Lett. **314**: 131-139.

8. **Fang, X., Gomelsky, M.** 2010. A post-translational, c-di-GMP-dependent mechanism regulating flagellar motility. Mol. Microbiol. **76**: 1295-1305.

9. **Greer-Phillips, S. E., Stephens, B. B., Alexandre, G.** 2004. An energy taxis transducer promotes root colonization by *Azospirillum brasilense*. J. Bacteriol. **186**: 6595-6604.

10. **Hamer, R., Chen, P. Y., Armitage, J. P., Reinert, G., Deane, C. M.** 2010. Deciphering chemotaxis pathways using cross species comparisons. BMC Syst. Biol. **4**:3.

11. **Hauwaerts, D., Alexandre, G., Das, S. K., Vanderleyden, J., Zhulin, I. B.** 2002. A major chemotaxis gene cluster in *Azospirillum brasilense* and relationships between chemotaxis operons in alpha-proteobacteria. FEMS Microbiol. Lett. **208**: 61-67.

12. **Hickman, J. W., Tifrea, D. F., Harwood, C. S.** 2005. A chemosensory system that regulates biofilm formation through modulation of cyclic diguanylate levels. Proc. Natl. Acad. Sci. **102**: 14422-14427.

13. **Katupitiya, S., Millet, J., Vesk, M., Viccars, L., Zeman, A., Lidong, Z., Elmerich, C., Kennedy, I.R.** 1995. A mutant of *Azospirillum brasilense* Sp7 impaired in flocculation with a modified colonization pattern and superior nitrogen fixation in association with wheat. Appl. Environ. Microbiol. **61**: 1987-1995.

14. **Keen, N. T., S. Tamaki, D. Kobayashi, and D. Trollinger.** 1988. Improved broad-host-range plasmids for DNA cloning in gram-negative bacteria. Gene **70**: 191–197.

15. **Kirby, J. R.** 2009. Chemotaxis-like regulatory systems: Unique roles in diverse bacteria. Ann. Rev. Microbiol. **63**: 45-59.

16. **Kovach, M. E., P. H. Elzer, D. S. Hill, G. T. Robertson, M. A. Farris, R. M. Roop II, Peterson, K. M.** 1995. Four new derivatives of the broad-host-range cloning vector pBBR1MCS, carrying different antibiotic-resistance cassettes. BioTechniques **166**: 175–176.

17. **Laszlo, D. J., Taylor, B. L.** 1981. Aerotaxis in *Salmonella typhimurium*: Role of electron transport. J. Bacteriol. **145**: 990-1001.

18. **McClaine, J. W., Ford, R. M.** 2002. Reversal of flagellar rotation is important in initial attachment of *Escherichia coli* to glass in a dynamic system with high- and low-ionic-strength buffers. Appl. Environ. Microbiol. **68**: 1280-1289.

19. **Merritt, J. H., Brothers, K. M., Kuchma, S. L., O'Toole, G. A.** 2007. SadC reciprocally influences biofilm formation and swarming motility via modulation of exopolysaccharide production and flagellar function. J. Bacteriol. **189**: 8154-8164.

20. **Miller, L. D., Yost, C. K., Hynes, M. F., Alexandre, G.** 2007. The major chemotaxis gene cluster of *Rhizobium leguminosarum* bv. *viciae* is essential for competitive nodulation. Mol. Microbiol. **63**: 348-362.

21. **Pilizota, T., Brown, M. T., Leake, M. C., Branch, R. W., Berry, R. M., Armitage, J. P.** 2009. A molecular brake, not a clutch, stops the *Rhodobacter sphaeroides* flagellar motor. Proc. Natl. Acad. Sci. U. S. A. **106**:11582–11587.

22. **Pereg Gerk, L., Paquelin, A., Gounon, P., Kennedy, I.R., Elmerich, C.** 1998. A transcriptional regulator of the *LuxR-UhpA* family, *FlcA*, controls flocculation and wheat root surface colonization by *Azospirillum brasilense* Sp7. Mol. Plant Microbe Interact. **11**: 177-187.

23. **Pereg Gerk, L., Gilchrist, K., Kennedy, I.R.** 2000. Mutants with enhanced nitrogenase activity in hydroponic *Azospirillum brasilense*-wheat associations. Appl. Environ. Microbiol. **66**: 2175-2184.

24. **Porter, S. L., Armitage, J. P.** 2004. Chemotaxis in *Rhodobacter sphaeroides* requires an atypical histidine protein kinase. *J. Biol. Chem.* **279:** 54573-54580.

25. **Sadasivan, L., Neyra, C. A.** 1985. Flocculation in *Azospirillum brasilense* and *Azospirillum lipoferum*: exopolysaccharides and cyst formation. J. Bacteriol. **163**: 716-723.

26. **Simon, R., U. Priefer, and A. Pülher.** 1983. A broad host range mobilization system for in vivo genetic engineering transposon mutagenesis in gram-negative bacteria. Bio/Technology **1:** 784-791.

27. **Siuti, P., Green, C., Edwards, A. N., Doktycz, M. J., Alexandre, G.** 2011. The chemotaxis-like Che1 pathway has an indirect role in adhesive cell properties of *Azospirillum brasilense*. FEMS Microbiol. Lett. **323**: 105-112.

28. **Sourjik, V.** 2004. Receptor clustering and signal processing in *E. coli* chemotaxis. Trends Microbiol. **12**: 569-575.

29. **Stephens, B. B., Loar, S. N., Alexandre, G.** 2006. Role of CheB and CheR in the complex chemotactic and aerotactic pathway of *Azospirillum brasilense*. J. Bacteriol. **188**: 4759-4768.

30. **Szurmant, H., and G. H. Ordal.** 2004. Diversity in chemotaxis mechanisms among the bacteria and archaea. Microbiol. Mol. Biol. Rev. **68**: 301-319.

31. **Tindall, M. J., Porter, S. L., Maini, P. K.. and J. P. Armitage.** 2010. Modeling chemotaxis reveals the role of reversed phosphotransfer and a bi-functional kinase-phosphatase. PLoS Comput. Biol. **6**: e1000896.

32. **Toutain, C. M., Caizza, N. C., Zegans, M. E. & O'Toole, G. A.** 2007. Roles for flagellar stators in biofilm formation by *Pseudomonas aeruginosa*. Res. Microbiol. **158**: 471–477.

33. **Wadhams, G. H., Warren, A. V., Martin, A. C., Armitage, J. P.** 2003. Targeting of two signal transduction pathways to different regions of the bacterial cell. Mol. Microbiol. **50**: 763–770.

34. **Wadhams, G.H., Armitage J. P.** 2004. Making sense of it all: bacterial chemotaxis. Nat. Rev. Mol. Cell Biol. **5**: 1024-1037.

35. **Wisniewski-Dye, F., Borziak, K., Khalsa-Moyers, G., Alexandre, G., Sukharnikov, L.O., Wuichet, K., Hurst, G.B., McDonald, W.H., Robertson, J.S., Barbe, V., Calteau, A., Rouy, Z., Mangenot, S., Prigent-Combaret, C., Normand, P., Boyer, M., Siguier, P., Dessaux, Y., Elmerich, C., Condemine, G., Krishnen, G., Kennedy, I.,**

Paterson, A.H., Gonzalez, V., Mavingui, P., Zhulin, I.B. 2011. *Azospirillum* genomes reveal transition of bacteria from aquatic to terrestrial environments. PLoS Genetics **7**: e1002430.

36. **Wuichet, K. and Zhulin, I. B.** 2010. Origins and diversification of a complex signal transduction system in prokaryotes. *Sci*. *Signal*. **3**: pa50.

37. **Xie, Z., Ulrich, L. E., Zhulin, I. B., Alexandre, G.** 2010. PAS domain containing chemoreceptor couples dynamic changes in metabolism with chemotaxis. Proc. Natl. Acad. Sci. **107**: 2235-2240.

38. **Xu, Q., Black, W. P., Cadieux, C. L., Yang, Z.** 2008. Independence and interdependence of Dif and Frz chemosensory pathways in *Myxococcus xanthus* chemotaxis. Mol. Microbiol. **69**: 714-723.

39. **Yang, Z., Ma, X., Tong, L., Kaplan, H. B., Shimkets, L. J., Shi, W.** 2000. *Myxococcus xanthus dif* genes are required for biogenesis of cell surface fibrils essential for social gliding motility. J. Bacteriol. **182**: 5793–5798.

40. **Zhulin, I. B., Bespalov, V. A., Johnson, M. S., Taylor, B. L.** 1996. Oxygen taxis and proton motive force in *Azospirillum brasilense*. J. Bacteriol. **178**: 5199-5204.

41. **Zhulin, I. B.** 2001. The superfamily of chemotaxis transducers: from physiology to genomics and back. Adv. Microbiol. Physiol. **45**: 157-198.

Chapter 3

Functional analysis of CheA1 domains in behaviors regulated by the Che1 pathway

Abstract

The *Azospirillum brasilense* Che1 pathway has been shown to directly regulate cell length and swimming speed. Che1-dependent control of the swimming speed may directly affect chemotaxis and aerotaxis, although Che1 has also been shown to modulate these locomotor behaviors indirectly, via an effect on the motility bias. In addition, Che1 control of the swimming speed was shown to indirectly affect clumping and flocculation behavior. Central to the chemotaxis signal transduction pathway is the histidine kinase, CheA. Signaling through CheA is not only important for responses (via interactions with CheY) to specific cues, but also to adaptation (via interactions with CheB). In order to gain further insight into how the Che1 pathway of *A. brasilense* could be involved in regulating multiple behaviors, either directly or indirectly, we chose to start by studying the function of CheA1. The *A. brasilense* Sp7 CheA1 is a hybrid histidine kinase with a seven-transmembrane HlyIII-like domain at its N-terminus and a second P5 domain at its C-terminus. Here, we characterize the functions of the *A. brasilense* Sp7 CheA1 domains by generating a set of constructs containing various domain deletions or site-specific mutations in order to determine their contribution to CheA1 function. Experimental evidence points to the N-terminal HlyIII-like TM domain as being cirtical for the proper localization of CheA1 at the cell poles, which in turn affects its function, including regulating the cell length. A regulatory role for the $P5_B$-Rec domain in modulating the TM function is also suggested by the behavior of mutant strains. Furthermore, other domains of CheA1 appear to impact chemotaxis and aerotaxis, most likely via effects on swimming sped and motility bias.

Section A. Introduction

Azospirillum brasilense are gram-negative alphaproteobacteria that live in the soil where they are capable of fixing atmospheric nitrogen and colonizing the root surfaces of various cereals and grasses. Within the soil, sensing of specific environmental cues such as nutrient availability can result in signals for chemotaxis (towards nutrients or away from toxins). *A. brasilense* has four different chemotaxis-like operons, one of which has been characterized and shown to regulate cell length and swimming speed (5, 6). Other behaviors such as clumping and flocculation seem to be indirectly regulated by this pathway and may involve cross-talk mechanisms with other Che pathways, a hypothesis currently under investigation (6).

The process of chemotaxis takes place using a two-component signal transduction system with CheA as the histidine kinase and CheY as the response regulator. Chemotaxis has been best characterized in the model organism *Escherichia coli*. *E. coli* possesses a single chemotaxis pathway and five different chemoreceptors (also referred to as methyl-accepting chemotaxis proteins, or MCPs). Signals are perceived by chemoreceptors which undergo a conformational change as a result. Conformational change within chemoreceptors is transduced to CheA via the adaptor protein CheW. CheA becomes autophosphorylated at a conserved histidine residue, His48 in *E. coli* (22, 36). CheA~P phosphorylates its cognate response regulator CheY at a conserved aspartate residue, Asp57 (33). The phosphorylated CheY (CheY~P) can then bind the flagellar motor in order to switch the direction of flagellar rotation from clockwise to counter-clockwise. Clockwise rotation stimulates the "tumble" behavior in *E. coli*. CheA~P also phosphorylates the methylesterase CheB, which together with the methyltransferase CheR, functions to add (CheR) and remove (CheB~P) methyl groups from conserved glutamate

residues on chemoreceptors, thus resetting these receptors to "sensing mode". Therefore, CheA not only serves to initiate a response to specific cues (by phosphorylating CheY), but it is also responsible for mediating a feedback response mechanism involving CheB by which new signals can be sensed by chemoreceptors (for a review, see 38 and 45).

CheA is a central component of the chemotaxis signal transduction pathway, and it is considered a Class II histidine kinase. Histidine kinases are identified by the presence of five conserved regions of amino acid sequences, and these are called the H, N, G1, F, and G2 boxes (1, 11, 30, 41). These regions contain the conserved amino acids, histidine, asparagine, glycine, and phenylalanine. The H-box domain contains a conserved histidine residue which is phosphorylated and the G-boxes consist of glycine-rich domains involved in nucleotide binding, kinase and phosphatase activities (Figure 22) (1). CheA differs from other prototypical histidine kinases in that it does not possess an H-box, and the phosphorylatable histidine is instead in a non-conserved region at the amino terminus (1). In CheA, the phosphorylatable histidine is located in the P1 domain in the model organism, *E. coli*, for which the NMR structure of the P1 domain has been determined (50, 51). Other domains found in the *E. coli* CheA are the P2, P3, P4, and P5 domains. The P2 domain contains the CheY/CheB recognition site and the crystal structure of the P2 domain in complex with CheY has been solved (46). It has also been shown that CheY and CheB bind to the P2 domain of CheA with micromolar affinity (24, 40); however, it was found that signaling specificity is not primarily determined by this domain (18). The crystal structure of the P3, P4, and P5 domains were determined from the CheA from *Thermatoga maritima* (Figure 22) (7). The P3 domain is required for dimerization and has been shown to play a critical role in signal transduction (28). The P4 domain is known as the kinase,

or catalytic domain, and it is in this region that the N, G1, F, and G2 boxes are located. The ATP-binding cavity contains four β strands and three α helices, sharing topology with the catalytic domains of GyrB and Hsp90, but differing from those of Ser/Thr/Tyr kinases (7). Surrounding the ATP-binding site are the regions containing the N, G1, F, and G2 domains (7). The P5 regulatory domain is homologous to SH3 domains, which are known to function in protein-protein interactions (7, 49). This regulatory domain has been shown to mediate interactions between CheA and CheW, and is thus essential to signaling via the chemotaxis signal transduction pathway (7, 8). Interestingly, while P1, P3, P4 and P5 are conserved in all CheA homologs, the P2 domain is not always present (46).

The Che1 pathway of *A. brasilense* Sp7 functions to coordinate multiple cellular behaviors, which is a departure from most other Che-like pathways in bacteria. Interestingly, CheA1, the histidine kinase for the Che1 pathway is unique in that it is not only a hybrid histidine kinase (it possesses a C-terminal Receiver domain), but it also has a second P5 domain at its C-terminus region and a 7-transmembrane domain of unknown function (COG1272) at its N-terminus. There are other CheA homologs that possess dual P5 domains at their C-terminus (such as *Rhodospirillum centenum*). No other CheA found thus far has been shown to possess this N-terminal transmembrane domain. Determining the roles of these unique CheA1 domains and how they contribute to the activity of CheA1 and thus, the Che1 pathway was undertaken in order to shed light on how they contribute to Che1 function in regulating multiple cellular behaviors.

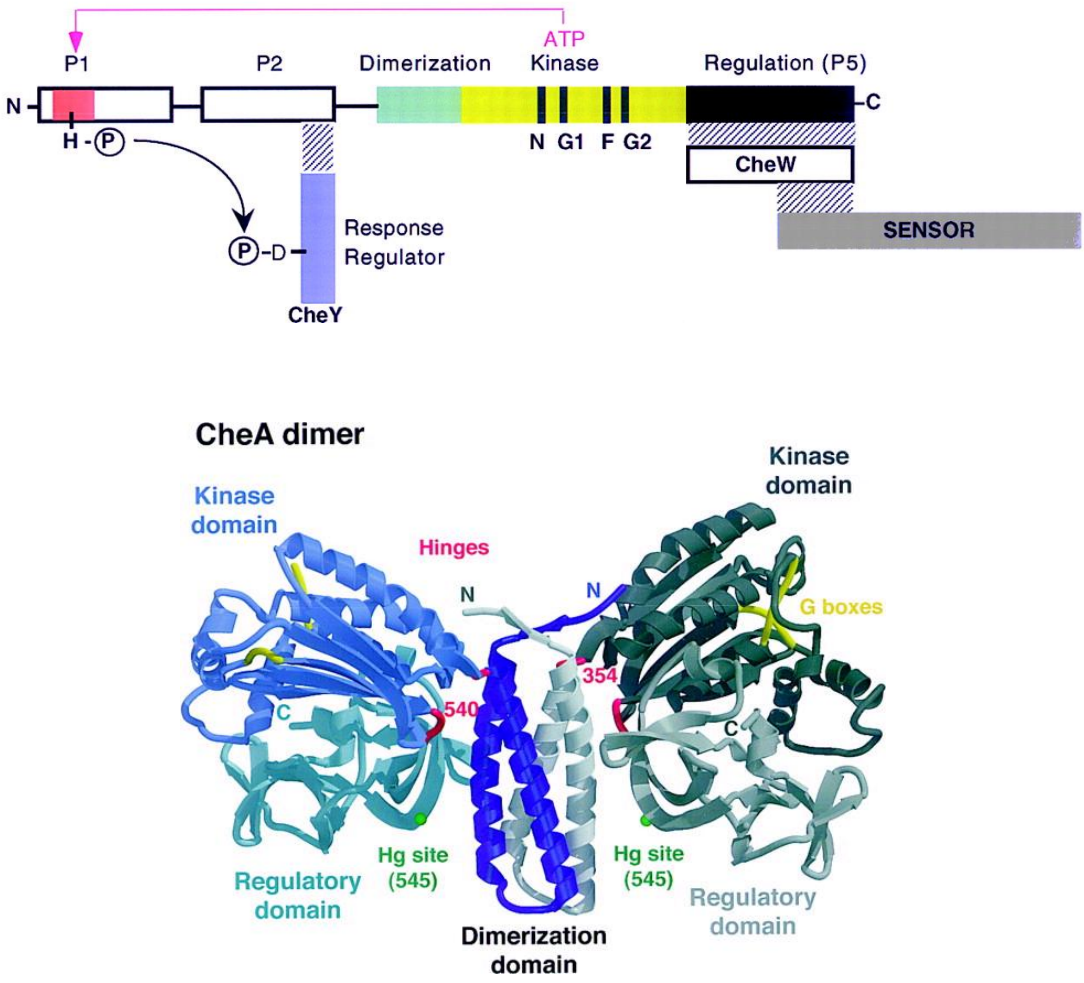

Figure 22. Structure of CheA, a class II histidine kinase. Image taken from Bilwes *et al*., 1999 (7). (Top) A representation of the domains of CheA, including the N, G1, F, and G2 regions. (Bottom) Crystal structure of CheA, highlighting the dimerization (P3), kinase (P4), and regulatory (P5) domains.

Section B. Materials and Methods

Bacterial Strains and Growth Conditions

Table 1 describes the strains and plasmids used in this study. Cells were grown at 28ºC with shaking in either rich TY (1 liter contains 10 grams Tryptone and 5 grams Yeast extract) media or MMAB (minimal media) supplemented with carbon and nitrogen sources of choice (16). For measurements of cell length, *A. brasilense* was first grown in MMAB semi-solid agar plates with ammonium chloride (18.7 mM) as the nitrogen source and malate (10 mM) as the carbon source and incubated at 28ºC for approximately 48 hours. Once the cells have grown and swam out from the inoculation point, cells from the outer ring of the semi-solid agar plate (about 20 µl) were inoculated into MMAB supplemented with ammonium chloride (18.7 mM), malate (5 mM), and fructose (5 mM) at 28°C overnight with shaking (about 225 rpm). Clumping behavior and flocculation was induced by inoculating 100 µl of an overnight culture of cells grown in TY media (OD_{600nm} = 1) into 5 ml of flocculation media (MMAB containing 0.5 mM sodium nitrate as sole nitrogen source and 8 mM fructose as sole carbon source) and then grown at 28ºC with shaking (about 225 rpm). Aliquots of cultures were observed microscopically at the time of inoculation, 3 hours post-inoculation (hpi), 6 hpi, 9 hpi, 14 hpi, and 24-30 hpi (time at which wild type cells are flocculated). Cells were visualized using a Nikon Eclipse E200 light microscope at 400X magnification.

Table 7. Strains and plasmids used in this study.

Strain or plasmid	Genotype, relevant characteristics	Reference or Source
Plasmids		
pBBR1MCS3	Cloning vector (Tc)	23
pRH005	Gateway destination vector with YFP (Cm, Km)	15
pBBR-*cheA1*	pBBR1MCS3 containing *cheA1*	5
pBBR-*cheA1ΔTM*	pBBR1MCS3 containing *cheA1* with the TM domain deleted	this work
pBBR-TM_{cheA1}	pBBR1MCS3 containing the TM domain of *cheA1* alone	this work
pBBR-*cheA1ΔRec*	pBBR1MCS3 containing *cheA1* with the C-terminal Rec domain deleted	this work
pBBR-*cheA1*$\Delta P5_B$-*Rec*	pBBR1MCS3 containing *cheA1* with the 2nd P5 (P5B) and C-terminal Rec domains deleted	this work
pBBR-*cheA1ΔTM*-$P5_B$-*Rec*	pBBR1MCS3 containing *cheA1* with the TM, 2nd P5 ($P5_B$), and C-terminal Rec domains deleted	this work
pBBR-*cheA1*$\Delta P5_A$	pBBR1MCS3 containing *cheA1* with the 1st P5 ($P5_A$) domain deleted	this work
pBBR-*cheA1*$\Delta P5_B$	pBBR1MCS3 containing *cheA1* with the 2nd P5 ($P5_B$) domain deleted	this work
pBBR-*cheA1*$\Delta P5_A$-$P5_B$	pBBR1MCS3 containing *cheA1* with both P5 domains ($P5_A$, $P5_B$) deleted	this work
pBBR-$cheA1_{H252Q}$	pBBR1MCS3 containing *cheA1* with the site-specific mutation H252Q	6
pBBR-$cheA1_{D1055N}$	pBBR1MCS3 containing *cheA1* with the site-specific mutation D1055N	this work
pRH-*cheA1*	pRH005 containing *cheA1*	this work
pRH-TM_{cheA1}	pRH005 containing the TM domain of *cheA1* alone	this work
pRH-*cheA1ΔTM*	pRH005 containing *cheA1* with the TM domain deleted	this work
pKGmob-Gm	mobilizable suicide plasmid (Gm)	21
pKGmob-*cheA1*	pKGmob-GM containing Sp245 *cheA1* (Gm)	this work
Strains		
Escherichia coli		
TOP10	General cloning strain	Invitrogen
OmniMAX	General cloning strain	Invitrogen
S17-1	*thi endA recA hsdR* with RP4-2Tc::Mu-Km::Tn7 integrated in chromosome	35
Azospirillum brasilense		
Sp7	Parental strain, "wild type"	ATCC29145
Sp245	Parental strain, "wild type"	4
cheA1 Sp245	*cheA1:Gm* insertion	this work

Table 7. Continued.

AB101	Δ(*cheA1*)::*gusA-Km* (Km)	5
AB103	Δ(*cheA1-cheR1*)::*Cm* (Cm), also named Δ*che1*	5
Wild type (pBBR)	Wild type strain (Sp7) containing pBBR1MCS3 (Tc)	5
AB101 (pBBR)	AB101 containing pBBR1MCS3 (Tc)	5
AB101 (pBBR-*cheA1*)	AB101 containing pBBR-*cheA1* (Tc)	5
AB101 (pBBR-*cheA1ΔTM*)	AB101 containing pBBR-*cheA1ΔTM* (Tc)	this work
AB101 (pBBR-TM_{cheA1})	AB101 containing pBBR-TM_{cheA1} (Tc)	this work
AB101 (pBBR-*cheA1ΔRec*)	AB101 containing pBBR-*cheA1ΔRec* (Tc)	this work
AB101 (pBBR-*cheA1Δ* $P5_B$*-Rec*)	AB101 containing pBBR-*cheA1Δ*$P5_B$*-Rec* (Tc)	this work
AB101 (pBBR-*cheA1Δ TM-P5B-Rec*)	AB101 containing pBBR-*cheA1ΔTM-P5B-Rec* (Tc)	this work
AB101 (pBBR-*cheA1Δ*$P5_A$)	AB101 containing pBBR-*cheA1Δ*$P5_A$ (Tc)	this work
AB101 (pBBR-*cheA1Δ*$P5_B$)	AB101 containing pBBR-*cheA1Δ*$P5_B$ (Tc)	this work
AB101 (pBBR-*cheA1Δ*$P5_A$-$P5_B$)	AB101 containing pBBR-*cheA1Δ*$P5_A$-$P5_B$ (Tc)	this work
AB101 (pBBR-$cheA1_{H252Q}$)	AB101 containing pBBR-$cheA1_{H252Q}$ (Tc)	6
AB101 (pBBR-$cheA1_{D1055N}$)	AB101 containing pBBR-$cheA1_{D1055N}$ (Tc)	this work
Wild type (pRH005)	Wild type strain (Sp7) containing pRH005 (Cm, Km)	this work
Wild type (pRH-*cheA1*)	Wild type strain (Sp7) containing pRH-*cheA1* (Cm, Km)	this work
Wild type (pRH-TM_{cheA1})	Wild type strain (Sp7) containing pRH-TM_{cheA1} (Cm, Km)	this work
Wild type (pRH-*cheA1ΔTM*)	Wild type strain (Sp7) containing pRH-*cheA1ΔTM* (Cm, Km)	this work
AB101 (pRH005)	AB101 containing pRH005 (Cm, Km)	this work
AB101 (pRH-*cheA1*)	AB101 containing pRH-*cheA1* (Cm, Km)	this work
AB101 (pRH-TM_{cheA1})	AB101 containing pRH-TM_{cheA1} (Cm, Km)	this work
AB101 (pRH-*cheA1ΔTM*)	AB101 containing pRH-*cheA1ΔTM* (Cm, Km)	this work
AB103 (pRH005)	AB103 containing pRH005 (Cm, Km)	this work
AB103 (pRH-*cheA1*)	AB103 containing pRH-*cheA1* (Cm, Km)	this work
AB103 (pRH-TM_{cheA1})	AB103 containing pRH-TM_{cheA1} (Cm, Km)	this work
AB103 (pRH-*cheA1ΔTM*)	AB103 containing pRH-*cheA1ΔTM* (Cm, Km)	this work

Antibiotic resistance abbreviations: Tc (tetracycline), Km (kanamycin), Cm (chloramphenicol), Gm (gentamycin)

Construction of domain deletions of CheA1 for complementation and YFP fusions

Generation of a construct for full complementation of Δ*cheA1* (AB101), as well as a construct containing the site-specific mutant, $cheA1_{H252Q}$, was performed previously (5, 6). Complementation of Δ*cheA1* (AB101) with domain deletions were performed by generating PCR products using primers which are listed in Table 8. The previously generated pBBR-*cheA1* was used as a template for generating the complementation constructs containing TM_{CheA1}, CheA1ΔTM (generated previously, Alexandre lab), CheA1ΔRec, CheA1Δ$P5_B$-Rec, CheA1Δ$P5_A$, CheA1Δ$P5_B$, and CheA1Δ$P5_A$-$P5_B$. The construct containing CheA1ΔTM was used as a template to generate the complementation construct containing CheA1ΔTM-$P5_B$-Rec. The site-specific mutant, $CheA1_{D1055N}$, was generated previously (Alexandre lab) using the QuikChangeII Site-directed Mutagenesis Kit (Stratagene). To generate the D1055N mutation, we used the primers listed in Table 8 in order to change the codon for Aspartate (GAC) to Asparagine (AAC). The promoter-less *cheA1* with the D1055N mutation was then cloned into pProEx-HTA and was then named pIZ106 (Alexandre lab strain collection, unpublished). In order to generate the pBBR-$cheA1_{D1055N}$, we used primers listed in Table 8 (CheA1prom Xho-F and CheA1 DNup HindIII-R) to clone the promoter sequence of *cheA1* using the pBBR-*cheA1* plasmid as a PCR template. We then used primers (CheA1 DNdn HindIII-F and CheA1full Xba-R) to clone the portion of *cheA1* containing the D1055N mutation. Each piece was inserted into the pCR2.1 TOPO vector and sequenced prior to cloning into pBBR-MCS3 (Kovach *et al*., 1995). Once verified, these pieces were isolated from pCR2.1 TOPO using the following enzymes: cheA1 DN up (XhoI and HindIII) and cheA1 DN down (HindIII and XbaI). Each fragment was then ligated into the pBBR-MCS3 vector which was cut with XhoI and XbaI. The

final constructs generated here were each introduced into *E. coli* S17-1 strain (35) to facilitate biparental mating into the Δ*cheA1* (AB101) mutant as described previously (39).

Construction of the cheA1 insertion mutant in the *Azospirillum brasilense* Sp245 strain took place by first amplifying by PCR a short (~500 bp) region of *cheA1* using the primers listed in Table 8. The amplified *cheA1* segment was cloned into pCR2.1 TOPO (Invitrogen) for sequencing purposes, then moved into the suicide vector, pKGmob-Gm. The final construct, pKGmob-*cheA1*, was then introduced into *E. coli* S17-1 cells (35) prior to biparental mating into the wild type Sp245 strain.

Gateway cloning technology from Invitrogen was used to clone *cheA1*, *cheA1ΔTM*, and TM_{cheA1} (TM domain alone) into the plasmid pRH005 in order to generate in-frame C-terminal gene fusions to yellow fluorescent protein (YFP) (15). The strategy for these gene fusions are as follows. First, using primers listed in Table 8, we generated each of these PCR products using pBBR-*cheA1* as a PCR template. PCR products were then incorporated into the donor vector, pDONR221 (Invitrogen), using the BP Clonase enzyme (Invitrogen) according to manufacturer's directions and transformed into OmniMax competent cells (Invitrogen). Afterwards, constructs were verified by sequencing (University of Tennessee, Molecular Biology Resource Facility). Next, constructs containing *cheA1*, *cheA1ΔTM*, and TM_{cheA1} were moved from the donor vector, pDONR, to the destination vector, pRH005, in a recombination reaction using the LR Clonase II enzyme (Invitrogen) according to manufacturer's directions. Final constructs were then introduced into wild type *A. brasilense*, Δ*cheA1* (AB101), and Δ*che1* (AB103) by biparental conjugation, as described above.

Table 8. List of primers used in this study.

Primer Name	Sequence (5'-3')
CheA1prom KpnI-F	CGGGGTACCCAGCGCGATGAACTGGTTG
CheA1prom XhoI-F	CCGCTCGAGCAGCGCGATGAACTGGTT
CheA1full XbaI-R	GCTCTAGATCATGCGGCACCTTTCTGC
CheA1ΔTM BglII-F	GAAGATCTTTCGCCGCGGTCGCGCGG
CheA1ΔTM BglII-R	GAAGATCTGACCGCGTCCGCCGCACG
CheA1 TM XbaI-R	TCTAGATCATTCCACGTCGAGCAACGA
CheA1ΔRec XhoI-R	CTCGAGTCATGGAGCGCCCTCTCC
CheA1ΔP5BRec XhoI-R	CTCGAGTCATCCTCCTGGCGGGTC
CheA1ΔP5Aup HindIII-R	AAGCTTGGGATCTTGATGACG
CheA1ΔP5Adn HindIII-F	AAGCTTAACGGCATCGCGTCG
CheA1ΔP5Bup HindIII-R	AAGCTTCTGGCGGGTCGCCTG
CheA1ΔP5Bdn HindIII-F	AAGCTTTCCTCGACCGATGCG
CheA1D1055N-sdm-F	CGTCATCGTCTCCAACATCGAGATGCCGG
CheA1D1055N-sdm-R	CCGGCATCTCGATGTTGGAGACGATGACG
CheA1 DNup HindIII-R	AAGCTTCACGGCGGTGACGTC
CheA1 DNdn HindIII-F	AAGCTTGAGAACGCCAACGAG
GW CheA1-F	GGGGACAAGTTTGTACAAAAAAGC AGGCTCAGCGCGATGAACTGGTT
GW CheA1-R	GGGGACCACTTTGTACAAGAAAGCTGG GTTGCGGCACCTTTCTGCTCG
GW CheA1 TM-R	GGGGACCACTTTGTACAAGAAAGCTGG GTTTCCACGTCGAGCAACGAC
Sp245 cheA1-F	GAATCACGTGACGTCGGA
Sp245 cheA1-R	CGACGCCGCGGCCCGACA

Restriction enzymes used are underlined as part of the primer name and the location of these restriction sites within the primers are underlined, as well. The underlined letters in primer sequences for the site-directed mutant, D1055N, represent the base that was changed.

Behavioral assays

Semi-soft agar assays: To compare chemotaxis responses of the Δ*cheA1* (AB101) mutant with those of strains carrying domain deletions of CheA1, minimal medium plates containing 0.3% agar, 18.7 mM ammonium chloride as a nitrogen source, and 10 mM malate as the carbon source were used. Semi-soft agar plates were inoculated with wild type *A. brasilense* strain Sp7 carrying pBBR-MCS3, Δ*cheA1* (AB101) carrying pBBR-MCS3, and Δ*cheA1* (AB101) complemented with various derivatives of CheA1 expressed from plasmids (39) (Table 8). Photographs of chemotactic rings were taken after 48 hours incubation at 28^{o}C.

Aerotaxis: Aerotaxis assays using the capillary method were performed as described previously (39).

Motility behavior: Analysis of the swimming motility bias was primarily qualitative. This analysis was performed using cells grown to a low density in MMAB supplemented with 10 mM malate. Cells were visualized and videos were taken using a Nikon Eclipse E200 light microscope at 400X magnification. From these videos, we analyzed the motility of cells in terms of "runs" (no change in direction) and the frequency at which cells changed directions (i. e. reversal frequency). Wild type cells show a mixture of "runs" and "reversals", thus having a "random" motility bias. Relative to the wild type, cells with lower reversal frequencies were referred to as "smoother", while cells with higher reversal frequencies were described as "more reversal" or "highly reversal". Analysis of swimming speed was performed from videos taken during the gas perfusion chamber assay (described below). These videos were analyzed using

the CellTrak software program in order to generate swimming tracks, by which swimming speed can be determined.

Gas perfusion chamber assay: In this assay, cells were grown as described previously in MMAB supplemented with 10 mM pyruvate and the gas perfusion chamber assay was performed as described in Chapter 2 (6), where cells under steady state conditions (atmospheric air flow) are subjected to changes in aeration (namely, removal of air by switching to N_2), under which conditions, we measure the response of cells in terms of swimming speed and clumping behavior. In this assay, the suspension of cells in the chamber initially experience a flow of air (normal atmospheric air with 21% oxygen) for approximately 30 seconds, which corresponds to steady state conditions. After 30 seconds, the atmosphere of air flowing over the cells is switched to N_2 for 30 seconds, for which we measure the response in terms of swimming speed and clumping behavior. Videos were taken for the entire 60 seconds. The 10 seconds prior to air removal and the 10 seconds after air removal were analyzed for swimming speed and clumping behavior, based on previously determined experimental conditions (6).

Measurements of cell length

Cell length measurements were performed as described previously (5). Briefly, each strain was first grown on MMAB plates containing 0.3% agar (similarly to that described in ***Behavioral Assays*** for chemotaxis ring formation). After cells formed chemotaxis rings (1-2 days later), approximately 20 μl of cells from the outer edge of the chemotaxis ring were inoculated into MMAB supplemented with 5 mM Malate and 5 mM Fructose as carbon sources and grown at 28°C with shaking. Actively growing cells ($OD_{600} \leq 0.5$) were stained with the live

fluorescent dye FM4-64 (Invitrogen Molecular Probes) in order to stain the cell membrane and facilitate visualization with the fluorescence microscopy and measurement. Cell staining was performed by adding 1 μl of 1 M FM4-64 to 1 ml of culture (final concentration at 1 μM) for 5 minutes at room temperature (Invitrogen Molecular Probes). Stained cells were concentrated by centrifugation (1 minute at max. speed in a microcentrifuge) and immobilized on slides using molten 1% low melting point agarose in PBS. Pictures were taken using a Nikon ECLIPSE 80i fluorescence microscope equipped with a Nikon CoolSnap HQ2 cooled CCD camera and cell lengths were measured using the NIKON NIS-Elements BR program for a minimum of 50 cells per sample taken from at least 4 different fields of view.

Fluorescence microscopy

Microscopy was performed for strains carrying YFP fusions to CheA1, CheA1TM, and CheA1 TM by taking cells grown in MMAB supplemented with 10 mM malate to a low density and concentrating them using centrifugation. Concentrated cells were then placed on a 1% agarose pad with a coverslip and allowed to settle for 2-3 minutes. Cells were then visualized using the Nikon ECLIPSE 80i fluorescence microscope equipped with a Nikon CoolSnap HQ2 cooled CCD camera, as described above. Fluorescent protein fusions could be observed using either the YFP or FITC filters.

Section C. Results

Domain architecture of CheA1

The chemotaxis histidine kinase, CheA1, from *Azospirillum brasilense* Sp7 differs from the prototypical CheA from *Escherichia coli* in its domain architecture: the *A. brasilense* Sp7 CheA1 lacks a P2 domain, it also possess two P5 domains and a CheY-like Receiver domain at the C-

terminus (Figure 23). The most unusual feature of CheA1 is the presence of a seven-transmembrane HlyIII-like domain at the N-terminus. The HlyIII-like domain is a conserved domain of unknown function (COG1272) with homology to the *Bacillus cereus* protein, HlyIII, the first of these domains to be identified (3). Homologs of this domain are found in the genomes of Eukarya and Bacteria, and absent from the genomes of Archaea. According to the pfam database (http://pfam.sanger.ac.uk), there were 3175 hits (as of March 2012) with sequences similar to that of HlyIII, with most of these proteins possessing HlyIII-like proteins as a single domain protein. Noticeably, the presence of the HlyIII-like domain at the N-terminus of CheA1 makes it membrane-bound (Alexandre, unpublished), a unique feature amongst CheA proteins, as these are soluble proteins in all other organisms. In fact, CheA1 from *A. brasilense* Sp7 is the only CheA found thus far to possess this HlyIII-like domain.

HlyIII-like domain of CheA1 is required for polar localization

It has been shown in *E. coli*, as well as in other organisms, that CheA localizes to the cell pole via interactions between the chemoreceptors, CheW, and the P5 domains of CheA (9, 14, 26, 34, 38). The role of the HlyIII-like domain in localization of CheA1 was first assessed by generating yellow fluorescent protein (YFP) fusions to the full length CheA1, the HlyIII-like (TM:YFP) domain alone, and the CheA1ΔHlyIII (CheA1ΔTM:YFP), each under the control of the native *cheA1* promoter for expression from a low copy plasmid. Each of these fusion proteins were expressed in the wild type Sp7, Δ*cheA1*, and Δ*che1* strain backgrounds. These fusions are functional in that cells swam normally in swarm plate assays and preliminary western blot analysis indicated similar expression levels for these fusion proteins and absence of

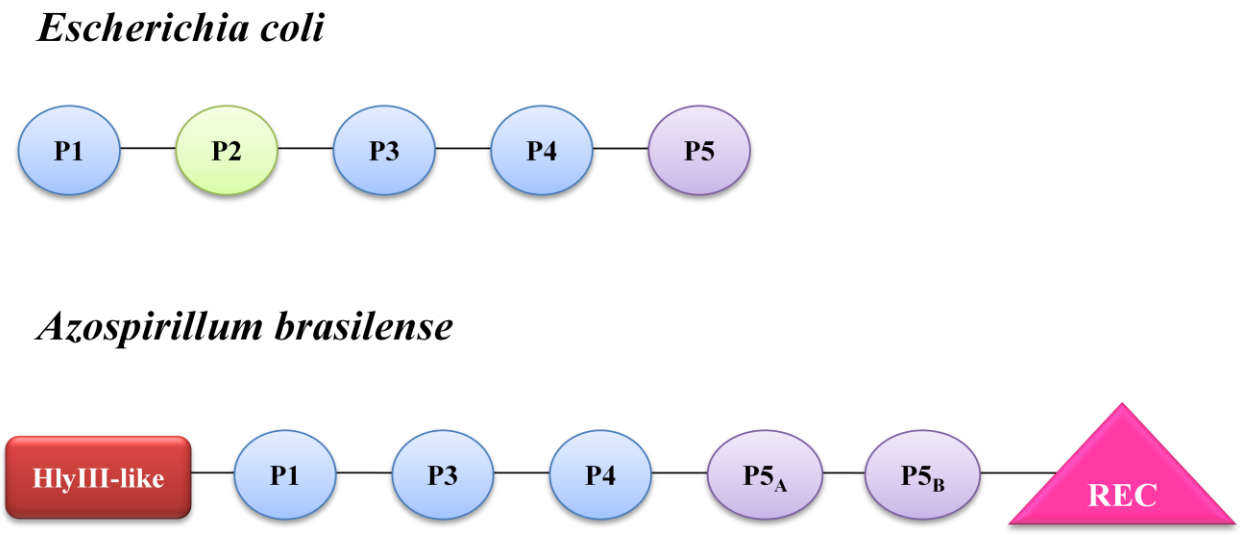

Figure 23. Domain organization of *Escherichia* coli CheA and *Azospirillum brasilense* CheA1. The domain architecture of CheA from *Escherichia coli* is similar to the CheA1 from *Azospirillum brasilense* in that both CheAs possess the P1, P3, and P4 domains. However, CheA1 from *A. brasilense* differs from CheA from *E. coli* in that the *A. brasilense* CheA1 lacks a P2 domain and possesses an N-terminal 7-transmembrane domain (HlyIII-like), two P5 domains ($P5_A$ and $P5_B$), and a Receiver (REC) domain.

degradation products (data not shown). Expressing the full length CheA1:YFP also restored the wild type phenotype for chemotaxis and cell length in the Δ*cheA1* mutant, further indicating that the fusion protein construct is functional. Strains containing CheA1:YFP showed localization at discrete polar foci in each strain background tested; whereas, strains carrying the CheA1 lacking the HlyIII domain (CheA1ΔTM:YFP) showed mostly diffuse localization with some weak polar localization observed (Figure 24), indicating a decreased ability of this truncated protein to localize at the cell poles. Interestingly, the HlyIII domain alone (TM:YFP) was able to localize to the cell poles, suggesting that this domain is the primary determinant of CheA1 polar localization (Figure 24). The localization of each YFP fusion protein expressed in the Δ*che1* (AB103) strain background, which is deleted for the Che1 operon, was analyzed next in order to determine whether the localization of CheA1 to the cell poles was also dependent on the presence of other Che1 chemotaxis proteins. Interestingly, CheA1, as well as the HlyIII-like domain alone, localized to the cell poles in the absence of other chemotaxis proteins (Figure 24). In the absence of the HlyIII domain (CheA1ΔTM:YFP), we observed a mixture of cells with diffuse localization and cells with some weak polar localization (about 70% weak localization in wild type and Δ*cheA1* mutant backgrounds, and about 20% weak localization in the Δ*che1* mutant background) (Figure 24). Together, these data indicated that the HlyIII domain of CheA1 is the primary determining factor in localization of CheA1 to the cell poles. This conclusion implies that the loss of this domain will likely impact the function of CheA1. However, because weak localization was still observed in variants lacking the HlyIII domain, this suggests that (soluble) CheA1 lacking the HlyIII domain remains able to localize at polar foci, although this

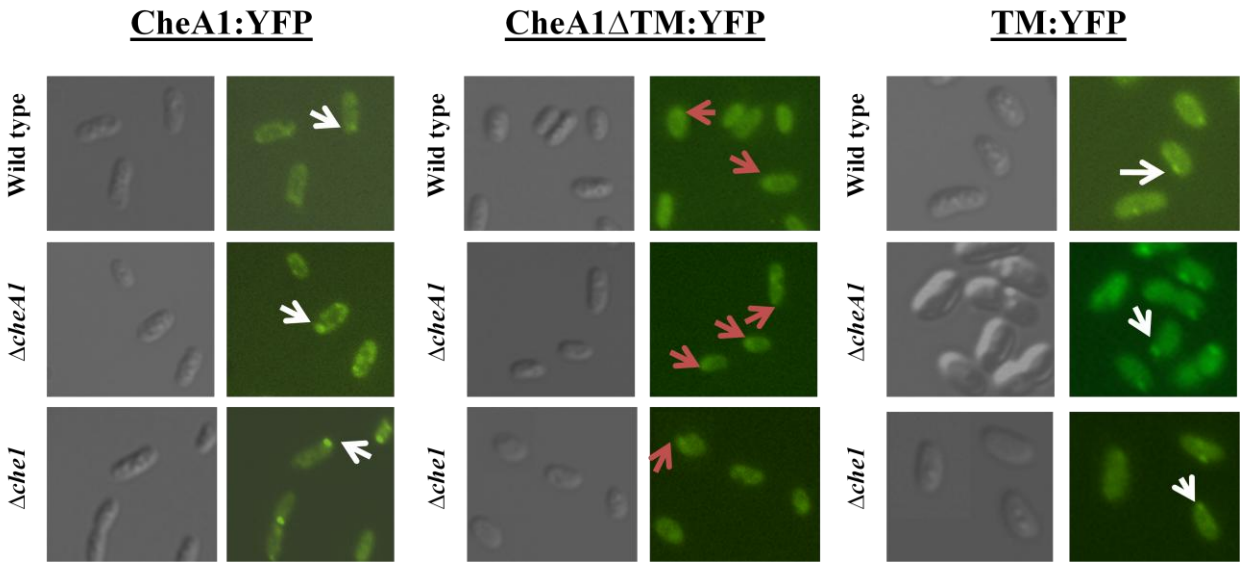

Figure 24. Polar localization of CheA1 is dependent on the TM domain. CheA1, CheA1ΔTM, and TM were localized in wild type *A. brasilense*, and in Δ*cheA1* and Δ*che1* mutant backgrounds. CheA1 and TM showed dicrete foci (white arrows) at the cell poles regardless of the presence or absence of other Che1 proteins, while CheA1ΔTM showed diffuse or weak polar localization (red arrows) in all backgrounds.

ability appears to be significantly reduced. Whether these constructs showing impaired localization of CheA1 retained some functions was analyzed in the following sections.

Complementation of ΔcheA1 (AB101) for functional analysis

In order to assess the roles of the HlyIII-like TM, the P5 ($P5_A$ and $P5_B$), and the CheY-like Receiver (Rec) domains in the overall function of CheA1, we generated a series of constructs that carry different in-frame deletions of these domains that are shown in Figure 25. Eight of these constructs contain in-frame domain deletions and two of them contain site-specific mutations affecting the predicted phosphorylation sites, His252 (from the P1 domain) and Asp1055 (from the receiver domain). Preliminary western blot analysis has indicated that these proteins are expressed at comparable levels and are stable (Chapter 2, other data not shown).

TM, $P5_B$, and Rec domains are essential for cell length regulation

The contribution of each domain of CheA1 to its activity in cell length regulation was analyzed by expressing the wild type *cheA1* and mutant derivatives of *cheA1* in a Δ*cheA1* (AB101) mutant strain background. In Δ*cheA1* (AB101) strains expressing *cheA1ΔTM*, *cheA1ΔTM-$P5_B$-Rec*, and *cheA1Δ$P5_A$-$P5_B$*, cell length phenotypes were similar to the Δ*cheA1* (AB101) mutant strain carrying an empty vector as a control, indicating that these constructs failed to complement the mutant phenotype (Figure 26). All other constructs expressed in the Δ*cheA1* (AB101) mutant background were able to restore cell length similar to the wild type, or longer. These data suggested that the HlyIII-like TM domain may play a critical role in cell length regulation, as well as the $P5_B$ domain when deleted in combination with $P5_A$ or Rec. Constructs that were able to restore cell length most similar to that of the wild type strain were *cheA1*, *cheA1Δ$P5_A$*, *cheA1Δ$P5_B$*, *cheA1$_{H252Q}$*, and *cheA1ΔRec* (Figure 26). Therefore, the wild

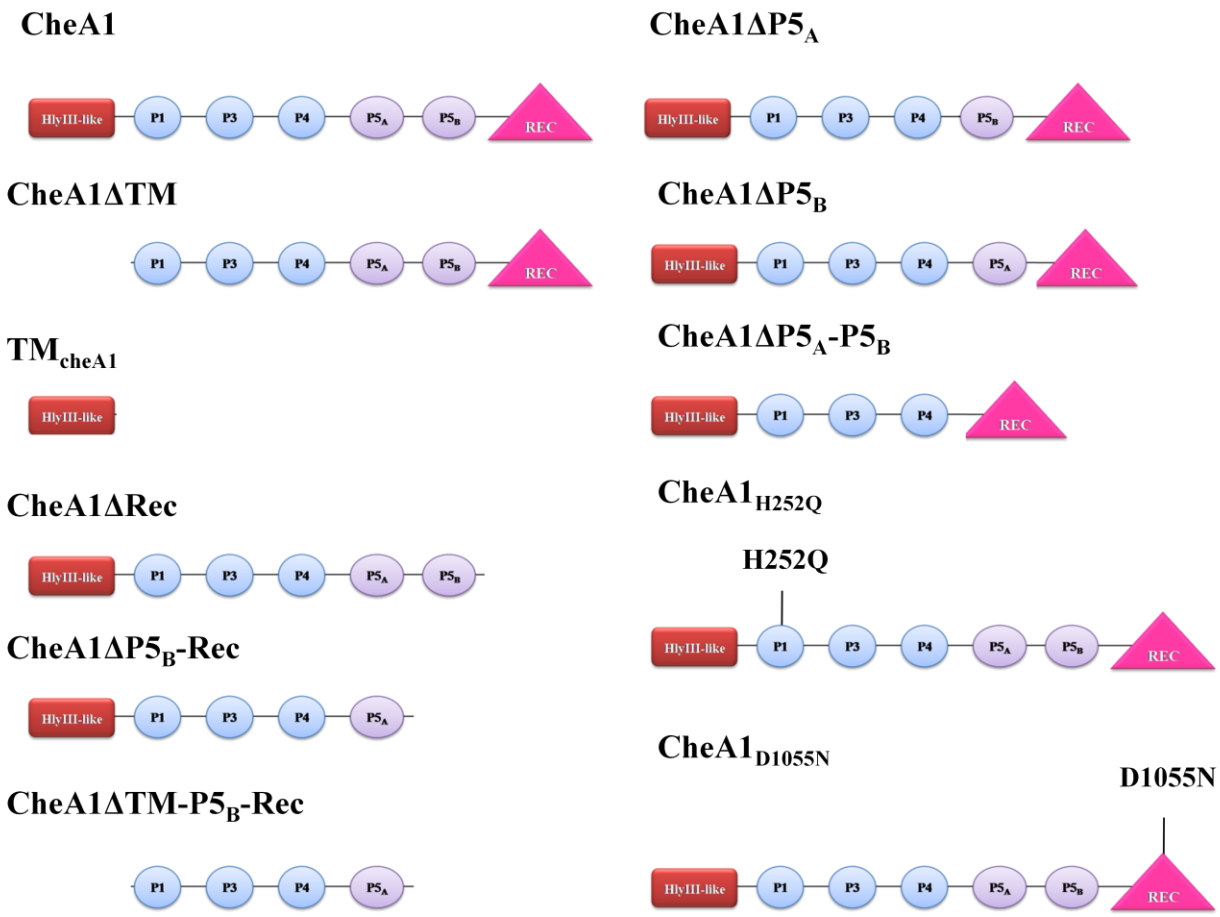

Figure 25. Schematic representation of constructs used in this study. Constructs generated in this work contained domain deletions in CheA1, as illustrated above, in order to analyze the function(s) of these domains, and how their function relates to the overall function of CheA1 in the Che1 chemotaxis-like pathway.

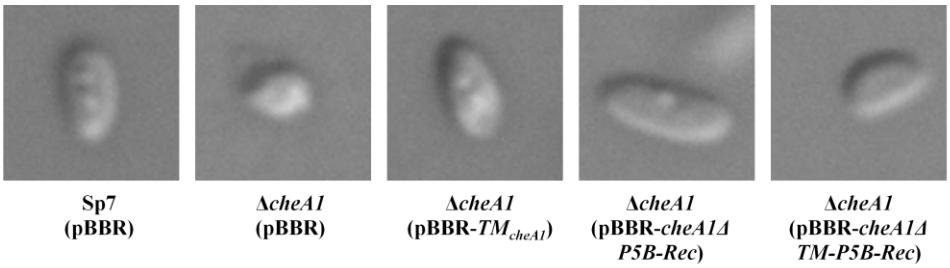

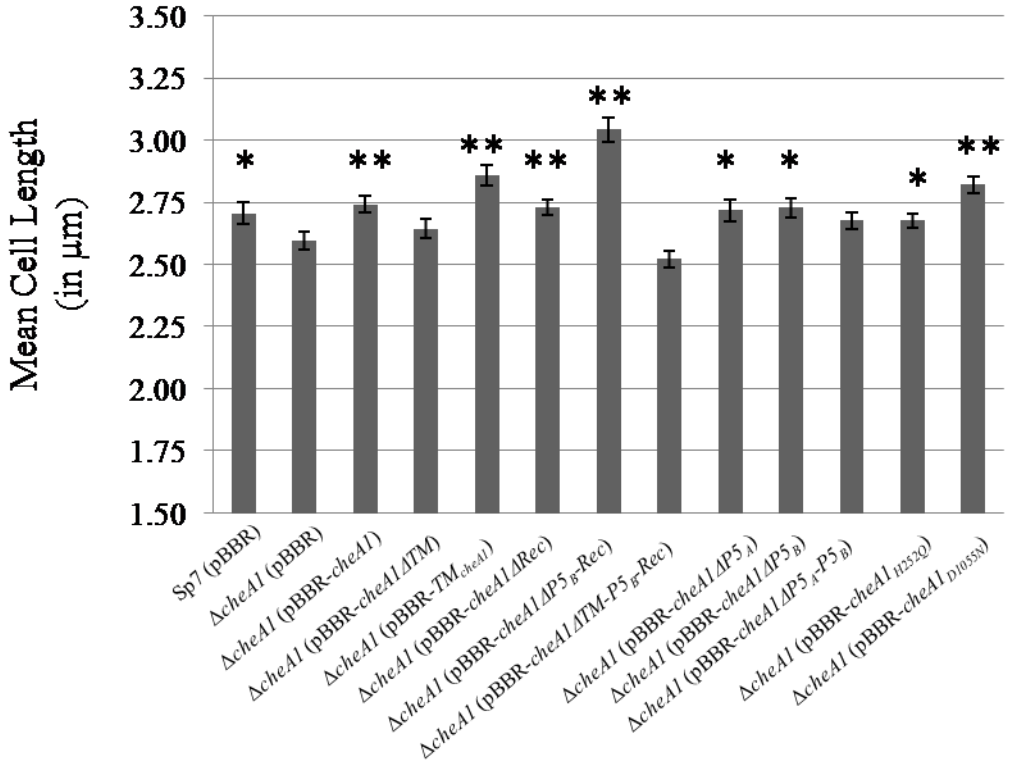

Figure 26. Mean cell lengths in wild type *A. brasilense*, Δ*cheA1* (AB101), and in Δ*cheA1* (AB101) strains complemented with truncated forms of CheA1. (Top) Representative pictures of strains with shorter cell lengths and longer cell lengths. (Bottom) Graph showing the mean cell lengths in each indicated strain. An (*) indicates statistically significant differences in cell size relative to Δ*cheA1* (AB101) at a p-value < 0.05, and (**) represents statistically significant differences in cell length relative to Δ*cheA1* (AB101) with a p-value < 0.0005 (n=50).

type protein or a protein variant in which the His252 or the P5A, P5B, or Rec domains are deleted alone yielded a functional construct for restoring the wild type cell length to a mutant, suggesting that they are dispensable for this function. Constructs which, when expressed in the Δ*cheA1* (AB101) mutant strain background, caused the cells to increase cell length longer than the wild type were TM_{cheA1}, $cheA1\Delta P5_B$-*Rec*, and $cheA1_{D1055N}$ (Figure 26). Taken together, these data suggest that the TM domain, along with the $P5_B$ and Rec domains, including a Rec in which the Asp1055 putative phosphorylation site is intact, all contribute to CheA1-dependent effects on cell length. Restoration of wild type cell length to a mutant was lost when the HlyIII (TM) domain was deleted, but the TM domain alone (TM_{cheA1}) was sufficient to rescue the cell length phenotype (Figure 26), but the cell length was greatly increased compared to the wild type.

However, the $P5_B$ domain, in combination with the Rec domain, that includes an intact Asp1055 residue, appears to form a functional module which can regulate the cell length phenotype: a strain complemented with $cheA1\Delta P5_B$-*Rec* is longer than a strain complemented with *cheA1ΔRec or* $cheA1\Delta P5_B$, yet when the TM domain is deleted in this construct ($cheA1\Delta TM$-$P5_B$-*Rec*), the long cell length phenotype is no longer observed (Figure 26). Taken together, these results suggest that the TM domain, as well as the $P5_B$ and Rec domains contribute to the function of CheA1 in cell length regulation. Interestingly, the presence of a phosphorylatable His252 residue was dispensable for CheA1-dependent cell length regulation. In contrast, mutating the putative phosphorylation site at the Asp1055 residue within the Rec domain caused the cells to be even longer than the wild type, suggesting a regulatory (inhibitory) role for this phosphorylatable residue in modulating changes in cell length. Together with results

obtained with the Rec and $P5_B$ domains, it is likely that $P5_B$-Rec with a functional phosphorylatable residue modulate the effect of the TM (HlyIII-like domain) on cell length.

The* A. brasilense *Sp245* cheA1 *mutant is affected in chemotaxis, but not cell length

The *Azospirillum brasilense* Sp245 strain is closely related to the *Azospirillum brasilense* Sp7 strain used throughout this study. Similarly to the Sp7 strain, *A. brasilense* Sp245 also possesses the Che1 chemotaxis-like pathway and the hybrid histidine kinase, CheA1. Whereas CheA1 in the Sp7 strain has the HlyIII-like domain at its N-terminus, CheA1 in Sp245 does not (HlyIII is encoded elsewhere on the genome); however, the other CheA1 domains are still present (Figure 27). Using a *cheA1* insertion mutant constructed in the *A. brasilense* Sp245 strain, we analyzed cell length phenotypes, as well as chemotaxis behavior. We found that mutations affecting *cheA1* in Sp245 caused significant defects in chemotaxis (Figure 27). However, cell length was not affected by mutating *cheA1* in strain Sp245 (Figure27). Together, these data confirm that the N-terminal HlyIII domain of CheA1 in the Sp7 strain is directly responsible for regulating the cell length phenotype.

Contribution of CheA1 domains to chemotaxis and aerotaxis behavior

The Che1 pathway has been shown to regulate the swimming speed of cells, with an indirect role in regulating the swimming motility bias (5, 6). However, it is also clear that despite its minor role, Che1 signaling contributes to chemotaxis and aerotaxis in *A. brasilense* (16). We have hypothesized that such indirect effects on the motility bias and chemotaxis/aerotaxis behavior may be mediated by cross-talk mechanisms between Che1 and other Che pathways (6). Although Che1 does not directly control the motility bias associated with chemotaxis and

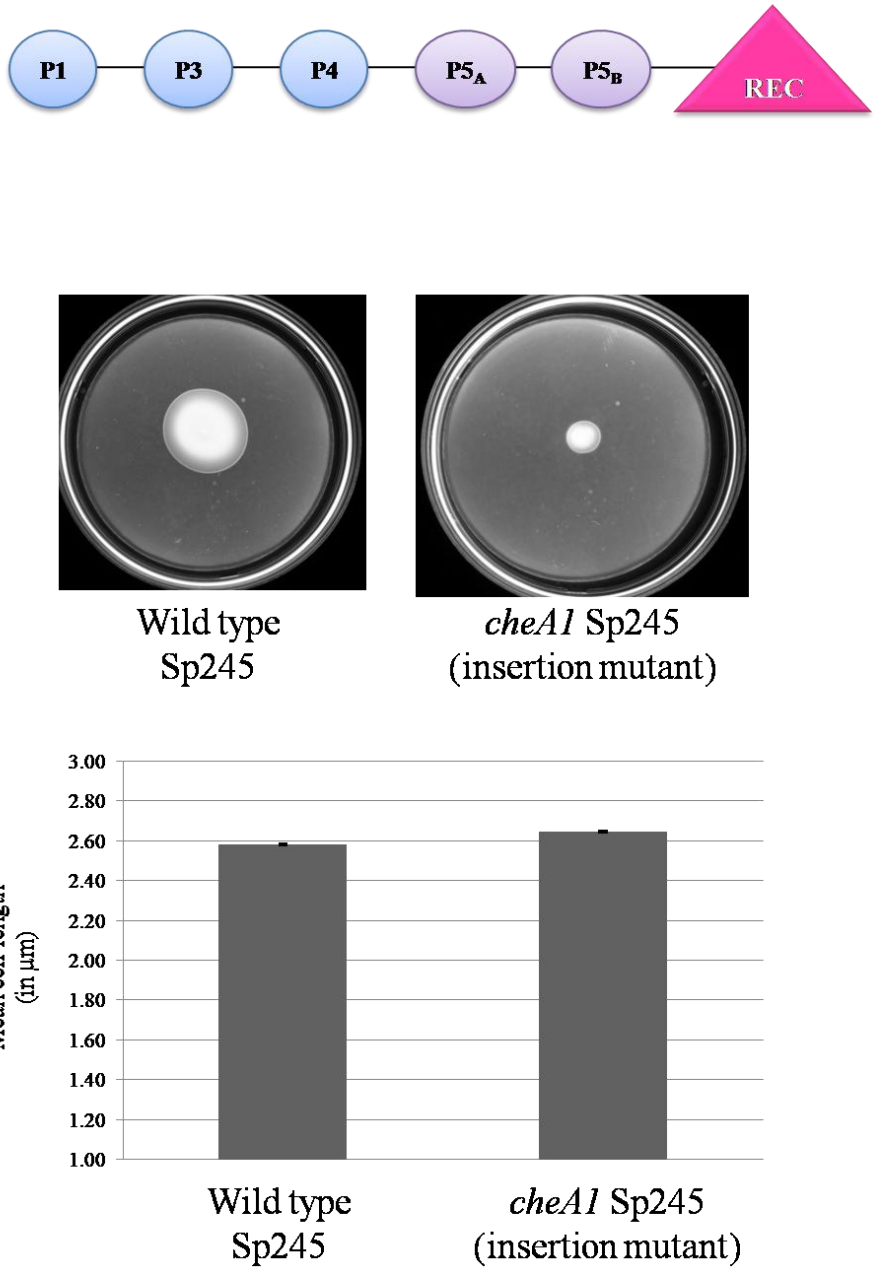

Figure 27. Behavioral defects in the HlyIII-less CheA1 from *A. brasilense* Sp245. (Top) Domain architecture of CheA1 from *A. brasilense* Sp245. (Middle) Chemotaxis semi-soft agar plate assays comparing chemotaxis abilities between wild type Sp245 and the Sp245 *cheA1* insertion mutant. Data shown is representative of at least 3 independent experiments. (Bottom) Comparison of mean cell lengths between wild type Sp245 and the Sp245 *cheA1* mutant (n=50). Cell length differences were not statistically different.

aerotaxis, we were curious to find whether mutations affecting the activity of CheA1 would affect these behaviors. In order to assess the roles of each domain of CheA1 in chemotaxis, we compared chemotaxis ring diameters formed in the semi-soft agar plate assay by the wild type *A. brasilense* Sp7 and the Δ*cheA1* (AB101) strain, carrying an empty vector (control) or plasmids expressing the wild type (Sp7) *cheA1* gene and mutant derivatives of *cheA1* (Figure 28). Relative to the fully complemented Δ*cheA1* (AB101) with the parental *cheA1*, each *cheA1* domain deletion mutant was affected in their chemotactic abilities to various degrees. Expression of *cheA1ΔTM*, *cheA1ΔP5$_B$-Rec*, and *cheA1ΔTM-P5$_B$-Rec* yielded chemotaxis phenotypes similar to that of the Δ*cheA1* (AB101) mutant strain carrying a control empty vector (Figure 28). These results suggest that the TM domain, as well as the P5B and Rec domains together, can affect chemotaxis behavior. Expression of *TM$_{cheA1}$*, *cheA1ΔP5A*, *cheA1ΔP5B*, *cheA1ΔP5A-P5B*, *cheA1ΔRec*, as well as the *cheA1$_{H252Q}$* and *cheA1$_{D1055N}$* in the mutant strain background caused an even greater defect in chemotaxis than that observed in the Δ*cheA1* (AB101) mutant carrying an empty vector (Figure 28). These results suggest that chemotaxis may be further reduced in the Δ*cheA1* (AB101) mutant strain by expressing non-functional variants of CheA1 lacking P5A, P5B, Rec domains alone or a phosphorylatable His252, Asp1055. Given that the wild type *cheA1* fully complemented the Δ*cheA1* mutant strain for chemotaxis, it is unlikely that the reduced chemotaxis is caused by indirect effects of copy numbers since the CheA1 variant proteins are expressed from the same plasmid as the wild type. It is thus possible that expressing these CheA1 variants "jam" chemotaxis under these conditions. Given that expressing *TM$_{cheA1}$* alone impairs chemotaxis, it implies that this TM domain affects chemotaxis machinery and impacts its ability to function properly. The effects of expressing

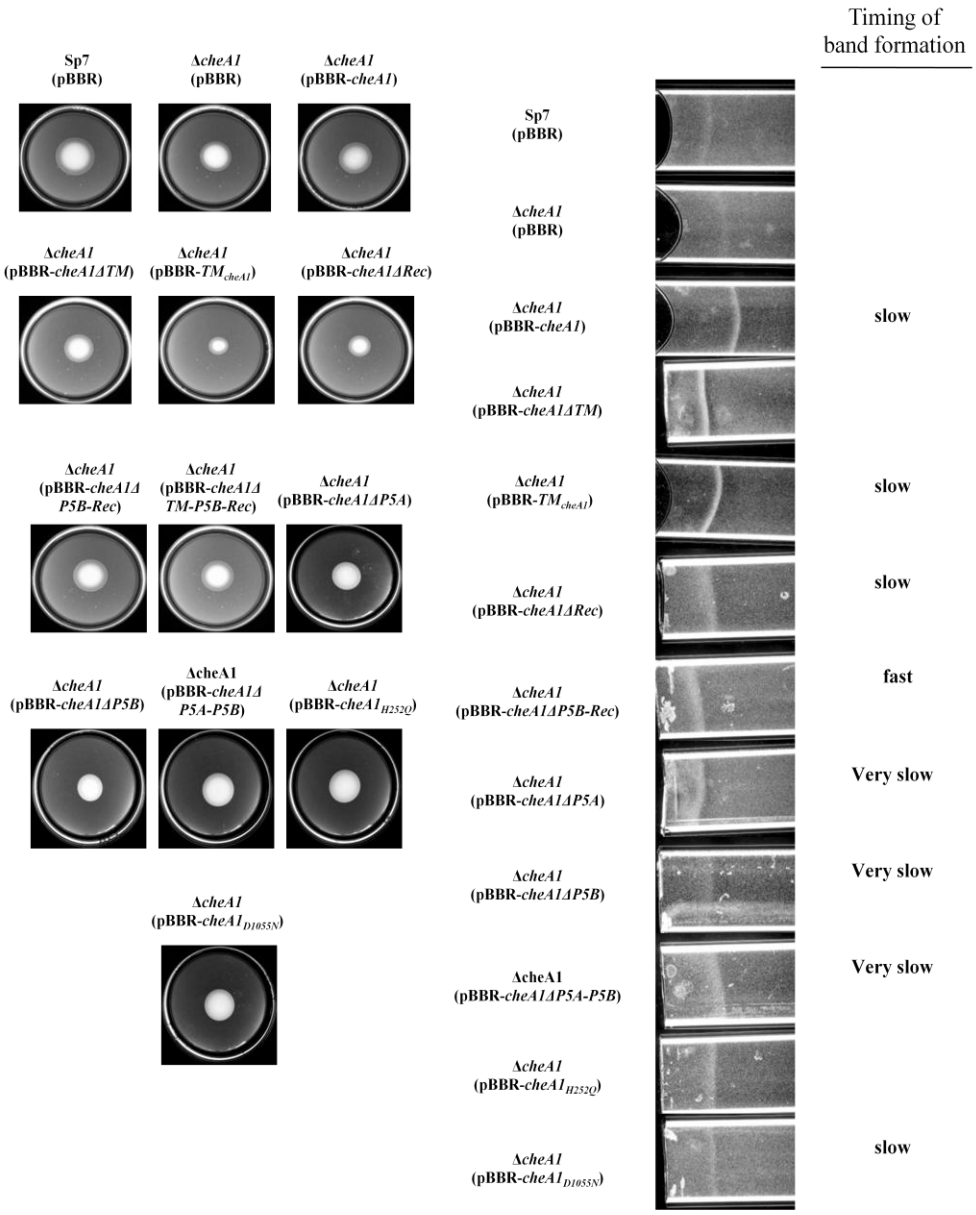

Figure 28. Chemotaxis and aerotaxis behaviors in wild type *A. brasilense*, Δ*cheA1* (AB101), and Δ*cheA1* (AB101) complemented with mutant derivatives of *cheA1*. (Left) Chemotaxis semi-solid agar assays comparing chemotaxis and motility behavior in each strain. Data shown is representative of at least 5 independent experiments. (Right) Capillary assay testing aerotactic behavior in all strains. Notes to the right of the picture refer to the relative timing of band formation. Those without notes formed bands within 1-2 minutes. Strains which were "slow" took 3-5 minutes to form a band, and strains that were "very slow" took more than 5 minutes. Strains that were "fast" formed a band in less than 1 minute. Data shown is from a single experiment.

TM$_{cheA1}$ alone on chemotaxis also suggest that the ability of TM to localize at the cell poles may account for these effects.

A. brasilense is known to form aerotactic bands in capillary tubes approximately 400-900 µm from the meniscus (air-liquid interface) within 0.5 to 3 minutes (53). Here, all strains tested were capable of producing an aerotactic band; however, the timing at which these aerotactic bands were formed was affected for some, but not all strains (Figure 28). Specifically, deletions of the P5$_A$, P5$_B$, and Rec domains alone caused the most significant delay in aerotactic band formation, suggesting that the cells are not able to sense and respond efficiently to the oxygen gradient established in the capillary tube. These strains were generally slow to form bands, and the bands that were formed were usually "fuzzy" and not as sharp as those bands formed by the wild type strain, further suggesting that the sensitivity of these cells to oxygen gradients is impaired. Expressing *TM*$_{cheA1}$ alone here appeared to affect chemotaxis machinery, as well. Expressing *TM*$_{cheA1}$ alone here appeared to affect chemotaxis machinery, as well. These results are in contrast with those that highlight the role of the HlyIII-like TM and P5$_B$-Rec domains in cell length regulation and suggest that domains other than TM, P5$_B$, and Rec, primarily affect aerotaxis responses.

Collectivelly, these results highlight the role of all domains of CheA1 (Sp7) in chemotaxis and aerotaxis behaviors. However, previous work has suggested that these phenotypes are also regulated by other unknown Che-like pathways with which Che1 is hypothesized to cross-talk (6, 39). Therefore, it remains possible that the effects of some or all of the mutations observed here are indirect. Because the Che1 pathway has been shown to control the swimming speed directly, we chose to analyze this next.

Swimming motility bias

In order to gain further insight into these observed defects in chemotaxis and aerotaxis behavior, the motility behavior and swimming bias of these strains, in the absence of any specific cue, was analyzed (Table 9). As observed previously, wild type cells display a random swimming bias consisting of a mixture of "runs" and "reversals", while mutants lacking *cheA1* showed a smoother swimming bias (i. e. more "runs" and fewer "reversals") (5). Strains expressing TM_{cheA1}, *cheA1ΔRec*, and *cheA1ΔTM-*$P5_B$*-Rec* each had a random swimming bias mostly similar to that of the wild type. The other strains tested (*cheA1*, *cheA1ΔTM*, *cheA1Δ*$P5_A$, *cheA1Δ*$P5_B$, *cheA1Δ*$P5_A$-$P5_B$, *cheA1Δ*$P5_B$*-Rec*) displayed an increase in the steady-state reversal frequency (probability of change in the swimming direction) (Table 9). In addition, strains complemented with *cheA1* lacking either of the P5 domains were also less motile, with *cheA1Δ*$P5_B$ showing the slowest motility. The TM_{cheA1} alone caused an increase in reversal frequency when expressed in the Δ*cheA1* (AB101) mutant background, suggesting either that TM_{cheA1} has a direct effect on the reversal frequency or that its localization at the cell pole accounts for these effects. In addition, these experiments indicated that the mutations affecting the P5 domains of CheA1 (Sp7) are the most affected in chemotaxis, aerotaxis, and motility behavior, suggesting critical roles.

CheA1 and swimming speed, the output of Che1

In previous work, we found that the Che1 pathway (Sp7) controls the swimming speed of cells upon experiencing a decrease in aeration conditions (air removal) in a gas perfusion chamber assay (Chapter 2, Bible *et al*., 2008). Compared to the wild type, a Δ*cheA1* (AB101)

Table 9. Motility bias of wild type *A. brasilense*, Δ*cheA1* (AB101), and Δ*cheA1* (AB101) complemented with wild type and mutant derivatives of *cheA1*.

Strain	Motility Bias*
Sp7 (pBBR)	random
Δ*cheA1* (pBBR)	smoother
Δ*cheA1* (pBBR-*cheA1*)	more reversal
Δ*cheA1* (pBBR-*cheA1ΔTM*)	more reversal
Δ*cheA1* (pBBR-TM_{cheA1})	random
Δ*cheA1* (pBBR-*cheA1ΔRec*)	random
Δ*cheA1* (pBBR-*cheA1Δ*$P5_B$-*Rec*)	more reversal
Δ*cheA1* (pBBR-*cheA1ΔTM-*$P5_B$-*Rec*)	random
Δ*cheA1* (pBBR-*cheA1Δ*$P5_A$)	more reversal, low motility
Δ*cheA1* (pBBR-*cheA1Δ*$P5_B$)	random, low motility
Δ*cheA1* (pBBR-*cheA1Δ*$P5_A$-$P5_B$)	more reversal, low motility

*****Motion analysis software was used to track the movement of cells grown under normal conditions. Analysis of swimming tracks indicated whether cells display a "random" swimming bias, or a "smoother" or "more reversal" swimming bias. Data was obtained from a single experiment.

mutant was unable to adjust their swimming speed in response to air removal. In this assay, we found that the TM_{cheA1} domain resulted in a significant decrease in swimming speed upon air removal (Figure 29), suggesting that expression of this domain alone is not sufficient to rescue the wild type swimming speed phenotype, but rather lead to a significant decrease in swimming speed upon air removal. The *cheA1ΔTM*, on the other hand, showed an increase in swimming speed similar to the wild type (Figure 29). These results suggest that the TM domain may affect swimming speed as a minor effect, which is detectable only when this domain is expressed at higher levels compared to wildtype. Mutations affecting the $P5_B$-Rec domain (*cheA1ΔP5$_B$-Rec*) resulted in a significant increase in swimming speed upon air removal, while deletion of the TM in this construct (*cheA1ΔTM-P5$_B$-Rec*) was unable to significantly adjust their swimming speed (Figure 29), suggesting that the $P5_B$ and Rec domains may affect swimming speed via interactions with the HlyIII-like TM domain, with the effect on cell length being perhaps related. Therefore, polar localization of CheA1 is likely important for the regulation of swimming speed. We also found that when *cheA1ΔRec*, *cheA1ΔP5A*, *cheA1ΔP5B*, *cheA1ΔP5$_A$-P5$_B$*, *cheA1$_{H252Q}$*, and *cheA1$_{D1055N}$* were expressed from plasmids in the Δ*cheA1* (AB101) mutant background strain, there was no response to changes in aeration (Figure 29), indicating that these constructs are not functional for restoring the ability of these cells to respond to changes in aeration conditions. These results suggest that when present at the cell pole, CheA1 requires $P5_A$, $P5_B$, and Rec, as well as a phosphorylatable His252 and Asp1055 for swimming speed modulation. The lack of response from variants that are defective in putative phosphorylation sites was expected, as these were shown to contribute to CheA1 function in swimming speed regulation previously (6).

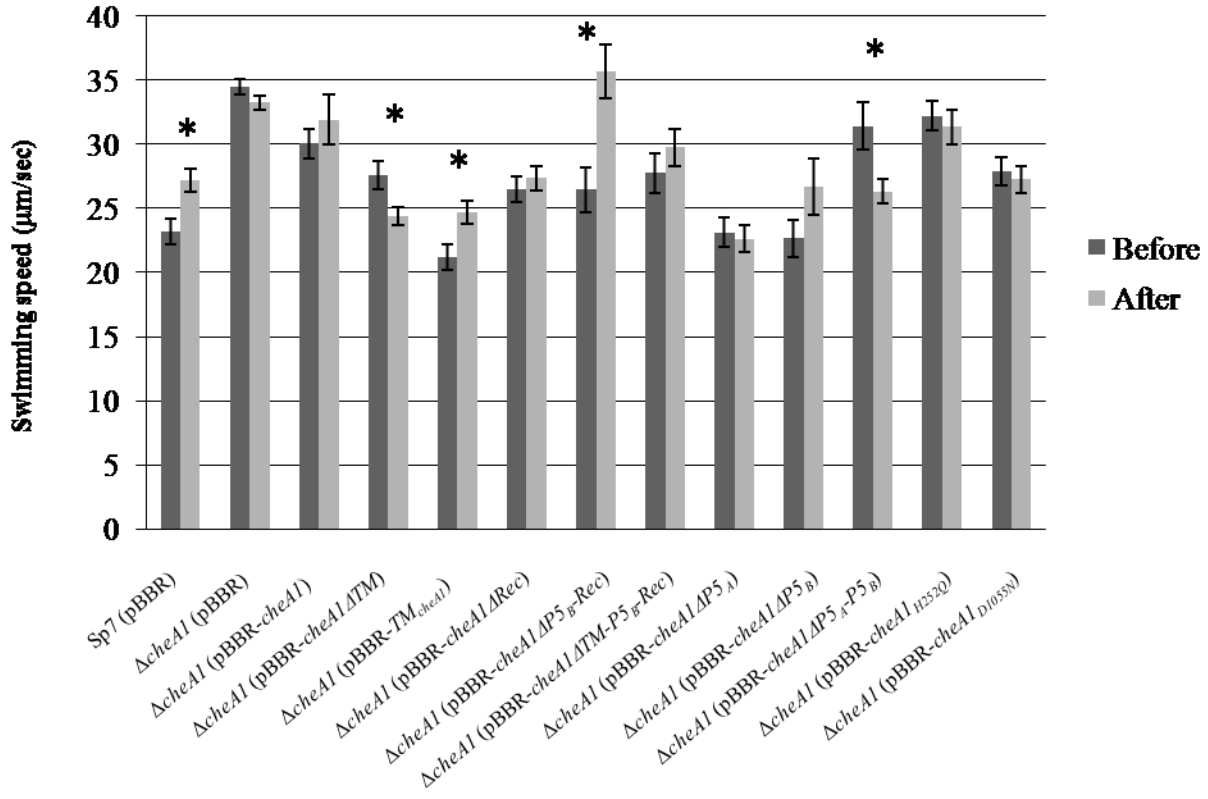

Figure 29. Mean swimming speed measurements in wild type *A. brasilense*, Δ*cheA1* (AB101), and Δ*cheA1* (AB101) complemented with derivatives of *cheA1* before and after air removal in the gas perfusion chamber assay. Dark gray bars represent the swimming speed 10 seconds prior to air removal (before), and light gray bars represent the swimming speed 10 seconds after air removal (after). (*) indicates statistically significant increases/decreases in swimming speed upon air removal ($p < 0.05$). Calculations were made from a minimum of 40 cells per sample.

Expression of *cheA1ΔP5$_A$-P5$_B$*, similarly to *cheA1ΔTM*, resulted in a significant decrease in swimming speed upon air removal in this assay (Figure 29). Such an inverted response would suggest that when these CheA1 variants are expressed, the signaling events involved in regulation of swimming speed in *A. brasilense* implicate other unknown protein(s) that appear to have opposite effects on swimming speed than those induced by CheA1 activity. Taken together, we can conclude that: 1. Mutations which affect signaling via the Che1 pathway inhibit the ability of Che1 to increase swimming speed upon air removal, consistent with previous findings (6); 2. Several domains of CheA1 (Sp7) evoke inverted swimming speed responses, suggestive of indirect effects, in addition to the direct CheA1-CheY1 effects demonstrated previously (6) and 3. The TM domain in CheA1 (Sp7), and likely the P5$_B$-Rec domains via regulatory effects on TM, also appears to affect the swimming speed of cells, likely via additional indirect effects that may depend on the ability of *TM$_{cheA1}$* to localize to cell poles.

Role of CheA1 domains in clumping and flocculation behavior

Clumping and flocculation behavior were shown to be affected by Che1 indirectly, via direct effects of Che1 on cell swimming speed (6). Specifically, strains which respond to air removal by increasing their swimming speed showed a reduction in the fraction of clumps formed. Conversely, strains which did not respond to air removal, showed an increase in clump formation. Using the gas perfusion chamber assay, we were unable to detect any clump formation in mutations affecting the TM (*cheA1ΔTM* and *TM$_{cheA1}$*), despite their swimming speed phenotypes (Figure 30), suggesting that CheA1 (Sp7) must be anchored at the cell pole via TM in order to link swimming speed changes with cell-to-cell interactions in clumping. Expression of *cheA1ΔP5$_B$-Rec* resulted in an increase in clump formation, similar to the Δ*cheA1* (AB101)

mutant; however, when TM was deleted from this construct (*cheA1ΔTM-P5$_B$-Rec*), there was a decrease in clump formation, similar to the wild type, supporting the idea that anchoring of CheA1 to the cell pole via TM is important in this behavior.

Other constructs which were not able to complement the Δ*cheA1* (AB101) mutant phenotype in terms of clumping include *cheA1ΔRec*, *cheA1ΔP5$_A$-P5$_B$,* and *cheA1$_{H252Q}$*. These constructs were also unable to increase their swimming speed upon air removal, as well, further suggesting that the P5$_A$, P5$_B$, Rec, and phosphorylatable His252 are important to the function of CheA1 (Sp7) in modulating swimming speed, thus affecting clumping behavior. However, strains expressing *cheA1ΔP5$_B$* and *cheA1$_{D1055N}$* were able to restore the wild type phenotype in clumping behavior, suggesting that although these domains may be important for regulating the swimming speed, they are not essential to the clumping response. Taken together, these results suggest that changes in the swimming speed contribute to transient changes in clumping upon changes in aeration conditions, but are not the only factors involved, in agreement with our previous observations (6). The results obtained here are also consistent with transient changes in clumping being regulated by CheA1-dependent and CheA1-independent effects.

Although the gas perfusion chamber assay is useful in measuring temporal changes in clumping behavior under aeration conditions, the flocculation assay can be more informative in terms of the overall sensitivity of the cells to changes in environmental conditions that occur during growth under nutrient-limiting conditons, such as nitrogen here. We have previously shown that indirect effects of Che1, suggested to depend on cross-talk with other Che-like

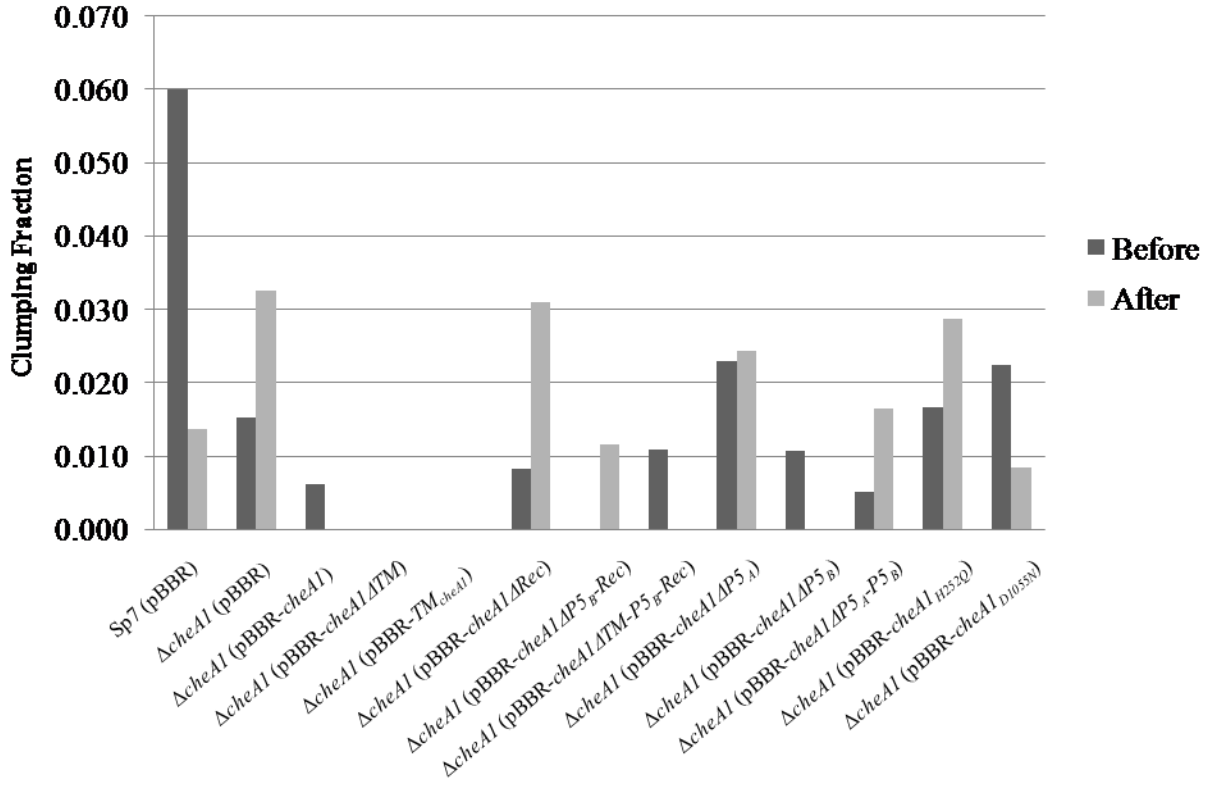

Figure 30. Fraction of clumping observed in wild type *A. brasilense*, Δ*cheA1* (AB101), and Δ*cheA1* (AB101) complemented with mutant derivatives of *cheA1* upon air removal in the gas perfusion chamber assay. Graph showing the fraction of clumps relative to the number of free-swimming cells observed in this assay. Data presented here represent a single experiment, therefore no data bars or statistical values are shown at this point. Dark gray bars represent the fraction of clumps prior to air removal (before), and light gray bars represent the fraction of clumps after air removal (after). Calculations were made from at least 100 cells per sample.

pathways, are readily apparent when cells are grown under flocculation-conducive conditions (6), allowing us to test the contribution of CheA1 domains to signaling cross-talk. In this assay, wild type *A. brasilense* typically formed transient clumps around 9-10 hours post-inoculation into flocculation media, with more stable clumps forming around 12-18 hours post-inoculation, and floc formation after approximately 24 hours. The Δ*cheA1* (AB101) mutant, however, formed stable clumps at 3-6 hours post-inoculation into flocculation media, and flocculated after approximately 17 hours (6).

In this assay, the strain expressing *cheA1ΔTM* resembled wild type flocculation behavior; whereas, the strain expressing TM_{cheA1} resembled the Δ*cheA1* (AB101) mutant (Figure 31). As above, this suggests that localization of CheA1 (Sp7) to the cell poles, mediated by TM_{cheA1}, may be key in the ability of CheA1 to cross-talk with other putative pathways. Mutations affecting $P5_A$ and $P5_B$ (*cheA1Δ*$P5_A$, *cheA1Δ*$P5_B$, and *cheA1Δ*$P5_A$-$P5_B$) resembled the wild type in clumping and flocculation behavior, suggesting that these domains of CheA1 are not required for modulating clumping and flocculation behavior (Figure 31). This is also true of the strain expressing *cheA1ΔRec*, suggesting that this domain is dispensable for this function. Interestingly, expression of *cheA1Δ*$P5_B$-*Rec* resulted in a phenotype similar to that of Δ*cheA1* (AB101) (Figure 31), suggesting that deletion of $P5_B$ and Rec domains together impairs the function of CheA1 in clumping and flocculation, which is consistent with a regulatory function for the $P5_B$-Rec domain suggested by other results obtained in this study. Deletion of the TM from this construct (*cheA1ΔTM-*$P5_B$-*Rec*), however, resulted in cells which clumped, but did not flocculate (Figure 31). This suggests that the P3, P4, and $P5_A$ domains of CheA1 may contribute

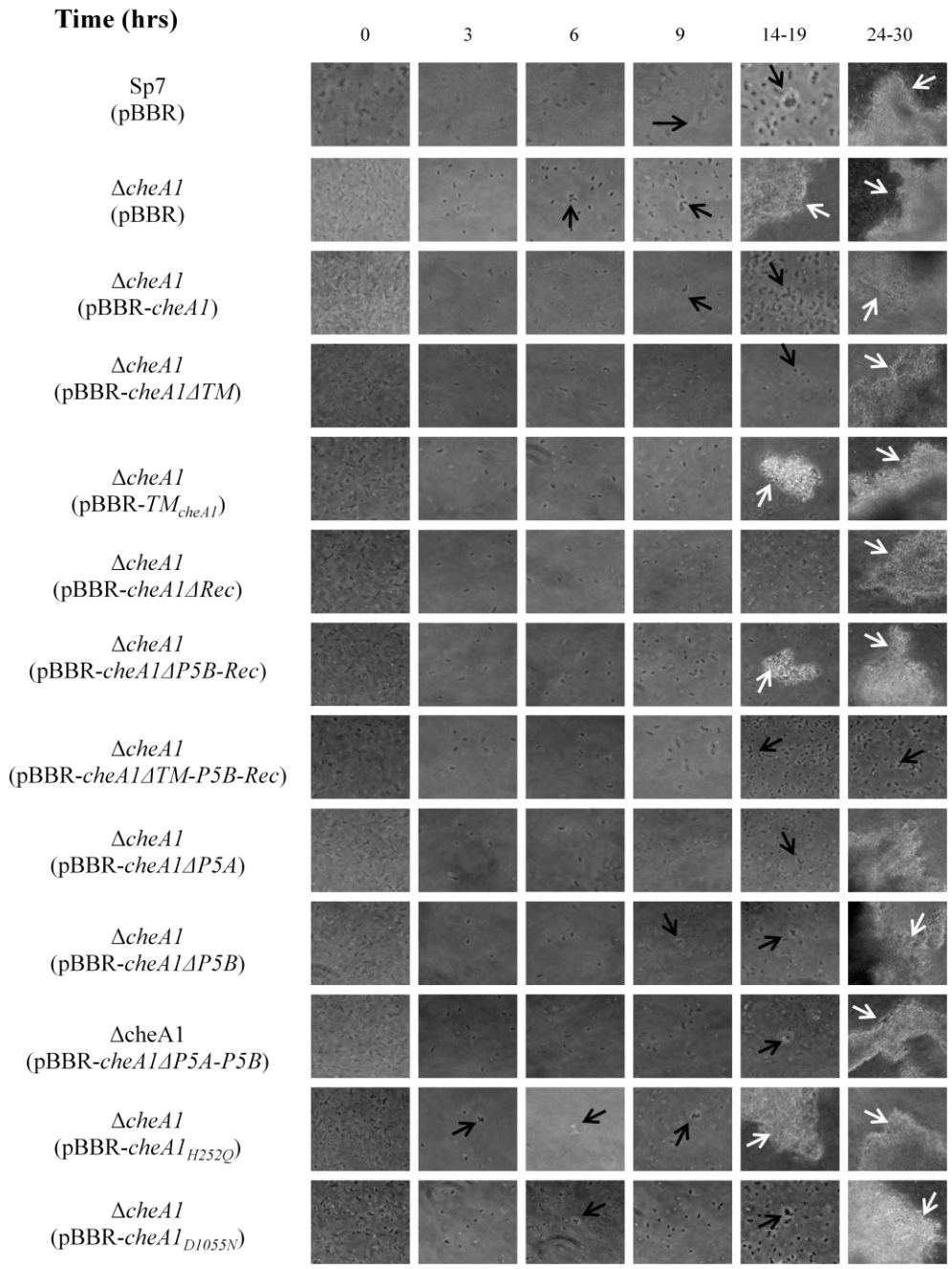

Figure 31. Timing of clumping and flocculation behavior in wild type *A. brasilense*, Δ*cheA1* (AB101), and Δ*cheA1* (AB101) complemented with mutant derivatives of *cheA1*. Time (in hours, post-inoculation) is noted above. Black arrows indicate clumps. White arrows indicate flocculation. Data is representative of at least 3 independent experiments.

to clumping, while other domains of CheA1 contribute to localization to the membrane, affecting both clumping and flocculation. This is further supported by the observation that expression of *cheA1*$_{H252Q}$ yielded clumping and flocculation phenotypes similar to Δ*cheA1* (AB101), suggesting that the predicted phosphorylation site, His252, plays a direct role in the regulation of clumping (and flocculation) behavior (Figure 31).

Section D. Discussion

A series of constructs were generated in order to analyze the functional domains of CheA1 (Sp7), including the HlyIII-like (TM) domain, as well as the $P5_A$, $P5_B$, and Rec domains. Our data show that the TM (HlyIII) domain controls changes in the cell length and that the $P5_B$-Rec domains modulate this effect. Furthermore, conservation of the autophosphorylation site of CheA1 does not appear to be required for this function, indicating that TM modulates cell length independently of other function(s) of CheA1. Chapter 4 will explore this function in greater detail. The Che1 pathway has been shown to regulate multiple cellular behaviors (Bible *et al*., 2008) and the results obtained here suggest that the role of CheA1 in this regulation is highly complex. This complexity is due, in part, to the presence of the N-terminal HlyIII (TM) domain which significantly affects CheA1 subcellular localization and thus could impact its function. The TM domain could also contribute to indirect effects that seem mediated by the functions of other domains of CheA1 (P5 and Rec), including participation in cross-talk with other putative pathways.

In terms of swimming motility-related behaviors, such as chemotaxis and aerotaxis, we hypothesize that defects in these behaviors may be secondary effects due to changes in the motility bias and swimming speed regulation. Mutations affecting CheA1 (Sp7) resulted in

various motility bias phenotypes, with some mutations showing a wild type "random" bias, and others having higher reversal frequencies (Table 9). Alterations in the motility bias can impair the ability of cells to respond appropriately to the presence of attractants (or repellents). Aerotactic and chemotactic behaviors may also be affected due to the impaired ability of certain strains to regulate the cell swimming speed in response to specific cues (Figure 29). Such effects on the swimming speed and motility bias (reversal frequency) may in turn affect clumping (and flocculation), perhaps via cross-talk mechanisms with other Che-like signal transduction pathways. Some evidence which may support this possibility includes the fact that localization of CheA1 (Sp7) is dependent on the presence of the HlyIII-like TM domain and not on the presence of other Che1 proteins. Chemotaxis proteins have been found to localize to the cell poles in other organisms (9, 14, 26, 34, 38); therefore, the ability of CheA1 to localize to the cell pole in the absence of other Che1 proteins could provide a mechanism by which cross-talk with other Che-like pathways could be regulated. The details of this process, however, remain to be elucidated.

Clumping and flocculation behaviors were also shown to be regulated by Che1 indirectly via effects on exopolysaccharide (EPS) production and direct effects on the swimming speed of cells (6). Interestingly, strains expressing *cheA1ΔTM* and *cheA1ΔP5*$_A$*-P5*$_B$ showed an "inverted response" to air removal, in that instead of not responding (like a Δ*cheA1* mutant), these strains decreased their swimming speed. Studies of "inverted responses" in other bacteria have shown that mutations affecting receptor modification (either by affecting the receptor directly or by affecting CheB) can result in "inverted responses" (10, 29, 43) (a model by which this may take place can be found in 44). Therefore, the "inverted response" that we observed in the strain

expressing *cheA1ΔTM* may be due to an inability to localize CheA1 properly (as suggested in Figure 24), while the strain expressing *cheA1ΔP5*$_A$*-P5*$_B$ may impair the ability of CheA1 to associate with receptors, thus affecting downstream signaling via CheA1 (including phosphorylation of CheB1 which in turn results in receptor modification) perhaps leading to the observed "inverted response".

The HlyIII-like TM domain regulates cell length

CheA1 from *A. brasilense* Sp7 is unique from all other CheAs studied thus far in that it is the only CheA with a seven-transmembrane domain at its N-terminus, resulting in a membrane-bound protein. Here, we show that the HlyIII-like TM domain is important for proper localization of CheA1 to the cell pole (Figure 24) and expression of this domain was able to complement Δ*cheA1* (AB101) mutant phenotypes in cell length, motility bias, and swimming speed. The HlyIII TM domain was not able to complement Δ*cheA1* (AB101) in terms of chemotaxis, aerotaxis, clumping and flocculation, suggesting that a functional CheA1 is required for these behaviors. In the absence of this domain, localization of CheA1 at the cell pole was weak and mostly diffuse; therefore, the activity of CheA1 in regulating any cellular behavior is expected to be greatly affected by the absence of this domain.

Our data support the hypothesis that many of the roles of TM_{cheA1} in CheA1 activity depend on its ability to localize at the cell poles. For example, our results suggest that the TM alone can restore cell length phenotypes, as well as the swimming motility bias and swimming speed; whereas, a soluble CheA1 construct (*cheA1ΔTM*) has opposite effects. However, even in membrane-localized constructs, different domains of CheA1 contribute to the behaviors

analyzed. In addition to our findings that the TM domain is essential and sufficient to restore cell length regulation to a Δ*cheA1* (AB101) mutant (Figure 26), our results also identified the $P5_B$-Rec domain combination as a modulator of the TM (HlyIII-like) effect on cell length. Together, these results suggest that the HlyIII (TM) domain may function as an "output" in the Che1 pathway, specifically in respect to regulation of cell length. This is a complete departure from the established function of other CheA homologs where the signaling output depends on a phosphorelay and autophosphorylation of CheA1 at a conserved His residue. Our data suggest that the effect of TM on cell length is independent of CheA1 autophosphorylation at His252. While we have no experimental evidence for autophosphorylation at this residue, previous evidence (6) indicated the presence of a functional His residue at this site is essential for CheA1 function and the Che1 signaling output in other Che1-dependent behaviors.

Weak localization of CheA1 which was observed in the absence of HlyIII (Figure 24, red arrows) indicated that this protein is still capable of localizing at polar clusters, albeit at reduced levels. In *E. coli*, and other species possessing soluble CheA homologs, CheA localizes at chemotaxis signaling clusters by interaction with the CheW adapter protein that recruits and organizes CheA and receptors in signaling complexes (9, 14, 26, 34, 38). The weak localization of the soluble CheA1, in which there is no TM (HlyIII) domain, could therefore result from interaction of CheA1 with CheW1 and receptors. Consistent with this hypothesis, the CheA1ΔTM:YFP showed even weaker localization when expressed in a strain in which all Che1 protein components, including CheW1, have been deleted. It follows that the effects of expressing the soluble CheA1 variants (lacking TM) are thus likely resulting from the TM-

independent localization of CheA1 to polar clusters that are assumed to be signaling chemotaxis complexes.

Although we have not yet identified the mechanism by which the HlyIII-like TM domain functions, we have found that this domain is homologous to members of the Progestin and AdipoQ Receptor (PAQR) family of proteins, of which there are 11 homologs in humans. In humans and other eukaryotes, these proteins have been shown to function as receptors with varied ligand specificities (42). Among this family of proteins, there are three classes of PAQRs, based on sequence homology and predicted topology. PAQR1-4 belong to one class and these are classified as adiponectin receptors, for which they have been shown to have a role in lipid metabolism, fatty acid oxidation, and glucose uptake both in yeast and humans (12, 20, 48). PAQR5-9 belong to a second class of PAQRs, and this class has been shown to function as progestin receptors (52). The final class of PAQRs, PAQR10 and PAQR11, have similarity to bacterial HlyIII-like proteins; however, these have been poorly characterized (42). Among the studies performed thus far on these PAQR family and HlyIII-like proteins, the mechanism by which this protein functions remains largely unclear. Chapter 4 will begin to address the questions surrounding the mechanism by which this domain functions in more detail.

$P5_A$, $P5_B$, and Rec domains

P5 domains are known as the regulatory domains of CheA because they mediate the interactions between CheA, CheW, and the receptors, and are thus critical to signaling via the chemotaxis signal transduction pathway (7, 8). Mutations resulting in the loss of either of the P5 domains of CheA1, or both of them, affect chemotaxis and aerotaxis behavior (Figure 27), the

motility bias (Table 9), and swimming speed (Figure 29). These results indicate that both domains are critical to CheA1 function in the control of taxis responses and swimming speed, and suggest that both domains may mediate interactions between CheA1, CheWs, and receptors in order to modulate changes in chemotaxis, aerotaxis and swimming speed that are the signaling ouptut of Che1. Che1 has been shown to affect the swimming speed directly, i. e. via a phosphorylation cascade between CheA1 and CheY1 with phosphorylatable CheY1 being essential for changes in swimming speed (6); whereas, changes in the reversal frequency are indirectly affected by Che1 (5), depending in part on cross-talk amongst a diverse set of unidentified chemotaxis receptors and their methylation status (39). These results thus strongly suggest that the indirect contribution of CheA1 to the reversal frequency, as well as chemotaxis and aerotaxis, may depend more on the ability of CheA1 to associate with different signaling complexes, via the HlyIII domains and/or P5 domains. Further insight into the subcellular localization of CheA1 and its ability to form protein complexes with other chemotaxis proteins will be important to better understanding the role of CheA1.

CheA1 of *A. brasilense* Sp7 also possesses a Rec domain, the presence of which characterizes CheA1 as a hybrid histidine kinase (40). Hybrid histidine kinases are often involved in complex phosphorelays in which phosphates are transferred from a histidine residue in the H-box (in Class I histidine kinases) or P1 domain (in CheA, or Class II histidine kinases) to an aspartate residue in the Receiver domain. These phosphates are commonly transferred to another protein containing a phosphorylatable His and then to another response regulator in a complex phosphorelay (40). An example of this type of phosphorelay is in the ArcB-ArcA system in *E. coli* which is used for sensing various respiratory growth conditions. ArcB is a

hybrid histidine kinase consisting of two phosphorylatable histidine residues and one phosphorylatable aspartate, which together undergo a complicated phosphorelay mechanism in order to influence the phosphorylation state of the response regulator, ArcA (27). Another example is FrzE from *Myxococcus xanthus* which is a CheA homolog involved in the regulation of A- and S-motility in this organism. The *M. xanthus* CheA Rec-domain can act by negatively regulating the autophosphorylation of the kinase domain, but studies thus far do not suggest any role of this receiver domain in phosphorelay (17).

In *A. brasilense* Sp7, CheA1 is embedded in the membrane making *in vivo* or *in vitro* phosphorylation assays complicated and poorly feasible at this stage. Therefore, we cannot yet conclusively establish whether the receiver domain of CheA1 functions in a multi-part phosphorelay, or if it serves an inhibitory function, as in FrzE from *M. xanthus*. However, experiments analyzing swimming speed, clumping and flocculation behavior suggest that when the predicted phosphorylation sites (His252 and Asp1055) are mutated, the activity of CheA1 is affected. Specifically, mutations affecting His252 and Asp1055 result in swimming speed phenotypes similar to a Δ*cheA1* (AB101) mutant, suggesting a direct role for phosphorylation of these domains in this behavior. Similarly, clumping and flocculation behaviors which are indirectly regulated by the Che1 pathway were also affected in these mutants. Thus far, cell length is the only behavior we have observed in which mutations affecting His252 and Asp1055 were not affected, suggesting that phosphorylation of CheA1 is not essential for cell length regulation. This also clearly identifies cell length regulation as a unique phenotype associated with the TM_{cheA1} (HlyIII-like) domain; however, the presence of this domain has multiple effects on CheA1 function, with some related to the ability of CheA1 to localize to the membrane.

Constructs containing *cheA1ΔP5$_B$-Rec* seem to have phenotypes that are different from behaviors observed in complementation with *cheA1ΔP5$_B$* or *cheA1ΔRec* alone. Why would complementation be so different among these three complementation constructs? One possibility is that the P5$_B$ and Rec domains function together as a "CheV"-like protein. CheV was first described in *B. subtilis* as a novel protein with a CheW- and a CheY-like domain, i.e. a P5-Rec domain architecture (13). Since then, homologs have been found and characterized in *Helicobacter pylori* and *Salmonella enterica* serovar Typhimurium, (2, 19, 25, 31, 32). A recent review highlights this protein as a coupling protein which may "provide further routes to controlling the chemotaxis system" (2). Interestingly, the authors of this review analyzed completely sequenced bacterial and archaeal genomes to find that all organisms with a chemotaxis pathway contain a CheW, a CheV, or both (2). Based on the presence of the CheW-like domain, it is possible that CheV can bind to receptors, however this has yet to be experimentally determined. Whether the P5$_B$ and Rec domains of CheA1 function as a CheV remains to be determined. However, some of the behaviors examined in this study could suggest such a mechanism. Weak localization of soluble CheA1 (CheA1ΔTM:YFP) in the Δ*che1* (AB103) mutant background could also suggest a "CheV-like" mechanism in that the P5$_B$-Rec domains (which are still in place for this construct), could potentially bind to receptors resulting in the observed weak localization.

Chapter 3

Functional analysis of CheA1 domains in behaviors regulated by the Che1 pathway

References

1. **Alex, L. A., Simon, M. I.** 1994. Protein histidine kinases and signal transduction in prokaryotes and eukaryotes. Trends Genet. **10**: 133-138.

2. **Alexander, R. P., Lowenthal, A. C., Harshey, R. M., Otteman, K. M.** 2010. CheV: CheW-like coupling proteins at the core of the chemotaxis signaling network. Trends in Microbiol. **18**: 494-503.

3. **Baida, G. E., Kuzman, N. P.** 1995. Cloning and primary structure of a new hemolysin gene from *Bacillus cereus*. Biochimica et Biophysica acta. **1264**: 151-154.

4. **Baldani, V. L. D., Baldani, J. I., Dobereiner, J.** 1983. Effects of *Azospirillum* inoculation on root infection and nitrogen incorporation in wheat. Can. J. Microbiol. **29**: 924–929.

5. **Bible, A.N., Stephens, B.B., Ortega, D.R., Xie, Z., Alexandre, G.** 2008. Function of a chemotaxis-like signal transduction pathway in modulating motility, cell clumping, and cell length in the Alphaproteobacterium, *Azospirillum brasilense*. J. Bacteriol. **190**: 6365-6375.

6. **Bible, A. N., Russell, M. H., Alexandre, G.** 2012. The *Azospirillum brasilense* Che1 chemotaxis pathway controls the swimming speed which affects transient cell-to-cell clumping. J. Bacteriol. Just Accepted.

7. **Bilwes, A. M., Alex, L. A., Crane, B. R., Simon, M. I.** Structure of CheA, a signal-transducing histidine kinase. Cell. **96**: 131-141.

8. **Bourret, R. B., Davagnino, J., Simon, M. I.** 1993. The carboxy-terminal portion of the CheA kinase mediates regulation of autophosphorylation by transducer and CheW. J. Bacteriol. **175**: 2097-2101.

9. **Briegel, A., Ortega, D. R., Tocheva, E. I., Wuichet, K., Li, Z., Chen, S., Müller, A., Iancu, C. V., Murphy, G. E., Dobro, M. J., Zhulin, I. B., Jensen, G. J.** 2009. Universal architecture of bacterial chemoreceptor arrays. Proc. Natl. Acad. Sci. USA. **106**: 17181-17186.

10. **Dang, C. V., Niwano, M., Ryu, J., Taylor, B. L.** 1986. Inversion of aerotactic response in *Escherichia coli* deficient in *cheB* protein methylesterase. J. Bacteriol. **166**: 275-280.

11. **Dutta, R., Qin, L., Inouye, M.** 1999. Histidine kinases: diversity of domain organization. Mol. Microbiol. **34**: 633-640.

12. **Ferre, P., Carling, D., Kimura, S., Nagai, R., Kahn, B. B., Kadowaki, T.** 2002. Adiponectin stimulates glucose utilization and fatty-acid oxidation by activating AMP-activated protein kinase. Nat. Med. **8**: 1288–1295.

13. **Fredrick, K. L., Helmann, J. D.** 1994. Dual chemotaxis signaling pathways in *Bacillus subtilis*: A sigma-D-dependent gene encodes a novel protein with both CheW and CheY homologous domains. J. Bacteriol. **176**: 2727-2735.

14. **Güvener, Z., Tifrea, D. F., Harwood, C. S.** 2006. Two different *Pseudomonas aeruginosa* chemosensory signal transduction complexes localize to cell poles and form and remould in stationary phase. Mol. Microbiol. **61**: 106-118.

15. **Hallez, R., Letteson, J. J., Vandenhaute, J., De Bolle, X.** 2007. Gateway-based destination vectors for functional analysis of bacterial ORFeomes: application to the Min system in *Brucella abortus*. Appl. Environ. Microbiol. **73**: 1375-1379.

16. **Hauwaerts, D., Alexandre, G., Das, S. K., Vanderleyden, J., Zhulin, I. B.** 2002. A major chemotaxis gene cluster in *Azospirillum brasilense* and relationships between chemotaxis operons in α-proteobacteria. FEMS Microbiol. Letters. **208**: 61-67.

17. **Inclán, Y. F., Laurent, S., Zusman, D. R.** 2008. The receiver domain of FrzE, a CheA-CheY fusion protein, regulates the CheA histidine kinase activity and downstream signaling to the A- and S-motility systems of *Myxococcus xanthus*. Mol. Microbiol. **68**: 1328-1339.

18. **Jahreis, K., Morrison, T. B., Garzón, A., Parkinson, J. S.** 2004. Chemotactic signaling by an *Escherichia coli* CheA mutant that lacks the binding domain for phosphoacceptor partners. **186**: 2664-2672.

19. **Karatan, E., Saulmon, M. M., Bunn, M. W., Ordal, G. W.** 2001. Phosphorylation of the response regulator CheV is required for adaptation to attractants during *Bacillus subtilis* chemotaxis. J. Biol. Chem. **276**: 43618-43626.

20. **Karpichev, I. V., Cornivelli, L., Small, G. M.** 2002. Multiple regulatory roles of a novel *Saccharomyces cerevisiae* protein, encoded by *YOL002c*, in lipid and phosphate metabolism. J. Biol. Chem. **277**: 19609-19617.

21. **Katzen, F., A. Becker, M. V. Ielmini, C. G. Oddo, and L. Ielpi.** 1999. New mobilizable vectors suitable for gene replacement in gram-negative bacteria and their use in mapping of the 3' end of the *Xanthomonas campestris* pv. campestris gum operon. Appl. Environ. Microbiol. **65:** 278–282.

22. **Kofoid, E. C., Parkinson, J. S.** 1991. Tandem translation starts in the *cheA* locus of *Escherichia coli*. J. Bacteriol. **173**: 2116-2119.

23. **Kovach, M. E., P. H. Elzer, D. S. Hill, G. T. Robertson, M. A. Farris, R. M. Roop II, Peterson, K. M.** 1995. Four new derivatives of the broad-host-range cloning vector pBBR1MCS, carrying different antibiotic-resistance cassettes. BioTechniques **166**: 175–176.

24. **Li, J. Y., Swanson, R. V., Simon, M. I., Weis, R. M.** 1995. The response regulators CheB and CheY exhibit competitive binding to the kinase CheA. Biochemistry. **34**: 14626-14636.

25. **Lowenthal, A. C., Simon, C., Fair, A. S., Mehmood, K., Terry, K., Anastasia, S., Ottemann, K. M.** 2009. A fixed-time diffusion analysis method determines that the three *cheV* genes of *Helicobacter pylori* differentially affect motility. Microbiology. **155**: 1181-1191.

26. **Maddock, J. R., Shapiro, L.** 1993. Polar localization of the chemoreceptor complex in the *Escherichia coli* cell. Science. **259**: 1717-1723.

27. **Matsushika, A., Mizuno, T.** 1998. A dual-signaling mechanism mediated by the ArcB hybrid sensor kinase containing the histidined-containing phosphotransfer domain in *Escherichia coli*. J. Bacteriol. **180**: 3973-3977.

28. **Morrison, T. N., Parkinson, J. S.** 1997. A fragment liberated from the *E. coli* kinase that blocks stimulatory, but not inhibitory, chemoreceptor signaling. J. Bacteriol. **179**: 5543-5550.

29. **Muskavitch, M. A., Kort, E. N., Springer, M. S., Goy, M. F., Adler, J.** 1978. Attraction by repellents: an error in sensory information processing by bacterial mutants. Science. **201**: 63-65.

30. **Parkinson, J. S., Kofoid, E. C.** 1992. Communication modules in bacterial signaling proteins. Annu. Rev. Genet. **26**: 71-112.

31. **Pittman, M. S., Goodwin, M., Kelly, D. J.** 2001. Chemotaxis in the human gastric pathogen *Helicobacter pylori*: different roles for CheW and the three CheV paralogues, and evidence for CheV2 phosphorylation. Microbiology. **147**: 2493-2504.

32. **Rosario, M. M., Fredrick, K. L., Ordal, G. W., Helmann, J. D.** 1994. Chemotaxis in *Bacillus subtilis* requires either of two functionally redundant CheW homologs. J. Bacteriol. **176**: 2736-2739.

33. **Sanders, D. A., Gillece-Castro, B. L., Stock, A. M., Burlingame, A. L., Koshland, D. E., Jr.** 1989. Identification of the site of phosphorylation of the chemotaxis response regulator, CheY. J. Biol. Chem. **264**: 21770-21778.

34. **Scott, K. A., Porter, S. L., Bagg, E. A. L., Hamer, R., Hill, J. L., Wilkinson, D. A., Armitage, J. P.** 2010. Specificity of localization and phosphotransfer in the CheA proteins of *Rhodobacter sphaeroides*. Mol. Microbiol. **76**: 318-330.

35. **Simon, R., U. Priefer, and A. Pülher.** 1983. A broad host range mobilization system for *in vivo* genetic engineering transposon mutagenesis in gram-negative bacteria. Bio/Technology **1:** 784-791.

36. **Smith, R. A., Parkinson, J. S.** 1980. Overlapping genes at the *cheA* locus of *E. coli*. Proc. Natl. Acad. Sci. USA. **77**: 5370-5374.

37. **Sourjik, V.** 2004. Receptor clustering and signal processing in *E. coli* chemotaxis. Trends Microbiol. **12**: 569-575.

38. **Sourjik, V., Berg, H. C.** 2000. Localization of components of the chemotaxis machinery of *Escherichia coli* using fluorescent protein fusions. Mol. Microbiol. **37**: 740-751.

39. **Stephens, B. B., Loar, S. N., Alexandre, G.** 2006. Role of CheB and CheR in the complex chemotactic and aerotactic pathway of *Azospirillum brasilense*. **188**: 4759-4768.

40. **Swanson, R. V., Schuster, S. C., Simon, M. I.** 1993. Expression of CheA fragments which define domains encoding kinase, phosphotransfer, and CheY binding activities. Biochemistry. **32**: 7623-7629.

41. **Swanson, R. V., Alex, L. A., Simon, M. I.** 1994. Histidine and aspartate phosphorylation: two-component systems and the limits of homology. Trends Biochem. Sci. **19**: 485-490.

42. **Tang, Y. T., Hu, T., Arterburn, M., Boyle, B., Bright, J. M., Emtage, P. C., Funk, W. D.** 2005. PAQR proteins: a novel membrane receptor family defined by an ancient 7-transmembrane pass motif. J. Mol. Evol. **61**: 372-380.

43. **Taylor, B. L., Johnson, M. S.** 1998. Rewiring a receptor: negative output from positive input. FEBS Lett. **425**: 377-381.

44. **Taylor, B. L., Zhulin, I. B., Johnson, M. S.** 1999. Aerotaxis and other energy-sensing behavior in bacteria. Annu. Rev. Microbiol. **53**: 103-128.

45. **Wadhams, G.H., Armitage J. P.** 2004. Making sense of it all: bacterial chemotaxis. Nat. Rev. Mol. Cell Biol. **5**: 1024-1037.

46. **Welch, M., Chinardet, N., Mourey, L., Birck, C., Samama, J. P.** 1998. Struture of the CheY-binding domain of histidine kinase CheA in complex with CheY. Nat. Struct. Biol. **5**: 25-29.

47. **Wuichet, K., Alexander, R. P., and Zhulin, I. B.** 2007. Comparative genomic and protein sequence analyses of a complex system controlling bacterial chemotaxis. Methods Enzymol. **422**: 1-31.

48. **Yamauchi, T., Kamon, J., Ito, Y., Tsuchida, A., Yokomizo, T., Kita, S., Sugiyama, T., Miyagishi, M., Kara, K., Tsunoda, M., Murakami, K., Ohteki, T., Uchida, S., Takekawa, S., Waki, H., Tsuno, N. H., Shibata, Y., Terauchi, Y., Froguel, P., Tobe, K., Koyasu, S., Taira, K., Kitamura, T., Shimizu, T., Nagai, R., Kadowaki, T.**2003. Cloning of adiponectin receptors that mediate antidiabetic metabolic effects.Nature. **423**:762–769.

49. **Zhao, J., Parkinson, J. S.** 2006. Cysteine-scanning analysis of the chemoreceptor-coupling domain of the *Escherichia coli* chemotaxis signaling kinase CheA. J. Bacteriol. **188**: 4321-4330.

50. **Zhou, H., Lowry, D. F., Swanson, R. V., Simon, M. I., Dahlquist, F. W.** 1995. NMR studies of the phosphotransfer domain of the histidine kinase CheA from *Escherichia coli*: assignments, secondary structure, general fold, and backbone dynamics. Biochemistry. **34**: 13858-13870.

51. **Zhou, H., Dahlquist, F. W.** 1997. Phosphotransfer site of the chemotaxis-specific protein kinase CheA as revealed by NMR. Biochemistry. **36**: 699-710.

52. **Zhu, Y., Bond, J., Thomas, P.** 2003. Identification, classification, and partial characterization of genes in humans and other vertebrates homologous to a fish membrane progestin receptor. Proc. Natl. Acad. Sci. USA. **100**: 2237–2242.

53. **Zhulin, I. B., Bespalov, V. A., Johnson, M. S., Taylor, B. L.** 1996. Oxygen taxis and proton motive force in *Azospirillum brasilense*. J. Bacteriol. **178**: 5199-5204.

Chapter 4

Characterization of HlyIII-like proteins in *A. brasilense*, *E. coli*, and *B. subtilis*

Abstract

CheA1 from *A. brasilense* Sp7 is unique from all other CheAs studied thus far in that it possesses an N-terminal seven transmembrane HlyIII-like domain. These HlyIII-like proteins are representative members of the PAQR (Progestin and AdipoQ Receptor) family of proteins, with HlyIII-like proteins being the most "ancient" forms, found in all Bacteria and Eukarya. The HlyIII-like domain of CheA1 has a role in modulating cell length, and in ensuring the proper localization of CheA1 at the cell poles. However, the details of how HlyIII-like domains exert this function remains unclear. In chapter 3, evidence suggests that other CheA1 domains, such as the $P5_B$ and Rec domains, modulate the output of this transmembrane (TM) domain, making study of the TM domain alone in this organism difficult. Therefore, HlyIII-like proteins found in *Escherichia coli* and *Bacillus subtilis,* in which these HlyIII-like proteins are found as single domain proteins, were also analyzed. In both *E. coli* and *B. subtilis*, deletion of HlyIII-like proteins affected membrane properties, observed by defects in membrane staining and by defects in fatty acid composition of the cytoplasmic membranes. Such effects on membrane properties also affect the localization of membrane-associated proteins, which may impact other cellular behaviors.

Section A. Introduction

In chapter 3, we examined the roles of the N-terminal HlyIII-like TM domain, the two P5 domains ($P5_A$ and $P5_B$), and the C-terminal receiver domain of CheA1, and how they relate to signaling via the Che1 pathway. We also highlighted the fact that HlyIII domains are highly conserved and that homologs of HlyIII-like proteins are typically found as single-domain proteins which are widespread among Bacteria and Eukarya. Phylogenetic analysis of these HlyIII-like proteins in Bacteria and Eukarya suggests an activity of these proteins in lipid and fatty acid metabolism.

These HlyIII-like proteins belong to a newly described family of proteins known as the Progestin and AdipoQ Receptor (PAQR) family of proteins, named after homologs that have been found in humans. Interestingly, despite their sequence similarity, there is significant variation among this family in terms of function, topology, and ligand specificity (39). In humans, there are 11 PAQR family proteins that fall within three groups (39). The first group consists of PAQR1-4, the second consists of PAQR5-9, and the third group consists of PAQR10-11. The PAQR1-4 group includes the adiponectin receptors, which are classified from the rest based on their membrane topology (43). PAQR1-4 are predicted to have an intracellular N-terminus, and an extracellular C-terminus (39, 43). Two of these adiponectin receptors, AdipoR1 and AdipoR2, were shown to localize to skeletal muscle (AdipoR1) and the liver (AdipoR2) in humans and in mice, where they were found to mediate AMP kinase and PPARα ligand activities, which includes fatty acid oxidation as well as glucose uptake (43). On the other hand, PAQR5-9 are predicted to have an extracellular N-terminus and an intracellular C-terminus (39, 44), and these proteins make up the progestin receptor family of proteins, typically

found in reproductive tissues among mammals (44, 45). It was shown that PAQR5, 7, and 8 are found in human ovaries, where they are suggested to have an important role in the anti-tumorigenic properties of progesterone (8). It was also recently shown that the PAQR family of proteins is distantly related to alkaline ceramidases, based on sequence similarity, suggesting that these proteins may have membrane enzymatic activities, possibly even ceramidase activity (35). Interestingly, members of the PAQR1-4 adiponectin receptor group were recently shown to promote ceramidase activity, supporting this hypothesis (20). Homologs of group 1 PAQRs, called Izh1-4, have also been identified in the yeast, *Saccharomyces cerevisiae*, where one of these homologs, Izh2 has been shown to play a key role in lipid and phosphate metabolism (25), as well as zinc metabolism (29). Recently, the yeast Izh2p was also shown to have ceramidase activity, resulting in sphingoid base production as second messengers, lending further support to the hypothesis that members of the PAQR protein family have "ceramidase-like" activities (41).

Among the least characterized members of the PAQR protein family are the PAQR10 and PAQR11, which are the most similar to the bacterial HlyIII-like proteins (35, 39). Some recent studies involving PAQR10 and PAQR11 have suggested that these proteins are localized to the mitochondria where they may affect the mitochondrial pathway of apoptosis, thus affecting pancreatic endocrine cell development and survival (15). However, details surrounding how PAQR10 and PAQR11 are functioning within the mitochondria remain unclear. Most recently, PAQR10 and PAQR11 were shown to be localized to the Golgi apparatus where they were proposed to play an important role in Ras signaling (23). Ras proteins are trafficked to the Golgi from the plasma membrane where they are palmitoylated before trafficking back to the plasma membrane. In the study by Jin *et al*., it was found that PAQR10 and PAQR11 function

in MAPK signaling and play an important role in the retention of Ras proteins in the Golgi, with downstream effects on the ERK signaling cascade, although likely indirectly (23).

Bacterial homologs of the PAQR family of proteins are among the least studied thus far, which is especially interesting considering the first member of this family to be identified was from the bacterial organism, *Bacillus cereus*. In this organism, HlyIII was shown to function as a pore-forming cytolysin, a characteristic which was proposed to contribute to its virulence as an opportunistic pathogen (4). The *B. cereus* HlyIII protein is the only bacterial PAQR homolog studied thus far among bacteria. However, evidence for this function as a cytolysin is indirect at best, relying on overexpression of the seven-transmembrane protein in a heterologous *Escherichia coli* host; furthermore, no evidence was provided that HlyIII was actually expressed in the assays for cytolysin activity (4). As mentioned in chapter 3, a HlyIII-like domain is found at the N-terminus of CheA1 from *A. brasilense* Sp7 and we have shown that this domain is required for cell length regulation and localization of CheA1 at the cell poles. Our data also suggest that this protein domain may also modulate other motility-dependent effects of CheA1. Using *A. brasilense*, *E. coli* and *B. sublitis* as models, we explore the function of the HlyIII-like domain proteins in these bacteria in this chapter. Our data allow us to propose a model that accounts for the effect of HlyIII on cell length at division and also suggests that the regulation of cell division is not the primary target of HlyIII and that HlyIII-like proteins may have more general effects on the cell physiology, possibly by affecting the distribution and function of membrane proteins and via effects on cytoplasmic membrane composition and function.

Section B. Materials and Methods

Strains and Growth Conditions

Table 10 describes the strains and plasmids used in this study. All strains of *E. coli*, *B. subtilis*, and *A. brasilense* were grown at 28ºC with shaking. *E. coli* was grown in either rich LB (1 liter contains 10 grams Tryptone, 5 grams Yeast extract, and 10 grams NaCl) media, Tryptone media (10 grams Tryptone, 5 grams NaCl) or M9 minimal media (1 liter contains 6 grams Na_2HPO_4, 3 grams KH_2PO_4, 0.5 grams NaCl, 1 gram NH_4Cl and is supplemented with 10 ml each of 100 mM $MgSO_4$ and 10 mM $CaCl_2$, 0.001% Thiamine, 0.01% Methionine, as well as 0.4% glucose). *B. subtilis* was grown in rich NB (1 liter contains 8 grams Nutrient Broth and 5 grams NaCl) or biofilm/sporulation media (27). *A. brasilense* was grown in either rich TY (1 liter contains 10 grams Tryptone and 5 grams Yeast extract) media or MMAB (minimal media) supplemented with carbon and nitrogen sources of choice (19).

Chemotaxis swarm plate assays

Chemotaxis swarm plate assays were performed with *Escherichia coli* by first growing cells in LB media to a low optical density (OD600 $\leq$ 0.3). Cultures were each adjusted to a similar density prior to inoculation into swarm plates. Swarm plates consisted of tryptone media containing 0.3% agar and supplemented with either 20 mM aspartate, 20 mM serine, 20 mM nitrate, or buffer (as a control). Plates were incubated between 16 and 18 hours at 28ºC prior to observation.

Table 10. Strains and plasmids used in this study.

Strain or plasmid	Genotype, relevant characteristics	Reference or Source
Plasmids		
pBSKII	Cloning vector (Amp)	Stratagene
pBSK-*yqfA*	pBSKII containing *yqfA* (Amp)	this work
pJSB2-*ftsZ*	pBAD derivative, C-terminal Venus fusion to *ftsZ* (Cm)	34
pWM1079	*minDE-gfp* in pBAD33 (Cm)	38
pRH005	Gateway destination vector with YFP (Cm, Km)	16
pRH-*minCDE*	pRH005 containing *minCDE*	this work
pRH-*ftsZ*	pRH005 containing *ftsZ*	this work
Strains		
Escherichia coli		
TOP10	General cloning strain	Invitrogen
UB1005	wild type strain, λ^{-}*gyrA37*(NalR) *relA1spoT1metB1* λ^{R}	gift from J. Cronan
Δ*yqfA* UB1005	Δ*yqfA*::Km	this work
Wild type (pBSKII)	UB1005 containing pBSKII (Amp)	this work
Δ*yqfA* (pBSKII)	Δ*yqfA* UB1005 containing pBSKII (Amp, Km)	this work
Δ*yqfA* (pBSK-*yqfA*)	Δ*yqfA* UB1005 containing pBSK-*yqfA*) (Amp, Km)	this work
Wild type (Venus-FtsZ)	UB1005 containing pJSB2-*ftsZ* (Cm)	this work
Δ*yqfA* (Venus-FtsZ)	Δ*yqfA* UB1005 containing pJSB2-*ftsZ* (Cm, Km)	this work
Wild type (MinDE-GFP)	UB1005 containing pWM1079 (Cm)	this work
Δ*yqfA* (MinDE-GFP)	Δ*yqfA* UB1005 containing pWM1079 (Cm, Km)	this work
Azospirillum brasilense		
Sp7	Parental strain, "wild type"	ATCC29145
AB101	Δ(*cheA1*)::*gusA-Km* (Km)	5
BS104	Δ(*cheB1cheR1*)::*Km* (Km)	37
Sp7 (pRH-*minCDE*)	wild type strain containing pRH-*minCDE* (Cm, Km)	this work
AB101 (pRH-*minCDE*)	AB101 containing pRH-*minCDE* (Cm, Km)	this work
AB101 (pRH-*ftsZ*)	AB101 containing pRH-*ftsZ* (Cm, Km)	this work
Sp7 (pBBR)	wild type (Sp7) containing pBBR-MCS3 (Tc)	5
AB101 (pBBR)	AB101 containing pBBR-MCS3 (Tc)	5
AB101 (pBBR-TM_{cheA1})	AB101 containing pBBR-TM_{cheA1} (Tc)	Chapter 3
AB101 (pBBR-*cheA1Δ* $P5_B$-*Rec*)	AB101 containing pBBR-*cheA1Δ*$P5_B$-*Rec*	Chapter 3
Bacillus subtilis		
Wild type	Parental strain 168, "wild type"	INRA*
Δ*yplQ*	pMUTIN plasmid insertion in *yplQ*	INRA*

Antibiotic resistance abbreviations: Amp (ampicillin), Km (kanamycin), Cm (chloramphenicol), Tc (tetracycline)
*INRA: Institut National de la Recherche Agronomique

Construction of a* ΔyqfA *mutant and complementation

The Δ*yqfA* mutant was constructed by using the method of Datsenko and Wanner (11) using primers (pKD-YqfA-Up: 5'-ACGCTGGAGAGGTATACATGTGCGTGT ACGTTTCTCCGGAGTAAGTTATGGTGTAGGCTGGAGCTGCTTC-3' and pKD-YqfA-Do: 5'- ATGGGAATTAGCCATGGTCCCTGATGCGACGCTGGCGCGTCTTATCAGGCCTAC AAAGGCATACCCATTA-3'). Generation of a construct for complementation of the *yqfA* mutation was performed by cloning the full length *yqfA* gene from *E. coli* genomic DNA using the primers (yqfAexp_HindIII-For: 5'-AAGCTTATGGTTCAGAAGCCC -3' and yqfAexp_XbaI-Rev: 5'-TCTAGATTACGCCTGCCCAAT -3'). The amplified *yqfA* was then cloned into the pCR2.1 TOPO cloning vector according to manufacturer's instructions (Invitrogen). Afterward, *yqfA* was removed from the pCR2.1 TOPO vector using the enzymes, HindIII and XbaI, and then ligated into the pBSK II vector (Stratagene). The completed construct was then transformed into the *E. coli* Δ*yqfA* mutant.

Fluorescent protein fusion constructs

The plasmids pJSB2-FtsZ (gift from H. P. Erickson, Duke University) and pWM1079 (gift from W. Margolin, University of Texas Medical School, Houston) were used to transform wild type UB1005 cells and the Δ*yqfA* mutant. The pRH-*minCDE* and pRH-*ftsZ*, containing the *minCDE* and *ftsZ* genes from *A. brasilense*, were cloned using Gateway cloning technology from Invitrogen. To generate this fusion, we used the primers (gwMinCDE_for: 5'-GGGGACAAGTTTGTACAAAAAAGCAGGCTAAGGAGGAGTCCCTTATGGCAGCGGTG AGCAGC-3' and gwMinCDE_rev: 5'-GGGGACCACTTTGTACAAGAAAGCTGGGTG GCGACGCTTCTTGACGCC-3') to amplify the *minCDE* genes and (gwFtsZ_for: 5'-

GGGGACAAGTTTGTACAAAAAAGCAGGCTAAGGAGGAGTCCCTTATGATCAACGTG ACCATC-3' and gwFtsZ_rev: 5'-GGGGACCACTTTGTACAAGAAAGCTGGGTGGTTGG CCTGACGGCGCAG-3') to amplify the *ftsZ* gene from *A. brasilense* genomic DNA. PCR products were then incorporated into the donor vector, pDONR221 (Invitrogen), using the BP Clonase enzyme (Invitrogen) according to manufacturer's directions and transformed into OmniMax competent cells (Invitrogen), followed by sequencing (University of Tennessee, Molecular Biology Resource Facility). Next, *minCDE* was moved from the donor vector, pDONR, to the destination vector, pRH005 (Hallez *et al*., 2007), in a recombination reaction using the LR Clonase II enzyme (Invitrogen) according to manufacturer's directions. The final construct was then introduced into wild type *A. brasilense* and Δ*cheA1* (AB101) using biparental conjugation (37).

Measurements of cell length

Cell length measurements were performed as described previously, with the following differences (5). In *Escherichia coli,* cells were grown in either M9 minimal media supplemented with glucose, or in LB media to a low optical density (OD600 ≤ 0.3). Once cells were grown, staining and measurements were performed as described (5). In *Bacillus subtilis*, cells were grown in NB media to a low optical density (OD ≤ 0.3), stained and measured as described previously (5).

Membrane Staining

Membrane Staining for *A. brasilense*, *E. coli*, and *B. subtilis* took place using the same protocols for each dye. Staining with FM1-43 and FM4-64 took place as described above in

Measurements of cell length with the exception that whereas staining with FM4-64 was visualized using the TRITC (Texas Red Isothiocyanate) filter, staining with FM1-43 was visualized with the FITC (Fluorescein Isothiocyanate) filter set. Staining with 10-*N*-Nonyl Acridine Orange (NAO) was performed as described previously by incubating cells for 1 hour with 200 nM NAO, followed by visualization with the FITC filter set (32). Photographs were taken using a Nikon ECLIPSE 80i fluorescence microscope equipped with a Nikon CoolSnap HQ2 cooled CCD camera.

Fluorescence Microscopy

Microscopy was performed for strains carrying fluorescent protein fusions to FtsZ or MinDE (*E. coli*) by first growing cells in LB supplemented with 0.4% glucose and appropriate antibiotics overnight at 28ºC with shaking. Next, approximately 1 ml of cells was removed from the culture and washed twice with 0.8% KCl to remove excess glucose. Cells were then re-inoculated to a low cell density into fresh LB with the appropriate antibiotics and incubated at 28ºC with shaking for 2 hours. After the 2 hour incubation, L-arabinose was added to a final concentration of 0.001% and incubated for another 2 hours at 28ºC with shaking prior to visualization. DAPI staining was performed by adding 1 µl of a 5 mg/ml stock solution of DAPI (Molecular Probes, Invitrogen) to spproximately 200 µl of cells. DAPI stained cells were visualized using fluorescence microscopy with a UV filter. Strains carrying YFP fusions to MinCDE and FtsZ (*A. brasilense*) were prepared by growing cells in MMAB supplemented with 10 mM malate at 28ºC with shaking to a low cell density, with no induction required. For visualization in all strains, cells were first concentrated using centrifugation. Concentrated cells were then placed on a 1% agarose pad with a coverslip and allowed to settle for 2-3 minutes.

Cells were then visualized using the Nikon ECLIPSE 80i fluorescence microscope equipped with a Nikon CoolSnap HQ2 cooled CCD camera, as described above. Fluorescent protein fusions could be observed using either the YFP or FITC filters.

Immunofluorescence microscopy was performed using rabbit polyclonal antibodies against the following: *E. coli* CheB and *E. coli* CheR (A gift from Ann Stock, Princeton), *E. coli* Tsr (a gift from J. S. Parkinson, Univ. of Utah), and *B. subtilis* McpB (a gift from G. Ordal, Univ. of Illinois). For immunolocalization experiments, cells were grown as follows: *E. coli* cells were grown in M9 minimal media supplemented with 0.4% glucose, *A. brasilense* cells were grown in MMAB supplemented with 10 mM Malate, and *B. subtilis* cells were grown in NB, each to a low cell density (O. D. $\leq$ 0.3). Collected cells were first washed and resuspended in 100 µl PBS, then fixed in 1 ml of ice cold methanol for 1 hour at -20ºC. Afterwards, cells were placed onto poly-L-lysine coated coverslips and allowed to dry (about 10 minutes). Cells were then gently lysed using a 2 mg/ml lysozyme solution in GTE buffer (50 mM glucose, 20 mM Tris-HCl pH 8.0, 10 mM EDTA) for 10 minutes, prior to incubation overnight at 4ºC in a blocking solution consisting of 1% non-fat dry milk in PBS, pH 7.0. Next, coverslips were washed twice with PBS, prior to adding the antibody solution consisting of 1% non-fat dry milk in PBS with a 1:300 antibody concentration. Coverslips were incubated in the antibody for 2 hours at room temperature in the dark, then washed 10 times with PBS. Next, the coverslips were incubated with an Alexa Fluor 488 goat anti-rabbit IgG at a 1:500 dilution in 1% non-fat dry milk in PBS for 2 hours at room temperature. Afterwards, the coverslips were washed and then placed onto a slide and sealed with clear nail polish.

PLFA Analysis

Phospholipid-Fatty Acid (PLFA) analysis of *A. brasilense* and *E. coli* cells by Microbial Insights, Inc. (Rockford, TN) and analysis of *B. subtilis* was performed by Microbial ID (Newark, DE). Preparation of samples included growing *A. brasilense* in MMAB supplemented with 5 mM malate and 5 mM fructose, *E. coli* in M9 media with glucose, and *B. subtilis* in NB media, each at a low OD. Cells were collected and sent for analysis to the aforementioned companies.

Section C. Results

Loss of HlyIII-like proteins results in defective/altered membrane lipid staining

As mentioned in the introduction, phylogenetic analysis of HlyIII-like proteins among Bacteria and Eukarya, as well as studies on other PAQR family proteins, suggested a role for these proteins in lipid and fatty acid metabolism. In order to assess this possibility, we performed membrane staining among three different organisms: *Azospirillum brasilense*, *Escherichia coli*, and *Bacillus subtilis*. Membrane staining using the lipophilic dyes, FM1-43 and FM4-64 was performed in wild type *A. brasilense*, *E. coli*, and *B. subtilis*, along with the corresponding mutants lacking the following HlyIII-like proteins: CheA1 (*A. brasilense*), YqfA (*E. coli*), and YplQ (*B. subtilis*). Results from this experiment showed different staining patterns between wild type cells and the HlyIII-like protein mutants in all three organisms tested (Figure 32). Staining phenotypes in *A. brasilense* and *E. coli* were best observed when cells were grown under minimal media conditions, while growth in rich (Nutrient Broth) media provided the clearest results for *B. subtilis*. In both *A. brasilense* and *E. coli*, staining with FM4-64 was weaker in the HlyIII mutants, as compared to the wild type strains (Figure 32). In *B. subtilis,*

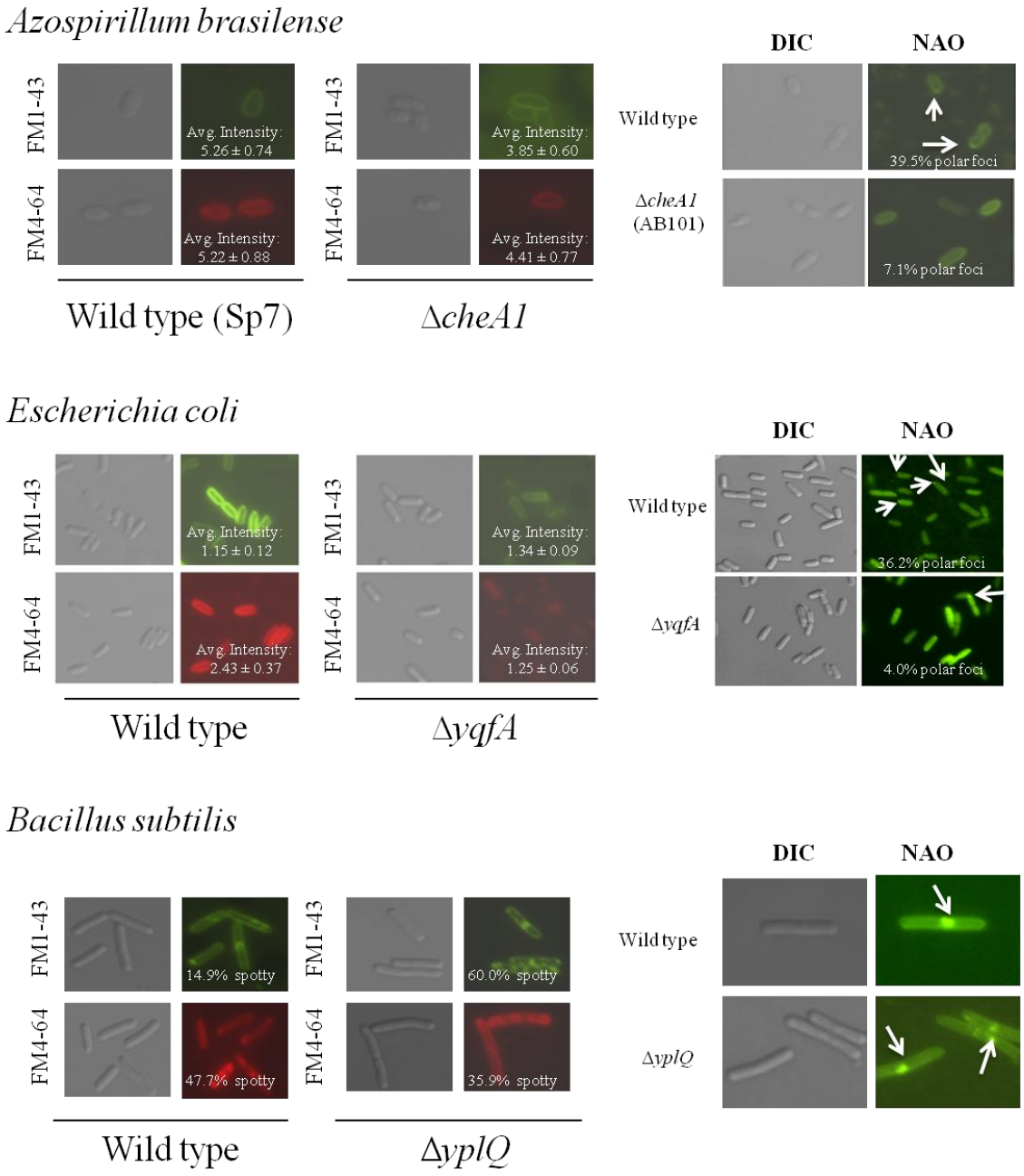

Figure 32. Comparison of membrane staining phenotypes in wild type *A. brasilense*, *E. coli*, and *B. subtilis* and corresponding HlyIII mutants. Panels on the left and middle show staining with FM1-43 and FM4-64 in each strain shown, with DIC photographs on the left and fluorescence images on the right. Numbers indicate the average fluorescence intensity, or the percentage of cells with "spotty" staining. Anionic phospholipid staining with NAO is shown in panels on the right. Arrows indicate foci in each strain. Differences in the percentage of cells showing polar foci are as indicated. Calculations are based on at least 30 cells per sample.

staining with FM1-43 showed increased "spotty" staining in the *yplQ* insertion mutant compared to the wild type; whereas, staining with FM4-64 showed increased "spotty" staining in the wild type strain, as opposed to the Δ*yplQ* mutant (Figure 32). These results suggested that mutations affecting HlyIII-like proteins affect properties of the membrane that allow for staining with the lipophilic dyes, FM1-43 and FM4-64. Interestingly, FM1-43 and FM4-64 differ in their structures, with FM4-64 having a longer carbon chain than FM1-43 for insertion into the membrane (Molecular Probes, Invitrogen). These differences in carbon chain length may influence the efficiency of dye uptake in cell membranes, particularly in different lipid environments. Therefore, we speculate that the observed differences in membrane staining with these two dyes could be due to differences in membrane composition.

To gain further insight into how membrane properties of these bacteria may be affected by HlyIII-like proteins, we chose to examine the localization of anionic phospholipids, such as cardiolipin, an important phospholipid in bacteria. To do so, we used NAO, which is known to stain all anionic phospholipids, including cardiolipin (32). In the Δ*cheA1* (AB101) mutant, there was a significant decrease in the localization of NAO-stained anionic lipids at polar foci, relative to the wild type *A. brasilense* (Figure 32). Similarly, the *E. coli* Δ*yqfA* mutant showed weaker polar localization of NAO compared to staining observed in the wild type strain (Figure 32). Interestingly, staining in *B. subtilis* did not result in any observable differences between the wild type and Δ*yplQ* mutant (Figure 32).

Loss of HlyIII-like proteins affects protein localization

We hypothesized that membrane properties affected in cells lacking HlyIII-like proteins could cause defects or changes in subcellular localization of membrane-associated proteins (either membrane proteins or cytoplasmic proteins which bind to membrane proteins). To test this hypothesis, the localization of the *E. coli* chemotaxis proteins CheB and CheR (which bind to membrane-bound chemoreceptors), Tsr (an *E. coli* chemoreceptor), as well as the localization of the McpB chemoreceptor in *B. subtilis*, were analyzed. Localization of these proteins was performed in wild type *E. coli* [wild type (pBSKII)], as well as the Δ*yqfA* mutant [Δ*yqfA* (pBSKII)], and a complemented Δ*yqfA* mutant in which the wild type parental gene is expressed from a plasmid [Δ*yqfA* (pBSK-*yqfA*)] (Figure 33). The complemented Δ*yqfA* mutant was functional, in that it restored the wild type cell length phenotype (see Figure 34). In wild type *E. coli* cells, localization of CheB and CheR was found primarily at the cell poles, with some localization observed at mid-cell. In the *E. coli* Δ*yqfA* (pBSKII) mutant, fewer polar foci were observed when CheB and CheR localization was analyzed, and this difference was no longer observed in the complemented strain, Δ*yqfA* (pBSK-*yqfA*). Similar experiments were performed with an antibody against Tsr from *E. coli* (Figure 33). Tsr localization showed primarily polar localization in the wild type strain, while the mutant showed a more "spotty" localization pattern for the Tsr chemoreceptor. This pattern of localization was also rescued in the complemented strain. This Tsr antibody was also used to assess the localization of receptors in wild type *A. brasilense*, as well as the Δ*cheA1* (AB101) mutant, since it has been shown to cross-react with several receptors in *A. brasilense* (S. Greer-Phillips dissertation) (Figure 33). However, no significant differences in localization patterns of cross-reacting proteins with this

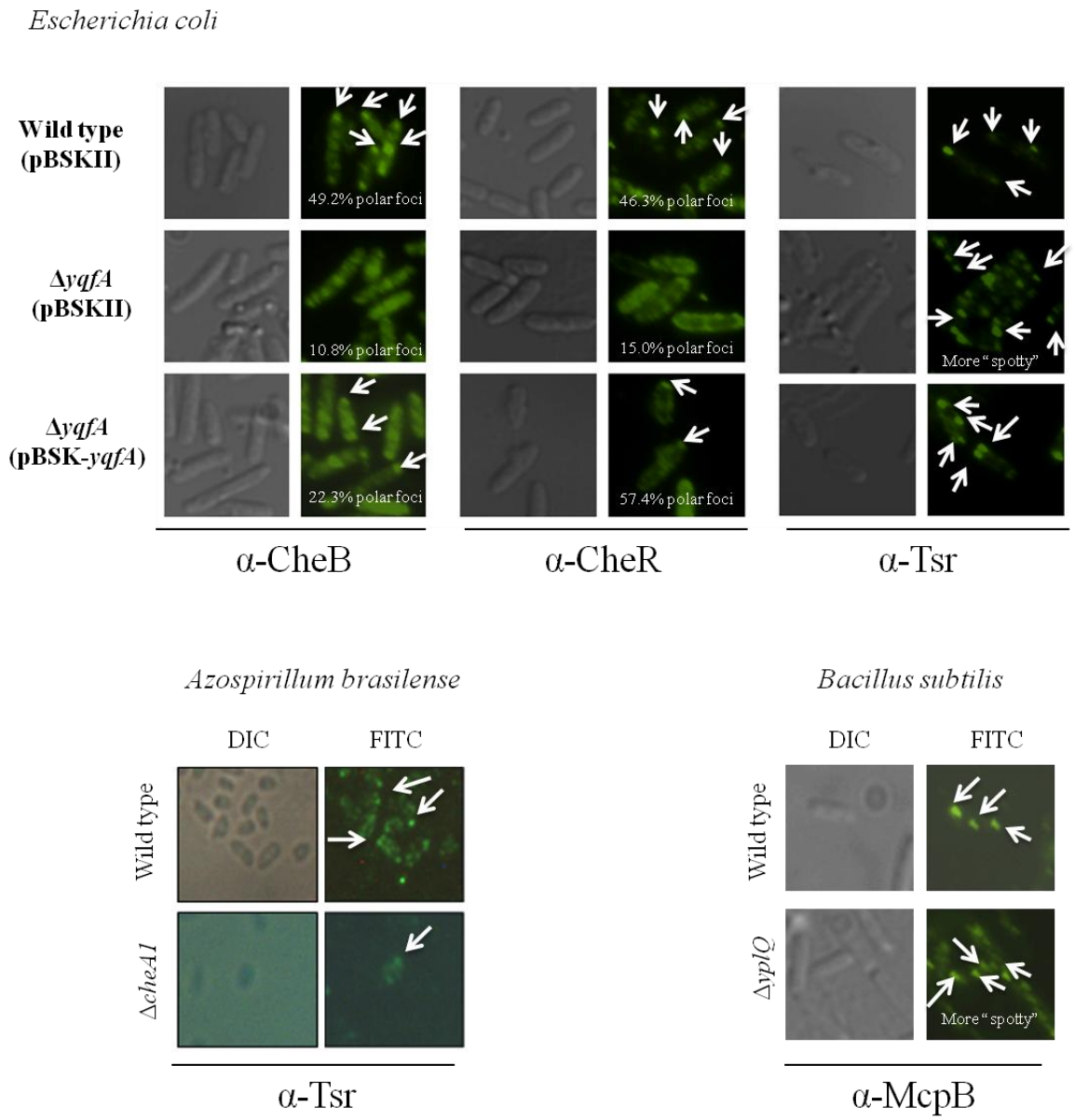

Figure 33. Effects of HlyIII-like proteins on localization of membrane-associated proteins in *E. coli, A. brasilense,* and *B. subtilis*.(Top) Localization of CheB, CheR, and Tsr in wild type *E. coli*, the Δ*yqfA* mutant, and the complemented mutant. (Bottom left) Localization of Tsr in wild type *A. brasilense* and the Δ*cheA1* mutant. (Bottom right) Localization of McpB in wild type *B. subtilis* and the Δ*yplQ* mutant. In all strains, the arrows point to foci and notes comment on localization patterns. Calculations for localization with α-CheB and α-CheR represent the number of cells with polar foci (more than 50 cells analyzed per sample). Localization experiments using α-Tsr or α-McpB resulted in more than 90% of cells showing polar foci in the wild type (and complemented strains) and more than 90% of cells showing "spotty" localization in mutants (more than 50 cells analyzed per sample).

antibody were detected. Given that recent genome analysis indicated the presence of 48 chemoreceptors in *A. brasilense* (42), the likelihood that Tsr cross-reacts with all of them is questionable. It will be interesting in the future to analyze the localization of chemoreceptors from *A. brasilense* either by gene fusions with YFP or immunolocalization, upon availability of antibodies against *A. brasilense* chemoreceptors.

Using an antibody against the *B. subtilis* McpB, we analyzed the localization of this receptor in the wild type *B. subtilis* and in the Δ*yplQ* mutant. Similar to Tsr localization in *E. coli*, we found that localization of McpB was more "spotty" in the Δ*yplQ* mutant, than in the wild type *B. subtilis* (Figure 33). Taken together, these data suggested that the effects of HlyIII-like proteins on membrane properties, can in turn affect the localization of some membrane-bound proteins, as well as membrane-associated proteins.

HlyIII-like proteins are involved in cell length regulation

Chapter 3 showed that the HlyIII-like domain at the N-terminus of CheA1 from *A. brasilense* plays an essential role in cell length regulation. Specifically, we showed that the cell length defect in mutants lacking *cheA1* (where mutant cells were shorter than the wild type) could be complemented with the HlyIII-like TM domain of CheA1 alone, and in strains expressing *cheA1ΔTM*, complementation of cell length was not observed. Further, in the closely related strain of *A. brasilense*, strain Sp245, in which the HlyIII-like domain is not found at the N-terminus of CheA1 (42), mutating the Sp245 *cheA1*gene doesn't have any effect on cell length, lending support to the assumption that the HlyIII-like domain of CheA1 in strain Sp7 is primarily responsible for the effect of mutating this gene on cell length regulation. Here, we

wanted to test the effect of HlyIII-like proteins on cell length in *E. coli* and *B. subtilis*. As compared to the shorter cell length phenotype of Δ*cheA1* in *A. brasilense* Sp7, we found that the *E. coli* Δ*yqfA* mutant was significantly longer than the wild type, and this phenotype was rescued in the complemented strain, Δ*yqfA* (pBSK-*yqfA*) (Figure 34). Although these results continue to suggest a regulatory effect of HlyIII on cell length, the observed phenotypes between *A. brasilense* and *E. coli* were opposite. Intriguingly, we were unable to observe any cell length defects in *B. subtilis* (Figure 34).

HlyIII-like proteins do not directly affect cell division machinery or process

In chapter 1, we showed that the observed cell length phenotypes of a Δ*cheA1* mutant and wild type *A. brasilense* were not due to cell division defects (i. e. cells divided normally, and cell length defects were still observed in dividing cells). Measurements of growth rates were also found to be similar, suggesting that the observed cell length differences in *A. brasilense* were not due to defects in cell division *per se*. Here, we examined the growth rate of the wild type *E. coli* and the Δ*yqfA* mutant under the conditions where we see the best differences in cell length and found that the growth rates in each strain were similar (division rates were approximately 1 hour in both strains when grown in LB at 28ºC with shaking). To further test for other cell division defects, we performed DAPI staining (for DNA) and examined the localization of FtsZ, an essential component of the cell division machinery in bacteria (Figure 35). The Z-rings assembled by polymerization of FtsZ appeared at midcell, as expected, and did not seem delayed or compromised, at least as visualized by fluorescence microscopy, in both the wild type and the Δ*yqfA* mutant background. There were no noticeable defects in chromosome segregation as

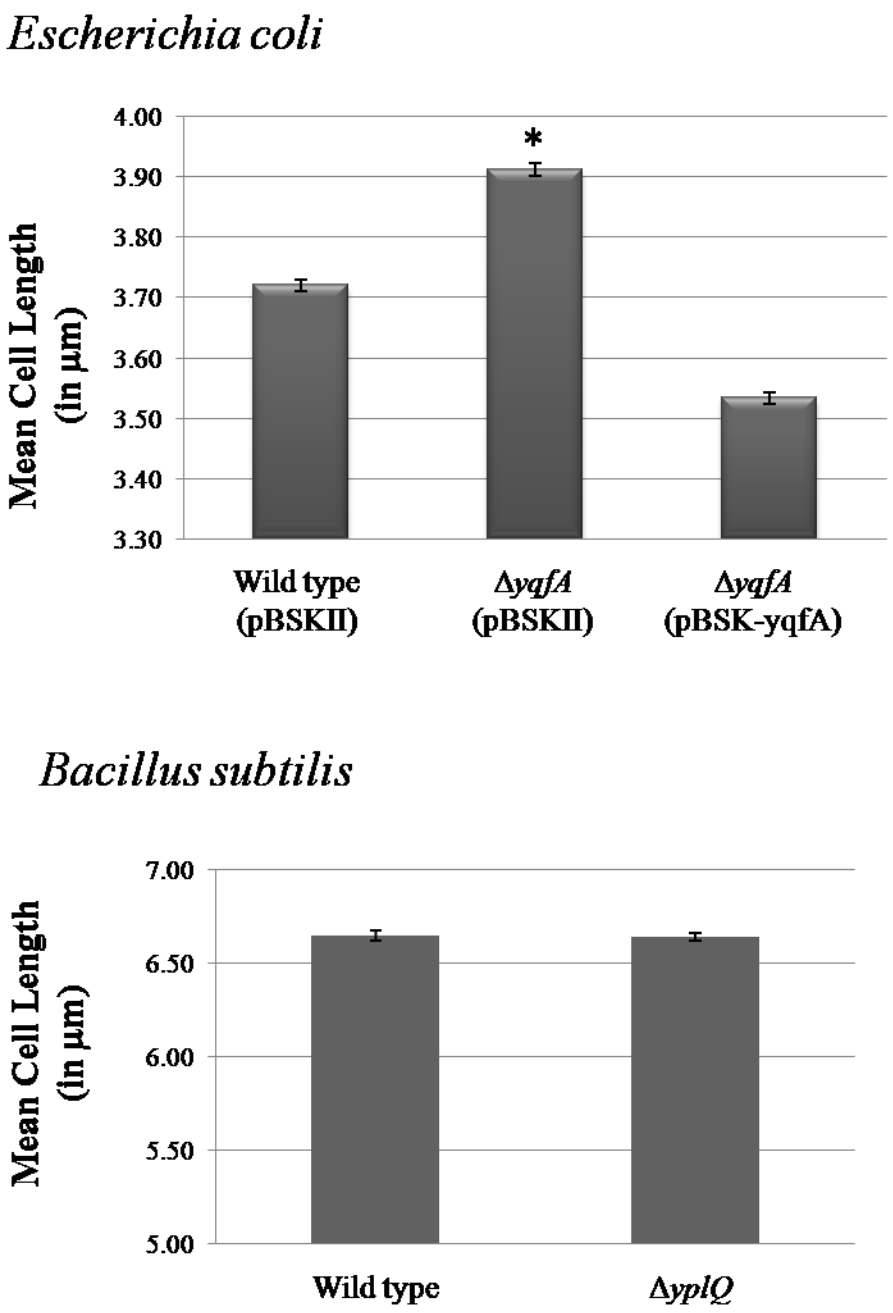

Figure 34. Measurement of mean cell length in wild type and HlyIII mutants of*E. coli* and *B. subtilis*. (Top) Mean cell lengths in wild type, mutant, and complemented strains of *E. coli*. (Bottom) Mean cell lengths in the wild type and Δ*yplQ* mutant in *B. subtilis*. (*) Indicates statistically significant differences in cell length relative to the wild type (n=50).

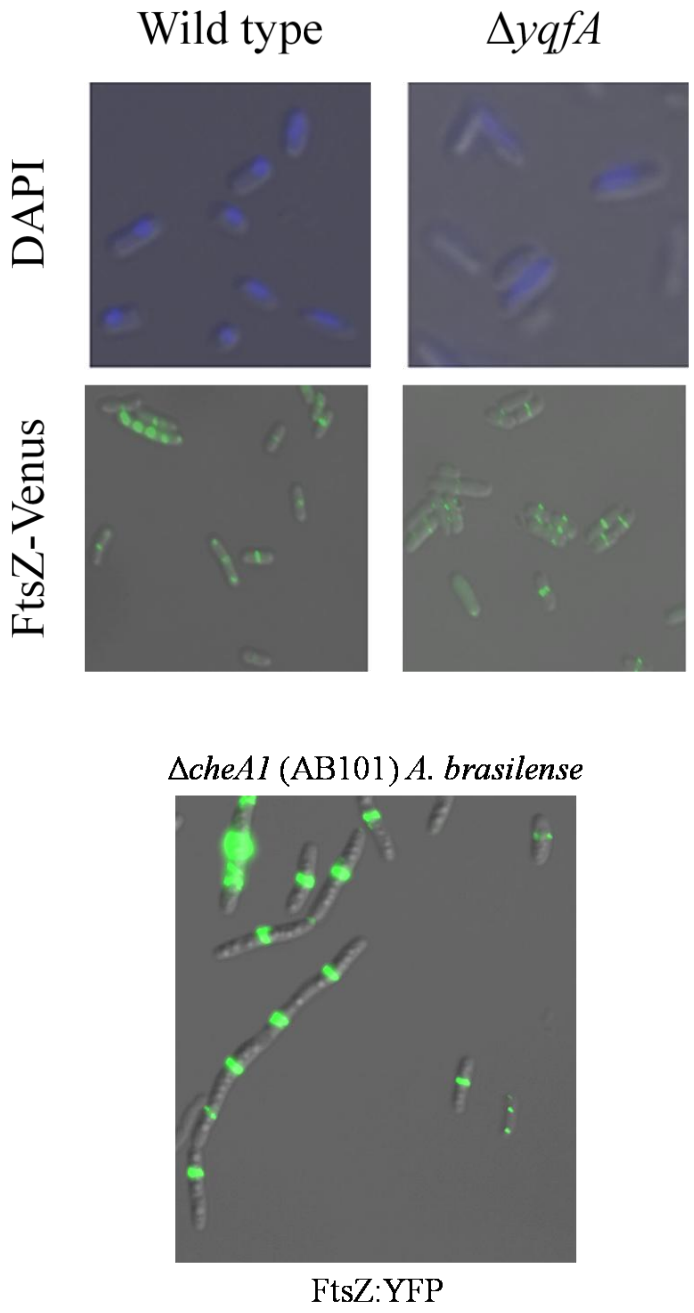

Figure 35. Localization of cell division components in wild type *E. coli*, the Δ*yqfA* mutant, and FtsZ:YFP localization in a Δ*cheA1* (AB101) mutant. (Top) Merged images of DIC and DAPI localization (blue). (Middle) Merged images of DIC and FtsZ-Venus (green) in E. coli. (Bottom) Merged image of DIC and FtsZ:YFP in a Δ*cheA1* (AB101) mutant of *A. brasilense*. Wild type images are not yet available.

revealed by DAPI staining, as well, suggesting that these HlyIII-like proteins do not directly affect cell division machinery.

Expression of a construct encoding FtsZ:YFP in *A. brasilense* Sp7 prevented growth in most strains and also lead to the production of filaments. Figure 35 shows a representative picture of cells from the Δ*cheA1* (AB101) mutant that is capable of forming FtsZ rings. However, a mixture of normal cells and filaments were observed in this culture, as shown in this figure. At this time, we do not have wild type cells expressing FtsZ:YFP; however, it does not appear that mutations affecting *cheA1* disrupt FtsZ ring formation, supporting the observations in *E. coli* that HlyIII-like proteins do not affect FtsZ ring assembly.

Perturbations in Min localization in HlyIII mutants

In order to gain insight into the possible mechanism(s) underlying cell length regulation via HlyIII-like proteins in *E. coli* and *A. brasilense*, the localization and oscillation behavior of Min proteins (MinC, MinD, and MinE), which are required for the proper placement of the FtsZ ring during cell division, in wild type and HlyIII mutants of *E. coli* and *A. brasilense* were analyzed next. In the following experiment, each of these organisms were grown to low densities under conditions where differences in cell length were best observed (see **Materials and Methods**) (5; Chapter 3). We found that in *E. coli*, when grown to an optical density of less than 0.3, wild type cells formed MinE rings that were capable of oscillating from pole-to-pole (Figure 36). However, localization of Min proteins in the Δ*yqfA* mutant was diffuse and MinE ring formation and oscillation was not observed in this mutant at low density. Interestingly, when cells were allowed to continue growing to densities ranging from 0.3 to 0.7, MinE ring

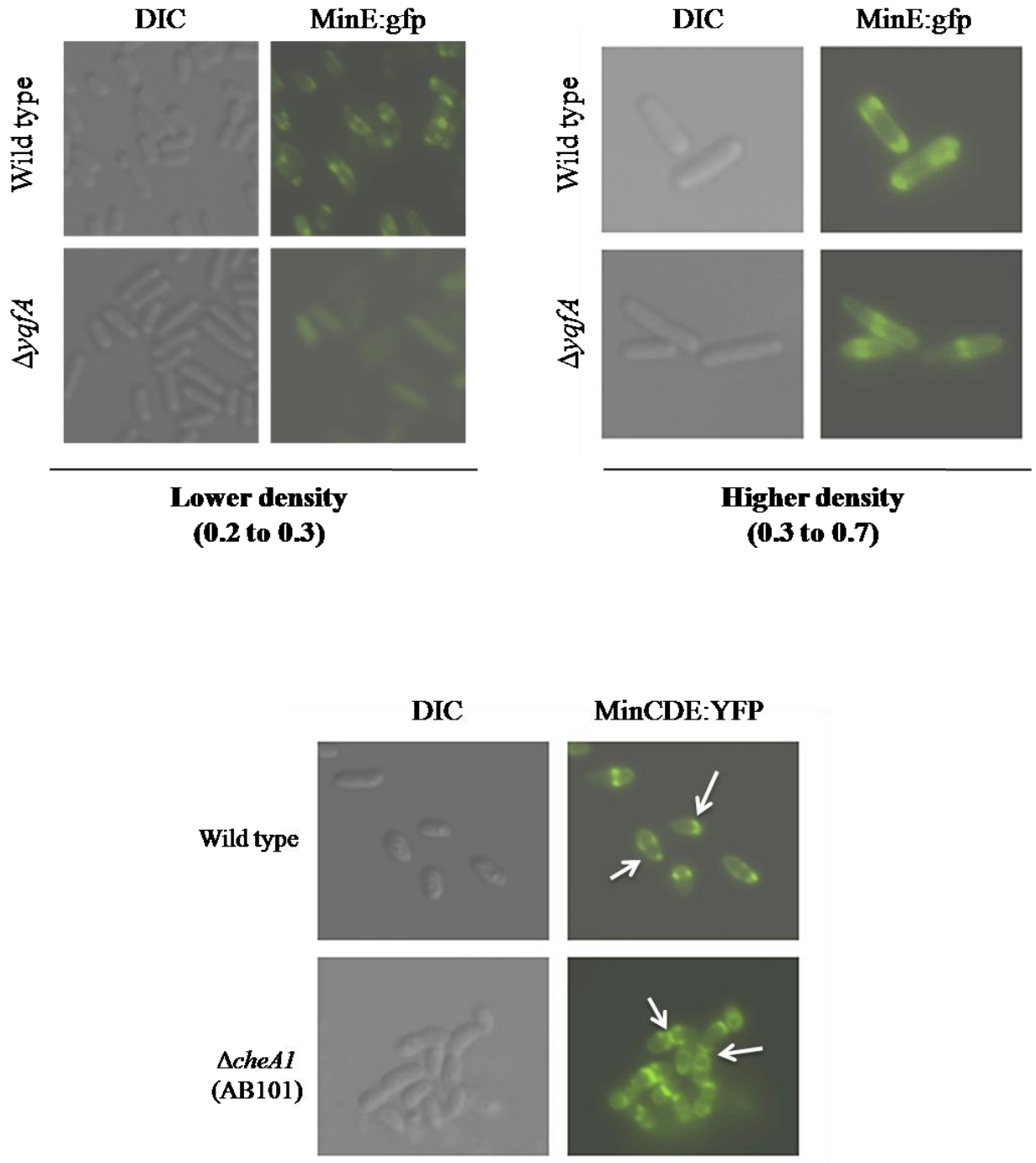

Figure 36. Localization of Min proteins is affected in HlyIII mutants of *E. coli* and *A. brasilense*. (Top) Comparison of Min localization between wild type and Δ*yqfA* in *E. coli* at low cell densities versus higher cell densities. (Bottom left) Example of Min oscilllation in wild type *A. brasilense*. (Bottom right) Comparison of Min localization between wild type and Δ*cheA1* in *A. brasilense*. Arrows indicate differences in Min localization.

formation and oscillations in the Δ*yqfA* mutant appeared to be similar to the ones observed in the wild type strain (Figure 36). These results suggest that the effect of HlyIII-like proteins in *E. coli* cell division may be to affect the localization of Min proteins, thereby affecting the ability of Min proteins to oscillate, ultimately delaying cell division site placement. Notably, once localization of Min proteins was observed in the Δ*yqfA* mutant, no differences with the wild type pattern could be detected in Min oscillations.

In *A. brasilense*, we did not observe a density-dependent localization phenotype for Min proteins in the wild type and Δ*cheA1* (AB101) mutant. We did, however, observe different patterns of localization of these proteins in the Δ*cheA1* (AB101) mutant, as opposed to the wild type (Figure 36). Specifically, Min proteins in the Δ*cheA1* (AB101) mutant (that also does not possess the HlyIII-like protein) appeared more diffuse (or spread out) within the cell membrane; whereas, localization of Min appeared more concentrated at specific regions in wild type cells. Taken together, these data suggest that the effect of HlyIII proteins on the cell membrane may in turn affect localization of proteins that are important for the placement of cell division machinery.

HlyIII-like proteins affect fatty acid profiles

The previous experiments have collectively suggested that HlyIII-like proteins affect properties of the cell membrane, which may explain defects in localization of membrane-associated proteins, including proteins that determine placement of the cell division machinery. To gain further insight into how the membrane of the cells may be affected, phospholipid-fatty

acid composition (PLFA) analysis of membranes of *A. brasilense*, *E. coli*, and *B. subtilis* was performed (by Microbial Insights, Inc. and Microbial ID).

In all three strains examined in this experiment, we did not find any specific fatty acid that was consistently affected in mutants lacking HlyIII. However, we did find that each of the mutant strains in which the gene encoding for HlyIII was mutated had fatty acid profiles which were different to the wild type strains. In *E. coli*, we found that there is a higher percentage of palmitate (16:0) in the Δ*yqfA* mutant, compared to the wild type, which appeared to be complemented by expressing the wild type parental gene (Figure 37). There was no difference in the composition or concentration of unsaturated fatty acids (monoenoics) in the presence or absence of YqfA.

B. subtilis differs from *E. coli* and *A. brasilense* in that the normal lipid composition in this organism consists primarily of saturated and branched chain (iso and anteiso) fatty acids, a trait common to *Bacillus* species (for a review, see 24). The fatty acid profiles of the *B. subtilis* wild type and the Δ*yplQ* mutant strains were quite similar with the exceptions that wild type has a higher percentage of the 17:1 iso fatty acid, compared to the mutant, while myristate (14:0) and stearate (18:0) were detected in the mutant (albeit at low levels), but not in the wild type (Figure 37).

Fatty acid profiles were the most similar amongst strains of *A. brasilense*, with little to no variation observed regardless of the presence of the HlyIII domain, even in the Δ(*cheB1cheR1*) (BS104) mutant which has a longer cell length than the wild type and HlyIII-like proteins are presumably more active. It did appear, however, that in a Δ*cheA1* mutant strain expressing

Escherichia coli

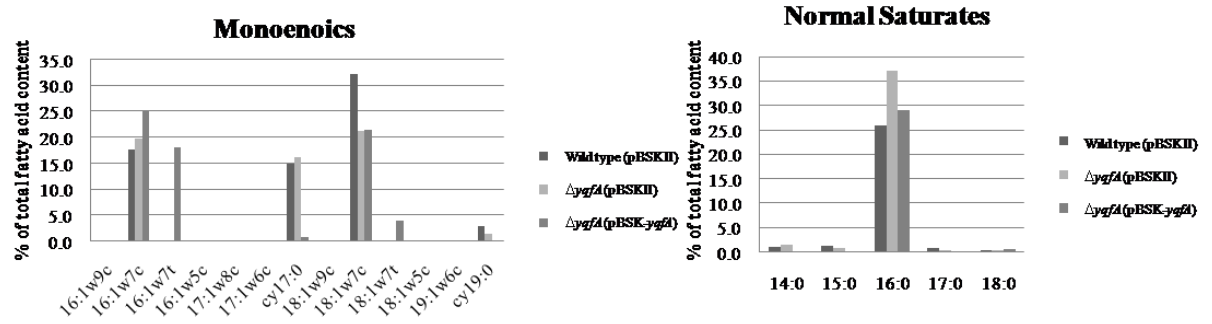

Bacillus subtilis

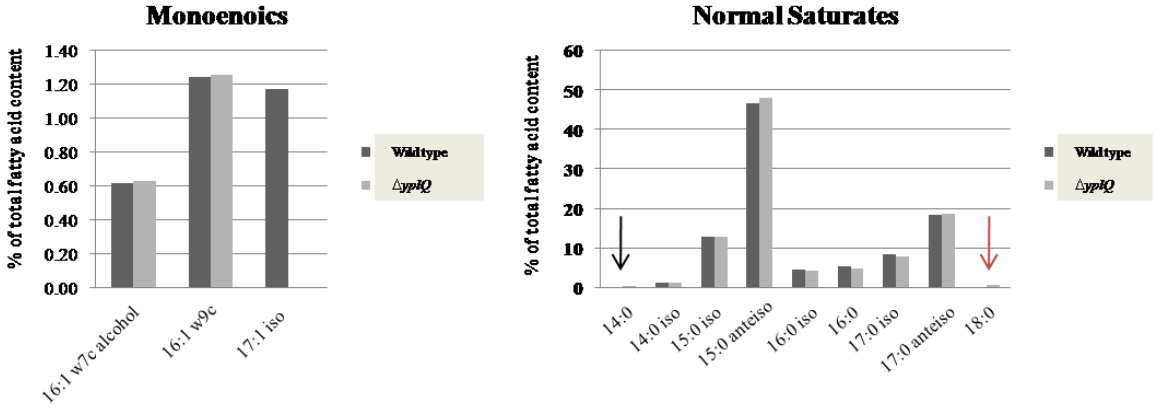

Figure 37. Phospholipid-Fatty Acid (PLFA) analysis among wild type and HlyIII mutants in *E. coli* and *B. subtilis*. (Left) Graphs comparing unsaturated fatty acid content in all strains tested. (Right) Graphs comparing saturated fatty acid content in all strains tested. Arrows highlight the presence of saturated fatty acids that are only found in the Δ*yplQ* mutant. Black arrow represents a value of 0.38% total fatty acid content. Red arrow represents a value of 0.49% total fatty acid content.

Azospirillum brasilense

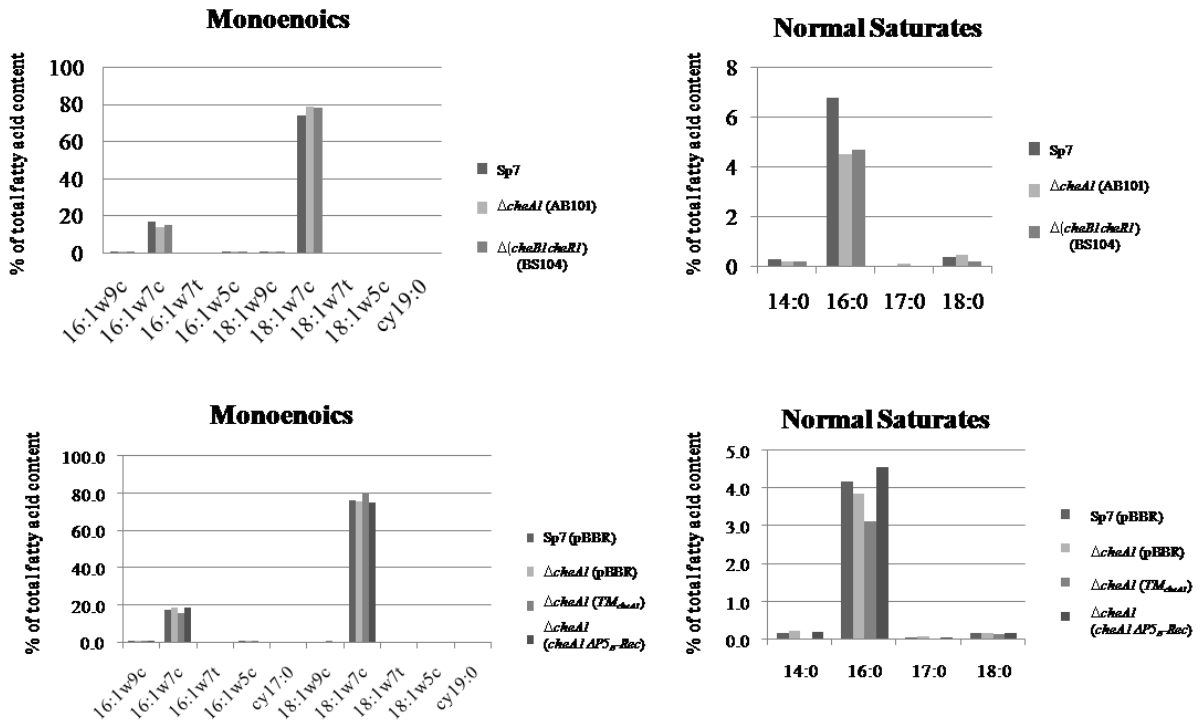

Figure 38. Phospholipid-Fatty Acid (PLFA) analysis among wild type and mutants in *A. brasilense*. (Left) Graphs comparing unsaturated fatty acid content in all strains tested. (Right) Graphs comparing saturated fatty acid content in all strains tested.

TM_{cheA1}, there were lower levels of palmitate (16:0) detected (Figure 38). Taken together, there is not a single specific pattern of fatty acid content that is affected by HlyIII-like proteins; however, alterations in fatty acid profiles do seem to be observed in all strains lacking HlyIII.

HlyIII-like proteins affect behavior of E. coli *and* B. subtilis

Because membrane properties, including protein localization appeared to be affected as a result of mutations in HlyIII, we were curious about how such effects would contribute to behavioral attributes in these organisms. We tested the effects of SDS and high salt concentrations on the growth of *E. coli* to determine if the lack of HlyIII affected membrane permeability, but no effect was detected (data not shown). Based on localization studies of CheB, CheR, and Tsr, we were curious to see how mis-localization of these proteins would affect chemotaxis behavior in the wild type versus the Δ*yqfA* mutant. Here, we found that chemotactic abilities of *E. coli* are impaired as a result of deleting *yqfA* (Figure 39). In tryptone media that was untreated, we observed that the wild type strain forms chemotactic rings, as expected; however, the mutant only forms a single chemotactic ring, suggesting a defect in chemotactic abilities. Taxis towards serine, which is sensed by the Tsr receptor (Springer *et al*., 1977), was tested using the same assay. We found that the Δ*yqfA* mutant showed a significant defect in chemotaxis toward serine, as compared to the wild type.

Early behavioral experiments using *B. subtilis* included examining the effect of HlyIII on biofilm formation, as well as cell morphology. In studies of biofilm formation in this organism, cells were grown in media conducive to sporulation and biofilm production (see Materials and Methods). Under these conditions, we found that the mutant lacking *yplQ* began to form

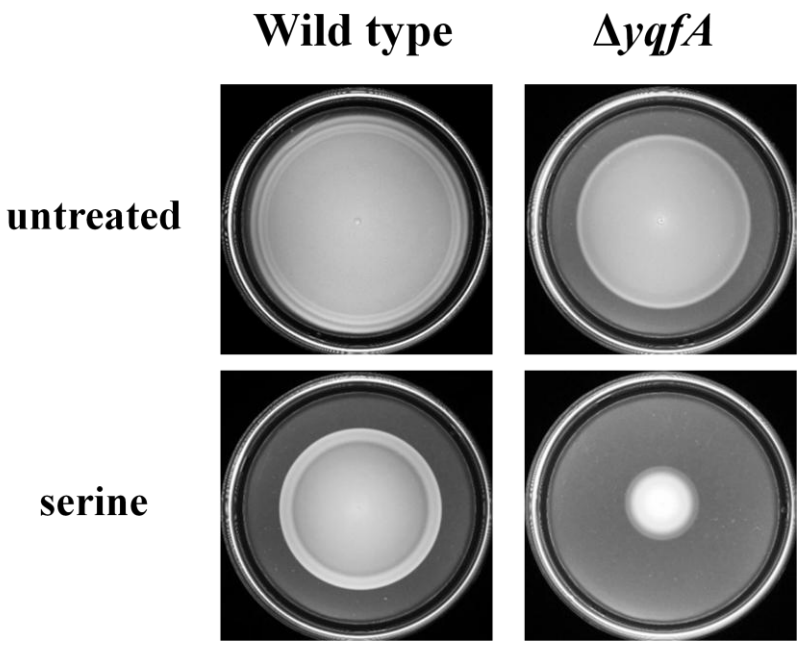

Figure 39. Chemotaxis semi-soft agar plate assays comparing chemotaxis abilities between wild type *E. coli* and the Δ*yqfA* mutant. Semi-soft agar plates were prepared as described (Materials and Methods) and photographs were taken 14-18 hours post-inoculation. Data shown here is representative of at least two independent experiments.

biofilms earlier than the wild type (Figure 40). Furthermore, after 2-3 weeks, cultures of wild type cells turned brownish in color and included thick biofilms. In contrast, the Δ*yplQ* mutant culture did not turn brown, and although this strain formed biofilms earlier compared to its parent, prolonged incubation led to a marked decrease in biofilm, suggesting biofilm degradation (Figure 40). In addition, the *B. subtilis* Δ*yplQ* mutant formed elongated cells in greater abundance compared to the wild type, in which such elongated cells are more seldom seen (Figure 40). Current literature suggests that the formation of these long cells is regulated by turning off the activity of the transcription factor, sigma D (σ^D) (28) when cells are grown to mid-exponential phase. It has been shown that the formation of long cells is a characteristic of biofilm formation (7), which would be supported by the fact that the Δ*yplQ* mutant forms biofilms earlier than the wild type.

Section D. Discussion

In this chapter, exploratory experiments were conducted to gain insight into the role of HlyIII-like proteins in bacteria. Our data collectively suggest that mutants lacking HlyIII-like proteins found in three phylogenetically distinct bacterial representatives, *A. brasilense*, *E. coli*, and *B. subtilis* are affected in membrane properties (Figure 32). Furthermore, membrane proteins, as well as proteins associated with membrane proteins (CheB and CheR), are mis-localized in strains in which the gene encoding for HlyIII has been deleted (Figure 33). In chapter 3, we showed that the N-terminal HlyIII domain of CheA1 in *A. brasilense* is responsible for regulating the cell length; here, we show that the HlyIII-like protein, YqfA, in *E. coli*, but not YplQ in *B. subtilis*, is also responsible for cell length regulation, although the cell length phenotypes as a result of these mutations are opposite between *E. coli* and *A. brasilense* (Figure

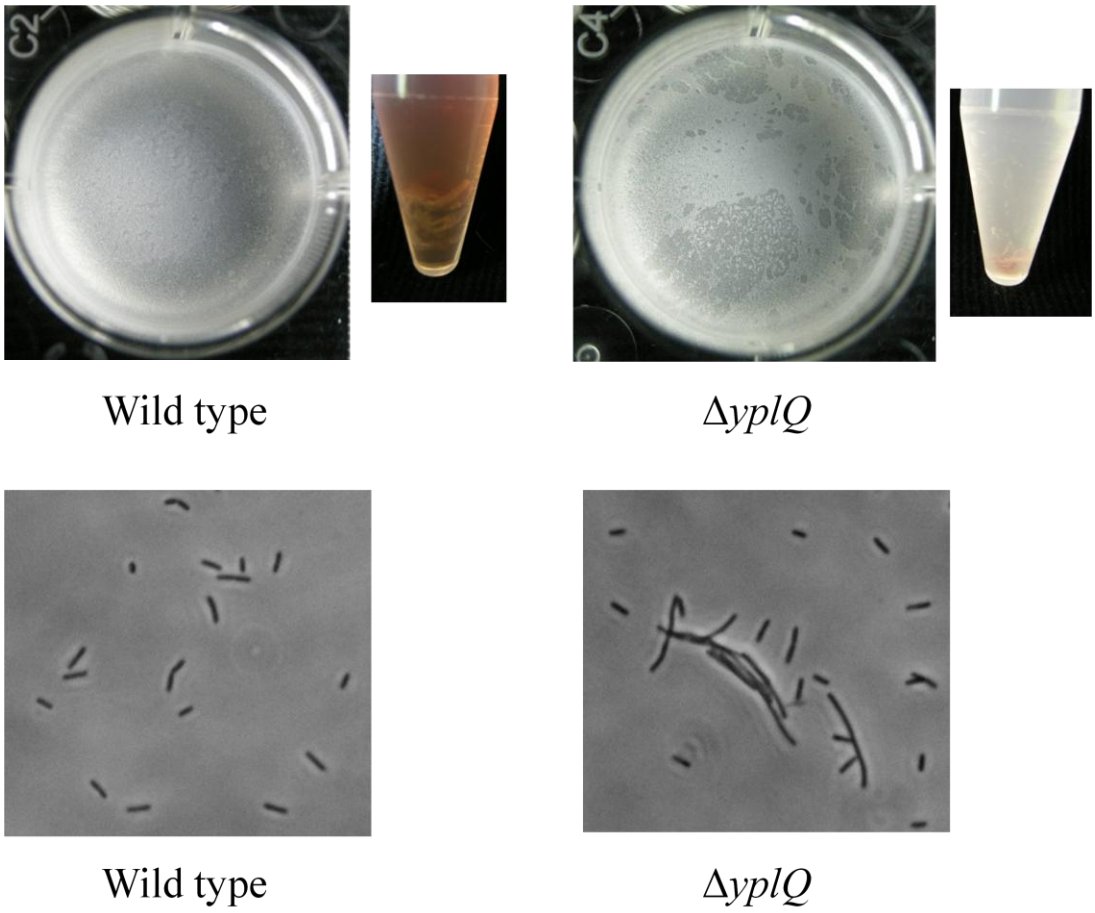

Figure 40. YplQ affects biofilm formation and cell morphology in *B. subtilis*. (Top) Photographs of biofilm formation in well plates and plastic tubes. Pictures of well plates were taken within 1 week of inoculation, whereas pictures of plastic tubes were taken after 2-3 weeks. (Bottom) Phase-contrast microscopy of cells grown under normal growth conditions. Wild type cells (left) have little to no formation of long cells, while the Δ*yplQ* mutant (right) has several long cells. Data shown here is representative of at least 3 independent experiments.

34). Each of these organisms also showed variation in fatty acid profiles as a result of mutations affecting HlyIII (Figure 38 and 39).

Although the experiments described in this chapter suggest that bacterial HlyIII-like proteins may be involved in regulating membrane properties, details surrounding how HlyIII specifically functions in the membrane remain elusive. Here, we will describe some possible mechanisms of HlyIII action, which are currently under investigation in the Alexandre lab.

Effects of HlyIII on the membrane

Lipid domains (or lipid rafts) have been described in eukaryotic cells as regions within the cell membrane consisting of specific phospholipid arrangements, often consisting of membrane proteins, that are of a more rigid nature, as opposed to the "fluid-mosaic" model proposed by Singer and Nicolson (for a review, see 40). Recently, the presence of lipid microdomains was shown in *Mycobacteria, Escherichia coli,* and *Bacillus subtilis* Marburg membranes (9, 14, 26, 32). It has been suggested that these lipid domains are functionally similar to those in eukaryotic cells in that they consist of a specific arrangement of lipids and membrane proteins (30). Evidence presented here supports a possible role for HlyIII-like proteins in organizing lipid domains, albeit indirectly. For example, in each strain tested, the differences in staining with 3 different lipid dyes indicated distinct staining patterns and differing dye affinities between parent strans and those in which the HlyIII domain protein was missing. Differences in the fatty acid composition of the membranes from each strain were observed, as well. Taken together, these results suggest a very general effect of HlyIII on membrane properties. Such effects on the membrane properties could explain the changes in localization of

membrane-associated proteins detected in the strains lacking HlyIII. Changes in the localization of these proteins caused a defect in function, suggesting a physiological relevance to the different staining and localization patterns observed.

Of particular significance is the observation that mutating HlyIII caused a change in the ability of Min proteins to localize properly, which could provide a mechanism by which this domain may affect cell length at division. Cell length phenotypes were affected in HlyIII mutants of *E. coli* and *A. brasilense*. We observed that localization of Min proteins was affected in these strains, possibly due to effects of HlyIII on the membrane, in terms of organization or composition, as mentioned earlier. MinD is known to associate directly with the membrane in an ATP-dependent manner (22) via its C-terminal region which binds directly to the lipid bilayer (21), and it is responsible for recruitment of FtsZ to the mid-cell at division (12, 21). It has also been shown that anionic lipids, such as cardiolipin, are found at the cell poles and at mid-cell, where cell division proteins such as FtsZ are known to localize and interact, thus suggesting an important role for lipid composition and organization in division site selection in bacteria (32, 33). Interestingly, although MinD is essential to FtsZ ring formation in *E. coli*, and presumably in *A. brasilense*, it has been shown that MinD is not required for FtsZ ring formation in *B. subtilis* (3), perhaps explaining why cell length phenotypes were not observed for the Δ*yplQ* mutant in *B. subtilis*. Furthermore, cell division site placement does not depend on the oscillation of MinCDE proteins in *B. subtilis*, but on a gradient of DivIVA that is a protein anchored at the cell poles (13). Similarly, chemotaxis phenotypes in *E. coli* shown in Figure 40 suggest that HlyIII-like proteins can affect the sensitivity of cells to environmental cues. One possible way this may happen is through disruption of membrane properties resulting in the mis-localization of

chemoreceptors and other chemotaxis proteins. This possibility is suggested by the data presented here (Figure 33). Because bacterial chemotaxis is a robust signal transduction pathway that depends on factors including specific protein concentrations and protein chemistry (2), it is likely that mis-localization or defective localization of chemotaxis proteins could affect the efficiency by which this signal transduction pathway functions.

In *B. subtilis*, mutations affecting HlyIII-like proteins result in early biofilm formation relative to the wild type, as well as early degradation. The regulation of biofilm formation, and degradation, is highly complex. There are many genes associated with biofilm formation which includes (but is not limited to): sporulation genes, EPS production genes, and genes for surfactant production (6, 7, 17, 18, 27). Additionally, there are several environmental factors that have been shown to trigger biofilm dispersal, including nutrient availability, changes in temperature, as well as quorum-sensing (for a review, see 31). Perhaps one of the most interesting factors that contribute to biofilm dispersal, in relation to HlyIII and the roles of PAQR family proteins in lipid modification and fatty acid oxidation, is the production of cis-2-decenoic acid (a short chain fatty acid) produced by *Pseudomonas aeruginosa*, which induces the dispersal of biofilms (10). Interestingly, this fatty acid resembles other short chain fatty acids that are known to have a role in signaling (10).

Another possible mechanism by which HlyIII-like proteins may affect membrane properties and membrane-associated protein localization is in the modification of fatty acids, and thus lipid composition, within the membrane. Indeed, several proteins have been shown to be associated with particular fatty acids within the membrane (1). It would thus be expected that a change in the fatty acid composition of the membrane could alter the proper insertion and

stability or function of these proteins. However, fatty acids are not known to be extensively modified post-synthesis and after incorporation into the membrane in bacteria. It is thus unclear how such modifications would occur post-synthesis. On the other hand, it is possible that HlyIII-like proteins modulate *de novo* fatty acid biosynthesis. Interestingly, the adiponectin receptors AdipoR1 and AdipoR2 of the PAQR family of proteins were shown to have a role in mediating AMP kinase and PPARα activities, which lead to downstream effects on fatty acid oxidation and glucose uptake (43). Additionally, the yeast PAQR homolog, YOL002c, was also shown to be involved in lipid metabolism (25). A recent paper classified HlyIII and PAQR proteins as part of the CREST protein family and suggested that, based on homology to alkaline ceramidases, HlyIII-like proteins and PAQR proteins may have membrane enzymatic functions, possibly ceramidase-like, in which short chain fatty acids (such as sphingosine) may be produced as second messengers in downstream signaling (35). In fact, it was recently shown that the PAQR homolog, Izh2p, from yeast has ceramidase activity and that sphingoid bases produced by this PAQR function as second messengers (41). Thus, it is possible that HlyIII directly affects fatty acid within the cell membrane. This intriguing function could also contribute to explaining the plethora of phenotypes affected by mutating HlyIII.

Chapter 4

Characterization of HlyIII-like proteins in *A. brasilense*, *E. coli*, and *B. subtilis*

References

1. **Alberts, B., Johnson, A., Lewis, J., Raff, M., Roberts, K., Walter, P.** 2002. Molecular Biology of the Cell (4th ed.). New York: Garland Science.

2. **Alon, U., Surette, M. G., Barkai, N., Leibler, S.** 1999. Robustness in bacterial chemotaxis. Nature. **397**: 168-171.

3. **Anderson, D. E., Gueiros-Filho, F. J., Erickson, H. P.** 2004. Assembly dynamics of FtsZ rings in *Bacillus subtilis* and *Escherichia coli* and effects of FtsZ-regulating proteins. J. Bacteriol. **186**: 5775-5781.

4. **Baida, G. E., Kuzmin, N. P.** 1996. Mechanism of action of hemolysinIII from *Bacillus cereus*. Biochim. Biophys. Acta. **1284**: 122–124.

5. **Bible, A.N., Stephens, B.B., Ortega, D.R., Xie, Z., Alexandre, G.** 2008. Function of a chemotaxis-like signal transduction pathway in modulating motility, cell clumping, and cell length in the alphaproteobacterium, *Azospirillum brasilense*. J. Bacteriol. **190**: 6365-6375.

6. **Branda, S.S., González-Pastor, J.E., Ben-Yehuda, S., Losick, R., Kolter, R.**2001. Fruiting body formation by *Bacillussubtilis*. Proc. Natl. Acad. Sci. USA. **98:** 11621–11626.

7. **Branda, S.S., González-Pastor, J.E., Dervyn, E., Ehrlich, D., Losick, R., and Kolter, R.** 2004. Genes involved in the formation of structured multicellular communities by *Bacillus subtilis*. J. Bacteriol. **186:** 3970–3979.

8. **Charles, N. J., Thomas, P., Lange, C. A.** 2010. Expression of membrane progesterone receptors (mPR/PAQR) in ovarian cancer cells: implications for progesterone-induced signaling events. Hormones and Cancer. **1**: 167-176.

9. **Christensen, H., Garton, N.J., Horobin, R.W., Minnikin, D.E., Barer, M.R.**1999. Lipid domains of mycobacteria studied with fluorescent molecular probes. Mol. Microbiol. **31:** 1561–1572.

10. **Davies, D. G., Marques, C. N.**2009. A fatty acid messenger is responsible for inducing dispersion in microbial biofilms. J. Bacteriol. **191**: 1393-1403.

11. **Datsenko, K. A., Wanner, B. L.** 2000. One-step inactivation of chromosomal genes in *Escherichia coli* K-12 using PCR products. Proc. Natl. Acad. Sci. USA. **97**: 6640-6645.

12. **de Boer, P. A., Crossley, R. E., Rothfield, L. I.** 1989. A division inhibitor and a topological specificity factor coded for by the minicell locus determine proper placement of the division septum in *E. coli*. Cell. **56**: 641-649.

13. Edwards, D. H., Errington, J. 1997. The *Bacillus subtilis* DivIVA protein targets to the division septum and controls the site specificity of cell division. Mol. Microbiol. **24**: 905-915.

14. Fishov, I., Woldringh, C.L.1999. Visualization of membranedomains in *Escherichia coli*. Mol. Microbiol. **32:** 1166–1172.

15. Góñez, L. J., Naselli, G., Banakh, I., Niwa, H., Harrison, L. C. 2008. Pancreatic expression and mitochondrial localization of the progestin adipoQ receptor PAQR 10. Mol. Med. **14**: 697-704.

16. Hallez, R., Letteson, J. J., Vandenhaute, J., De Bolle, X. 2007. Gateway-based destination vectors for functional analysis of bacterial ORFeomes: application to the Min system in *Brucella abortus*. Appl. Environ. Microbiol. **73**: 1375-1379.

17. Hamon, M.A., Lazazzera, B.A.2001. The sporulationtranscription factor Spo0A is required for biofilm developmentin *Bacillus subtilis*. Mol. Microbiol. **45**: 1199–1209.

18. Hamon, M.A., Stanley, N.R., Britton, R.A., Grossman, A.D., Lazazzera, B.A.2004. Identification of AbrB regulated genes involved in biofilm formation by *Bacillus subtilis*. Mol. Microbiol. **52:** 847–860.

19. Hauwaerts, D., Alexandre, G., Das, S. K., Vanderleyden, J., Zhulin, I. B. 2002. A major chemotaxis gene cluster in *Azospirillum brasilense* and relationships between chemotaxis operons in α-proteobacteria. FEMS Microbiol. Letters. **208**: 61-67.

20. Holland, W. L., Miller, R. A., Wang, Z. V., Sun, K., Barth, B. M., Bui, H. H., Davis, K. E., Bikman, B. T., Halberg, N., Rutkowski, J. M., Wade, M. R., Tenorio, V. M., Kuo, M. S., Brozinick, J. T., Zhang, B. B., Birnbaum, M. J., Summers, S. A., Scherer, P. E. 2011. Receptor-mediatedactivation of ceramidase activity initiates the pleiotropicactions of adiponectin. Nat. Med. **17**: 55-63.

21. Hu, Z., Lutkenhaus, J. 2001. Topological regulation of cell division in *E. coli*, spatiotemporal oscillation of MinD requires stimulation of its ATPase by MinE and phospholipid. Mol. Cell. **7**: 1337-1343.

22. Hu, Z., Saez, C., Lutkenhaus, J. 2003. Recruitment of MinC, an inhibitor of Z ring formation, to the membrane in *Escherichia coli*: role of MinD and MinE. J. Bacteriol. **185**: 196-203.

23. Jin, T., Ding, Q., Huang, H., Xu, D., Jiang, Y., Zhou, B., Li, Z., Jiang, X., He, J., Liu, W., Zhang, Y., Pan, Y., Wang, Z., Thomas, W. G., Chen, Y. 2011. PAQR10 and

PAQR11 mediate Ras signaling in the golgi apparatus. Cell Res. Advanced online publication.

24. Kaneda, T. 1991. Iso- and anteiso-fatty acids in bacteria: biosynthesis, function, and taxonomic significance. Microbiol. Mol. Biol. Rev. **55**: 288-302.

25. Karpichev, I. V., Cornivelli, L., Small, G. M. 2002. Multiple regulatory roles of a novel *Saccharomyces cerevisiae* protein, encoded by yOL002c, in lipid and phosphate metabolism. J. Biol. Chem. **277**: 19609-19617.

26. Kawai, F., Shoda, M., Harashima, R., Sadaie, Y., Hara, H., Matsumoto, K.2004. Cardiolipin domains in *Bacillussubtilis* Marburg membranes. J. Bacteriol. **186:** 1475–1483.

27. Kearns, D. B., Chu, F., Branda, S. S., Kolter, R., Losick, R. 2005. A master regulator for biofilm formation by *Bacillus subtilis*. Mol. Microbiol. **55**: 739-749.

28. Kearns, D. B., Losick, R. 2005. Cell population heterogeneity during growth of *Bacillus subtilis*. Genes and Development. **19**: 3083-3094.

29. Lyons, T. J., Villa, N. Y., Regalla, L. M., Kupchak, B. R., Vagstad, A., Eide, D. J. 2004. Metalloregulation of yeast steroid hormone receptor homologs. Proc. Natl. Acad. Sci. USA. **101**: 5506-5511.

30. Matsumoto, K., Kusaka, J., Nishibori, A., Hara, H. 2006. Lipid domains in bacterial membranes. Mol. Microbiol. **61**: 1110-1117.

31. McDougald, D., Rice, S. A., Barraud, N., Steinberg, P. D., Kjelleberg, S. 2012. Should we stay or should we go: mechanisms and ecological consequences for biofilm dispersal. Nat. Rev. Microbiol. **10**: 39-50.

32. Mileykovskaya, E., Dowhan, W. 2000. Visualization of phospholipid domains in *Escherichia coli* by using the cardiolipin-specific fluorescent dye 10-*N*-Nonyl Acridine Orange. J. Bacteriol. **182**: 1172-1175.

33. Mileykovskaya, E., Dowhan, W. 2005. Role of membrane lipids in bacterial division-site selection. Curr. Opin. Microbiol. **8:** 135-142.

34. Osawa, M., Erickson, H. P. 2005. Probing the domain structure of FtsZ by random truncation and insertion of GFP. Microbiology. **151**: 4033-4043.

35. Pei, J., Millay, D. P., Olson, E. N., Grishin, N. V. 2011. CREST – a large and diverse superfamily of putative transmembrane hydrolases. Biology Direct. **6**: 37.

36. Springer, M. S., Goy, M. F., Adler, J. 1977. Sensory transduction in *Escherichia coli*: two complementary pathways of information processing that involve methylated proteins. **74**: 3312-3316.

37. Stephens, B. B., Loar, S. N., Alexandre, G. 2006. Role of CheB and CheR in the complex chemotactic and aerotactic pathway of *Azospirillum brasilense*. **188**: 4759-4768.

38. Sun, Q., Margolin, W. 2001. Influence of the nucleoid on placement of FtsZ and MinE rings in *Escherichia coli*. J. Bacteriol. **183**: 1413-1422.

39. Tang, Y. T., Hu, T., Arterburn, M., Boyle, B., Bright, J. M., Emtage, P. C., Funk, W. D. 2005. PAQR proteins: a novel membrane receptor family defined by an ancient 7-transmembrane pass motif. J. Mol. Evol. **61**: 372-380.

40. Vereb, G., Szöllösi, J., Matkó, J., Nagy, P., Farkas, T., Vígh, L., Mátyus, L., Waldmann, T. A., Damjanovich, S. 2003. Dynamic, yet unstructured: the cell membrane three decades after the Singer-Nicolson model. Proc. Natl. Acad. Sci. USA. **100**: 8053-8058.

41. Villa, N. Y., Kupchak, B. R., Garitaonandia, I., Smith, J. L., Alonso, E., Alford, C., Cowart, L. A., Hannun, Y. A., Lyons, T. J. 2009. Sphingolipids function as downstream effectors of a fungal PAQR. Mol. Pharmacology. **75**: 866-875.

42. Wisniewski-Dye, F., Borziak, K., Khalsa-Moyers, G., Alexandre, G., Sukharnikov, L.O., Wuichet, K., Hurst, G.B., McDonald, W.H., Robertson, J.S., Barbe, V., Calteau, A., Rouy, Z., Mangenot, S., Prigent-Combaret, C., Normand, P., Boyer, M., Siguier, P., Dessaux, Y., Elmerich, C., Condemine, G., Krishnen, G., Kennedy, I., Paterson, A.H., Gonzalez, V., Mavingui, P., Zhulin, I.B.2011.*Azospirillum* genomes reveal transition of bacteria from aquatic to terrestrial environments. PLoS Genetics. **7**: e1002430.

43. Yamauchi, T., Kamon, J., Ito, Y., Tsuchida, A., Yokomizo, T., Kita, S., Sugiyama, T., Miyagishi, M., Kara, K., Tsunoda, M., Murakami, K., Ohteki, T., Uchida, S., Takekawa, S., Waki, H., Tsuno, N. H., Shibata, Y., Terauchi, Y., Froguel, P., Tobe, K., Koyasu, S., Taira, K., Kitamura, T., Shimizu, T., Nagai, R., Kadowaki, T.2003. Cloning of adiponectin receptors that mediate antidiabetic metabolic effects. Nature. **423**: 762–769.

44. Zhu, Y., Rice, C. D., Pang, Y., Pace, M., Thomas, P. 2003. Cloning, expression, and characterization of a membrane progestinreceptor and evidence it is an intermediary in meiotic maturation of fish oocytes. Proc. Natl. Acad. Sci. USA. **100**: 2231–2236.

45. Zhu, Y., Bond, J., Thomas, P. 2003. Identification, classification, andpartial characterization of genes in humans and other vertebrateshomologous to a fish membrane progestin receptor. Proc. Natl. Acad. Sci. USA. **100**: 2237–2242.

Conclusions

Prior to this dissertation project, the study of taxis behaviors in *Azospirillum brasilense* established that aerotaxis is a dominant behavior and that chemotaxis takes place using a methylation-independent mechanism, in which chemotaxis is driven by metabolism-dependent cues, rather than methylation/demethylation of chemoreceptors. Despite the Che1 pathway being originally identified as a key pathway in the regulation of chemotaxis behavior in *A. brasilense*, later experimental evidence characterizing mutations which were affected in individual protein components of the Che1 pathway failed to show null chemotaxis phenotypes, and they also provided evidence that *A. brasilense* uses both methylation-independent and methylation-dependent forms of chemotaxis. These results initially draw quite a complex and unexpected picture regarding the role of the Che1 pathway in the control of chemotaxis and aerotaxis behavior in this organism. These data also raised intriguing possibilities regarding the unique functions of Che1 and some of its components, including CheA1 from *A. brasilense* Sp7 in modulating these usnusaual functions.

During the course of this dissertation project, we have worked to characterize the function of this Che1 pathway. Interesting to the study of chemotaxis, as a whole, we found that a single Che pathway, with presumably a single output, can coordinate and influence a variety of cellular behaviors. Specifically, we have shown that the Che1 pathway directly affects cell swimming speed, which indirectly affects the ability of cells to clump together, as well as their ability to navigate by chemotaxis and aerotaxis. The indirect function of Che1 has intriguing implications. In work performed by Siuti, *et al*., (see reference 27, Chapter 2) flagellar motility and chemotaxis were shown to modulate the ability of cells to attach to surfaces and form

biofilms. However, the exact function of this property is often unclear. The finding that modulation of swimming speed *per se* can alter the ability of cells to regulate cell-to-cell interactions offers a new testable hypothesis for the role of this function in the formation of biofilms. We have also learned from recent genome sequencing that Che1 is one of four Che-like pathways in *A. brasilense*. It has been shown in recent years that the majority of bacterial organisms are not like *E. coli* or other model organisms which possess a single chemotaxis pathway, but most organisms have multiple Che-like pathways. In addition, recent studies are starting to find that these organisms which possess multiple chemotaxis-like pathways have mechanisms in place by which they can cross-talk with one another in order to regulate more than one behavioral output. The work that we have presented here has also provided evidence to suggest that the Che1 pathway can affect multiple cellular behaviors via cross-talk with other Che-like pathways.

Not surprisingly, research among bacteria with multiple Che-like pathways including (but not limited to) *Rhodobacter sphaeroides, Myxococcus xanthus,* and *Rhodospirillum centenum* has also shown that the paradigm of a single chemotaxis pathway with a single behavioral output, as set forth in the model organism *E. coli*, is rather the exception and not the rule when it comes to chemotactic signaling. The study of chemotaxis in these organisms, as well as *A. brasilense,* is starting to highlight the necessity of studying this signal transduction pathway in organisms with multiple Che-like pathways.

What we've learned about chemotaxis in *A. brasilense* during the course of this dissertation project can be summarized in a few words: it's not that simple. The presence of CheBs (which we find are important to behaviors such as clumping and flocculation), CheRs, as

well as CheDs in the genome suggest that this organism can use both methylation-dependent (i.e. chemotaxis based on receptor methylation) and methylation-independent mechanisms (i.e. chemotaxis based on metabolism) for chemotaxis. It has four different Che-like pathways with various behavioral outputs, not to mention the presence of individual chemotaxis genes scattered throughout the genome which are not organized into operons. In addition, there are 48 chemoreceptors (i. e. sources of signaling input) which presumably utilize these four Che-like pathways. To further complicate things, there is likely cross-talk taking place between these Che-like pathways, perhaps at the level of cross-methylation of receptors.

In our proposed model shown in Fig. 41, we summarize findings made during this dissertation project, along with possible mechanisms by which Che1 indirectly regulates such behaviors as clumping, flocculation, and chemotaxis (motility bias) based in part on data obtained in the Alexandre lab that is not presented here. The predicted mechanisms shown in this model will provide the groundwork for understanding how a single bacterial organism can sense a variety of environmental cues and then "decide" how to respond. Some interesting questions for the future could include: 1) do these Che-like pathways always cross-talk with one another, and 2) if not, how do they "decide" when to cross-talk and when not to? Together, studies in *A. brasilense*, as well as other organisms with multiple Che-like pathways, will start to shape the future of how chemotaxis behavior in bacteria is understood.

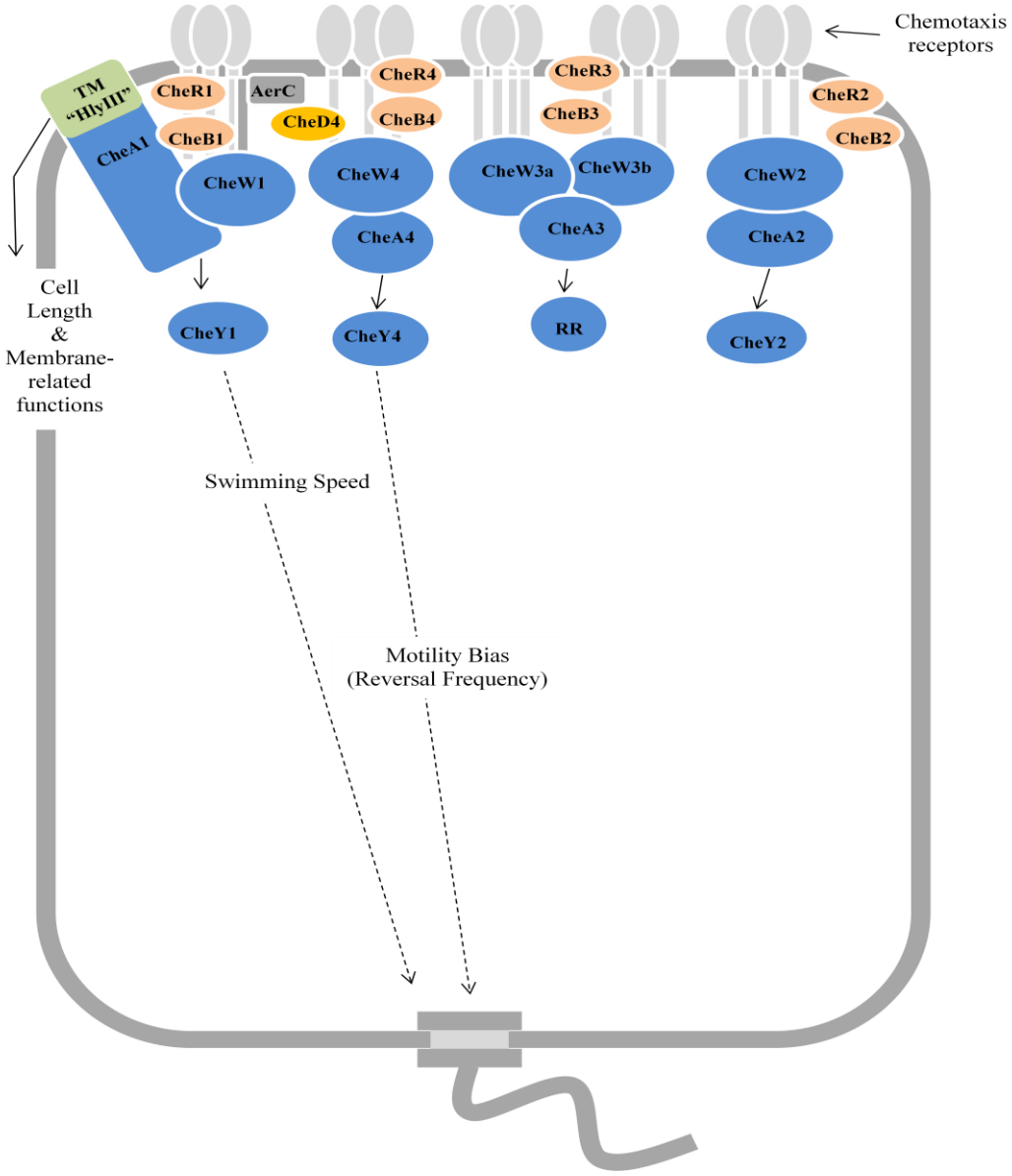

Figure 41. Proposed model for the function of Che1 in *A. brasilense*. Che1 has been shown to regulate the cell swimming speed (Chapter 2) and cell length regulation has been shown to take place via the N-terminal TM domain ("HlyIII") of CheA1 (in Sp7) (Chapter 3). The N-terminal TM domain of CheA1 has also been shown to play a role in membrane-related functions (Chapter 4). Arrows indicating phosphorylation of CheB by CheA are not shown and arrows indicating methylation/demethylation of receptors by CheB, CheR, or CheD are also not shown.

Vita

Amber Nicole Bible was born August 15, 1981 in Knoxville, Tennessee. During her early years of education, she was schooled at home by her mother, Carolyn Bible, with the help of her grandfather, William Warwick. During these years, she developed an interest in science while doing science experiments at home and visiting the American Museum of Science and Energy at Oak Ridge. In 1994, Amber started attending Knoxville Baptist Christian Schools (KBCS) and remained there until she graduated as class valedictorian in 2000. During her sophomore/junior years of high school, her mom was diagnosed with breast cancer. Watching her mother deal with this disease and witnessing the effects that chemotherapy and radiation had on her, Amber developed a strong desire to contribute to the field of cancer research. In fall 2000, she began her undergraduate education at the University of Tennessee, Knoxville and pursued a Bachelor's degree in Biology, concentrating on Biochemistry, Cellular, and Molecular Biology. During her undergraduate career, she worked as a supervisor at a local grocery store and also worked as a clerk at the medical library at the University of Tennessee Medical Center. During the summer of 2004, she volunteered in the lab of Dr. Jay Wimalasena at the University of Tennessee Medical Center as an undergraduate. During her time there, she had the opportunity to participate in breast cancer research and upon graduating with her Bachelor's degree, Dr. Wimalasena hired her as a laboratory assistant. Some of the work that she participated in resulted in a publication where she is an author. Upon the advice of Dr. Jay Wimalasena, she chose to pursue a graduate school career at the University of Tennessee, Knoxville. During her first year, she searched for a lab where she could continue to participate in cancer research. However, she was not able to find the right kind of research environment that

suited her. Surprisingly, during her second rotation with Dr. Gladys Alexandre, she discovered that bacteria were far more interesting than she had ever given them credit for being before. In the summer of 2006, she decided to join Dr. Alexandre's lab, during which time she has had the opportunity to present her research at four different conferences, as well as being the first author on two publications and a recipient of the Alexander Hollaender Fellowship Award.